Proteome analysis of dissected barley seed tissue during germination and radicle elongation

Heterologous expression of barley limit dextrinase inhibitor

Bønsager, Birgit Christine; Svensson, Birte; Finnie, Christine

Publication date:
2007

Document Version
Publisher's PDF, also known as Version of record

Proteome analysis of dissected barley seed tissues during germination and radicle elongation
&
Heterologous expression of barley limit dextrinase inhibitor

Ph.D. Thesis

Birgit Christine Bønsager
Department of Chemistry, Carlsberg Laboratory
and
Enzyme and Protein Chemistry, BioCentrum-DTU

Supervisors:

Prof. Birte Svensson
Enzyme and Protein Chemistry
BioCentrum-DTU
Technical University of Denmark

Associate Prof. Christine Finnie
Enzyme and Protein Chemistry
BioCentrum-DTU
Technical University of Denmark

Preface

This Ph. D. project was initiated at the Department of Chemistry, Carlsberg Laboratory in January 2003 under the supervision of Professor Birte Svensson and Christine Finnie. Carlsberg Laboratory financed the project from January 2003 to March 2004, during which time I was enrolled as a Ph. D. student in the Department of Biochemistry and Molecular Biology at University of Southern Denmark. On April 1st, 2004, Professor Birte Svensson and the project transferred to Enzyme and Protein Chemistry (EPC), BioCentrum-DTU. DTU funded my Ph. D. scholarship from April 2004 to January 2007, including one year of maternity leave.

The project was initially divided into two parts. The first was a proteome analysis of dissected barley tissues during germination. The second was an investigation of structure and functional relationships of barley limit dextrinase inhibitors. The second part, however, did not progress far due to problems with production of recombinant protein, despite several production attempts. The proteome analysis component began on the basis of an extensive four year research project "Barley proteome project" at the Carlsberg Laboratory, which started in 2000 and ended in the spring of 2004. The present dissertation furthermore includes a study of functional aspects of enzymes involved in the ascorbate-glutathione cycle, in particular ascorbate peroxidase. This study was inspired by the results of the proteome analysis of dissected barley tissues during germination.

The thesis contains an Introduction (Chapter 1) including the objectives and the strategies used, Materials and methods (Chapter 2), and the Results of the work (Chapter 3) are given in three parts:

1) Proteome analysis of dissected barley seed tissues during germination and radicle elongation (Chapter 3.1)
2) Proteomics-based description of enzymes of the ascorbate-glutathione cycle (Chapter 3.2)
3) Study of the limit dextrinase inhibitor (Chapter 3.3)

These three Result sections will each have a Discussion. A final Discussion and Conclusions chapter addresses the major points of the thesis (Chapter 4). Future perspectives are given in Chapter 5.

The work has resulted in the following publications:

B. Svensson, K. Fukuda, P.K. Nielsen, **B.C. Bønsager.** (2004) Proteinaceous α-amylase inhibitors. Biochim. Biophys. Acta, 1696, 145-156. (Appendix 4)

B.C. Bønsager, C. Finnie, P. Roepstorff, B. Svensson. Spatio-temporal changes in germination and radical elongation of barley seeds tracked by proteome analysis of dissected embryo, aleurone layer and endosperm tissues. Submitted to Proteomics. (Appendix 5)

B.C. Bønsager, C. Finnie, A. Shahpiri, B. Svensson. Monitoring enzymes of the ascorbate-glutathione cycle during germination and radicle elongation of barley seed embryo. In prep. (not included in the thesis)

Several posters and oral presentations at international conferences and meetings. (Appendix 6)

Acknowlegdement

During my Ph.D., I have received help and enjoyed stimulating discussions with a number of people, whom I would like to thank. In particular I would like to thank my supervisors, **Professor Birte Svensson** and **Associate Professor Christine Finnie**, without whom the project would not have been possible. Birte has provided a great scientific environment and support and advice when needed. Christine has provided excellent technical help, advice and feed-back. Furthermore I would like to mention:

Carlsberg Laboratory
Klaus Bock for a Ph.D. stipend for the first 15 months of the study.
Ole Østergaard for setting up a proteomics system.
Kristian Sass Bak-Jensen for general discussion on protein chemistry.
Mette Hersum Bien for technical assistance.
Sidsel Ehlers for purified barley limit dextrinase.
Birgitte Skadhauge for providing barley seeds.
Ella Meiling for advice with germination conditions.

Enzyme and Protein Chemistry, BioCentrum-DTU
Kenji Maeda for help with experiments with thioredoxin h, modeling of APX and DHAR structures, and general discussions on protein chemistry.
Per Hägglund for help with experiments with thioredoxin h, general discussions on protein chemistry, and for reading part of the thesis prior to printing.
Azar Saphiri for gene expression analysis.
Dale Shelton for help with mass spectrometry and general discussions on protein chemistry.
Torben Steenholdt for discussions about mass spectrometry and identification of a few proteins.
Jannick Prentø for the work on heterologous production and refolding of recombinant LDI and construction of the *L. lactis* expression vector.
Jørn Hejgaard for reading part of the thesis prior to printing.
Sophie Bozonnet for many good discussions, company, and support.
Birgit Andersen for technical assistance, especially with mass spectrometry.
Marina Rybaltover for always being helpful in the laboratory, when time was limited.

The rest of the present and former group members and other people in the building are thanked for being great colleagues and always being helpful when needed.

Center for Microbial Biotechnology, BioCentrum-DTU
Jan Martinussen for providing the vector for *L. lactis* expression of LDI and for help with transformation and cell growth.

University of Southern Denmark
Peter Roepstorff and **Ole Nørregaard Jensen** for access to the mass spectrometry facility.
Andrea Lorenzen for technical assistance with mass spectrometry.

Metropolotanian University, Tokyo, Japan
Prof. T. Koshiba for providing APX specific antibodies.

Grain Research Laboratory, Canadian Grain Commission, Winnipeg, Canada
Dr. A.W. MacGregor for providing anti-LDI antibodies and purified barley LDI.

I would also like to thank my family for support, patience, and flexibility during busy times.

Summary

Cereal grains are vital components of our diet, and therefore understanding of the biology of breakage of dormancy and initiation of germination very important. These processes are far from fully understood, despite extensive studies, and no specific markers for germination have been identified at the protein or the DNA level. In addition, germination of barley seeds is of interest for the brewing industry since this process corresponds to the steeping process that starts the industrial malting.

In the present study a proteomics approach was employed to understand the initial changes in the water soluble protein composition of the barley seed upon imbibition and the following events that occur until to 72 h post imbibition (PI). 2D gel electrophoresis of proteins extracted from dissected barley seeds tissues during germination (0-24 h) and the subsequent radicle elongation (24-72 h) describes spatio-temporal variations in the protein patterns. Seeds from 8 time points (0, 4, 12, 24, 36, 52, 60, and 72 h PI) were dissected into embryo, aleurone layer and endosperm and small scale protein extractions enabled us to obtain good resolution 2D gels. The 2D gels were compared between the time points and the different tissues and protein spots of changing intensity were tracked and identified by in-gel digestion, mass spectrometry, and database searches. Forty-eight different proteins in 79 protein spots were tracked through-out the processes and the distribution of these protein spots differed among embryo, aleurone, and endosperm emphasizing individual tissue functionalities. The most significant changes occurred in the two living tissues, namely the embryo and the aleurone layer, both of which resume metabolic activity upon imbibition. The earliest and the largest number of changes were observed in the embryo. This is in contrast to the endosperm which serves as storage reserve, where the hydrolytic enzymes, produced in the aleurone layer, take action in order to provide nutrients for the embryo growth.

β-Type proteasome subunit and a fragment of heat shock protein 70 were identified at 4 h PI as the first proteins to appear in embryo together with changes in the spot pattern of desiccation stress related proteins such as late embryonic abundant (LEA) proteins and abscisic acid induced proteins. After 12 h well-known desiccation stress related proteins and other proteins (putative embryonic protein and abscisic acid induced protein), that we suggest are involved in desiccation, rapidly disappear. Other proteins including several redox-related proteins, which are involved in protection against water stress and reactive oxygen species, changed in abundance at the end of germination and start of radicle elongation. These proteins had different tissue distribution and most of them either remained constant or decreased in abundance during radicle elongation, except for ascorbate peroxidase (APX) which was only present in the germinating barley embryo after 24 h. Other proteins involved in osmotic and salinity stress, storage breakdown, folding, and housekeeping were identified and tracked through 72 h PI.

APX and the other enzymes involved in the ascorbate-glutathione cycle (dehydroascorbate reductase, monodehydroascorbate reductase, and glutathione reductase) were thought to have an important function during germination and radicle elongation, since the high energy demand upon imbibition generates reactive oxygen species, especially in the metabolically active and dividing embryo tissue. These four enzymes were subjected to activity assays carried out using barley embryo protein extracts and the activity profiles were compared

to the 2D gel patterns. This gave both concordant and deviating enzymes activity and 2D gel spot intensities during radicle elongation. APX activity detection in zymograms and gene expression analysis indicated that at least two APX isoforms are present in the germinated embryo extract. The APX mRNA of both isoforms were present in the dry mature seed, whereas increasing activity was only observed after 36 h, which supports that the ascorbate-glutathione cycle is not functioning in the desiccated seed, but that the mRNA is ready for translation. Both APX and DHAR are suggested targets of Trx h-linked redox regulation, and this is discussed based on the present results, although it was not possible to detect changes in the dehydroascorbate reductase activity by addition of reduced, recombinant Trx h to the embryo extract. Post-translational modification of APX was further studied by mass spectrometry based on the 2D gel pattern of APX in germinated barley embryos, which indicated the presence of several APX forms with different pI values.

The barley limit dextrinase inhibitor (LDI) is thought to be at least partly responsible for the presence of non-fermentable branched dextrins (α-limit dextrins) in barley malt by inhibiting the starch debranching enzyme limit dextrinase (LD). By producing the low abundant LDI in a heterologous host organism, the aim was to characterize the interaction between LD and LDI and the influence of Trx h on the interaction. Trx is suggested to reduce LDI and thereby indirectly increasing the activity of LD during malting. LDI cDNA was cloned from developing barley seeds and several vector constructs were made for heterologous expression; however, LDI was only successfully produced as a fusion protein with *E. coli* Trx h attached to the N-terminus. The fusion protein showed 16 fold lower activity than LDI purified from barley seeds. By removing the Trx tag by the endoprotease, enteropeptidase, the inhibitory activity further decreased 3-10 fold. This activity decrease was probably caused by unspecific cleavage by enteropeptidase in the LDI sequence due to non-native folding.

Dansk resumé

Frø fra cerealer er vitale komponenter i vores kost, og derfor er det vigtigt at forstå biologien bag brydning af dvaletilstanden og start på spiringsprocessen. Disse processer er langt fra fuldt forstået på trods af omfattende studier, og der er endnu ikke identificeret specifikke markører på protein eller DNA niveau. Spiring af bygfrø er desuden interessant for ølbrygning, da denne proces stort set svarer til støbningsprocessen, som indleder industriel maltning.

I det nærværende projekt har vi brugt proteomanalyse til at forstå de tidlige ændringer i mønstret af bygkerners vandopløselige proteiner efter vandoptagelse og de efterfølgende processer, der sker indtil 72 timer efter vandoptagelsens start. 2D gel elektroforese af de vandopløselige proteiner fra dissekerede væv under spiring (0-24 timer) og rodforlængelse (24-72 timer) beskriver de rum- og tidsmæssige variationer i proteinmønstret. Frø fra 8 tidspunkter (0, 4, 12, 24, 36, 52, 60, 72 timer efter vandoptagelse) blev dissekeret og protein ekstraktioner i lille skala gjorde det muligt at fremstille 2D geler med god opløsning. 2D geler fra forskellige tidspunkter og forskellige væv blev sammenlignet, og pletter med varierende intensitet blev fulgt og identificeret ved hjælp af in-gel fordøjelse, massespektrometri og databasesøgninger. Otte-og-fyrre proteiner i 79 pletter blev identificeret og fulgt gennem spiringsprocessen. Fordelingen af disse proteiner varierede mellem embryo (kimen), aleuronlaget og endosperm (frøhviden), hvilket understreger de individuelle vævsfunktioner. De fleste og de første ændringer skete i embryo, som sammen med aleuronlag er levende væv, der genoptager metabolisk aktivitet efter vandoptagelse. Derimod er endospermen et dødt forrådslager, hvor hydrolytiske enzymer, som produceres i aleuronlaget, er aktive for at frigøre næring til vækst af embryo.

β-Type proteasome subunit og et fragment af ”heat shock protein 70” blev identificeret som de første proteiner, der viser sig allerede 4 timer efter vandoptagelse i embryo sammen med en ændring i pletmønstret for udtørringsstress-relaterede proteiner så som ”late embryonic abundant (LEA) proteiner” og ”abscisin syre-induceret proteiner”. Efter 12 timer forsvinder velkendte udtørringsstress-relaterede proteiner og andre proteiner (”putative embryonic protein” og ”abscisin syre-induceret protein”), som, vi formoder, er involverede i udtørring. Andre proteiner, blandt andet redoxrelaterede proteiner, der er involverede i beskyttelse mod vandstress og reaktive oxygenforbindelser, ændrede mængde ved slutningen af spiringsprocessen og begyndelse af rodforlængelsen. Disse proteiner viste forskellig fordeling i vævene og de fleste forblev konstant eller faldt i mængde ved slutningen af spiring og ved begyndelse af rodforlængelse, undtagen ascorbate peroxidase (APX), som kun var til stede i det spirende embryo efter 24 timer. Andre proteiner, som er involverede i osmotisk og saltstress, nedbrydning af lagerstoffer, foldning, og almindelig ”housekeeping” blev identificeret og fulgt gennem de 72 timer efter vandoptagelse.

APX og de andre enzymer, der er involverede i ascorbate-glutathion cyklus (d.v.s. dehydroascorbate reduktase, monodehydroascorbate reduktase og glutathione redutase) har sandsynligvis en vigtig funktion i spiringen og rodforlængelsen, da det store energikrav efter vandoptagelse genererer reaktive oxygenforbindelser, særligt i embryo. Aktivitetsmålinger af disse enzymer i embryo protein ekstrakter blev foretaget og aktivitetsprofilerne blev sammenlignet med de tilsvarende 2D gel mønstre. Dette gav både samstemmende og afvigende enzymaktiviteter og 2D gel profiler under rodforlængelsen. APX aktivitet blev sporet i zymogrammer og gen ekspressionsanalyse indikerede, at mindst to APX isoformer er til stede i

embryoekstrakter. mRNA for begge for isofomer var til stede i det tørre modne frø, hvorimod stigende aktivitet blev observeret fra 36 timer, hvilket støtter at ascorbat-glutathion cyklus ikke fungerer i det udtørrede frø, men at mRNA er til stede og parat til translation. Både APX og DHAR er foreslåede målenzymer for thioredoxin h redox regulation. Dette blev diskuteret baseret på de opnåede resultater, selvom det ikke var muligt at detektere en ændring i DHAR aktivitet ved tilsættelse af reduceret rekombinant Trx h til embryoekstraktet. Post-translationelle modifikationer af APX blev yderligere studeret ved hjælp af massespektrometri baseret på 2D gel mønstret af APX i spirende byg embryoer, som indikerede tilstedeværelse af adskillige APX former med forskellige pI værdier.

Byg limit dextrinase hæmmeren (LDI) er tænkt at være delvist ansvarlig for tilstedeværelsen af ufermenterede forgrenede dextriner (α-grænsedextriner) i bygmalt ved at hæmme stivelsesafgreningsenzymet limit dextrinase (LD). LDI er til stede i små mængder i bygfrøet, og ved at producere den i en heterolog værts organisme var formålet at karakterisere vekselvirkningen mellem LD og LDI, og hvordan denne påvirkes af Trx h. Trx h reducerer muligvis LDI og øger derved aktiviteten af LD under maltning. LDI cDNA'et blev klonet fra udviklende bygfrø, og adskillige ekspressionsvektorer blev konstrueret for heterolog ekspression, men LDI blev kun produceret som et fusionsprotein med *E. coli* Trx påsat N-terminalen. Fusionsproteinet havde aktivitet, der var 16 gange lavere end vildtype LDI oprenset fra byg. Ved at fjerne Trx delen med enteropeptidase, faldt hæmningsaktiviteten yderligere 3-10 gange. Dette fald i aktivitet efter kløvning skyldtes sandsynligvis forkert foldning af LDI under ekspressionen, som kunne bevirke uspecifik kløvning med enteropeptidase.

Table of Contents

Abbreviations

2D	Two dimensional
2DE	Two dimensional gel electrophoresis
1DE	One dimensional gel electrophoresis
ABA	Abscisic acid
AL	Aleurone layer
AMY1	α-Amylase isozyme 1
AMY2	α-Amylase isozyme 2
APX	Ascorbate peroxidase
AsA	Ascorbic acid
BASI	Barley α-amylase/subtilisin inhibitor
BLAST	Basic local alignment search tool
bLDI	Limit dextrinase inhibitor purified from barley seeds
BSA	Bovine serum albumin
CAPS	3-[cyclohexylamino]-1-propanesulfonic acid
cCBB	Colloidal coomassie brilliant blue
CHC	α-cyano-4-hydroxy cinnamic acid
cDNA	Complementary deoxy nucleic acid
CM-protein	Chloroform/methanol protein
cv	Cultivar
DHA	Dehydroascorbic acid
DHAR	Dehydroascorbate reductase
DIGE	Differential in-gel electrophoresis
DNA	Deoxy nucleic acid
DTT	D/L-Dithiothreitol
ECS	Enteropeptidase cleavage site
E. coli	*Escherichia coli*
EDTA	Ethylene-dinitrilo-tetra-acetic acid
EM	Embryo
EN	Endosperm
EST	Expressed sequence transcripts
GA	Gibberellic acid
Gdm	Guanidinium
GR	Glutathione reductase
GSH	Glutahione, reduced
GSSG	Glutathione, oxidized
GST	Glutathione *S*-transferase
HEPES	N-(2-morpholine)ethanesulfonic acid
h	Hours
HSP	Heat shock protein
IAA	Iodoacetamide
ICAT	Isotope-Coded Affinity Tag
Id	Identification
IEF	Isoelectric focussing
IPG	Immobilised pH gradient
IPTG	Isopropyl-β-thiogalactopyranoside
JIP	Jasmonate induced protein
kDa	kilo Dalton
LC	Liquid chromatography
LD	Limit dextrinase
LDI	Limit dextrinase inhibitor
LEA protein	Late embryonic abundant protein
L. lactis	*Lactococcus lactis*

Mw	Molecular weight
m/z	Mass to charge ratio
MALDI	Matrix assisted laser desorption/ionization
MDHAR	Monodehydroascorbate reductase
mRNA	messenger RNA
MS	Mass spectrometry
MS/MS	Tandem mass spectrometry
MutPIT	Multidimensional protein identification technology
NCBInr	National Center for Biotechnology Information non-redundant sequence database
NADH	Nicotinamide adenine dinucleotide
NADPH	Nicotineamide adenine dinucleotide phosphate
PCR	Polymerase chain reaction
PDI	Protein disulfide isomerase
pI	Isoelectric point
PI	Post imbibition
PMF	Peptide mass fingerprinting
PPA	Porcine pancreatic α-amylase
P. pastoris	*Pichia pastoris*
RBI	Ragi bifunctional inhibitor
RNA	Ribonucleic acid
ROS	Reactive oxygen species
SOD	Superoxide dismutase
Rpm	Revolutions per minute
sbCBB	Silver blue coomassie brilliant blue
SDS	Sodium dodecyl sulfate
SDS-PAGE	Sodium dodecyl sulfate polyacryl amide gel electrophoresis
sHSP	Small heat shock protein
SPR	Suface plasmon resonance
TC-sequence	Tentative consensus sequence
TIGR	The Institute of Genome Research
TMA	*Tenebrio molitor* α-amylase
TOF	Time of flight
TPI	Triose phosphate isomerase
Tris-HCL	Tris(hydroxymethyl)aminomethane hydrochloride
Trx h1	Thioredoxin h1
Trx h2	Thioredoxin h2

Chapter 1 - Introduction

1.1 The barley seed

1.1.1 Physiology and structure

Barley belongs to the *Gramineae*, the grass family, which contains all cereals including wheat, rice, rye, maize, oats, millet, and sorghum. The structure of the dry mature barley seed is well characterized (shown schematically in Figure 1.1). The barley seed belongs to the class of orthodox seeds that can be dried and stored for a long time without loosing or reducing the germination efficiency.

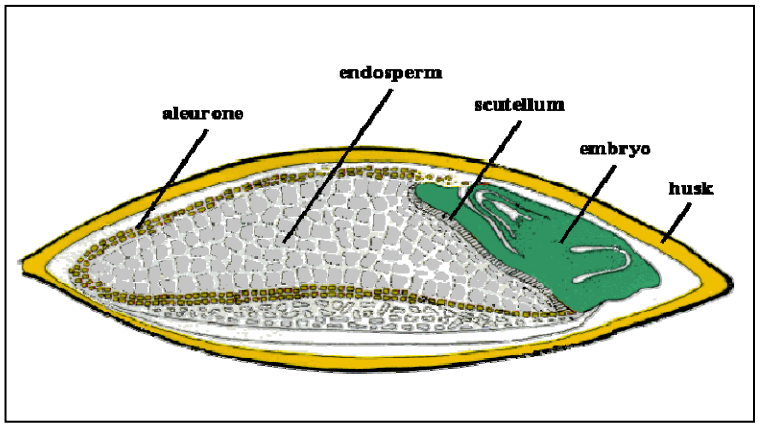

Figure 1.1. A cross section through the crease of the dry mature seed. The seed consists of the embryo, which develops into the new plant. The endosperm contains most of the starch and storage proteins and is separated from the embryo by the scutellum. The endosperm is surrounded by the aleurone layer, which synthesizes and releases hydrolytic enzymes into the endosperm upon germination. An outer layer of cellulose called the husk (seed coat) protects the seed towards the surroundings (From www.crc.dk).

The dry mature barley seed consists of several differentiated tissues that fulfill different functions during seed germination and seedling growth. The embryo comprises 3-4% of the dry weight of the seed. It is a living tissue and contains all necessary components for growth of a new plant when supported by nutrients from the endosperm. The vast majority of the seed is made up of the starchy endosperm, which is dead tissue that protects and contains nutrients for the embryo, i.e. mainly starch (amylose and amylopectin) and storage proteins, but also lipids and other nutrients. The endosperm cell walls consist of β-glucan, arabinoxylan and cellulose and a small amount of protein, glucomannan and phenolic acids (Briggs, 1978; Fincher and Stone, 1986). The aleurone layer is only 2-4 cell layers thick and surrounds the starchy endosperm. It is a non-dividing highly specialized tissue that produces hydrolytic enzymes in response to gibberellic acid (GA) during radicle elongation. The aleurone cells do not contain starch but are rich in other reserve substances such as lipids and proteins and undergo programmed cell death at approximately 4-6 days after water up-take, referred to as imbibition (Fath et al., 2000; Bethke et al., 1999). The scutellum is a single cell layer thick tissue located between the embryo and the endosperm. It carries out some of the same functions as the aleurone

layer in addition to transport of nutrients to the embryo. The seed coat (the same as husk on Figure 1.1) protects the seed from the surroundings. It is dead tissue and at the end of germination the radicle will break through the seed coat.

1.1.2 Germination of barley

By definition germination comprises those events that commence with the uptake of water by the quiescent dry seed and terminate with the elongation of the embryonic axis (Bewley and Black, 1994). The time frame of this process is approximately 24-36 h depending on the temperature, and it is followed by the radicle elongation and growth of the new plant.

Uptake of water is triphasic: an initial phase (imbibition) is followed by a plateau phase (increase in metabolic activity). In the third phase an increase in water up-take occurs after the germination is completed, as the embryonic axis elongates (initiation of growth). Dormant seeds for unknown reasons do not enter the third phase (Bewley and Black, 1994). The phytohormone abscisic asid (ABA) plays a central role in embryo maturation, both to suppress precocious germination and to induce the expression of maturation-associated genes for storage product accumulation and acquisition of desiccation tolerance. Mutants of Arabidopsis deficient in ABA synthesis have impaired seed maturation and dormancy (Koornneef and Karssen 1994).

The germination seems to be programmed during the massive water loss occurring late in maturation, where a switch in cellular activities from an exclusively developmental program to an exclusively germination/growth program takes place (Kermode, 1990; 1995). The cellular structures and enzymes necessary for the initial resumption of metabolic activity are generally assumed to be present within the dry seed, having survived, at least partially intact, the desiccation (Bewley and Black, 1994). Moreover, preserved mRNA is present in the dry seed (Bewley, 1997) and seems to be used for translation during germination since seeds do germinate in the presence of the transcriptional inhibitor, α-amanitin, however, strongly delayed (Rajjou et al., 2004). This suggests that regulators of the rate of seed germination are under transcriptional control. In contrast, seed germination was completely blocked by the translational inhibitor cycloheximide (Rajjou et al., 2004). Together these results enlighten the importance of protein synthesis from the pool of stored mRNAs for radicle protrusion.

Resumption of respiratory activity can be detected within minutes post imbibition (PI) (Bewley, 1997). Newly synthesized ribosomes appear in the seed within hours (Dommes and Van de Walle, 1990). Proteins involved in normal cellular metabolism are synthesized and no specific marker exclusive to germination has been found. The high levels of GA present in developing grains decrease during maturation so that the mature dry grain normally contains very low levels of GA (Jacobsen et al., 1995). Upon germination GA is synthesized in the embryo secreted as a gradient to the scutellem and aleurone layer, where it induces production of hydrolytic enzymes, α-amylase being the most abundant (Zentella et al., 2002). The hydrolytic enzymes act in the endosperm to release nutrients for embryo growth (Figure 1.2). The scutellum seems to account for 5-10% of the total α-amylase, which is produced in 1-2 days PI. In the aleurone layer, α-amylase production peaks after 3-4 days PI (Jacobsen et al., 1995).

GA has been widely associated with seed germination and this has been confirmed by the identification of GA-deficient mutants of Arabidopsis and tomato, seeds of which will not germinate unless exogeneously supplied with GAs (Koornneff and van der Veen, 1980; Groot and Karssen, 1987). Furthermore, the fact that inhibitors of GA biosynthesis prevent germination (Karssen et al., 1989; Nambara et al., 1991; Jacobsen and Olszewski, 1993) indicated the requirement for *de novo* synthesis of GAs in germination. However, the precise role of GA in

germination is not known. At the protein level GA-deficient seeds seemed to complete germination and only one protein, cytoskeleton component α-2,4 tubulin, appeared to depend on the GA action (Gallardo et al., 2002). Fewer than 60 genes respond specifically to GA in rice aleurone cells during germination as revealed in a comprehensive cDNA microarray study (Bethke et al., 2006). A role of GA in germination could be softening of the seed coat for penetration of the radicle as reported for Arabidopsis (Rajjou et al., 2004).

Starch hydrolysis in the endosperm proceeds through the action of four different enzymes, collectively known as diastase. Low and high pI α-amylase and β-amylase act in synergy on the α-1,4-glycosidic linkages yielding glucose, maltose, and limit dextrin. Limit dextrinase hydrolyses the α-1,6-glycosidic bonds and α-glucosidase catalize the last step in starch degradation of maltose into glucose units (Bewley and Black, 1994). α-Amylase and α-glucosidase are synthesized in the aleurone layer during germination. β-Amylase accumulates in the starchy endosperm during development and maturity and exists in the endosperm of the dry grain mostly in an inactive form that is disulfide bound to a component of protein bodies (Hejgaard, 1978). Release of GA induces synthesis of cysteine endopeptidases that cleave β-amylase into an active form. Limit dextrinase is synthesized in the aleurone layer during germination and radicle elongation, but some is already present in the endosperm during maturation (Burton et al., 1999).

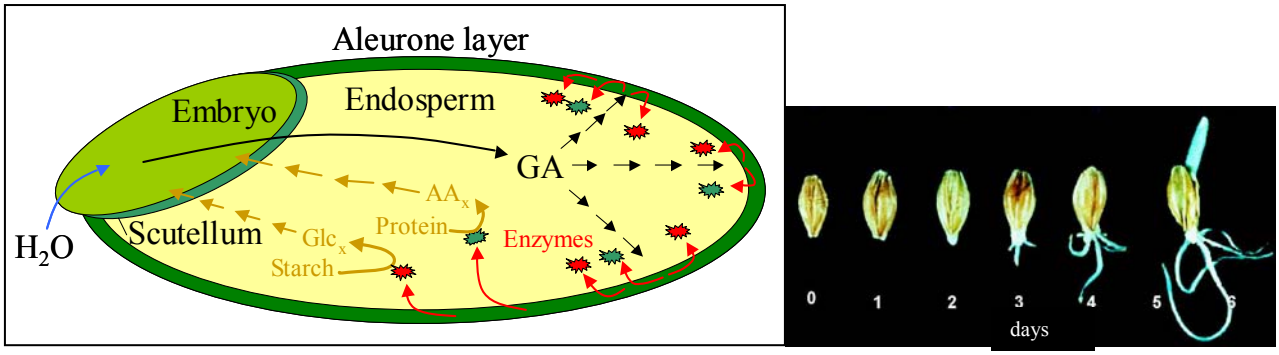

Fig. 1.2. Summary of events taking place during germination and radicle elongation. Left: Water up-take through the embryo elicits a signal of gibberellic acid (GA) from the embryo into the endosperm. GA diffuse to the aleurone layer initiating activation and/or *de novo* synthesis of hydrolytic enzymes, which are released to the starchy endosperm. One group of enzymes catalyses the degradation of starch to maltose, glucose and oligosaccharides (Glc_x), while others degrade storage proteins to peptides and free amino acids (AA_x). The released peptides and oligosaccharides diffuse to the embryo, where they are taken up and used as building blocks or as energy source. Rigth: The barley seed during germination and radicle elongation.

Removal of cell walls of starchy endosperm cells is a crucial early event that is necessary for the starch and protein degrading enzymes to reach their substrates. Cell wall degrading enzymes include (1,3-1,4)-β-glucanase, (1,3)-β-glucanase, β-glucosidase, cellulase and enzymes involved in degradation of arabinoxylans (Bewley and Black, 1994).

1.1.3 Stress conditions during germination

Development of orthodox seeds (including barley) culminates in the loss of water that is either coincident with or subsequent to the acquisition of desiccation tolerance by the embryo (Figure 1.3). This induces proteins protecting the seed from permanent damage. Some of these proteins also play a role during germination and are often termed desiccation stress related proteins.

However, since it is a normal physiological condition for orthodox seeds, it is more correct to use the term desiccation tolerance. This is described in section 1.1.3.1. During germination and radicle elongation the barley seed is exposed to changes in the external environment and is able to defend itself against abiotic stresses (drought, high salinity, low and high temperatures, high light, mechanic stress) and biotic stresses like pathogen attack. Stress generates reactive oxygen species (ROS) but a tight redox control system in the seed can cope with this and prevent cellular damage. This will be described in section 1.1.3.2.

1.1.3.1 Desiccation tolerance

Desiccation tolerance refers to an organism's ability to remain organized with the stresses of almost complete water loss and of rehydration (Hoekstra and Golovina, 2003). The rate of metabolism drops significantly upon drying and ABA is important for this process since slow drying without ABA is generally insufficient for somatic embryos to acquire tolerance. The ABA-inducible late embryonic abundant proteins (LEA proteins) and small heat shock protein (sHSPs) are suggested to play an important role in desiccation tolerance. The accumulation of these proteins to high concentrations coincides with the acquisition of desiccation tolerance. LEA proteins have a high number of polar residues that are suggested to form structures that can protect other proteins and cell membranes from disruption or damage in the near-dry state (Ingram and Bartels, 1996). sHSP's might act as molecular chaperones during seed dehydration and the first few days of rehydration. Generally HSPs are able to maintain partner proteins in a folded or un-folded state, to minimize the aggregation of non-native proteins, or to target non-native or aggregated protein for degradation and removal from the cell (Hoekstra and Golovina, 2003).

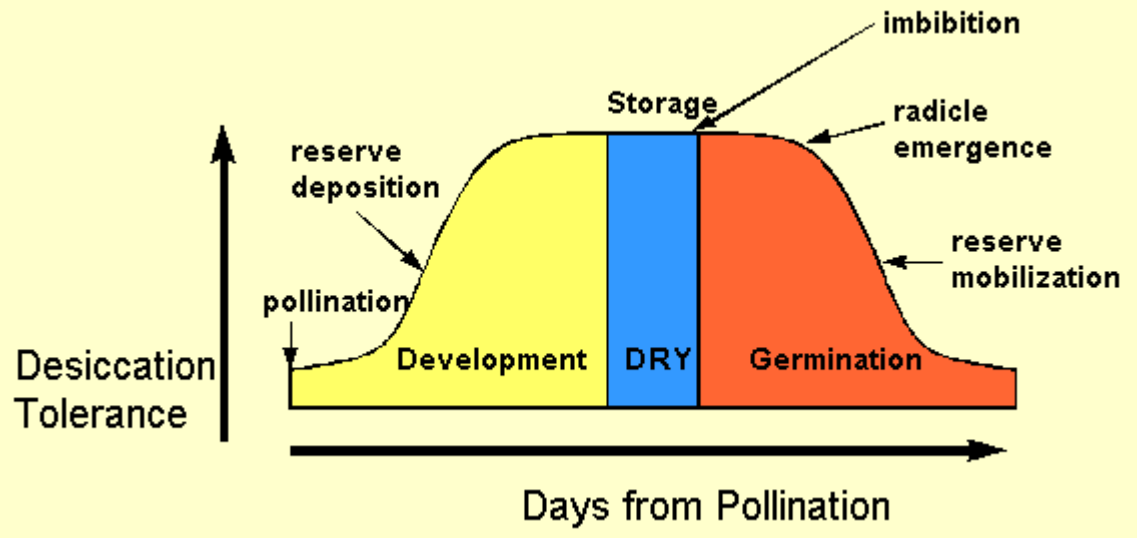

Figure 1.3. The acquisition and loss of desiccation tolerance in an orthodox seed showing the major development stages. The figure is from www.agronomy.psu.edu/courses.

1.1.3.2 Redox control

In plants reactive oxygen species (ROS; hydrogen peroxide, superoxide and hydroxide radicals) are continuously produced as by-products of various metabolic pathways localized in the different cellular compartments. They are usually considered as toxic molecules that lead to cell injury and disturbances in seed development or germination processes. However, ROS are also involved in cellular signaling in a wide range of responses to various stimuli (Bailly, 2004; Foyer

and Noctor, 2005). The dual role of ROS relies on tight control of ROS by the antioxidant machinery, which involves detoxifying enzymes and antioxidant compounds.

H_2O_2 is the most studied of the ROS and is involved in tolerance to abiotic stress (Prasad et al., 1994) cellular defense against pathogens (Levine et al., 1994), programmed cell death (Jabs, 1999; Amor et al., 2000; Fath et al., 2001), somatic embryogenesis (Cui et al., 1999) and response to wounding (Orozco-Cardenas et al., 2001), root gravitropism (Joo et al., 2001) and ABA-mediated stomatal closure (Pei et al., 2000; Zhang et al., 2001).

1.1.3.3 ROS scavenging including enzymes of ascorbate-glutatione cycle

Redox homeostasis is governed by the presence of large pools of antioxidants that absorb and buffer reductants and oxidants. These include ascorbate (AsA), glutathione (GSH) as well as tocopherol, flavonoids, alkaloids and carotenoids. Antioxidants continuously scavenge ROS and determine the lifetime and the specificity of the ROS signal. AsA is oxidized to form monodehydroascorbate (MDHA) which disproportionates to form dehydroascorbate (DHA), and GSH is oxidized to form oxidized glutathione (GSSG).

Table 1.1. Major antioxidative enzymes in plants and commonly used abbreviations

Superoxide dismutase	SOD
Ascorbate peroxidase	APX
Monodehydroascorbate reductase	MDHAR
Dehydroascorbate reductase	DHAR
Glutathione reductase	GR
Catalase	CAT
Glutathione peroxidase	GPX
Guaiacol-type peroxidases	-
Glutathione-*S*-transferase	GST
Peroxiredoxin	PRX
Thioredoxin	Trx
Glutaredoxin	GTX

Several enzymes, including the enzymes in the ascorbate-glutathione cycle (Figure 1.4), in the plant are involved in the protection of ROS. The major antioxidative enzymes are given in Table 1.1. Superoxide dismutase (SOD) catalyzes the reduction of O_2^- to H_2O_2 (Figure 1.4), which is a much less reactive compound. H_2O_2 is broken down to H_2O and molecular oxygen (O_2) by catalase and peroxidases. Catalase is only present in the peroxisomes whereas peroxidases are present throughout the cell. There are several types of peroxidases, which use different types of reductants (Table 1.1). Ascorbate peroxidase (APX) is present throughout plant systems and is found in different isoforms in different compartments (cytosol, stroma, thylakoid, mitchondria) along with the other enzymes in the ascorbate-glutathione cycle. APX catalyzes the first step in the ascorbate-glutathione cycle (Figure 1.4) and generates H_2O and O_2 with the oxidation of AsA to MDHA. Two molecules of MDHA can dispropoinate non-enzymatically and spontaneously generate DHA and AsA. The additional three enzymes in the ascorbate-glutathione cycle are involved in regeneration of AsA. Monodehydroascorbate reductase (MDHAR) and dehydroascorbate reductase (DHAR) reduce MDHA and DHA to AsA, respectively, and

glutatione reductase (GR) reduces GSSG to GSH which functions as an electron donor for DHAR. MDHAR and GR use NADPH as an electron donor. The relative importance of the DHAR and MDHAR pathways is not known, but the specific activity of MDHAR is 10 fold higher than that of DHAR in both mitochondria and chloroplasts of tomato as determined by activity assays using the purified organelles (Mittova et al., 2000). The various scavenging enzymes encoded by the ROS network (including the ascorbate-glutathione cycle and other enzymes listed in Table 1.1) can be found in almost every subcellular compartment.

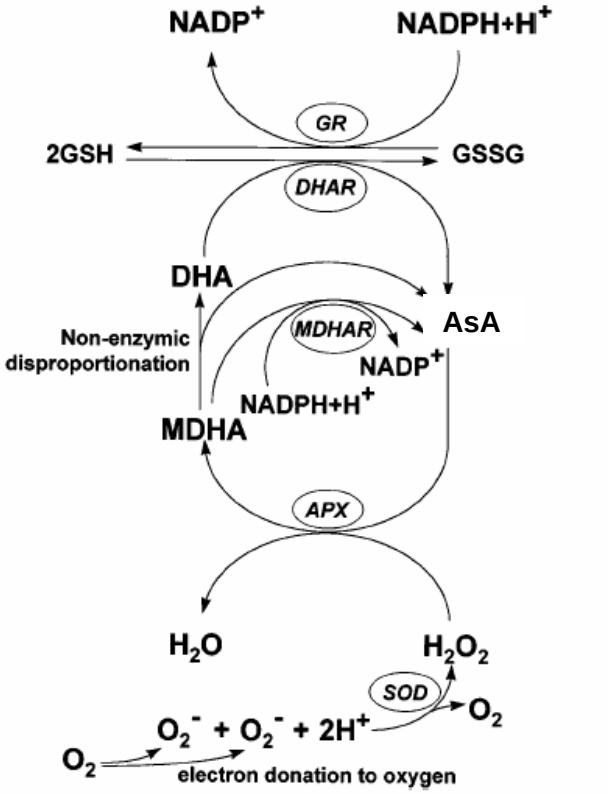

Figure 1.4. The ascorbate-glutathione cycle. Not all reactions are depicted stoichiometrically. Figure modified from Noctor and Foyer (1998).

The ascorbate-glutathione cycle has been studied during different physiological processes of the seed. During development of wheat and broad bean seeds the levels of AsA and DHA, MDHA and GSH increase but they decrease again during the desiccation phase and AsA disappears completely (Arrigoni et al., 1992; De Gara et al., 2003). Accordingly the enzyme activities involved in the ascorbate-glutathione cycle also decrease during desiccation. As shown in wheat and pine seeds the AsA content increases significantly and DHA increases slightly after 24 h PI (De Gara et al., 1997; Tommasi et al., 2001). This is in agreement with the fact that presence of the last precursor (galactono-γ-lactone) in the AsA biosynthesis increase during germination of wheat seeds (De Gara et al., 1997). The absence of APX in 2D gels of mature barley embryo extracts (Section 3.1.7) and absence of APX activity in the mature seeds of wheat and pine (Asada, 1997; Tommasi, 2001; De Gara, 2003; Section 3.1) indicate that the ascorbate-glutathione cycle does not function during desiccation (Bailly, 2004). DHAR activity decreases and MDHAR and GR activities increase slightly PI. The residual levels of DHAR and MDHAR in the dry seed may be necessary for the immediate generation of AsA upon imbibition as new AsA biosynthesis starts after 10-20 h of germination (De Gara et al., 1997).

1.1.3.4 Oxidative stress

The production of ROS is frequently considered to be a deleterious event since oxidant accumulation invariably leads to oxidative stress damage (Creissen et al., 1999). Abiotic and biotic stress conditions may give rise to excessive concentrations of ROS and result in oxidative damage of protein, DNA, and lipids.

Many studies have correlated increases in one or more of the antioxidant enzymes with either stress conditions or decreased stress resistance. Abiotic stress conditions that have been studied include low temperature, high salinity, herbicide challenges, drought, wounding, ultraviolet irradiation, and ozone exposure (Noctor and Foyer, 1998 and refs therein). Generally oxidative defense enzymes are elevated during these stress conditions but sometimes this elevated level is minor and moreover these enzymes exist in several isoforms that have different characteristics. Therefore it is a challenge to achieve an overview of the oxidative stress defense system in the different cell compartments and how the enzymes co-operate. A number of mRNA microarrays studies in Arabidopsis regarding changes in gene expression as a consequence of different stress conditions (heat, drought, salt, cold, and high light) or lines deficient in SOD, APX or CAT have been carried out and reviewed (Mittler et al., 2004). Together these data indicate that the network of genes involved in oxidative stress shows redundancy as deficiency in APX1 results in enhanced gene expression of type 2 Peroxiredoxin and ferritin, and deficiency in CAT2 results in enhanced gene expression of a cobber-binding protein, glutaredoxin and thioredoxin. Also flexibility of the gene network was observed as the ROS network responds in a highly specific manner to each of the studied stresses.

1.1.4 The malting process

The interest in barley germination and seedling growth has its origin from the large volumes of malted (essentially germinated) barley used by the brewing industry.

Malting is basically germination of non-dormant seeds carried out under controlled environmental conditions in order to maximize endosperm degradation and to minimize rootlet and radicle growth. Furthermore, conditions are selected to maximize the fraction of seeds that germinate and to achieve as uniform germination as possible. Unmodified parts of the endosperm result in extraction losses, and seedlings that develop too far may cause filtration problems in the brewing process. The first part of the malting, termed steeping, involves mixing of the dry seeds with excess water for imbibition. This is repeated three times with air-rest periods within the first 48 h to decrease water sensitivity. The result of steeping is an increase of the water content of the seeds from approximately 14% to 45%. After steeping, the rehydrated seeds are transferred to a germination tank, where the seeds continue the germination and seedling growth. When the endosperm structure is fully degraded (typically after 5-6 days) development is stopped by drying the seeds in hot air, resulting in a storage stable product. The effect of the aeration during malting on germination efficiency was studied by measuring the activity of alcohol dehydrogenase (Wilhelmson et al., 2006). Alcohol dehydrogenase is expressed in barley aleurone layer at oxygen deficiency and can therefore be regarded as an indicator of the efficiency of the aeration in malting. Oxygen deficiency during the first steeping process had no effect on the germination or malt quality and therefore it is likely that air introduced into the steeping step does not reach the embryo because of the seed coat. The importance of aeration increases as the malting process proceeds (Wilhelmson et al., 2006).

During the seedling growth phase of malting the speed of endosperm modification can be controlled by temperature, watering and by the possible addition of GA to the spraying water.

In order to determine malt quality several parameters are verified including protein content, β-glucan content, β-amylase activity, predicted diastatic power, germination index and germination percentage. Protein content refers to the amount of storage protein. The diastatic power represents the combined activity of the four starch-degrading enzymes, α-amylase, β-amylase, limit dextrinase and α-glucosidase. Besides storage proteins and hydrolytic enzymes, enzyme inhibitors can play an important role in the malt quality. These inhibitors mainly include CM proteins (α-amylase and protease inhibitors that are extractable from flour in chloroform/methanol), but also the endogenous α-amylase/subtilisin inhibitor (BASI), which is a well characterised strong proteinaceous inhibitor of the major α-amylase isoform (AMY2) in barley (Mundy et al. 1983; Abe et al., 1993; Bønsager et al., 2005) and limit dextrinase inhibitor (LDI). The physiological roles of BASI and LDI are not known, but BASI is abundant in the dry seed (Bak-Jensen et al., 2004) and is thus present prior to the production of large amounts of active starch degrading enzymes. BASI may be implicated in regulation of the starch degrading activity by inhibiting AMY2 in premature sprouting seeds (Mundy et al., 1983). The presence of LDI in germinated barley seeds may cause the presence of non-fermentable branched dextrins in malt by inhibition of a fraction of the LD (MacGregor et al., 1994; Walker et al., 2000; Bringhurst et al., 2001).

The cytosolic thioredoxin h (Trx h) is thought to be an important protein during seed germination. It is a small disulfide oxidoreductase that reduces the disulfide bonds in storage proteins and small cysteine-rich protein (including enzyme inhibitors) rendering them more soluble and susceptible to the proteolytic breakdown that takes place in the endosperm during radicle elongation (Kobrehel et al., 2002; Wong et al., 1995; Lazano et al., 1996). Many Trx h targets proteins have been suggested using two different proteomic approaches in barley, wheat and Arabidopsis. In the first case, affinity column using monocystenic mutants of either Trx h have been used, allowing the formation of stable mixed disulfides between the potential targets and the mutant. The trapped targets were then eluted with DTT and characterized in Arabidopsis (Yamazaki et al., 2004; Rouhier et al., 2005; Merchand et al., 2006). In the second case, targets were detected after direct reduction of the targets followed by labeling of free thiols in barley (Yano et al., 2001, 2005; Maeda et al., 2004, 2005), in wheat (Wong et al., 2003), and in Arabidopsis (Merchand et al., 2004, 2006). Further analysis need to confirm the interactions with Trx h as the biological role of many of these remains unanswered. Both BASI and LDI are suggested targets of Trx h and the structure of the Trx h/BASI complex has recently been solved (Maeda et al., 2006). Transgenic barley overexpressing Trx h showed enhanced LD activity (Cho et al., 1999; Stahl et al., 2004). This could indicate that LDI is reduced by Trx h followed by proteolysis, thus counteracting normal level of LDI inhibition of LD (Section 1.3).

1.1.5 Thioredoxin h (Trx h) interaction with redox-related enzymes

Trx h has been suggested to be involved in cellular protection against oxidative stress, in particular during desiccation and germination, where Trx h expression pattern and localization correlate with the presence of superoxide radicals (Serrato and Cejudo, 2003). This was supported by the identification of peroxiredoxin as a Trx h target by using a catalytic inactive Trx mutant for fishing targets *in vivo* in *Saccharomyces cerevisiae* (Verdoucq et al. 1999), in Arabidopsis (Broin et al., 2002), and in *Populus trichocarpa* (Rouhier et al., 2001). Other redox related proteins: peroxidase, glutathione *S*-transferase, APX and DHAR are suggested to be Trx h targets (Wong et al., 2003; Marchand et al., 2004; Yamazaki et al., 2004) and Trx h may facilitate redox control via regulation of these enzymes.

1.1.5.1 Trx h interaction with ascorbate peroxidase (APX)

The possible Trx h-dependent inactivation of APX has been studied using recombinant proteins (Gelhaye et al., 2006). This showed that the Trx h system reduced APX activity by 50% after 40 min incubation, but the same effect was seen when DTT and GSH was added to APX during catalysis (Gelhaye et al., 2006). Cytosolic APX's from barley and other plants are highly conserved and, according to the crystal structure of APX from soybean and pea (Patterson and Poulos, 1995; Sharp et al., 2003), the disulfide bonds in barley APX1 are unlikely to be accessible to reduction by Trx h. However, APX contains a conserved Cys32 of which mutation (Cys32Ser) caused 70% drop in activity towards AsA, while full activity towards guaiacol was retained (Lad et al., 2002). Thus Cys32 is located in the vicinity of the substrate binding site, as also seen in the crystal structure, and may be a target for oxidation. ROS can mediate redox regulation by reversible oxidation of essential cysteine residues (Jones et al., 2004), and this type of regulation may occur during radicle elongation, where ROS continuously are formed.

1.1.5.2 Trx h interaction with dehydroascorbate reductase (DHAR)

Identification of DHAR as a Trx h target has recently (Hägglund et al., in prep) been corroborated by a quantitative redox proteomics approach based on the use of isotope coded affinity tags (ICAT). In this approach a protein extract from 48 h germinated barley embryo was divided in two tubes, incubated in the presence and absence of barley Trx h, respectively. Cysteines reduced by Trx h were alkylated by iodoacetamide, followed by dialysis to remove excess iodoacetamide. Then proteins were denatured, remaining non-alkylated cysteines were fully reduced and labeled with iodoacetamide-based ICAT reagents containing a linker with 9 isotopically coded carbon atoms (the Trx h-treated sample was labelled with the "light" version ($9 \times {}^{12}C$), the control sample was labelled with the "heavy" version ($9 \times {}^{13}C$). The proteins were digested with trypsin and ICAT labeled peptides were purified on an avidin affinity column. Peptides were separated on a nanoLC column and detected by mass spectrometry (MS). With the exception of mass difference, the ICAT reagents are chemically equivalent and will co-elute and appear as paired signals with a mass difference 9 Da. Trx h target peptides should have a ratio of "heavy"/"light" ICAT higher than one. The peptide ${}_{8}AAVGHPDTLGDCPFSQR_{24}$ from DHAR displayed one of the highest "heavy"/"light" ratios and was thus concluded to be preferentially reduced by Trx h.

It may be speculated that Trx h replaces GSH as an electron donor during catalysis by DHAR. Based on the proposed DHAR catalytic mechanism (Dixon et al, 2002), Trx h may reduce the mixed disulfide bond between Cys19 (located in the active site) of DHAR and GSH yielding electrons for reduction of DHA. Trx h has previously been shown to reduce GSH-mixed disulfide bonds (Jung and Thomas, 1996); however, this is normally the target of glutaredoxin (Ghezzi, 2005). It is also possible that DHAR has a disulfide bond between the two cysteines in the enzyme (Cys5 and Cys19) that undergoes reduction prior to catalysis.

1.2 Plant proteomics

A proteome is defined as "the complete protein complement expressed by a cell at a specific time including the sets of all protein isoforms and protein modifications". Proteomics is defined as "the systematic analysis of the protein population in a tissue, cell, or subcellular compartment". The different cell types within a multicellular organism will have different proteomes whereas the genome is constant. The proteome will vary with respect to the physiological state of the cell, changes in the surrounding environment, stress, heath and disease. Further variation between a gene and its corresponding protein includes splicing and post-translational modifications. There are two basic categories of proteomic studies: the first one involves protein profiling of biological material with the aim of separating, sequencing and cataloging as many proteins as possible. This includes subcellular proteomes. The second is comparative proteomics where the objective is to characterize differences between different protein populations.

Proteomes are complex compared to the genome (Figure 1.5). Thus in order to give a global integrated view on changes in protein composition in large scale, methods for proteome analysis have to be able to resolve thousands of proteins in a single experiment.

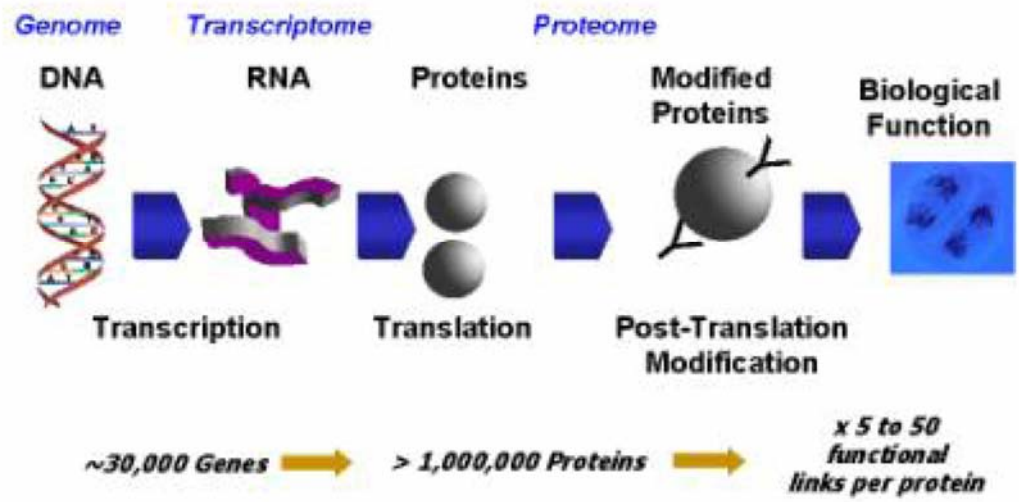

Fig. 1.5. The interrelationship between genomics, transcriptomics and proteomics. Genomics encompasses the genome (denoting the entire DNA sequence of an organism), which is constant for all cell types within the same organism. This is in contrast to the transcriptome and proteome, which are different for the various cell types within the same organism, and furthermore also changes with time. The numbers are approximate and give a general idea of the distinct complexity of genomes, transcriptomes and proteomes.

Proteins are difficult to handle and present numerous challenges. They are physico-chemically highly heterogeneous and structurally complex. This complicates extraction, solubilization, handling, separation and identification. Plant materials are typically more problematic for proteome analysis than tissues from other organisms. Rigidity of cell walls, relatively low protein concentrations, proteases and various natural compounds severely interfere with downstream protein stability, separation and analysis. These compounds include cell wall, polysaccharides, lipids, phenolics and a broad array of secondary metabolites (Granier, 1988; Gegenheimer, 1990; Tsugita et al., 1996). Moreover, plants regularly possess a large number of related isogenes increasing the number of closely related protein forms. Despite these

difficulties, proteomics have now been widely applied in plant studies. A brief overview of proteome analysis of plant seeds will be presented in Section 1.2.3 as this is highly relevant for the present study.

1.2.1 The proteomics tools

When working with proteomics one needs large scale and high through-put methods in order to obtain a comprehensive quantitative picture of the proteome. Both gel-based and gel-free methods are used and both will be described below. Mass spectrometry (MS) has now become a widely available technique for protein identification and will be briefly described in Section 1.2.1.3. To enhance proteome resolution and coverage, it is often necessary to use several technologies that provide complementary results (Whitelegge, 2004).

1.2.1.1 2D gels based proteomics

The 2D gel electrophoresis technique was developed in the mid 1970's (O'Farrell, 1975) but the high expansion came with development of microanalytical techniques that are able to identify protein in the amounts available from 2D gels. These microanalytical techniques were first Edman sequencing (Aebersold et al., 1987; Matsudaira, 1987; Rosenfeld et al., 1992). More recently the expansion of proteomics has been driven by rapid advances in MS and commercialization of MS equipment, together with increasing EST and genomic sequence data. The MS technique is much more productive and sensitive than Edman degradation (Yates et al., 1993; Cottrell, 1994; James et al., 1994)

2D gel based proteomics is a relatively quantitative method for comparing two or more samples and up to 3000 spots can be resolved in a single 2D gel. In addition this method is ideal for identification of many post-translational modifications, because one can obtain high sequence coverage by MS of a protein from a spot on a gel.

Several image analysis software programs have been developed that are capable of multiple gel analysis (reviewed in Biron et al., 2006). However, it is often necessary with manual intervention to correct the step of detection of protein spots (i.e. deletion of false protein spots and correction of the shape of protein spots), as well as the pairing step of protein spots within replicates of gels and between series of gels.

Although 2DE is widely used in proteomic analysis, it has some limitations:

- It is not sufficient to compare the enormous diversity possible of cellular proteins despite the use of zoom, i.e. narrow pH range gels.
- The dynamic range of 2DE is at maximum 10^4 (Rabilloud, 2002) and therefore low abundant proteins e.g. transcription factors are not visible. This limitation can sometimes partly be overcome by enrichment or pre-fractionation.
- The chemical heterogeneity of a proteome of a simple organism exceeds the range of a 2D gel (Wasinger, 2000) in terms of molecular weight and pI, but worse is the problem with protein extraction as well as solubility during 2DE. Especially membrane proteins remain a major limitation in 2DE.
- Another limitation is the lack of quantitative determination of proteins between two samples. This can be overcome, however, by use of the 2D difference gel electrophoresis (2D DIGE) technique (Ünlü et al., 1997). Here each protein sample is labeled with a fluorescent dye with distinct excitation and emission properties. The labeled samples are mixed and separated in the same 2D gel whereby identical separation conditions are ensured for comparison of the samples. Identical proteins labeled with different dyes

have the same electrophoretic mobility independently of the used dye. The labeled protein can be visualized by SyproRuby fluorescent staining and a software package (DeCyder, GE Healthcare) is designed specifically to compare levels of protein from different samples in the gel and to guide spot picking for protein identification.

1.2.1.2 Gel-free proteomics approaches

Gel-free proteomics approaches have been developed and they overcome some of the limitations in 2DE. One method is the multi-dimensional protein identification technology (MudPIT; Link, et al., 1999), where total protein mixtures are digested with several endopeptidases and subjected to a multidimensional peptide chromatography separation prior to MS/MS (LC/LC MS/MS; LC: liquid chromatography). In this approach also insoluble protein (including membrane proteins) can be digested and analyzed for protein identification. MudPIT does not provide quantitative comparison of proteomes and is not suitable for analysis of post-translational modifications, but it gives an impressive overview of the proteome. A way to simplify the complex MS data often obtained from the MudPIT approach is to run a 1D SDS-PAGE of the proteins prior to proteolytic digest of individual bonds and MS/MS.

Another gel-free MS approach is the isotope coded affinity tags (ICAT; Gygi, 1999), which is used for quantitative comparison of proteomes. In this approach two samples are labeled with a heavy and a light mass tag, respectively, prior to mixing of the samples and tryptic digestion. The tags contain three functional units; biotin, which can bind an avidin affinity column, a linker, and iodoacetamide, which links the tag to cysteine residues. The two tags differ in mass by 8 Da. The labeled peptides are purified on an avidin affinity column prior to LC MS/MS. The peptides derived from the same protein but different samples thus differ by 8 Da, and the ratio between their peak areas enables relative quantification. The corresponding parent protein is identified by tandem MS sequencing.

1.2.1.3 Mass spectrometry

Mass spectrometry (MS) has become an indispensable technique in protein chemistry and is now suitable in use also for non-MS specialists. Sub-picomoles of quantities of peptides can be analyzed with a mass accuracy better than an error of 0.1 Da in 1000 Da. In the present work all protein identification are based on matrix assisted laser desorption/ionization-time of flight (MALDI-TOF) and MALDI-TOF/TOF MS and therefore this technique will receive attention. The general procedure used in the present study for protein identification is illustrated in Figure 1.6.

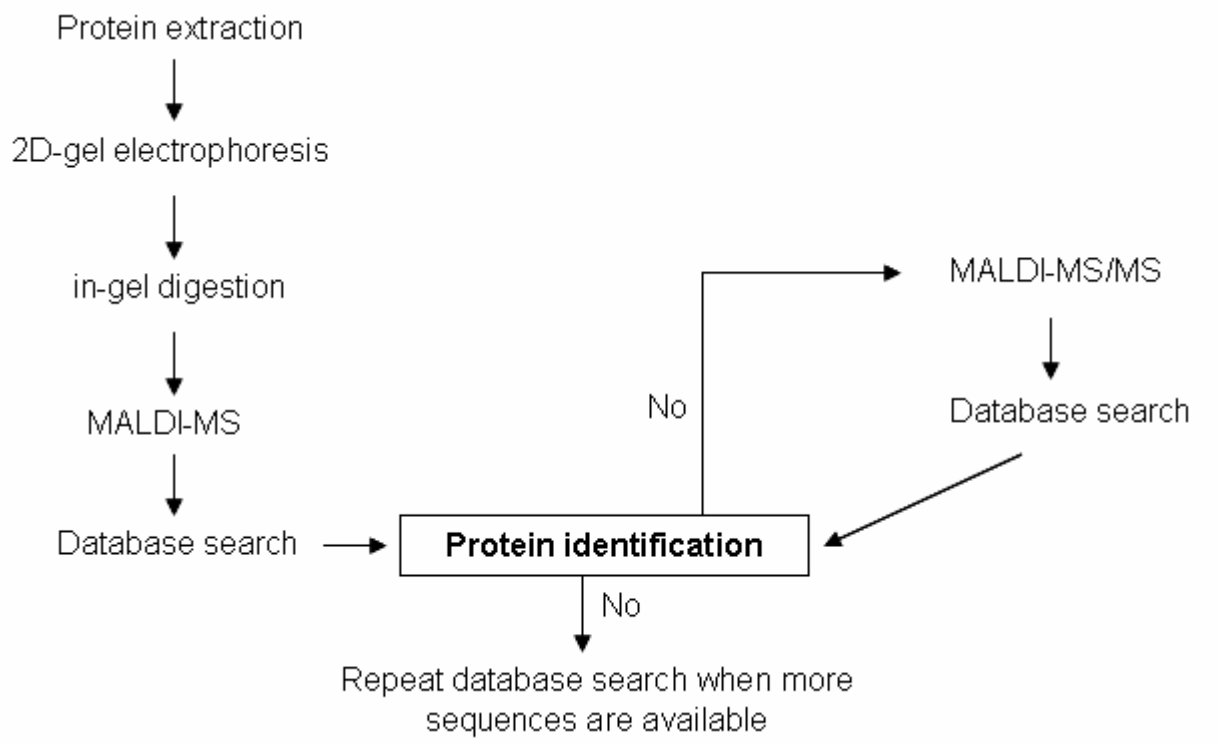

Figure 1.6. Overview of protein identification strategy of spots from 2D-gels by in-gel digestion, MS and database search (based on Shevchenko et al., 1996).

Preparation of samples for MS from a 2D gel includes spot picking, in-gel tryptic digestion and micro purification of peptides. The latter method purifies and concentrates the peptides using nano-scale reversed-phase columns before MS analysis to increase both sensitivity and signal-to-noise ratio (Gobom et al., 1999). The peptides are eluted directly onto the target in the matrix, where several benzoic acid and cinnamic acid derivatives are good candidates, especially α-cyano-4-hydroxycinnamic acid (CHC; Beavis et al., 1992) used in the present work. The sample preparation for MS is fairly labor-intensive, but it is possible to automate the spot-picking and tryptic digest with a robot. An alternative to the microcolumn purification is the anchor chip method (Sjødal et al., 2005), where a few microliters of the peptide mixture is applied to a hydrophilic surface area of the target. This method has shown to decrease ion suppression effects.

In MALDI-TOF MS the ions are generated by applying laser pulse UV light to a mixture of the peptides and the concentrated matrix solution, which are deposited and co-crystallized onto the target. The aromatic group of the matrix material absorbs the laser pulse UV light (desorption) and the acidic group donates a proton to the peptides (ionization) while the associated sublimation of the matrix brings the analyte ions into the gas phase (Karas et al., 1990). Then the analyte molecules are accelerated into a fieldless vacuum of the flight tube due to a high electrical field between the target and a grid, converting the potential energy of the molecules into kinetic energy. The velocity by which the individual molecules reach the detector can be converted into the according mass using calibration with molecules of known mass. MS can be recorded in positive and negative mode, which ionize positive and negative ions, respectively, depending on the settings of laser pulse potential.

MS generates a large amount of numerical data, therefore bioinformatics tools are essential to match these MS data to protein, EST, and genome sequence databases. The increase in database accessions has increased the risk for false-positive identifications. The most classical criterium used to confirm protein identifications is the MOWSE (molecular weight search) score. Reasons for failing to match MS data (especially for the MS/MS and LC-MS/MS) when searching a protein database are as follows: (i) the peptide sequence is not in databases; (ii) an unsuspected PTM; (iii) the peptide is a result of nonspecific cleavage; and (iv) the product-ion data is poor quality (Choudhary et al., 2001; Jamet, 2004). Careful validation of results from a database search is therefore important.

1.2.1.4 cDNA microarray

The non-proteomic approach by using cDNA microarray chips enables comparison of mRNA levels between two or more samples. This method is widely used also in plant studies as RNA is easy to extract compared to proteins. mRNA levels appear not to be a consistent indication of cognate protein abundance and several studies have revealed poor correlation between changes in the abundance of specific mRNAs and their corresponding proteins (Gygi et al., 1999; Tian et al., 2004). Proteome and microarray analysis are two large scale approaches that can provide complementing results for detailed studies of a process. This is addressed in Section 4.3.

1.2.2 Barley seed proteomics studies

The dry mature barley seed has a 10% protein content of the dry weight. The proteins can be divided into two major groups; storage proteins and metabolically active proteins. The storage proteins are called hordeins in barley and are the main protein component in the endosperm, but also present in small amounts in embryo and aleurone layer. These proteins are soluble in alcohol/water mixtures (Osborne, 1907) and are therefore avoided in a water-based protein extraction.

After the establishment of high resolution 2DE this technique was exploited in several studies of barley seeds from 1983-1992 (Shewry et al., 1983; Görg et al., 1988; Flengsrud and Kobro, 1989; Görg et al, 1992; Görg et al, 1992; Weiss et al., 1992; Flengsrud, 1993). These works included discrimination of barley varieties by their 2D patterns, year-to-year variations, studies of germination and radicle elongation (day 1-7 PI) and cultivar differences. The results lacked identifications but 12 proteins were identified by Edman sequencing in cultivar Bomi in the pH range 4.2 – 6.9 (Flensgrud, 1993), including superoxide dismutase, glycogen synthase precursor, triose phosphate isomerase, CM-proteins, γ-hordein-1 precursor, and a fragment of C-hordein. Kristoffersen and Flengsrud (2000) mapped additional 11 proteins also by Edman sequencing in the pH range 7-9 including the α-amylase/subtilisin inhibitor (BASI), hordeins, trypsin inhibitor, and peroxidase.

Recently extensive use of 2DE and MS identification assigned approximately 260 soluble barley proteins to about 450 spots in developing, mature and germinated seeds of malting barley (Finnie et al, 2002, 2006; Østergaard et al., 2002, 2004; Bak-Jensen et al., 2004, 2007). The proteins used for these studies were extracted from whole seeds in water (5 mM Tris-HCL pH 7.5, 1 mM $CaCl_2$) to avoid the storage proteins. Many house keeping proteins, stress-related protein, defence related protein, etc. were identified. Several proteins were shown to vary between cultivars during development and malting. Subfractionation was done by dissection of the barley seed tissues into endosperm, embryo and aleurone layer in order to visualize low abundant proteins and to assign the different proteins to the specific tissues (Finnie and

Svensson, 2003). Recently 46 proteins associated with aleurone plasma membranes were identified using reverse-phase chromatography followed by LC-MS/MS (Hynek et al., 2006). Many details in these studies are relevant for the present work and will be discussed throughout Section 3.1.

The genome of barley is 5000 Mb and due to the large size compared to certain other cereal species (i.e. rice: 45 Mb and Arabidopsis: 120 Mb) it has not bee sequenced. However, the database of barley EST is constantly growing, which is helpful for the attempt to identify proteins from the barley seed. However, EST's are short and some do not have a good overlap with others, and therefore it is difficult and cumbersome to identify proteins this way.

Two cDNA microarray studies have been carried out of dissected barley seed tissues during germination and radicle elongation (Potokina et al., 2002; Watson and Henry, 2005). Potokina et al. (2002) analyzed differential gene expression in embryo, scutellar epithelium and endosperm (the endosperm preparation included also the aleurone layer) from 0 to 72 h PI. Spatial and/or temporal differential gene expression was detected of 154 genes divided into 26 categories based on putative function. Sixty-nine of these genes showed the highest mRNA level in endosperm, 58 were up-regulated in both embryo and scutellum, 11 were specifically expressed in embryo and 16 in scutellum tissue. In this work a cDNA array was based on clones of a cDNA library of developing caryopsis and therefore proteins like α-amylase that are absent during development are not represented. Watson and Henry (2005) analyzed the barley embryo during 0-96 h PI and detected 76 genes that changed in abundance during this period. Thirty-four genes changed in abundance during the first 12 h; 14 were up-regulated and 20 down-regulated, and can therefore be assigned a function during germination. The up-regulated genes include nucleotide binding protein, expansin-like protein, serine carboxypeptidase 1A, polyubiquitin, NADP dependent oxidoreductase P-like, phosphatidylinositol-4-phosphate 5-kinase type II alpha.

1.2.3 Non-barley plant seed proteomics studies

During the last 15 years there has been considerable progress in plant proteomics which is of high relevance for the present work. Several reviews summarize the large amount of data and discuss the used methods and challenges (Thiellement et al., 1999; Kersten et al., 2002; Rakwal and Agrawal, 2003; Peck, 2005; Agrawal and Rakwal, 2006; Komatsu and Yano, 2006). Most of these reviews focus mainly on rice proteomics since this is the most well studied plant organism with respect to proteomics. Also Arabidopsis is well characterized by proteomics methods. The genomes of rice and Arabidopsis have been fully sequenced and therefore they serve as reference organisms in plant proteomics studies. Many barley proteins in 2DE analysis are identified based on homology between barley EST's and rice and Arabidopsis genes. This section is focused on proteomics analysis of seeds of wheat and rice, which are relatively closely related to barley, and Arabidopsis.

Seeds from wheat were investigated by 2DE focused on cultivar discrimination from 2D patterns (Dunbar, 1985) and followed up by 2DE of wheat endosperm (Skylas et al., 2001; Amiour et al., 2002; Islam et al., 2002). The development of wheat seeds has also been studied by 2DE where developing and mature seed proteomes were compared (Skylas et al., 2000) and 250 proteins were identified in developing endosperm (Vensel et al., 2005). Another study separated whole wheat endosperm amyloblasts or amyloblast membrane proteins during development and protein were identified by LC-MS/MS (Andon et al., 2002).

In rice the first data file of proteins from seed embryos and endosperm (from dry mature seeds and leaves 20-25 days after germination) was reported by Komatsu et al. (1993). More than 600 protein spots including 100 embryo protein spots and 150 leave protein spots were separated and detected by CBB. Thousands of rice proteins were resolved in chloroplasts and tissues including leaf, stem root, germ, seedling, seed, bran, chaff, and callus in the pH range 3-10 (Tsugita et al., 1994, 1996; Sadimantare et al., 1999). Fifty-six were sequenced, but no proteins from the seed were identified. Koller and co-workers (2002) made a comprehensive study of rice seed, root and leaf protein extracts by 2DE and MS/MS and LC/LC-MS/MS. This led to identification of 2528 unique proteins of which 877 (152 from 2D gels) were from seeds. Another research group performed analysis of rice proteins from endosperm and embryos of seeds, leaves and roots by 2DE. Fifty-nine embryo proteins were identified by sequencing and 46 proteins (from all three tissues) were unambiguously identified by MALDI-TOF MS (Hirano, 1997).

A composite pH 3-10.5 2D pattern of Arabidopsis leaf, stem, root, and callus protein with 4763 spots, including 984 from seeds, has been published (Kamo et al. 1995; Tsugita et al., 1996). Forty-eight proteins were identified by Edman sequencing. More recently, around 1300 proteins were separated from Arabidopsis seeds during the initial stages of germination, during priming (pre-germination treatment followed by drying used to synchronize the germination of individual seeds in a batch) and at radicle emergence (Gallardo et al., 2001). During germination and radicle elongation 74 spots changed in abundance of which only 39 were restricted to germination (Section 1.1.2). Finally a study of the impact of treatment with a specific GA synthesis inhibitor (paclobutrazol) of wild type and mutant Arabidopsis seeds was done (Gallardo et al., 2002). Only the cytoskeleton component α-2,4 tubulin that changed during germination seemed to be dependent on GA. In contrast, GA appeared to be important for a number of proteins associated with emergence of the radicle.

A number of plant proteomics studies present comparative analysis of tissues exposed to abiotic and biotic stresses in order to understand stress mechanisms in plants (Noctor and Foyer, 1998), but it is beyond the scope of the present thesis to address the details of these studies.

1.3. Limit dextrinase inhibitor

1.3.1 Limit dextrinase (LD)

Limit dextrinase (LD) belongs to glycoside hydrolase family 13, which contains α-amylase and enzymes involved in debranching of starch, glycogen, pullulan, and maltodextrins, as well as branching enzymes and transglycosidases (http://afmb.cnrs-mrs.fr/CAZY/). The enzymes apply a retaining catalytic mechanism and LD catalyses hydrolysis of the 1,6-α-glycosidic bonds.

LD is present in low levels in developing seeds and increase in germinating barley seeds (Sissons, et al., 1993; Burton et al., 1999). In developing seeds LD has been detected by northern blot and zymogram analysis in endosperm and embryo, and it has been suggested that LD is involved in control of the branching and debranching activity in the synthesis of amylopectin (Sissons et al, 1993). The presence of LD is low in the mature dry seed, but increases in response to GA in abundance during radicle elongation (Burton et al., 1999). LD is synthesized in the aleurone layer and acts in the endosperm, where it degrades amylopectin in concerted action with α-amylase, β-amylase, isoamylase and α-glucosidase (Section 1.1.3). The LD activity increases after 3-5 days of germination and reaches a maximum at 6-7 days (Longstaff and Bryce, 1993; MacGregor et al., 1994; Kristensen et al., 1999). Using specific antibodies, LD was detected in aluerone layer incubated 24 h in 20 mM succinic acid, 20 mM $CaCl_2$, pH 4.6 with 5 μM ABA, 5 μM GA, or no hormone, respectively, however, mostly in the GA treated sample (Shaphiri et al., in prep). LD peaks at 48 h and after 24 h part of the LD was secreted to the medium when aleurone was incubated with GA or no hormone. This is in agreement with the fact that LD is produced in the aleurone layer in response to imbibition and GA, and secreted to the endosperm to participate in starch degradation.

During germination LD is present in a free and an inactive bound form, which can be released and activated by treatment with reducing agents (Longstaff and Bryce, 1993). It is thought that bound LD may be a limiting factor in the conversion of starch to sugars during malting (Sissons et al., 1993; Section 1.1.4) and furthermore, that it is complexed in a 1:1 molar ratio with the proteinacious limit dextrinase inhibitor (LDI; MacGregor et al., 2003). Limit dextrinase has been purified from barley malt with a yield of 2 mg × kg^{-1} (Kristensen et al., 1998). In attempts to produce recombinant protein, the cDNA sequence has been cloned from germinating barley seeds (cv. Maud) and the protein was recently produced in *Pichia pastoris* as an active enzyme in a high cell density fermentor (Vester-Christensen, in prep).

1.3.2 Limit dextrinase inhibitor (LDI)

The barley limit dextrinase inhibitors (LDI) are endogenous inhibitors of barley LD. Peptide sequencing of the two LDIs showed that they have the same amino acid sequence identical to the deduced sequence of a barley cDNA encoding a putative α-amylase/trypsin inhibitor (Lazaro et al., 1988; Figure 4.2). The LDI consists of 114 amino acids and has nine cysteines forming four disulfide bonds. The free cysteine (Cys59) is modified by either a GSH or cysteine molecule, which generates the two LDI mixed disulfide forms with pI of 6.7 and 7.2, respectively (MacGregor et al., 2000).

LDI is present in the barley seed endosperm of mature and germinating seeds and maybe also during the development (Macri et al., 1993). Presumably the protein is being degraded during germination together with α-amylase/trypsin inhibitors (CM-proteins; Section

1.2) belonging to the same protein family as LDI. It is suggested, however, that the LDI inhibits the function of LD in the radicle elongation (Section 1.3.1; Sisson et al., 1993).

LDI has been purified from mature barley seeds (cv. Harrington) in a few mg × kg^{-1} of each of the two LDI forms (MacGregor et al., 1994), but only little characterization of the LD/LDI complex has been conducted. Generally characterization of CM-proteins is sparse. Available information is summarized in Table 1.2 (Payan, 2004; Svensson et al., 2004). Only very few of these proteins have been expressed recombinantly and little mutational work has been done in order to understand the inhibitory mechanisms. The structures of two members of the CM protein family has been solved; the bifunctional α-amylase/trypsin inhibitor from ragi seeds (Strobl et al., 1995) and the 0.19 α-amylase inhibitor from wheat (Oda et al., 1997), and 0.28 in complex with TMA (Payan, 2004). The binding constants are determined to 0.11 nM for the *Bacillus subtilis* α-amylase/0.53 wheat inhibitor pair and 11 nM and 15 nM for RBI in complex with PPA and TMA, respectively.

Table 1.2. Summary of known information CM-proteins in cereals

Characteristics	Known information	Reference
Source:	Barley, wheat, ragi, rye	Svensson et al., 2004
α-amylase targets:	Mammalian, insect, bacterial	Svensson et al., 2004
Protease inhbitory activity:	RBI	Campos et al., 1983
Size:	124-160 aa, 5 disulfide bonds	Garcia-Maroto et al., 1991 Barber et al., 1986 Campos et al., 1983
Names:	RBI	Campos et al., 1983
	0.19	Franco et al., 2000
	0.28 (WMAI-1)	Garcia-Maroto et al., 1991
	0.53	Franco et al., 2000
	WRP25	Feng et al., 1996
	WRP26	Feng et al., 1996
	BMAI-1	Sanchez-Monge et al., 1992
Solved structures:	Free RBI (NMR)	Strobl et al., 1995
	TMA/RBI complex (x-ray)	Strobl et al.,1998
	Free 0.19 (x-ray)	Oda et al, 1997
	TMA/0.28 (x-ray)	Payan, 2004
Inhibition constants:	0.11 nM (*B. subtilis* α-amylase/0.53)	Takase, 1994
	15 nM (TMA/RBI competitive binding)	Alam et al., 2001
	11 nM (PPA/RBI)	Maskos et al., 1996
Mutational work:	0.19 and 0.53 and *B. subtilis* α-amylase (mutants in the amylase)	Takase, 1994
	RBI and TMA (Ser1Ala)	Alam et al., 2001
	WMAI-1 (position 1 and 4, insertion segments at position 4 and 58)	Garcia-Maroto et al., 1991

The structure of LDI has been modeled based on the three-dimensional structure of the trypsin/α-amylase inhibitor from ragi, which shares 52% sequence identity with LDI (MacGregor et al., 2000), including the nine cysteines (Figure 4.2). The model shows four helices as commonly seen in this protein family. Cys59 seems to be free cysteine whereas the remaining eight cysteines form disulfide bonds (Figure 1.8).

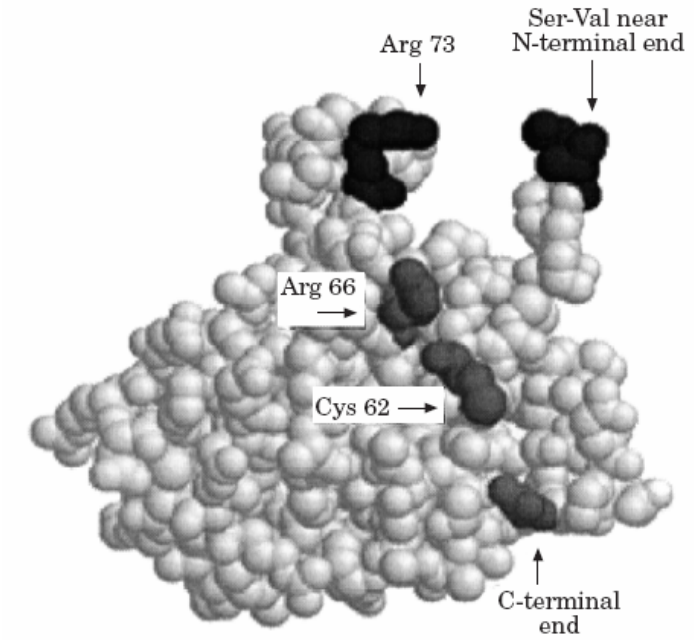

Figure 1.8. Model of limit dextrinase inhibitor based on the structure of RATI showing Ser7-Val8 and Arg73, Cys62, and Arg66 and the C-terminal end, Gly117. Arg 73 and Arg66 may be involved in inhibition of LD. (From MacGregor et al., 2000). The numbering is according to the sequence of (Lazaro et al., 1988) shown in alignment with LDI in Section 3.3.3.3. Cys62, Arg66, and Arg73 correspond to Cys59, Arg64, and Arg71 in the LDI sequence.

1.3.3 Complex formation of LD/LDI

The binding of LDI to LD has been described as "strong", but the binding constant (K_D) has not been determined (MacGregor., 2004). Based on the crystal structure of the complex of *Tenebrior molitor* α-amylase and ragi trypsin/α-amylase inhibitor (TMA/RBI; Figure 1.9) and mutational work of RBI it was revealed that the N-terminal $Ser1_{RBI}$ and $Val2_{RBI}$ interact directly with the putative catalytic acids of the α-amylase. Moreover, two areas of RBI are directly involved in the interaction. Area 1 contains Ser1-Ala11 and Pro52-Cys55 and area 2 contains Arg61, Val67-Ser70, Gly72, Thr107-Gly110, Leu115-Leu117. Since LD belongs to the same structural family as α-amylase, the catalytic sites have the same geometry and the complex of LD/LDI may structurally be similar to that of TMA/RBI. Ser1 and Val2 in RBI are equivalent to Ser4 and Val5 in LDI, and this extension of three amino acids in LDI may abolish α-amylase inhibition and turn the protein into a LD inhibitor. The N-terminal residues of LDI are therefore thought to be important for binding to LD (MacGregor et al., 2000). By specifically modifying arginines in LDI, the inhibitory effect on LD was reduced suggesting that one or more arginines are involved in inhibition (Figure 1.8).

The trypsin inhibitors belonging to the CM-protein family all share a loop sequence Gly-Pro-Arg-Leu (see Figure 3.34), which is believed to be the protease inhibitory site. In LDI, the equivalent loop sequence is Gly-Pro-Ser-Arg and this alteration causes a conformational change of the loop and consequently LDI posses no trypsin inhibitory activity (MagGregor et al., 2000).

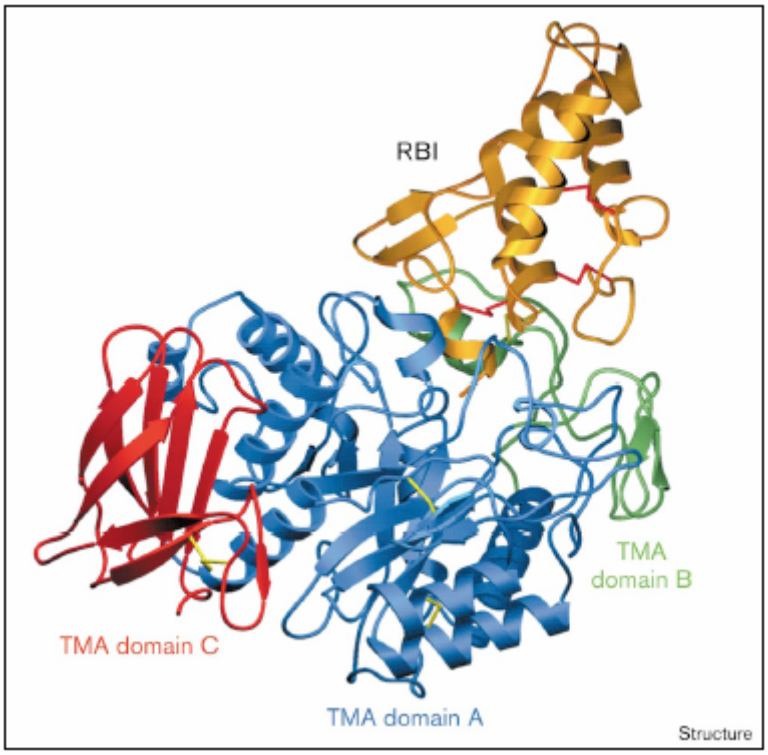

Figure 1.9. A ribbon diagram of the TMA/RBI complex. RBI is shown in yellow. The three TMA domain, A, B and C are shown in blue, green and red, respectively. Disulfide bridges in RBI and TMA are shown in red and yellow, respectively (Strobl et al., 1998).

1.4 Objectives and strategies of the present study

1.4.1 Proteome analysis of barley seed during germination and radicle elongation

1.4.1.1 Objectives

The grains of the *gramineae* family (barley, wheat, rice, rye, maize, oats, millet and sorghum) are important in nutrition for animals and humans and are therefore subjected to extensive studies. Barley seed germination is in addition central for obtaining good industrial malting quality. Little is known about the early changes in the germination and so far no protein marker with a specific role in germination has been identified. It is reported in the literature that the mRNA necessary for resumption of metabolic activity upon imbibition is present in the dry seed (Bewley and Black, 1994) and therefore the first germination specific changes may occur at the protein level.

The present work was based on comprehensive proteome analysis of developing, mature, and germinating malting barley seeds. 2D gels of whole barley seed protein extract at 72 and 144 h of the malting process indicated that tremendous changes occurred at the protein level (Østergaard et al., 2002, 2004; Bak-Jensen et al., 2004). Moreover, proteome analysis of dissected barley seeds (embryo, aleurone layer and endosperm) revealed the behavior of less abundant proteins and facilitated the assignment of proteins to specific tissues (Finnie and Svensson, 2003). Based on this previous work, a remaining question concerned the spatio-temporal protein profiles of the different tissues at the initial stages of germination.

1.4.1.2 Strategies

The proteomic approach used in the present study benefited from previous experience with related work in our laboratory. Seeds were germinated at conditions corresponding to micromalting experiments and the earlier used reference cultivar Barke was maintained in the present study (Østergaard et al., 2002). Proteins were extracted from the dissected tissues according to an existing protocol (Finnie and Svensson, 2003). 2DE and protein identification by MS were carried out according to standard procedures with minor changes (Østergaard et al., 2002). The use of already established protocols enables comparison of the present with previous data; however, the present work is substantially more detailed.

1.4.2 Study of enzymes of the ascorbate-glutatione cycle during radicle elongation

1.4.2.1 Objectives

Most protein changes in the 2D gel pattern during germination and radicle elongation were observed and identified in the embryo as a consequence of the resumption of metabolic activities upon imbibition. Many changes during the radicle elongation concerned proteins involved in redox control. In particular the H_2O_2 scavenging enzyme APX had an interesting profile during development and germination/radicle elongation as it appeared in the endosperm of developing seeds (Finnie and Svensson, 2003) and in the germinated embryo but not in the dry mature seed. It is possible to measure enzymatic activity of APX and the other enzymes in the ascorbate-glutathione cycle (DHAR, MDHAR, and GR) in protein extracts. This gives a functional aspect that importantly expands the information achieved by 2DE. For understanding germination related processes it is important to understand regulatory mechanisms of enzymes and this was approached in case of DHAR and APX.

1.4.2.2 Strategies

APX, DHAR, MDHAR, and GR were subjected to analysis by enzyme activity assays and furthermore, APX was studied with respect to presence of different forms (differing in post-translational modifications) and isoforms by aid of specific antibodies, MS, and gene expression analysis. Recombinant barley Trx h was available (Maeda et al., 2003) and used to investigate a possible interaction with DHAR.

1.4.3 Study of the limit dextrinase inhibitor

1.4.3.1 Objectives

Barley wort and beer contain unfermentable branched dextrins caused by lack of complete degradation of starch during malting. This may be caused by insufficient level of activity of LD due to inhibition by the endogenous limit dextrinase inhibitor. LDI is not well characterized and no K_i or K_D values have been reported.

Based on our experience with another glycoside hydrolase family 13 enzyme, barley α-amylase 2 and its proteinaceous inhibitor, barley α-amylase/subtilisin inhibitor (BASI), we wanted to pursue characterization of the interaction between LD and LDI. This required establishing a heterologous expression system for LDI, as LDI is present in low amounts in the barley seed. In addition LDI is thought to be a Trx h target and this could be further investigated by aid of recombinant Trx h.

Finally, in order to understand the function of LDI in the barley seed, knowledge about the expression patterns of LD and LDI in the barley seed tissues during radicle elongation is desirable.

1.4.3.2 Strategy

The LDI gene had to be cloned from barley seeds. The idea was first of all to try to produce the protein in *Escherichia coli* preferably without a tag, but a construct with a C-terminal His_6 tag was also made for easy purification. MacGregor et al. (2000) suggested that the N-terminal residues were important for inhibition based on modeling of the three-dimensional structure, and we therefore aimed at keeping this part of the protein authentic, which means that no additional amino acids were attached from added tags. A cleavable Trx h tag was added to the N-terminus of LDI in order to facilitate disulfide bridge formation and increase the solubility in *E. coli*. If *E. coli* was unable to produce inhibitory active LDI, *Pichia pastoris* was the next choice since this yeast host is able to post-translationally modify and secrete the protein to the medium. Other recombinant plant proteins including α-amylase (Juge et al., 1996), α-glucosidase (Naested, et al., 2006), BASI (Bønsager et al., 2003), and lipid transfer protein (Klein et al., 1998) have been produced in *P. pastoris* and the yield can be optimized enormously by high cell-density fermentation (Naested et al., 2006). A third choice of expression host was the gram-positive bacteria *Latococcus lactis*, which exports the produced protein to the periplasma where the folding machinery is situated and where problems with toxicity of foreign proteins can be avoided (Sarvas et al., 2004).

The produced LDI was planned to be characterized with respect to interaction with LD by using LD activity inhibition assays and binding studies by surface plasmon resonance (SPR). The next step would be to design and construct mutants in LDI by site-directed mutagenesis for further characterization of the LD/LDI interaction.

The well established methods for protein extraction from barley seeds, 2DE and MS (Finnie et al., 2002; Østergaard et al., 2002) and the availability of LD antibodies could facilitate

identification of production patterns and possible post-translational modifications of LD in the barley seed during germination and radicle elongation.

Chapter 2 - Materials and methods

2.1 Preparation of plant material

2.1.1 Germination of barley seeds and embryos

Seeds from the malting cultivar Barke (2002 harvest) were provided by Sejet Plantbreeding. A preliminary test showed that the germination was acceptably homogenenous when seeds in 9 cm Petri dishes (100 seeds in each) were added tap-water (4 mL) and incubated in the dark at 20^{o}C. At 4, 12, 24, 36, 52, 60, and 72 h PI 100 seeds (germinated at 15^{o}C) from each time point were frozen in liquid nitrogen and stored at -80^{o}C until use.
Embryos were dissected from the seeds (Section 2.1.2) and germinated on water/agar plates with or without 5 μM ABA at 15^{o}C for 24, 48 and 72 h and frozen on liquid nitrogen.

2.1.2 Dissection of barley seeds

Five seeds were selected carefully with respect to visual homogenity and used for dissection and protein extraction. Husk was removed from the seeds after incubation in 50% H_2SO_4 for 30 min and rinsing 5 times in a large volume of water. First the embryo including the scutellar epithelium was removed and remains of endosperm were scraped away from the embryo fraction. The aleurone layer was cut away from the endosperm and with repeated washing (in ice cold water) and scraping of the aleurone layer, remains of endosperm was removed from the aleurone layer. The tissues from five seeds were individually freeze dried for 24 h.

2.1.3 Small scale protein extractions

Proteins were extracted from the endosperm by crushing and grinding to a fine powder using a pre-cooled ceramics mortar. The powder was transferred to a 2 mL Eppendorf tube and resuspended in 750 μL ice cold extraction buffer (5 mM Tris-HCL, 1 mM $CaCl_2$, pH 7.5). The aleurone layers were ground in a pre-cooled mortar with 250 μL extraction buffer and transferred with another 250 μL to a 2 mL Eppendorf tube. The embryos were ground to a fine powder using a plastic pestle in an Eppendorf tube on ice with 250 μL ice cold extraction buffer, and transferred with another 250 μL extraction buffer to a 2 mL Eppendorf tube. One glass bead was added to each tube for homogenization of the extraction. The tubes were shaken in an Eppendorf shaker at top speed for 30 min at 4^{o}C. The samples were centrifuged for 30 min at 18000 × g at 4^{o}C. Supernatants containing soluble protein were de-salted using a NAP-5 column (GE Healthcare) and transferred to clean tubes and stored at -80^{o}C. Protein concentrations in the extracts were determined by the Popov assay (Popov et al., 1975) with bovine serum albumin (BSA) as a standard.

2.1.4 Protein extraction for enzyme activity assays

Embryos used for protein extractions for enzyme activity measurements were not freeze-dried. Proteins were extracted in 100 mM Tris-HCl pH 8.0, 0.5 mM AsA. The extracts were de-salted using a NAP-5 column (GE Healthcare) and eluted in the extraction buffer. Protein extracts used for 1DE and IEF were concentrated 10 fold using a Microcon spin column (MWCO = 3500; Millipore).

2.2 1D and 2D gel electrophoresis

2.2.1 1D gel electrophoresis

The protein sample was mixed with one fourth volume of sample buffer (Invitrogen; prepared either for native or non-native gels) and for non-native gels also 1/10 volume of DTT (0.5 M) to a total volume of maximum 25 μL. Samples for non-native gels were boiled for 2 min and then applied to either a NuPAGE 4-12% Bis Tris gel or a 4-12% Tris-glycine gel (Novex system, Invitrogen) along with the Mark12 marker or the pre-stained SeeBlue marker (Invitrogen). For native gels the gel container was placed on ice and the gel was pre-run with 1 mM AsA in the upper chamber for 20 min. The proteins were stained with blue silver coomassie brilliant blue (bsCBB; Candiano et al., 2004) or colloidal coomassie brilliant blue (cCBB; Rabilloud et al., 2000) and destained in Milli-Q water, blotted onto a nitrocellulose membrane (Section 2.5.1 and 2.5.2), or subjected to APX activity staining (Section 2.4.6).

2.2.2 Isoelectric focusing

10 μL protein extract was mixed with an equal volume of sample buffer (20 mM lysine, 20 mM arginine, 15% glycerol) and applied to an IEF gel (Novex system, Invitrogen). The gel container was placed on ice and the gel was pre-run with 1 mM AsA in the cathode buffer (20 mM lysine, 20 mM arginine) for 20 min. As anode buffer 7 mM phosphoric acid was used. APX was detected by western blotting (Section 2.5.1 and 2.5.2) and activity staining (Section 2.4.6)

2.2.3 2D gel electrophoresis

40 μg protein from embryo and aleurone layer and 80 μg from the endosperm was precipitated in 4 volumes of acetone at -20^{o}C for > 24 h. The proteins were redisolved in reswelling buffer (8 M urea, 2 % (w/v) CHAPS, 0.5 % (v/v) IPG buffer 4-7 (GE Healthcare), 20 mM DTT and a trace of bromophenol blue) and first dimension separation was carried out using 18 cm IPG strips with a linear gradient of pI 4-7 on a IPGphor (GE Healthcare) as previously described (Finnie et al., 2002). The IPG strips were equilibrated for 20 min in equilibration buffer (50 mM Tris-HCl pH 8.8, 6 M urea, 30 % (v/v) glycerol, 2 % (w/v) SDS and a trace bromophenol blue) containing 10 mg/mL DTT followed by incubation for 20 min in equilibration buffer containing 25 mg/mL iodoacetamide. Second dimension (12-14%, 18 × 24 cm, GE Healthcare) was run on a Pharmacia Multiphor according to manufacturer's recommendations. Gels were stained with silver nitrate (Heukeshoven and Dernick, 1985). cCBB stained gels were run of non-germinated and 72-h germinated tissues (250 μg loaded) as described above.

For detection of LD in the barley seed extracts, 11 cm IPG strips (pH range 4-7) were used and these were cut after focusing to fit into the NuPAGE 4-12% Bis Tris Zoom gel (Novex system, Invitrogen). The proteins were blotted onto a nitrocellulose membrane (Section 2.5.1).

2.2.4 Analysis of 2D gels

The 24 silver stained gels made for different time points PI (8 gels from each of the three tissues) were carefully compared manually. Proteins that were by experience found to be constant during the germination process were used as markers for spot intensity and mobility, i.e. spot 220 and 103: superoxide dismutase, spot 142: GSH-dependent dehydroascorbate reductase, and spot 95: triose phosphate isomerase (Figure 3.1). Spots that increased or decreased in abundance in the different tissues over the time course of 0-72 h were identified in the corresponding cCBB stained gels from which they were excised. The spots were subjected to trypsin (Promega)

digestion (Shevchenko et al., 1996) and MS as previously described (Finnie et al., 2002). APX spot were also digested with AspN and LycC (Roche) using the same conditions as for trypsin digestion.

2.3 Mass spectrometry

Trypsin, AspN or LysC digestion of the excised spots were analyzed by MALDI-TOF or MALDI-TOF/TOF MS (Voyager DE-STR mass spectrometer; Applied Biosystems Inc. or Bruker Reflex II or III).. The peptide maps were subjected to a Mascot search in the NCBI database or in the EST-database for green plants. If the peptide map resulted in unsuccessful or uncertain identification, the peptides were analyzed by MALDI-TOF/TOF in order to obtain sequence information.

2.3.1 Protein identification

Tryptic digests were analyzed by MALDI-TOF-MS (Voyager DE-STR mass spectrometer; Applied Biosystems Inc. or Bruker Ultraflex II). Proteins were identified by peptide mass mapping and searching the National Center for Biotechnology Information non-redundant database (NCBInr) and if necessary an EST database, using the internet version of the search engine MASCOT [29]. The searches were carried out from November 2003 to October 2004 and following parameters were set: Taxonomy: viridiplantae; fixed modifications: carbamidomethyl cysteine; variable modifications: oxidized methionine; peptide tolerance: 0.1 Da; up to one missed cleavage. Identifications were considered positive when at least 5 peptides combined with a significant MASCOT score and a sequence coverage of at least 20% (see supplemental data). Tentative consensus (TC) sequences of matched ESTs were found by searching the Institute for Genome Research (TIGR) barley (or in a few cases wheat) index (www.tigr.ord/tdb/hvgi). Proteins not identified by this approach were analyzed by MS/MS (Bruker Ultraflex II or III) to obtain peptide fragmentation data. In a few cases the MASCOT search results became significant when the ion score was included.

2.4 Enzyme activity assays

2.4.1 Ascorbate peroxidase (APX) activity

The activity of APX was assayed at room temperature from the decrease in absorbance at 290 nm as AsA was oxidized to MDHA (Nakano and Asada, 1981). The activity of APX was detected in 50 μL embryo extract (30 μg protein) in 50 mM potassium phosphate pH 7.0, 0.1 mM EDTA, 1 mM AsA, and 1 mM H_2O_2 in a final volume of 1 mL. The reaction was started by addition of H_2O_2 and followed at 290 nm for 9 minutes. Correction was done for the low, non-enzymatic oxidation of AsA by H_2O_2. No correction for the oxidation of AsA in the absence of H_2O_2 was necessary, which shows the lack of or the presence of very low activity of ascorbate oxidase in barley seeds.

2.4.2 Dehydroascorbate reductase (DHAR) activity

The activity of DHAR was assayed at room temperature from the increase in absorbance at 265 nm as DHA was reduced to AsA (Nakano and Asada, 1981). The activity of DHAR was detected in 20 μL embryo extract (12 μg protein) in 50 mM potassium phosphate pH 7.0, 0.1 mM EDTA, 2.5 mM GSH, 0.2 mM DHA (made fresh) in a final volume of 1 mL (Dalton et al., 1986). The

reaction was started by addition of DHA and followed at 265 nm for 9 min. Correction was done for the non-enzymatic reduction of DHA, and as GSSG has a low absorbance at 265 nm, the reaction rate was corrected by multiplying by a factor of 0.98 (Nakano and Asada, 1981).

2.4.3 Glutathione reductase (GR) activity

The activity of GR was assayed at room temperature from the decrease in absorbance at 340 nm as NADPH was oxidized (Foster and Hess 1980; O'Kane et al., 1996). The activity of GR was detected in 50 µL embryo extract (30 µg protein) 100 mM HEPES pH 7.8, 2 nM EDTA, 0.3 mM NADPH, 1 mM GSSG. The reaction was started by addition of GSSG and followed at 340 nm for 9 min.

2.4.4 Monodehydroascorbate reductase (MDHAR) activity

The activity of MDHAR was assayed at room temperature from the decrease in absorbance at 340 nm as NADPH was oxidized (de Pinto et al., 2000). The activity of MDHAR was detected in 350 µL embryo extract (220 µg protein) in 100 mM Tris-HCl pH 8.0, 0.2 mM NADPH, 1 U ascorbate oxidase, 2.5 mM AsA in a volume of 1 mL. The reaction was started by addition of AsA and followed at 340 nm for 9 min.

2.4.5 Calculation of enzyme activity

The activity was calculated by the change in absorbance per minute per µg total protein in extract divided by the extinction coefficients for either AsA at 265 nm (14 $M^{-1} \times cm^{-1}$) or 290 nm (2.8 $M^{-1} \times cm^{-1}$) or NADPH at 340 nm (6.22 $M^{-1} \times cm^{-1}$), respectively (Hiner et al., 2000). A quantitative determination of the enzyme was not possible because the amount of each enzyme in the protein extracts was unknown.

2.4.6 Detection of APX activity in gels

The native 1D PAGE was run (Section 2.1.1). The following procedure was described by Mittler and Zilinskas (1993) and was performed at room temperature. Subsequent to the gel electrophoretic separation, the gel was equilibrated with 50 mM sodium phosphate pH 7, 2 mM AsA 3 × 10 min. The gel was then incubated with 50 mM sodium phosphate pH 7.0, 4 mM AsA, 2 mM H_2O_2 for 20 min. H_2O_2 started the reaction. The gel was subsequently washed with 50 mM sodium phosphate pH 7.0 for 1 min and submerged in a solution containing 50 mM sodium phosphate pH 7.8, 28 mM TEMED, 2.45 mM nitroblue tetrazoium (NBT). The APX activity was observed as an achromatic band on a purple background.

2.4.7 LD activity inhibition assay

The LD inhibition activity of LDI was determined by pre-incubation of 0.006 nmol LD and 0.03-0.7 nmol of LDI for 10 min at 40°C in a total volume of 200 µL 0.2 M sodium-acetate pH 5.0, 5 mM $CaCl_2$, 0.1% BSA. This gives a concentration of 0.03 µM LD and 0.15-3.5 µM LDI during pre-incubation.100 µL Red Pullulan (2% in 0.5 M KCl) was added at the degradation of the insoluble substrate into soluble units continued for 20 min at 40°C. The reaction was stopped by addition of 600 µL cold 85% ethanol. The samples were left at room temperature for 10 min and then centrifuged 8 min, 10000 rpm. The residual activity of LD was measured at A_{540} in a microtiter plate.

As positive control bLDI (0.485 mg/mL) purified from barley seeds was used (kind gift of Dr. A.W. MacGregor; MacGregor et al., 1994). The concentration was determined by Popov assay using BSA and barley rTrx h2 as standards (Popov et al., 1975; Maeda et al., 2003).

2.5 Immuno-detection of proteins

2.5.1 Western blotting of 1D and IEF gels

After running of 1D SDS-PAGE, native PAGE or IEF, proteins were electroblotted onto a nitrocellulose membrane using the Novex system (Invitrogen) according to the method described by the manufacturer.

2.5.2 Western blotting of 2D gels

After 2nd dimension separation, the 2D gels was equilibrated in transfer buffer (Invitrogen) containing 15% methanol for 30 min. Proteins were electroblotted onto a nitrocellulose membrane (equilibrated 10 min in Milli-Q H_2O and 15 min in transfer buffer) for 5 h (60 V, 120 mA, 20W; 0.3 mA/cm^2) in a semidry blotting apparatus (Multiphor II system; GE Healthcare) according to the manufacturer's recommendations.

2.5.3 Immuno-detection of APX, LD, and LDI

The nitrocellulose membrane with electroblotted proteins (Section 2.5.4) was incubated in TBST buffer (25 mM Tris-HCL pH 8, 150 mM NaCl, 0.1% Tween-20) for non-specific blocking followed by 1 h incubation with primary antibody (dilution 1:1000-3000) in TBST buffer. The membrane was washed 3 × 5 min in TBST and blocked again for 30 min in TBST. Secondary antibody (goat anti-rabbit/alkaline phosphatase conjugated; 1:2000) was added and incubation continued for 30 min. the membrane was washed 3 × 5 min and immunoreactive proteins were stained in 100 mM Tris Base pH 9.5, 100 mM NaCl, 5 mM $MgCl_2$ containing 0.33 mg/mL NBT and 0.17 mg/mL 5-bromo 4-chloro indolyl phosphate (BCIP) for 5 min. The reaction was stopped by change to Milli-Q H_2O. Anti-LD antibodies were raised against LD from the malt enzyme from cv. Natasha (Manners et al., 1970). Barley LDI antibodies were provided by Dr. A.W. MacGregor, and maize APX antibodies were provided by Prof. T. Koshiba (Koshiba, 1993).

2.6 RT-PCR analysis

Total RNA for RT-PCR analysis was isolated from embryo by the RNeasy Plant Mini Kit (Qiagen). Contaminating genomic DNA was digested using RNase-Free DNase Set (Qiagen) during RNA purification. 18S rRNA was used as internal control and was amplified with primers 18S rRNA1 (5′-CTACGTCCCTGCCCTTTGTACA-3′) and 18S rRNA2 (5′-ACACTTCACCGGACCATTCAA-3′). Primers apx1F (5′-CAGGCAGGTGTTTTCCACTC-3′) and apx1R (5′-CCTTGTCGGTCGGCAACT-3′) were designed based on sequence of APX with accession number Q945R5 and primers apx2F (5′-GCAAGTCTTTGGGAAGCAGA-3′) and apx2R (5′-AGTTTTGTCACTTGGAAGCTGAAG-3′) were designed based on APX with accession number O23983. RT-PCR analysis was performed using One-Step RT-PCR Kit (Qiagen). The amplification reaction was performed according to the manuscript with minor modifications. A 25 µL standard RT-PCR mixture contained 1× reaction buffer, 1 × Q solution, 0.4 mM deoxynucleotide triphosphates, 0.6 µM primers, 2 units RNase inhibitor and 1 µL of

reverse transcriptase-DNA Taq polymerase enzyme mix. A total of 50 and 100 ng of RNA was used for analysis of APX and 18SrRNA, respectively. The thermal cycling consisted of 50ºC for 30 min to synthesize the first-strand cDNA; 95ºC for 15 min to inactivate the reverse transcriptase and to activate Taq DNA polymerase; 15 and 30 cycles of 94ºC for 1 min, 63ºC for 1 min, and 72ºC for 1 min for PCR amplification; and a final elongation at 72ºC for 10 min. A total of 17 μL of RT-PCR products was analyzed on a 1.2% (w/v) agarose gel with TAE (Tris-acetate-EDTA) running buffer and stained with 0.5 μg/mL of ethidium bromide. RT-PCR products were purified with QIAquick Gel Extraction kit (Qiagen) and were ligated into pDrive cloning vector (Qiagen) for subsequent nucleotide sequencing.

2.7 Heterologous expression of limit dextrinase inhibitor

2.7.1 Cloning of the LDI gene

The protein sequence was known from MS data and N-terminal sequencing. The sequence of the LDI cDNA was found in an EST database. The protein sequence was obtained by aid of MS (MacGregor et al., 2000). A tblastn database search gave several hits with almost identical sequences. Primers covering the 5' and 3' sequences were designed and synthesized (DNA Technologies).

Husk from the frozen barley seeds was removed and milling of the seeds was carried out in a mortar cooled in liquid nitrogen. RNA was extracted from developing barley seeds (cv. Morex) using RNeasy Plant Mini Kit (Qiagen). RT-PCR was carried out using a Qiagen kit. The PCR product was cloned into a TOPO vector (Invitrogen) and sequenced using TOPO forward and reverse primers.

2.7.2 Design and construction of expression vectors

pET11a (Novagen) and pET32a (Novagen) were used for heterologous expression in *E. coli*, pPICZa (Invitrogen) for *P. pastoris* and pAMJ399 for *L. lactis* (Gasson, 1983). The *L. lactis* expression system was kindly provided by Associate Professor Jan Martinussen, Center for Microbial Biotechnology, BioCentrum-DTU. The His_6 tag constructs were made using a C-terminal primer encoding the six histidines adjacent to the LDI sequence. pET32a encoded the N-terminal thioredoxin tag. An enteropeptidase cleavage site (ECS) was added between thioredoxin and LDI. The constructs were made by amplification of the LDI sequence by PCR using the TOPO-LDI vector as template and subcloning the PCR product into the expression vector of interest using encoded cleavage sites (*BamH*1, *Nde*1, *Msc*1, *EcoR*1; *Xho*1). Primers used for all constructs are listed in Table 2.1.

Furthermore a construct in pET11a with optimized codon usage in the 5' end was made. Three synthesized primers of 78 bp, with an overlap of 24 bp, encoding the LDI N-terminus with optimized codon usage for *E. coli* and *P. pastoris* were combined using PCR (Lin et al., 2002). This covered the first 123 bp of LDI. The generated PCR product was used as a 5' primer and the LDI cDNA was amplified using standard PCR with an annealing temperature of 45°C for 90 s. Inserts in all constructs were confirmed by sequencing.

Table 2.1. Primers used for cloning of LDI and for construction of expression vectors. Bold represents restriction sites

Primers for cloning of LDI

Name	Sequence
LDI Forward	5' GAGAGA **CATATG** ACCCTGGAGAGCGTCAAGGACG 3'
LDI R	5' **GGATCC** CCTTA TCCCGGCTCCTGGACGGACGA 3'
LDICHIS N:	5'**GGATCC** CCTTA GTGGTGGTGGTGGTGGTG TCCCGGCTCCTGGACGGACGA 3'

Primers for E. coli constructs

Name	Sequence
LDI N P32	5'GAGAGA**TGGCCA**TGATGATGATGATAAAACCCTGGAGAGCGTCAAGGACG 3'
LDI R	5' GAGAGA **GGATCC** CCTTA TCCCGGCTCC 3'
LDI CHIS	5' GAGAGA **GGATCC** CCTTA GTGGTGGTGG 3'

Primers for P. pastoris constructs

Name	Sequence
LDI P S forward	5' GAGAGA **GAATTC** ACCCTGGAATCTGTTAAAGATG 3'
LDI P Xho	5' GAGAGA **CTCGAG** TTA TCCCGGCTCCTGGACGGACG 3'
LDI P HisXho	5'GAGAGA **CTCGAG** TTA GTGGTGGTGGTGGTGGTG 3'

Primers with optimized codon usage

Name	Sequence
LDI-1:	5'GAGAGA**CATATG**ACCCTGGAATCTGTTAAACATGAATGTCAGCCAGGTGTTTTT CCACATAACCCACTGGCCACCTGT 3'
LDI-2:	5' CAGCATTGGTCTGGATGGACCTCTACCACAAACTCTTTTAATAACATAGGTATG ACAGGTGGCCAGTGGGTTATCTGG 3'
LDI-3:	5' AGAGGTCCATCCAGACCGATGCTGGTTAAAGAAAGATGTTGTAGAGAACTGGCC GCCGTTCCAGATCATTGTAGATGT 3'

Primers for L. lactis constructs

Name	Sequence
F lacto	5' GAGAGA **AGATCT** ACCCTGGAGAGCGTCAAGGACG 3'
R lacto	5' GAGAGA **CTGCAG** TTA TCCCGGCTCCTGGACGGACG 3'
R lactoHis	5' GAGAGA **CTGCAG** TTA GTGGTGGTGGTGGTGGTG 3'

2.7.3 Transformation

The expression vectors were transformed into the chemical competent *E. coli* strains Oregami, Tunar, BL21, and Rosetta using standard procedures (Sambrook and Russells, 2001).

pPICZa/LDI-CHIS was linearized by *Pme* I and transformed into *P. pastoris* X-33 according to standard procedures and spread on YPDS plates (yeast extract peptone dextrose medium with sorbitol). Plates were left for 48 h at 30^{o}C.

pAMJ399/LDI and pAMJ399/LDI-CHIS were transformed into *L. lactis* subsp. *cremoris* strain MG1363 using standard procedures (Gasson, 1983) under supervision of Jan Martinussen.

2.7.4 Growth and harvest of cells

E. coli cells containing the expression plasmids were grown at 15, 20 or 37°C and at an OD_{600} = 0.8 the cells were induced by 5 or 100 μM IPTG. The growth was continued either overnight at 15°C or 20°C and 2-3 h at 37°C. Stressing of the cells was done by addition of 5% ethanol at the time of induction or cold shock by placing the cells on ice for 10 min before induction. The level of expression was tested using western blot on samples of 200 μL cell culture, which was spun down and resuspended in 15 μL SDS sample buffer containing DTT and boiled for 7 min before running of SDS-PAGE and blotting onto a nitrocellulose membrane.

Cells were harvested by centrifugation (4°C, 4000 rpm, 10 min) and resuspended in BugBuster (Novagen) including DNase for 20 min at room temperature for rupture of the cell wall. Cell debris was spun down at 4°C, 12000 rpm, 30 min and the supernatant was used for protein purification.

Twenty transformed colonies of *P. pastoris* X-33 containing pPIZα-LDI-CHIS were tested for LDI production by immunostaining of the colonies. Cells were grown on BMM (buffered minimal methanol) plates with nitrocellulose membrane on top for three days at 30°C. LDI was detection by using specific antibodies.

100 mL M17 medium containing 1 μg/mL erythromycin and 5 g/L glucose was inoculated with MG1363/pAMJ399-LDI and MG1363/pAMJ399-LDI-CHIS. A pH shift during fermentation induced the P170 promotor. Cells were spun down and the pellet washed with 0.9% NaCl and resuspended in 5 mL 50 mM Tris pH 8.0. 20 μL of the resuspended pellet and 20 μL of the supernatant were applied to SDS-PAGE. The supernatant was concentrated 3-fold and 150 μL was used for LD activity inhibition assay.

2.7.5 Protein purification

The protein extract was filtered using a 0.22 mm filter and applied manually using a syringe to a 1 mL HiTrap chelating HP nickel column (GE Healthcare) pre-equilibrated with 50 mM Tris, pH 8.0, 0.5 M NaCl, 50 mM imidazole. The column was washed with 10 mL 50 mM Tris, pH 8.0, 0.5 M NaCl, 50 mM imidazole and 5 mL 50 mM Tris-HCl, pH 8.0, 0.5 M NaCl, 100 mM imidazole and Trx-ECL-LDI-His_6 was eluted in 50 mM Tris, pH 8.0, 400 mM imidazole and fractions of 1 mL were collected. The protein was eluted in fraction 2-4 and these were combined and dialyzed against 20 mM Tris-HCl, pH 8.5, 50 mM NaCl, 2 mM $CaCl_2$.

2.7.6 Cleavage of Trx-ECL-LDI-His_6

100 μL Trx-ECL-LDI-His_6 fusion protein (3.4 mg/mL) was cleaved with 3.5 μL enteropeptidase (2 U/μL; Novagen) overnight at 16°C.

2.7.7 Refolding of Trx-ECL-LDI-His_6

This protocol was based on (Jaenicke and Rudolph, 1989). The fusion protein was denatured in 100 mM Tris-HCl, pH 8.5, 6 M Gdm-HCl, 22 nM DTT with a final concentration of 5 mg/mL fusion protein. The protein was diluted into the renaturation buffer to a concentration of 50 μg/mL. Renaturation was carried out in 0.1 M Tris-HCl 1 mM EDTA with all combinations of the following conditions: pH 7.5 or 9.0, GSH:GSSG 2:1 (2 mM :1 mM) and 10:1 (3 mM : 0.3 mM), $(NH_4)_2SO_4$ 0 M, 0.2 M, 3½ or 22 h incubation time. In addition 1 M Gdm-HCl in the renaturation buffer and different protein concentrations during renaturation were tested. Renaturation efficiency was tested using LD inhibition assays.

2.7.8 Immuno-detection of LD and LDI in barley seed protein extracts

For LDI detection proteins were extracted from a single barley seed or from endosperm from 5 seeds (Finnie et al., 2002) in 0.2 mM sodium acetate pH 5.0 with or without 20 mM DTT. The extracts (18 μL) were applied to SDS-PAGE and LDI was detected using specific antibodies.

For LD detection proteins were extracted from whole dry seeds, 3 days or 6 days germinated seeds as described in section 2.1. Nine μL protein extract (9-22.5 μg, depending on extract) from each time point was applied to SDS-PAGE and LD was detected using specific antibodies.

Chapter 3 - Results

The Results Chapter of the present work has been divided in three parts. The first part describes 2DE analysis of dissected barley seed tissues during germination and radicle elongation, the second part concerns the analysis of enzymes involved in the ascorbate-glutathione cycle, and the last part presents the results from several attempts of producing recombinant LDI. Each part will end with a discussion, while in Chapter 4 a discussion regarding the main points of the thesis work is presented.

3.1 Proteome analysis of dissected barley seed tissues

The work presented and discussed here is related to the proteome analysis of germination and radicle elongation in dissected barley seed tissues. Protein spots from 2D gels are tracked through 8 time points (0-72 h PI) in each tissue (embryo, aleurone layer and endosperm) and spatio-temporal profiles of the proteins will be addressed. Only protein spots that have been identified by MS and that change in abundance in the studied time period will be mentioned; this concern 48 proteins in 79 spots. An overview of the identified protein spots that change in abundance are given in Figures 3.1, 3.2, and 3.3 for the embryo, aleurone layer, and endosperm, respectively. These figures present the 2D gels from non-germinated and 72 h germinated seeds tissues. Selected examples of protein profiles will be shown in figures throughout the chapter. 2D gels from each time point in each tissue are presented in Appendix 1a-c for further details. Appendix 2 contains 2D gels of embryos germinated in isolation compared to embryos from whole-seed germination.

3.1.1 Plant material and protein extraction

Tissues from five barley seeds were used for each protein extraction, making it important that the seeds germinated homogeneously. Germination efficiency and homogeneity were determined by a preliminary test where 100 seeds in 9 cm Petri dishes were incubated with 4 mL tap water at 20^{o}C in the dark (standard germination conditions according to European Brewing Convention). After 24 h and 48 h, 88.3% and 99.3% of the seeds germinated, respectively, corresponding to a germination index of 8.87 (Riis et al., 1991; Riis et al., 1995). A germination index above 7 is required for malting barley (Riis et al., 1991; Riis et al., 1995), thus the seeds were considered to be of sufficient quality for the analysis. The chosen malting cultivar was previously used as reference in related proteomics studies (Østergaard et al. 2002, 2004; Finnie et al. 2002, 2006; Bak-Jensen et al., 2004). Portions of hundred seeds (germinated at 15^{o}C as in related studies, Østergaard et al. 2002, 2004, Bak-Jensen et al., 2004) were frozen in liquid nitrogen at 4, 12, 24, 36, 52, 60, and 72 h PI and stored at -80^{o}C until use. At these conditions germination was finished by 24-36 h PI, where the radicle penetrated the seed coat and radicle elongation began. Seeds were carefully selected with respect to visual homogeneity and used for dissection and small scale protein extractions under conditions that excluded the vast majority of the storage proteins (i.e. hordeins) to enable identification of the less abundant metabolic proteins.

The small scale protein extractions from the dissected tissues were difficult to compare directly. Therefore exact determination of protein concentrations was necessary and the same

amount of protein was applied onto the gels. The amount of water soluble proteins from whole seeds increased approximately 2.5 fold during the germination mainly due to release of bound proteins in the endosperm. This fact had to be taken into account when gels of endosperm were compared since decreased spot intensity could result from increase in abundance of other proteins.

3.1.2 2D gels from the analyzed tissues

Generally an enormous number of changes take places in the protein pattern of the 2D gels from the point of imbibition and the following 72 h. The three analyzed tissues have different functions in the germination and the subsequent radicle elongation as illustrated by the 2D gel protein patterns of the different tissues.

The increase in the number of protein spots on the 2D gels observed from embryo was due to the many cellular processes that take place upon imbibition (Figure 3.1). Many of the proteins are low abundant and only visible as small spots on a silver stained gel and could therefore not be identified by MS (Section 3.1.3).

The aleurone layer is a living tissue that regains metabolic activity PI along with the embryo and there are several similarities between the 2D patterns of these tissues (Figure 3.2). However, the aleurone layer undergoes programmed cell death at approximately day 4-6 PI, when the production of hydrolytic enzymes is finished.

The endosperm 2D gel protein patterns is dominated by the abundant α-amylase and trypsin inhibitors (CM-proteins) at the low molecular, low pH range of the gel (Figure 3.3; Østergaard et al., 2004). These proteins are inhibitors of α-amylase and proteases of pathogens and are involved in defense. The main starch degrading enzyme, α-amylase, appears in several spots during radicle elongation along with a number of serpin spots.

3.1.3 Comparison of 2D gels and protein identification

Prior knowledge of 2DE of barley seed protein extracts combined with running of two-three 2D-gels for each time point of the present samples ensured high reproducibility of the gels. Analysis with 12 h intervals was necessary to follow the individual proteins during the process, and a first time point of 4 h was chosen to detect immediate changes PI. An example from three replicates of 2D gels of embryo extract from non-germinated seed is given in Figure 3.4. Silver staining is generally sensitive, but it has been reported that protein spots from silver stained gels give low sequence coverage by MS compared to CCB stained gels (Biron et al., 2006). Moreover, silver staining is not quantitative because the staining intensity differs from protein to protein and has no linear dynamic intensity range corresponding to quantitative changes in protein contents. The latter disadvantage of silver staining was a minor problem in this study, because spot intensities of the same protein throughout germination and radicle elongation were compared. Proteins were identified from CBB stained gels from non-germinated or 72 h germinated seed tissues based on the protein patterns in the silver stained gels. The comparison of gels was complex since the individual spots were followed through gels from eight time points and also between the three tissues. Therefore the gels were compared manually by overlay of two-three gels at the time. Proteins that were by experience found to be constant during the germination process were used as markers for spot intensity and mobility, i.e. spot 220 and 103 (superoxide dismutase), spot 142 (GSH-dependent dehydroascorbate reductase) and spot 95 (triose phosphate isomerase; Figure 3.1). Due to the high reproducibility spots could be followed and identified from previously run 2D gels of extract of whole dry seeds, malt and developing seeds (Østergaard et al., 2002, 2004,

Finnie et al., 2002, 2006). Seventy-nine protein spots were analyzed of which 25 new identifications were made in the present study.

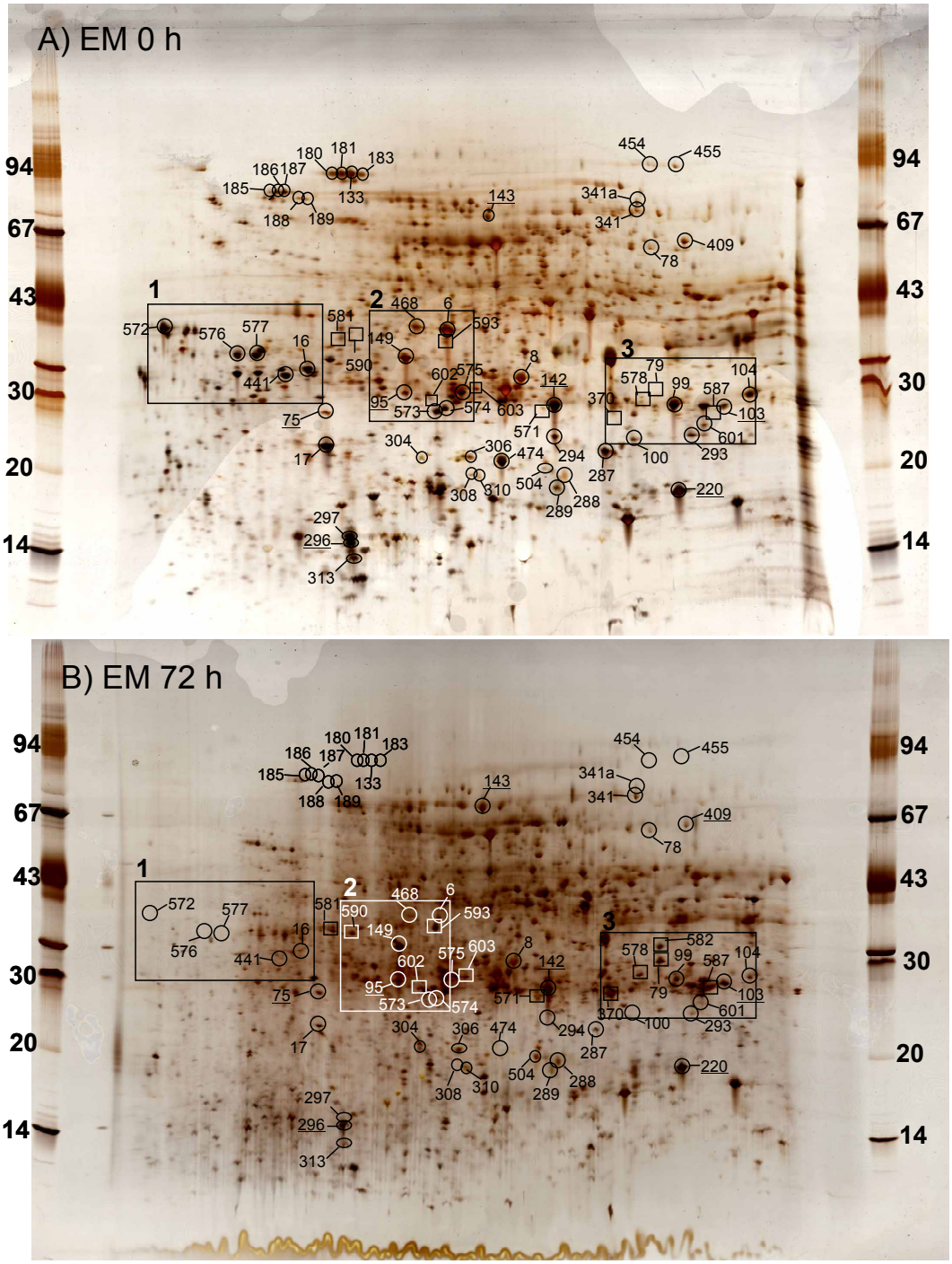

Figure 3.1. 2DE patterns pH range 4-7 of embryo of A) non-germinated seeds and B) 72 h PI. Encircled and squared spots are identified proteins that decrease and increase in abundance during germination and radicle elongation. Underlined numbers mark spots that remain constant during 0-72 h PI. Boxes 1-3 indicate regions for which close-up views are shown in Figures 3.6, 3.7, and 3.8, respectively.

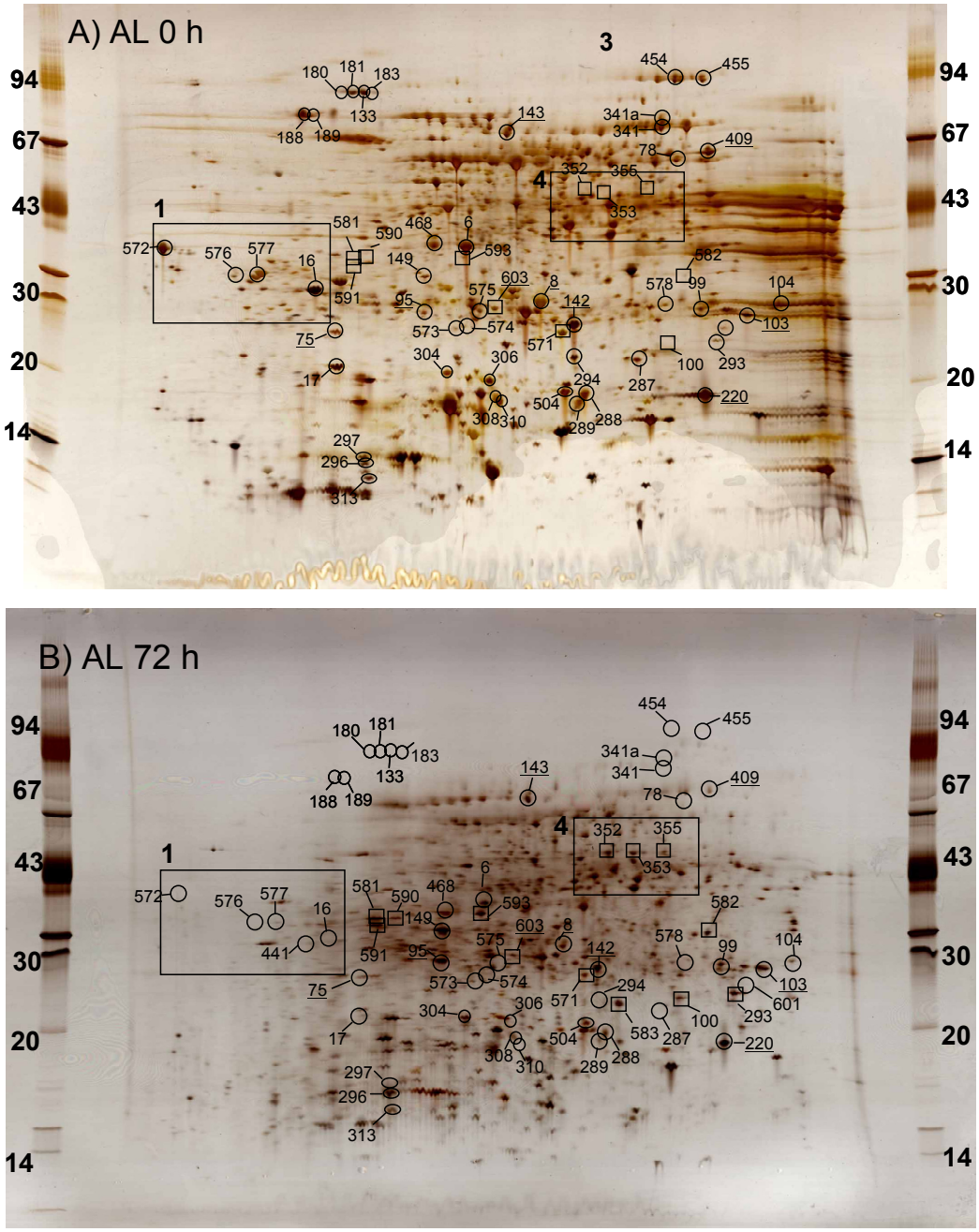

Figure 3.2. 2DE patterns pH range 4-7 of aleurone layer of A) non-germinated seeds and B) 72 h PI. Encircled and squared spots are identified proteins that decrease and increase in abundance during germination and radicle elongation. Underlined numbers mark spots that remain constant during 0-72 h PI. Boxes 1 and 4 indicate regions for which close-up views are shown in Figures 3.6 and 3.9, respectively.

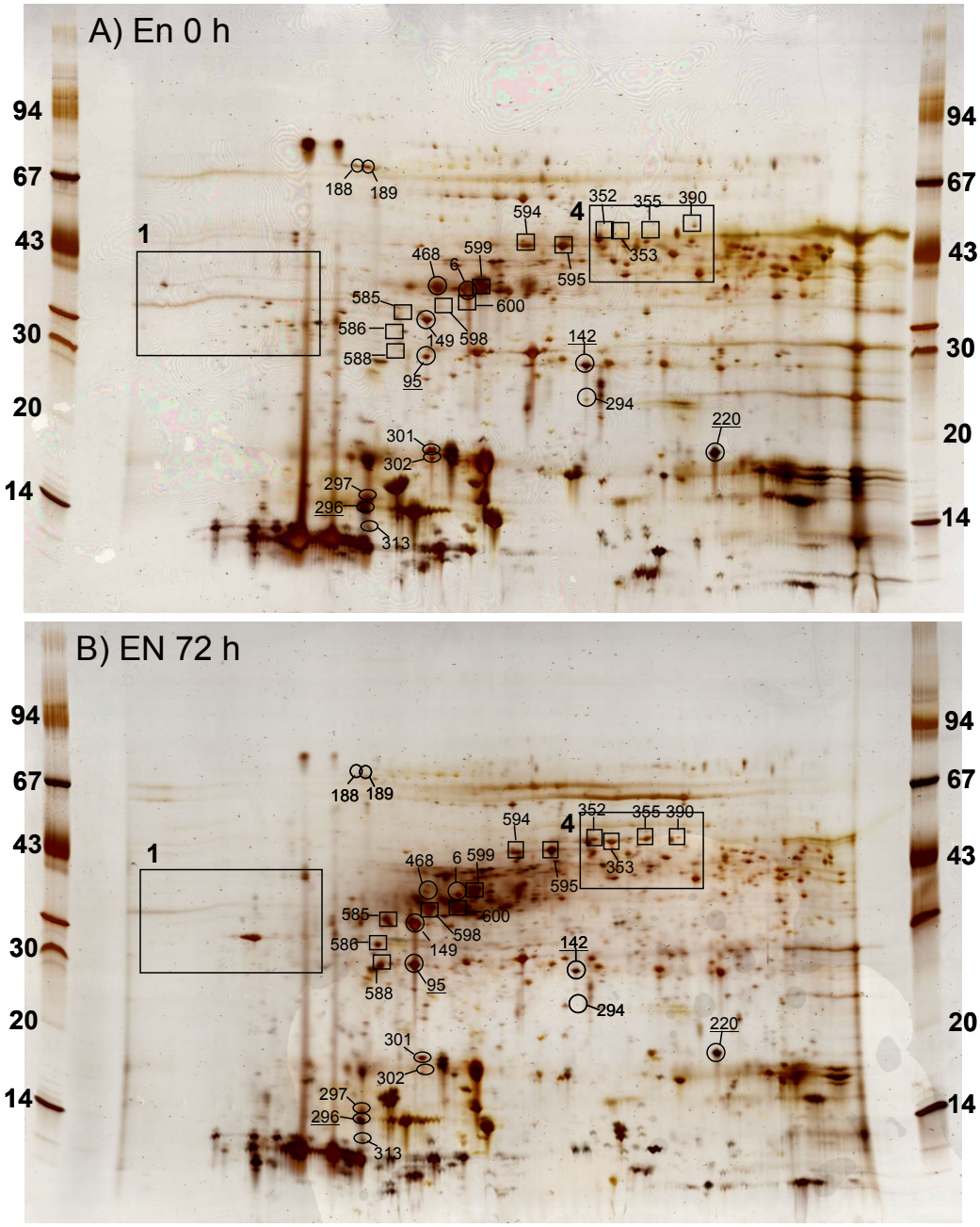

Figure 3.3. 2DE patterns of pH range 4-7 endosperm of A) non-germinated seeds and B) 72 h PI. Encircled and squared spots are identified proteins that decrease and increase in abundance during germination and radicle elongation. Underlined numbers mark spots that remain constant during 0-72 h PI. Boxes 1 and 4 indicate regions for which close-up views are shown in Figures 3.6 and 3.9, respectively.

Table 3.1. Identification and spatio-temporal appearance of proteins 0-72 h PI.

Functional class[a]	Spot ID	Protein	Change in abundance			Accesion #
			Embryo	Aleurone layer	Endosperm	
S (D)	254[c]	Late embryogenesis abundant proteinB19.1A*	↓ 24 h	÷	÷	Q05190
S (D)	579[b]	Late embryogenesis abundant protein B19.1B*	↓ 24 h	÷	÷	P46532
S (D)	474[d]	Late embryogenesis abundant protein B19.3	↓ 24 h	÷	÷	Q02400
S (D)	572[b]	Late embryogenesis abundant protein [wheat EST]	↓ 24 h	↓ 24 h	÷	TC191711
S (D)	16[d], 441[d]	Late embryogenesis abundant protein [EST]	↓ 24 h	↓ 24 h	÷	BG366433
S (D)	576[b]	Homolog to rice putative abscisic acid-induced protein [EST]	↓ 24 h	↓ 24 h	÷	TC191428
S (D)	577[b]	Homolog to rice putative abscisic acid-induced protein [EST]	↓ 24 h	↓ 24 h	÷	TC191428
S (D)	573[b], 574[b]	Homolog of rice putative embryonic protein [EST]	↓ 12 h	↓ 24 h	÷	TC142245
S (D)	575[b]	Homolog of rice putative embryonic protein [EST]	↓ 24 h	↓ 12 h	÷	TC142245
S (D)	17[d]	Cold-regulated protein Cor14b (barley)	↓ 36 h	↓ 60 h	÷	AJ29125
S (D)	100[c]	Aldose reductase (fragment)	↓ 12 h	↑ 72 h	÷	P23901
S (D)	293[c]	Aldose reductase (fragment)	↓ 24 h	↑ 24 h	÷	P23901
S (D)	583[b]	Aldose reductase (fragment)	÷	↑ 52 h	÷	P23901
S (D)	6[d], 468[c]	Homologous to glyoxalase I from rice (fragment) [EST]	↓ 24 h	↓ 52 h	↓ 52 h	Q9ZWJ2
S (D)	149[c]	Homologous to glyoxalase I from rice (fragment) [EST]	→	↑ 36 h	↑ 24 h	Q9ZWJ2
S (D)	585[b]	Homologous to glyoxalase I from rice (fragment) [EST]	÷	÷	↑ 24 h	Q9ZWJ2
S (D)	586[b]	Homologous to glyoxalase I from rice (fragment) [EST]	÷	÷	↑ 36 h	Q9ZWJ2
S (O)	409[d]	Glutathione reductase	→	↓ 52 h	÷	AV916384
S (O)	103[d]	Superoxide dismutase Mn	→	→	÷	T06258
S (O)	301[d]	Superoxide dismutase Cu-Zn, (chloroplast) [EST]	÷	÷	↓ 36 h	T06800
S (O)	302[d]	Superoxide dismutase Cu-Zn 2 (chloroplast) [EST]	÷	÷	↓ 60 h	T06800
S (O)	99[c]	Peroxiredoxin (1-Cys peroxiredoxin)	↓ 36 h	↓ 36 h	÷	P52571
S (O)	104[d]	Peroxiredoxin (1-Cys peroxiredoxin)	↓ 36 h	↓ 36 h	÷	P52571
S (O)	571[b]	Barley seed peroxidase 1 (fragment) [EST]	↑ 4 h ↓ 52 h	↑ 12 h ↓ 52 h	↑ 60 h	Z34917
S (O)	75[d]	Thioredoxin peroxidase (2-Cys peroxiredoxin)	→	→	÷	BM376549
S (O)	296[d]	Thioredoxin h1	→	↓ 60 h	→	BM374793
S (O)	297[d]	Thioredoxin h1	↓ 36 h	↓ 36 h	↓ 36 h	BM445252
S (O)	313[d]	Thioredoxin h2	↓ 52 h	↓ 60 h	↓ 36 h	BM445252
S (O)	79[c]	Ascorbate peroxidase	↑ 36 h	÷	÷	AJ006358
S (O)	142[c]	GSH-dependent dehydroascorbate reductase 1 [EST]	→	→	↓ 12 h	BE601917

S (O)	294[c]	GSH-dependent dehydroascorbate reductase 1 [EST]	↓ 24 h	↓ 12 h	↓ 12 h	BE601917
P	185[d], 186[d], 187[d], 188[d], 189[d]	Protein disulphide isomerase	↓ 60 h	↓ 36 h	↓ 4 h	P80284
P	133[d], 180[d], 181[d], 183[d]	Heat shock protein 70	↓ 60 h	↓ 36 h	÷	P11143
P	603[b]	Heat shock cognate protein 70 (fragment) [EST]	↑ 4 h	→	÷	TC138918
P	304[d]	sHSP- Class I small heat shock protein	÷	↓ 12 h	÷	CAA69172
P	305[d]	sHSP- Class I small heat shock protein	↓ 36 h	↓ 12 h	÷	TC135297
P	306[d]	sHSP- Low molecular mass heat shock protein	↓ 52 h	↓ 36 h	÷	TC56126
P	288[d]	sHSP- Class II small heat shock protein [EST]	↓ 36 h	→	÷	TC45769
P	310[d]	sHSP- Class II small heat shock protein [EST]	↓ 36 h	↓ 12 h	÷	TC45769
P	308[d]	sHSP- Class II small heat shock protein [EST]	↓ 36 h	↓ 36 h	÷	TC45773
P	504[d]	sHSP 16.9B	↓ 36 h	→	÷	S21600
P	289[d]	sHSP 17.3 kDa	↓ 36 h	→	÷	S16525
P	598[b], 599[b], 600[b]	Protein Z (Z4) serpin	÷	÷	↑ 52 h	CAA66232
P	582[b]	sHSP70 (fragment)	÷	↑ 60 h	÷	TC169366
E	352[d]	α-Amylase	÷	↑ 60 h	↑ 72 h	P04063
E	353[c]	α-Amylase	÷	↑ 52 h	↑ 60 h	P04063
E	355[c]	α-Amylase	÷	↑ 52 h	↑ 72 h	P04063
E	390[d]	α-Amylase	÷	÷	↑ 72 h	P04063
E	593[b]	CPase I A carboxyepeptidase	↑ 36 h	↑ 52 h	÷	1314177A
H	95[d]	Triose phosphate isomerase	→	→	↑ 36 h	P34937
H	588[b]	Triose phosphate isomerase	÷	÷	↑ 60 h	P34937
H	454[d]	Aconitate hydratase (cytoplasmic)	↓ 52 h	↓ 24 h	÷	BQ458967
H	455[d]	Aconitate hydratase (cytoplasmic)	↓ 52 h	↓ 24 h	÷	BQ466008
H	341a[d]	2,3-Bisphosphoglycerate-independent phosphoglycerate mutase [EST]	↓ 52 h	↓ 12 h	÷	BM371359
H	341[d]	2,3-Bisphosphoglycerate-independent phosphoglycerate mutase [EST]	→	↓ 52 h	÷	BM371359
H	143[d]	2,3-Bisphosphoglycerate-independent phosphoglycerate mutase [EST]	→	→	÷	TC63693
H	590[b]	Enolase (fragment) [EST]	↑ 24 h	↑ 36 h	÷	AW039978
H	581[b]	Enolase (fragment) [EST]	↑ 24 h	↑ 36 h	÷	CA017808
H	591[b]	Enolase (fragment) [EST]	÷	↑ 36 h	÷	CAA63121
H	287[c]	Initiation Factor 5A (eIF-5a)	↓ 24 h	↓ 12 h	÷	BF259508
H	578[b]	Proteasome subunit β-type [EST]	↑ 4 h	↓ 52 h	÷	O64464
H	602[b]	Proteasome α-subunit [EST]	↑ 24 h	÷	÷	TC147115
H	78[d]	Alanine aminotransferase	↓ 72 h	↓ 36 h	÷	P52894

H	601[b]	Transcription factor homolog BTF3-like protein [EST]	↓ 24 h	÷	÷	TC131691
U	587[b]	Probable jasmonate induced protein	↑ 52 h	÷	÷	X98124
U	370[c]	Probable jasmonate induced protein	↑ 52 h	÷	÷	X98124
U	8[c]	Embryo specific protein [EST]	↓ 52 h	↓ 52 h	÷	Q9ZNS9

The arrows indicate at what time point the protein spot start to either increase ↑ or decrease ↓ in abundance. Some proteins disappear, others only decrease in abundance (most spots can be followed in Figures 1-5). → indicates that the protein spot is constant during 0-72 h PI and ÷ indicates that the protein spot is not present in the specific tissue.

*appears only in CCB stained gels because it is negatively stained by silver staining.

[a] Functional categories: S (D): desiccation-, osmotic-, and salt stress; S (O): oxidative stress; P: protein synthesis, folding and storage; H: housekeeping; E: enzymes for storage compound degradation; U: proteins with unknown function.

[b] Identified in the present work.

[c] Published in (Østergaard et al., 2002, 2004) and re-identified in the present work.

[d] Published in (Østergaard et al., 2002, 2004).

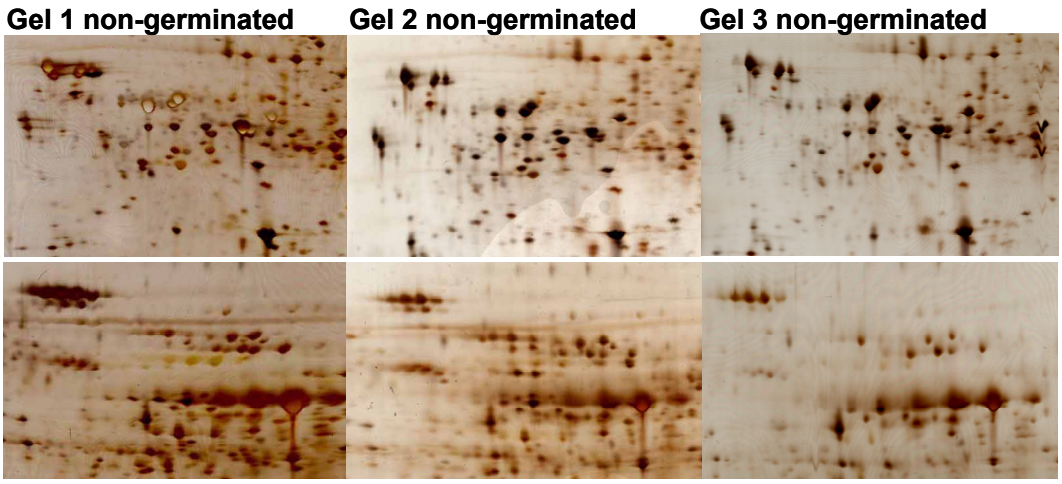

Figure 3.4. Reproducibility of the 2D gels. Two areas of 2D gels of non-germinated embryos shown for three replicates. The amount of loaded protein varies slightly. The gel sections represent an area of Mw: 25-49 kDa and pH: 4.1-4.9 (top row) and Mw: 50-100 kDa and pH 4.7-5.7 (bottom row).

3.1.4 Germination of isolated embryos

The influence of the other barley seed tissues (aleurone layer and endosperm) on germination of the embryo were tested by germination of isolated embryos on agar plates. 2D gels of these embryo extracts were compared to 2D gels of corresponding embryo extracts from whole seed germination. The degradation of LEA proteins happened equally fast and APX appeared at the same time and with same intensity in isolated germinating embryos as in embryos dissected from germinating whole seeds (Figure 3.5B, Appendix 2). This suggests that aleurone layer and endosperm tissues have no influence on the embryo during germination, supporting the hypothesis that the embryo is self-sufficient until the GA induced degradation of storage products during radicle elongation (Bewley and Black, 1994). At this stage 2DE patterns remained similar, but several high molecular weight protein spots were slightly reduced in abundance from the isolated embryos (Figure 3.5A). Addition of ABA during germination and radicle elongation of isolated embryos seemed without influence on germination, as the 2DE patterns were very similar to those of embryos isolated from germinating whole seeds (Figure 3.5, Appendix 2). We therefore suggest that ABA maintains dormancy and plays a minor role in the present non-dormant seeds.

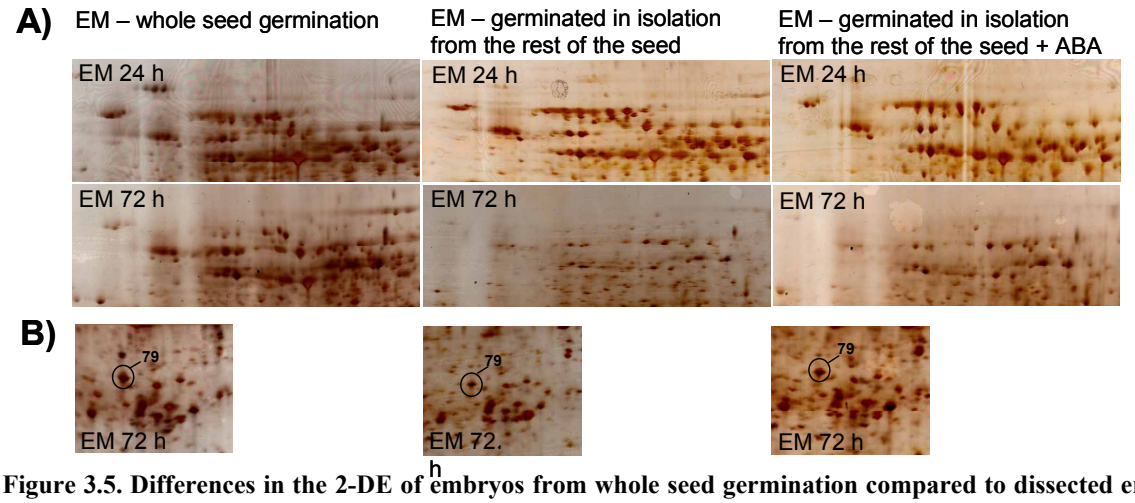

Figure 3.5. Differences in the 2-DE of embryos from whole seed germination compared to dissected embryos germinated in isolation from the rest of the seed with and without ABA. A) Presence of high molecular protein at 24 h PI (top row) compared to 72 h PI (bottom row). Mw 56-86 kDa and pH 4.7-6.0. B) Presence of APX at 72 h PI in three two spot patterns. Mw: 25-39 kDa and pH: 6.05-6.42.

3.1.5 Changes in the barley seed proteome during germination

Comparison of the 2D gels revealed many changes at the protein level in the three tissues during the germination and the radical elongation of the three tissues (Figures 3.1, 3.2, and 3.3; Table 3.1). Changes in spot pattern can reflect degradation and synthesis of proteins, as well as post-translational modifications, for example phosphorylation. Furthermore it is possible that some spots vary due to altered extractability of certain protein forms during the 72 h period.

The first protein that appeared in the 2DE patterns after imbibition was a β-type proteasome subunit (at 4 h PI) from embryo (Figure 3.8, spot 578) accompanied by an increase in a heat shock protein 70 fragment (Figure 3.7, spot 603). This was followed by appearance of an α-type proteasome subunit at the end of germination (24 h PI; Figure 3.7, spot 602). Other early changes were observed in the acidic part of the embryo proteome represented by late embryonic abundant (LEA) proteins (Figure 3.6, spot 572) and ABA-induced protein (Figure 3.6, spots 576, 577) present also in non-germinated aleurone, but absent in endosperm (Figure 3.6 B and C). Proteins that decrease during germination included LEA proteins in six spots (Fig. 3.1, spots 16, 254, 272, 441, 474, 579) corresponding to five different accessions (Table 3.1), a putative embryonic protein (Figure 3.7, spots 573, 574, 575), full length glyoxalase 1 (Figure 3.7, spots 6, 468), GSH-dependent dehydroascorbate reductase (Figure 3.1, spot 294), aconitate anhydrase (Figure 3.1, spots 454, 455), transcription factor homolog BTF3-like protein (Figure 3.8, spot 601), and two fragments of aldose reductase (Figure 3.8, spots 100, 293). All of these proteins are either associated with desiccation, osmotic, salt and oxidative stresses, or participate in the citric acid cycle. These changes underline the increased metabolic activity after start of imbibition. At the end of germination, i.e. the start of radicle protrusion (at approximately 24-36 h PI) modifications in spot patterns were highly significant and complex with proteins decreasing in abundance being involved in oxidative stress, glycolysis, citric acid cycle, and protein translation or acting as chaperones (Table 1).

The greatest number of new spots appeared at 36-72 h PI. These included ascorbate peroxidase (APX; Figure 3.8, spot 79), jasmonate-induced protein (Figure 3.8, spots 370, 587),

carboxypeptidase 1A (Figure 3.7, spot 593), α-amylase (Figure 3.2 and 3.3, spots 352, 353, 355, 390), the serpin protein Z (Z4) (Figure 3.3, spots 598, 599, 600), and fragments of HSP70 (Figure 3.2, spot 582), barley seed peroxidase 1 (Figure 3.1 and 3.2, spot 571, Laugesen et al., submitted) and an aldose reductase (Figure 3.2A, spot 583), respectively. The appearance of these fragments indicated degradation of the corresponding full length proteins.

The identified proteins were categorized (Table 3.1) into six functional classes; desiccation-, osmotic-, and salinity stress (S (D)), oxidative stress (S (O)), protein synthesis, folding and storage (P), housekeeping (H), enzymes for storage compound degradation (E), and proteins with other or unknown function (U). In general the proteins in a functional class share a similar temporal profile at germination and radicle elongation which makes it relevant to discuss each class individually.

3.1.6 Desiccation tolerance related proteins

The initial changes of germination were observed after 4 h in the acidic part of the embryo spot pattern (Figure 3.6) and some of the proteins involved were identified as LEA proteins and ABA induced protein. LEA proteins were much degraded at 12 h PI and very faint at 36 h PI in embryo and occurred in lower amounts in aleurone (Figure 3.6A and B). LEA proteins belong to the dehydrin superfamily that are known to contain a number of phsophorylation sites (Irar et al., 2006) which can be related to subcellular localization (Jensen et al., 1998), binding and retention of specific targets (Goday et al., 1994), and in the ion binding capacity and chaperone calcium-dependent functions (Heyen et al., 2002; Alsheikh et al., 2003). Although shifts in spot pattern at 4 h PI may reflect phosphorylation, it is not possible to assign changes to specific proteins as it is not clear from the spot pattern, which proteins are shifting (Figure 3.6) and MS provided only little sequence information. The change in spot pattern could also reflect a change in extractability of these proteins as an indirect effect of the imbibition.

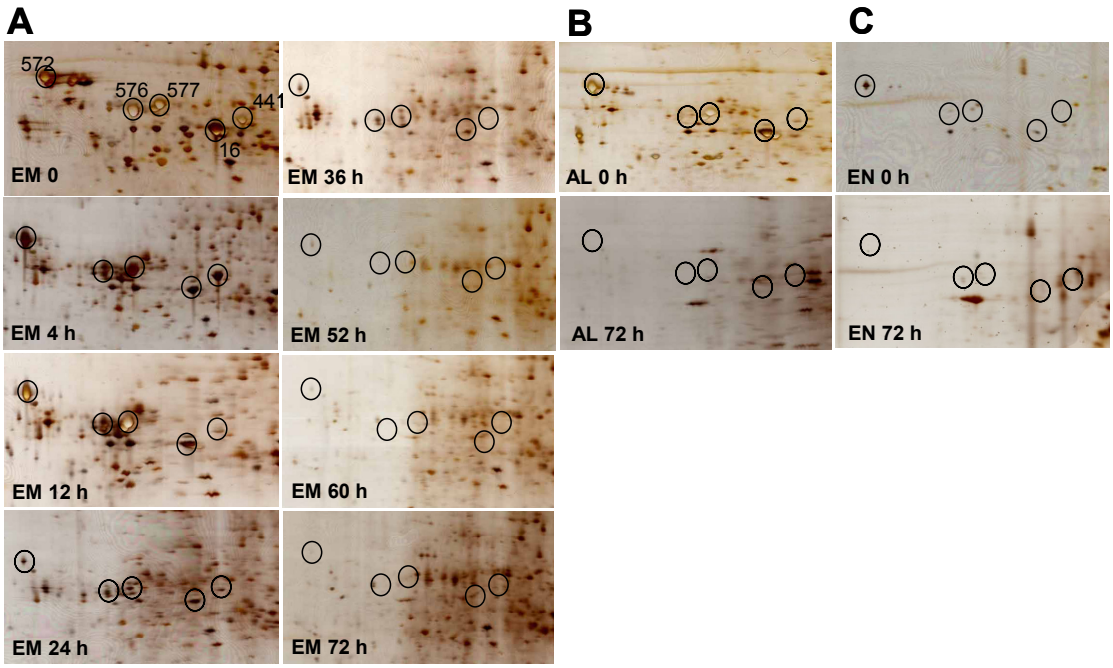

Figure 3.6. Temporal changes focusing on subpattern 1 (Figure 3.1, 3.2, and 3.2, box 1) of the A) embryo and comparison to B) aleurone layer and C) endosperm 2D gel patterns. Encircled spots are identified proteins which decrease in abundance and squared spots increase in abundance during germination and radicle elongation. Underlined numbers emphasize spots that remain constant during 0-72 h PI.

Other spots share spatio-temporal appearance with LEA proteins, including two charge variants of ABA-induced protein (Figure 3.6, spots 576, 577) and three forms of embryonic cell protein varying in size and pI (Figure 3.7, spots 573, 574, 575). The function of these proteins is unknown, but disappearance simultaneously with LEA proteins, proposes a role in desiccation. The precise function of these proteins is not known. LEA proteins are induced by cold, osmotic stress or exogenous ABA (Section 1.1.3.1). The cold regulated protein (Figure 3.1, spot 17) involved in desiccation stress (Crosatti et al, 1999) and present both in embryo and aleurone, decreased slightly after 4 h and then remained constant.

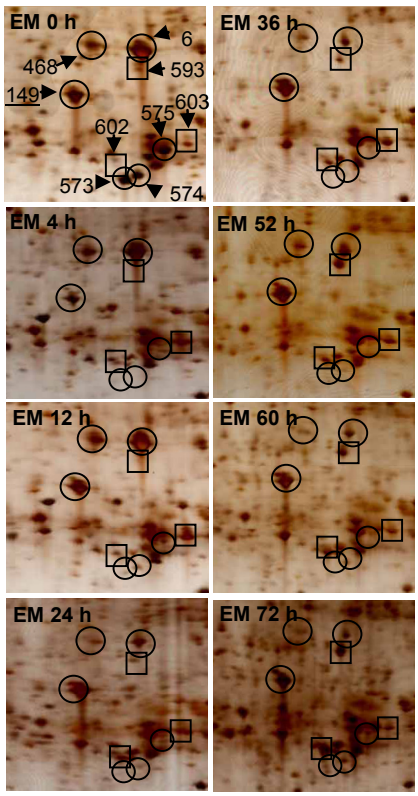

Figure 3.7. Temporal changes focusing on subpattern 2 (Figure 3.1, box 2) of the embryo 2D gel patterns. Encircled spots are identified proteins which decrease in abundance and squared spots increase in abundance during germination and radicle elongation. Underlined number emphasize spots that remain constant during 0-72 h PI.

Two full length forms of the highly abundant glyoxalase 1 that differed slightly in pI, decreased in all three tissues during germination (Figure 3.7, spots 6 and 468). In the endosperm, however, this decrease was slower and two additional spots containing glyoxalase I fragments appeared during the radical elongation (Figure 3.3, spots 585 and 586). These five forms of glyoxalase I originated from the same gene. The MS data provided no clues to the differences in molecular weight and pI and it is not known whether all the observed forms are active. Glyoxalase I is involved in the detoxification of methylglyoxal, which is a by-product of glycolysis. The role of glyoxalase I in seeds is not known, but it has been identified from wheat bran and a role during cold, salinity and desiccation tolerance was suggested (Johansen et al., 2000; Singla-Pareek et al., 2003). In contrast to the other desiccation stress related proteins it is also abundant in endosperm. The glyoxalase cycle is not essential for germination, but is important for seedling establishment and survival as demonstrated by characterization of two mutants in Arabidopsis, which lack the key enzyme isocitrate lyase (Eastmond et al., 2000).

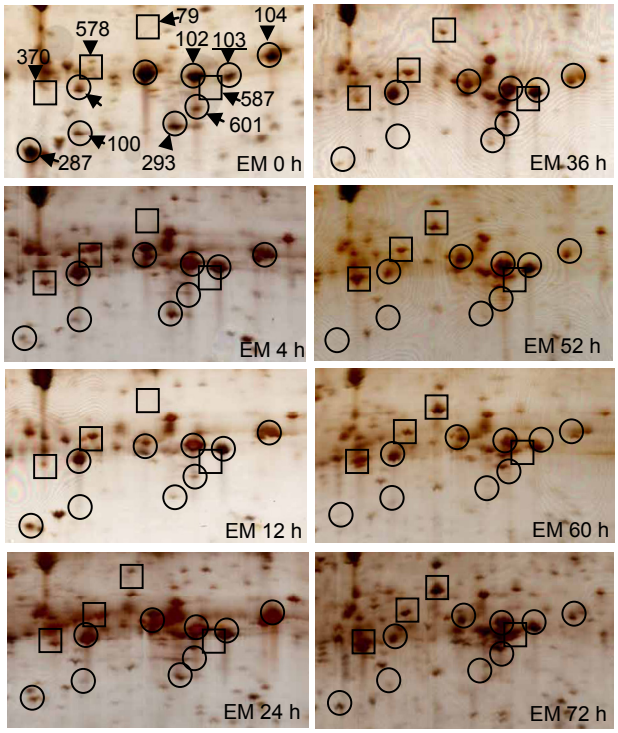

Figure 3.8. Temporal changes focusing on subpattern 3 (Figure 3.1, box 3) of the embryo. Encircled spots are identified as proteins with decreasing abundance and squared spots are identified as proteins with increasing abundance. Underlined numbers emphasize spots that remain constant during 0-72 h PI.

Several fragments of aldose reductase were present both in the embryo and aleurone layer, but with different spot patterns in the two tissues. Spots 100 and 293 (Figure 3.8) were present in both embryo and aleurone of non-germinated seeds and disappeared in embryo after 12-24 h, but increased in abundance in the aleurone at 24-72 h along with appearance of a third fragment of the same gene product (Figure 3.2, spot 583). This suggested that degradation of aldose reductase occurred at different speed in the embryo and in the aleurone layer, respectively. Three full-length forms of aldose reductase and one fragment, that all stem from the same gene, were identified in the pH range 6-11 gel of whole-seed extracts. The full-length forms decrease and the spot containing the fragment increased during 72 h PI in agreement with the present data (Bak-Jensen et al., 2004). Aldose reductase is produced at late stages of embryogenesis in response to ABA and was found also by Bartels et al. (1991) and Roncarati et al. (1995). The enzyme is normally considered the key enzyme in the polyol pathway leading to sorbitol from glucose (Jeffrey and Jörnvall, 1983), a common osmolyte helping to balance the cell osmotic strength with that of the environment during drought (Bartels, 1991).

The small heat shock proteins (sHSPs) also function in desiccation tolerance by the ability to bind to other proteins and to prevent protein aggregation. Several sHSP's (Figure 3.1 and 3.2, spots 288, 289, 304, 308, 310, 504) have been identified in the embryo and aleurone layer from non-germinated seeds and most of them decrease in abundance during radicle elongation in agreement with the literature (Hoekstra and Golovina, 2003).

3.1.7 Redox related proteins

Most proteins involved in oxidation stress that were identified in the present 2D gels were present in all three tissues and remained constant during germination. However, the low molecular weight form of GSH-dependent dehydroascorbate reductase (DHAR) decreased in abundance after 12 h in the aleurone layer and endosperm and after 24 h in the embryo (Figure 3.1, spot 294). The high molecular weight form remained constant in all tissues (Figure 3.1, spot 142). During radicle elongation the change in oxidative state of the seed upon imbibition apparently causes decrease in abundance of some of the oxidative stress related proteins whereas others remained constant.

APX removes hydrogen peroxide using ascorbate as an electron donor (Agrawal et al., 2003) and was found only in the germinated embryo (Figure 3.8, spot 79). The same spot was identified in the endosperm at the start of grain filling in addition to a spot containing a different APX isoform (Finnie et al., 2003). This appearance pattern in developing and germinating seeds agreed with the previous studies of APX activity during desiccation of cereal seeds suggesting that the ascorbate system was not involved in desiccation tolerance (Bailly, 2004). The level of an APX mRNA was up-regulated in the embryo during germination (Potokina et al., 2002) in accordance with the present protein profile.

In the endosperm one spot containing superoxide dismutase decreased during germination and another disappeared (Figure 3.3, spots 301 and 302, respectively). This protein form was not visible in 2D gels of embryo and aleurone layer. Two different superoxide dismutase-containing spots remained constant in all tissues during 72 h PI (Figure 3.1, spots 220, 103). Peroxiredoxin (Figure 3.8, spots 99, 104) decreased after 24 h and was only observed from embryo and aleurone layer. This protein was studied in detail during barley seed development (Finnie et al., 2006) where it appeared as three different forms of distinct temporal profiles during grain filling and desiccation. Barley seed peroxidase 1 was found in a single spot from all three tissues at 60 h PI as what appeared to be a fragment of Mw of 28.8 kDa (Figure 3.1 and 3.2, spot 571) of a 36.1 kDa full-length form found in the basic pH range, that includes a total of 13 peroxidase spots from whole seed extracts, representing three accessions (Bak-Jensen et al., 2004; Laugesen et al., submitted). Based on the present identification a barley seed peroxidase 1 fragment seems to be present in all three tissues. Glutathione reductase (Figure 3.1, spot 409) decreased slightly in embryo and aleurone during radicle elongation and was not found in endosperm.

Two thioredoxin h1 (Trx h1) spots and one thioredoxin h2 (Trx h2) spot were found from the three tissues (Maeda et al., 2003). Trx h1 (Figure 3.1, 3.2, and 3.3 spot 296) was most abundant in embryo, but essentially remained constant in the three tissues, whereas the other Trx h1 (Figure 3.1, 3.2, and 3.3, spot 297) and Trx h2 (Figure 3.1, 3.2, and 3.3, spot 313) in all tissues decreased during radicle elongation. As decribed in Section 1.4, Trx h is thought to play a central role in the malting process for mobilization of storage proteins and a large number of proteins have been suggested to be Trx h targets. Some of these have been studied in the present work, i.e. LD, LDI, APX and DHAR and this will be discussed in Section 3.2 and 3.3. Trx h is under control of GA and reaches maximum in the endosperm at 48 h PI and in the embryo it increases up to 72 h PI (Lazano et al., 1996; Marx et al., 2003)

3.1.8 Housekeeping proteins

Enzymes involved in glycolysis were present and decreased during germination and radicle elongation, respectively, reflecting the high energy demand of germination. Although this seems to be fulfilled mainly by glycolysis, strong expression of pentose-phosphate pathway transcripts in germinating seeds has been reported (Zhang et al., 2004). Full length enolase was represented in all three tissues in two-three isoforms, although only weakly in the metabolically inactive endosperm. Fragments of enolase appeared in embryo and aleurone (Figure 3.1 and 3.2, spots 581, 590, 591) suggesting that turn-over of enolase takes place even though no significant decrease of full length forms seems to occur. Three spots (Figure 3.1, spots 143, 341, 341a), containing 2,3 bisphosphoglycerate-independent phosphoglycerate mutase from two different genes found from embryo and aleurone. Spot 341a decreased in abundance after 24 h and 52 h, respectively, whereas spots 143 and 341 remained constant (Figure 3.1). These and one additional 2,3 bisphsophoglycerate-independent phosphoglycerate mutase containing spot (all shared the same database accession) were previously reported to differ in timing of appearance during grain filling (Finnie et al., 2006). Aconitate hydratase (Figure 3.1, spots 454, 455), involved in the citric acid cycle was also present in embryo and aleurone layer and decreased during radicle elongation. Four spots containing triose phosphate isomerase have been identified in the barley mature seed proteome pattern (Østergaard et al., 2004). These four spot are present in all three tissues at a constant level and an additional spot appears in the endosperm during germination (Figure 3.3, spot 588).

3.1.9 Protein synthesis, folding and storage

Five spots containing protein disulfide isomerase (PDI), four full length forms and two fragments of HSP70 and six spots containing various sHSPs were observed in all tissues and generally decreased in intensity at radicle elongation. The fastest loss occurred in the endosperm where PDI may serve as a storage protein. PDI was present throughout seed development, whereas HSP70 and sHSPs appeared during grain filling and after onset of desiccation, respectively (Finnie et al., 2006). sHSPs might act as molecular chaperones in seed dehydration and during the first few days of rehydration (Hoekstra and Golovina, 2003).

The serpin protein Z4 was identified in endosperm of non-germinated seed in three spots in three new intense spots appearing at 52 h PI (Figure 3.3; spots 598, 599, 600). After imbibition protein Z is released from a bound form by cysteine proteases (Hejgaard, 1982). The serpins cover the central part of the 4-7 pH range 2D gels (Østergaard et al., 2004) and it is difficult to monitor other proteins in this area. This emphasizes the importance of dissecting the barley seed before 2DE analysis. The biochemical role of plant serpins is still unclear, however, serpins behave as storage proteins because they respond as hordeins to the change in nitrogen level (Giese and Hejgaard, 1994) They may also provide protection against insect pathogens (Østergaard et al., 2000).

3.1.10 Enzymes for storage compound degradation

α-Amylase, the main starch degrading enzyme, was identified in three and four spots from both the aleurone layer and endosperm at 52 h and 60 h PI, respectively (Figure 3.9). A few additional spots containing α-amylase fragments appeared in endosperm from 72 h PI as identified by western blotting and MS (Bak-Jensen et al., 2007). Carboxypeptidase 1A (Figure 3.6, spot 593) appeared in the embryo 2DE at 36 h PI and in aleurone at 52 h PI. According to cDNA microarray data carboxypeptidase 1A is found in the scutellum and not the embryo (Potokina et

al., 2002), but in the present work these two tissues were not separated. This protein has been suggested to be a marker for malting quality as it provides amino acids for *de novo* synthesis of proteins (Potokina et al., 2006).

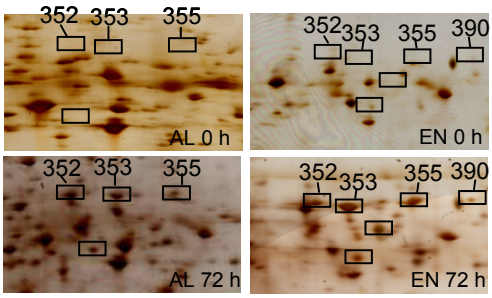

Figure 3.9. Temporal changes focusing on subpattern 4 (Figure 3.2 and 3.3, box 4). Appearance of α-amylase containing spot in the aluerone layer (AL) and the endosperm (EN) at 72 h PI. Numbered spot are identified by MS and un-numbered squared boxes are α-amylase spots identified based on western blotting (Bak-Jensen et al., 2007).

3.1.11 Proteins with other functions

Two spots from the 2DE pattern from 72 h days germinated barley extracts were identified as probable jasmonate induced protein 23 (JIP-23; Figure 3.8, spots 370, 587). The proteins in both spots were identical according to the MS and were identified as an EST with high homology to the known barley JIP-23 (Müller-Uri et al., 2002). Expression of JIP-23 is related to environmental stresses such as desiccation stress and osmotic stress. In accordance with the present observations JIP-23 expression has been found in developing seeds and in growing seedlings, but not in dry seed (Demus, 1999). The jasmonate pathway is important for wounding and production of JIP-23 during radicle elongations may be induced by the rupture of the seed structures. JIP-23 expression was identified in an mRNA microarray study of barley seed germination (Watson and Henry, 2005).

The CM-proteins are trypsin and α-amylase inhibitors that are highly abundant in the endosperm of the barley seed. Their name refers to the appearance in chloroform/methanol extracts of flour and these inhibitors also referred to as “cereal-type (Franco et al., 2002). They are involved in defense against pathogens but also serve as storage proteins that are degraded during seedling growth. They are highly abundant in the endosperm and found in a much lesser amount in aleurone layer, where they may represent contamination from the endosperm. The levels of most CM-proteins appeared to be constant during the first two days of germination, followed by a decrease in spot intensities (Figure 3.3; Østergaard et al., 2004).

3.1.12 Discussion

3.1.12.1. The proteomics approach

The approach used for proteome analysis clearly shows many changes during germination and in particular during radicle elongation. Germination of seeds is generally difficult to study because a population of seeds does not germinate synchronously and no visible signs of germination can be observed until 24 h PI. By using barley seeds with a high germination index, selecting 5 seeds

for each extraction, repeating extractions, and running replicate 2D gels ensured high reliability of the changes in the 2D gels. Also by careful tracking of protein spots through 8 relatively close time points, valid spot detection was ensured and protein could be assigned to the individual tissue functionalities. In spite of many proteins changing in abundance, only a limited number of proteins were identified. Many of the low abundant proteins were not visible on CBB stained gels, from which most of the identifications were made. Small spots on a silver stained gel are often below the detection limit for MS identification (Biron et al., 2006). A number of protein spots were not identified due to lack of sequence data in the NCBI and EST databases. Spectra from these spots can be subjected to searches when more barley EST's are available. The 2D-DIGE technique would be well suited for the present study and yield better quantitative comparison of spots even for low abundant proteins since this technique employ the sensitive and MS-compatible fluorescent dyes. However, equipment for this technique was not available in the laboratory.

3.1.12.2. Germination and radicle elongation of barley seeds

During germination, many of the proteins observed to increase or decrease in abundance were related to changes in the desiccation state of the seeds, including loss of desiccation-related LEA proteins from embryo and aleurone layer. These proteins were suggested to be induced by the dormancy-promoting hormone ABA (Jiang and Zhang, 2002) and were proposed to protect living tissues of the mature dry seeds by mimicking water molecules thus stabilizing proteins and the cell wall (Ingram and Bartels, 1996). Notable, LEA proteins decreased under cold and drought stress in barley, maize, and Arabidopsis (Seki et al., 2001; Kollipara et al., 2002; Ozturk et al., 2002) and were shown to be involved in heat tolerance in wheat (Skylas et al., 2002), Arabidopsis (Wehyer et al., 1996) and pea seeds (DeRocher et al., 1994).

During radicle elongation the seed seemed to respond to variations in oxidative, salt and osmotic stress as well as to changes in glycolysis, citric acid cycle, and hydrolysis of storage compounds. Rehydration of the seeds thus alters both water balance and ROS production and the living tissues – embryo and aleurone layer – respond to this by regulating stress protective enzymes. The present data show clearly that the regulation differs in the two tissues and may take place at the transcriptional, translational or post-translational level, giving rise to differences in the 2-DE patterns.

In the endosperm most changes occurred during radicle elongation where the tissue fulfills its function as storage reserve mobilized by an array of hydrolases. PDI spots decreased rapidly and may be some of the first endosperm proteins degraded to provide amino acids for seedling growth along with other storage proteins that are not water-soluble and therefore not detected in the present study. The low molecular weight CM-proteins and the serpins, which are highly abundant in the endosperm, are not discussed in detail, because they are non-metabolic proteins and of low interest for understanding germination.

3.2 Study of enzymes of the ascorbate-glutathione cycle during radicle elongation

3.2.1 Protein extraction for enzyme assays

Enzyme activity assays were established for the four enzymes involved in the ascorbate glutathione cycle (APX, DHAR, MDHAR and GR, Figure 1.4) based on existing protocols previously applied to plant protein extracts (Nakano and Asada, 1981; Dalton et al., 1986; O´Kane et al., 1996). The activity assays were carried out using embryo protein extracts only during 4-144 h PI. The ascorbate-glutathione cycle is expected to be important in the embryo since this is a metabolically active and dividing tissue PI, where redox regulation is essential to avoid cellular oxidative damage. APX is present in only the germinated embryo according to 2D gels and MS identification (Section 3.1). The ascorbate-glutathione cycle may be less important in the aleurone layer where many enzymes are degraded as part of cell death and finally, the endosperm is dead tissue, where protection against ROS plays a minor role.

Small scale protein extraction from the embryo followed by desalting allowed detection of the activity of enzymes of interest. The protein extraction protocol was modified (no vacuum-drying, extraction scaled up to 7 seeds, higher buffer concentration) relative to the extraction used for 2D gel analysis, but the protein composition should remain very similar. This was done in order to avoid a buffer change prior to the assays and to ensure comparable protein concentrations for different time points. The enzyme activities were analyzed in triplicate using a freshly prepared embryo extract for each replicate. The amount of protein present in the individual protein extractions was estimated to be approximately the same (based on several determinations of protein concentrations by the Popov assay; Popov et al., 1975). However, relatively large standard deviations (Appendix 3) were unavoidable due to the difficulties in working with small scale protein extractions. The fact that seeds do not germinate synchronously and the change in the mixture of proteins in the extracts during 0-144 h PI, as observed in the 2DE patterns (Østergaard et al., 2004; Section 3.1), also contributed to the size of the standard deviations. For two of the enzymes (GR and MDHAR), the change in activity over 72 h was minor and the analysis was extended to include embryos from seeds imbibed up to 144 h resulting in more clear trends of the activity profiles. The enzyme activities were corrected for non-enzymatic side-reactions as described in the literature (Nakano and Asada, 1981; Section 2.4). The 4 h PI time point was used instead of 0 h PI to indicate the background activity level, since it was much easier to dissect and more reliable to remove remains of endosperm in 4 h imbibed seeds compared to dry seeds. In this way errors due to contaminating endosperm proteins were reduced. The change in enzyme activity of APX, DHAR, MDHAR, and GR during the first 4 h of germination was assumed to be insignificant according to similarity of the 2DE patterns of embryo extracts at 0 and 4 h PI (Section 3.1; Appendix 1a).

The measured activities of enzymes involved in the ascorbate-glutathione cycle are shown in Figure 3.10, 3.12, 3.13, 3.15 (activity diagrams) and Appendix 3 (table with activity values including standard deviations). An example of raw data from one of the APX activity assays is also shown in Appendix 3. The units are calculated based on the total protein content of the extract in micrograms as done previously (De Gara et al., 1997; Tommasi et al., 2001); specific activities could not be ascribed the individual enzymes. The aim of these assays was to analyze changes in enzyme activities during radicle elongation and not to obtain absolute values of specific activities.

3.2.2 Activity of GR

GR activity remained constant 4-72 h in agreement with the 2D spot pattern and 1.8 fold increase in activity occurred from 72 to 144 h (Figure 3.10). GR was identified in the 2D gel pattern of barley embryos in one spot (spot 409), which was present during 72 h of germination and seemed to decrease slightly (Figure 3.11). This visual change in spot intensity could be due the increase in the amount of other proteins in the extract being used for normalization and thus dominating the GR spot intensity (Section 3.1.2).

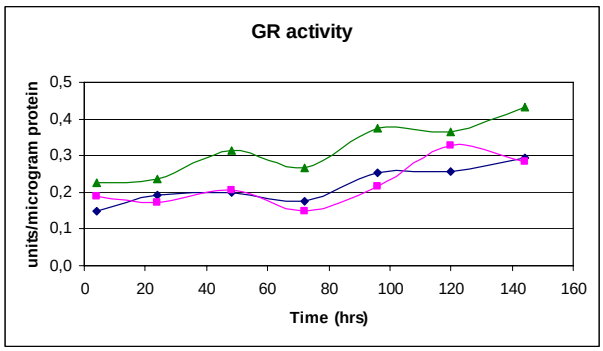

Figure 3.10. GR Activity from 4-144 h PI measured in the embryo extract using a direct spectrophotometric assay that measure depletion of NADPH (Section 2.4.3). One unit is defined as the amount of protein (microgram) that catalyzes conversion of 1 millimole substrate per minute. The individual curves represent replicates using freshly prepared extract each time.

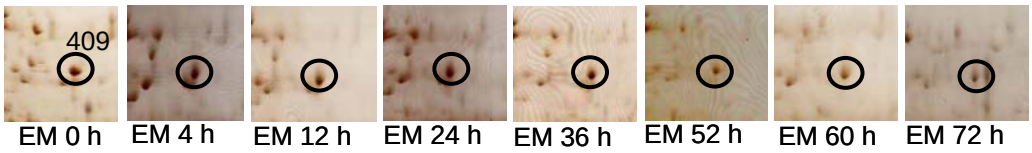

Figure 3.11. 2D gel pattern of the GR spot (spot 409; accession # AV916384) during germination and radicle elongation. The gel section represent the area of Mw: 58-80 kDa and pH: 6.1-6.44

3.2.3 Activity of MDHAR

MDHAR activity increased 2.7 fold during 4-144 h PI (Figure 3.12), which is in relatively good agreement with 2 fold increase in activity during 48 h PI previously found in wheat embryos (De Gara et al., 1997).

MDHAR was not identified in the 2D gels of neither non-germinated nor germinated embryos, but it has recently been identified in two spots, representing two different TC accessions (TC132872 and TC132873) in the aleurone layer incubated 18 h in 20 mM Succinic acid, 20 mM $CaCl_2$, pH 4.6, 5 µM GA (Christine Finnie, unpublished). These two MDHAR spots had apparent isoelectric points close to 6 and molecular weights around 45 kDa, which is in the range covered by the 2D gels of embryo and aleurone layer extracts of this study (Section 3.1). If the MDHAR spots were present in these 2D gels, they may not change in abundance and were therefore not selected for MS in this study, or are low abundant and not visible in the 2D gels.

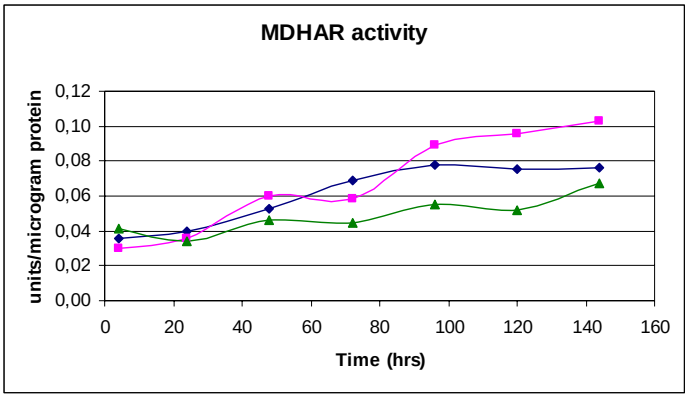

Figure 3.12. MDHAR Activity from 4-144 h PI measured in the embryo extract using a direct spectrophotometric assay that measure depletion of NADPH (Section 2.4.4). One unit is defined as the amount of protein (microgram) that catalyzes conversion of 1 millimole substrate per minute. The individual curves represent replicates using freshly prepared extract each time.

3.2.4 Activity of DHAR

The activity of DHAR decreased between 4-72 h PI, and then remained constant until 120 h PI, and then a small significant increase at 144 h (Figure 3.13). The small activity increase at 144 h PI (Figure 3.10) was significant but it is not known if the increase would continue if seeds were germinated for longer than 144 h. The activity profile for DHAR during radicle elongation has not been previously reported, but it decreased 3-4 fold during 48 h PI in wheat embryos (De Gara et al., 1997).

The 2D gel showed two spots containing DHAR of the same pI but differing in mass (Figure 3.14, spots 149, 294). The high molecular weight form remained constant during germination and radicle elongation, whereas the low molecular weight form decreased rapidly in abundance. Both originated from the same gene product. MS data confirmed the active site residues, CPFS, located in the N-terminal part of the protein, were present in the fragment, and it is therefore possible that the fragment is fully or partially active. The difference in Mw was probably caused by a truncation of the C-terminus or large post-translational modification. If the full-length DHAR form account for the majority of the activity, the DHAR activity profile did not reflect the spot appearance profile. This could indicate a post-translational mechanism of DHAR activity during radicle elongation. Such a mechanism could be induced by ROS and involve Trx h (Section 1.1.5.2) and was further analyzed (Section 3.2.4.1).

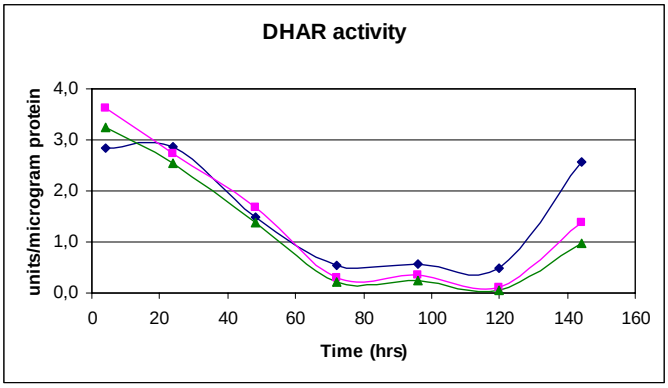

Figure 3.13. DHAR Activity from 4-144 h PI measured in the embryo extract using a direct spectrophotometric assay that measure generation of AsA (Section 2.4.2). One unit is defined as the amount of protein (microgram) that catalyzes conversion of 1 millimole substrate per minute. The individual curves represent replicates using freshly prepared extract each time.

The DHAR activity profile during radicle elongation could be due to activity profiles of other isoforms of DHAR present in the different cellular compartments (Mittler, 2002). Three tentative consensus (TC) sequences thought to encode DHAR, with 52% sequence identity between all three and 90% between two of them were identified in the barley gene index (www.compbio.dfci.harvard.edu/tgi/plant.html) and therefore it cannot be excluded that more unidentified DHAR proteins were present in the 2D gel patterns.

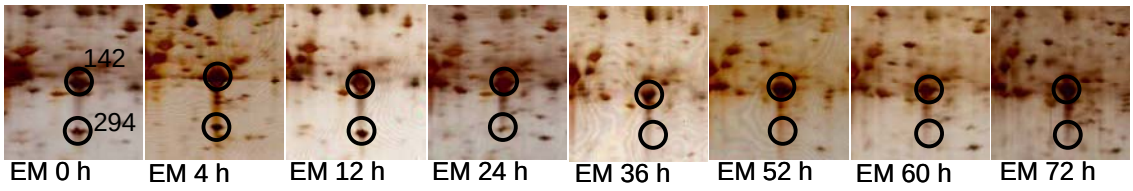

Figure 3.14. 2D gel spot pattern of DHAR spots (spots 142, 294, both having accession # BE601917) during germination and radicle elongation. The gel section represent the area of Mw: 23-35 kDa and pH: 5.6-6.15.

Another possibility is that the change in DHAR activity is due to activity of other enzymes that are known to possess DHA reducing activity. This has been proven *in vitro* for glutaredoxin, PDI, thioredoxin m and f, Kunitz type trypsin inhibitor, and thioredoxin reductase (Wells et al., 1990; Ahn and Moss, 1992; Trümper et al., 1994; Park and Levine, 1996; May et al., 1997). These proteins all contain a redox active di-cysteine or cysteine-serine site (as in DHAR), however, it is not known if their DHA reducing activity has any physiological role.

3.2.4.1 DHAR activity regulation by Trx h

The influence of reduced recombinant barley Trx h2 on the DHAR activity was tested in the embryo extract with low and high DHAR activity, respectively (Figure 3.13). Trx h was reduced by two fold excess of DTT (in 30 mM Hepes pH 7.0) and added to 18 µL embryo extract (0.4 µg/µL) to a final concentration of 10 µM, which represented a large excess of Trx h2 compared to the endogenous amount already present in the embryo extract. Control experiments included no addition of Trx h2, addition of DTT instead of Trx h2, and Trx h2 without embryo extract. These experiments could not confirm a Trx h-linked effect on the DHAR activity (not shown).

In order to validate the probability of DHAR-Trx h interaction, the DHAR structure was modeled based on the three-dimensional structure of Chloride Intracellular Channel 1 (CLIC1) complexed with GSH (PDB entry: 1k0n; Harrop et al., 2001). CLIC1 belongs to the GST family along with DHAR (Dulhunty et al., 2001, Dixon et al., 2002) and shares 28% sequence identity with DHAR. In the DHAR model, the distance between the two C-alpha atoms of Cys19 and Cys5 is 12 Å and it is not likely that a disulfide bond can be formed. However, this is a model and presence of a possible disulfide bond targeted by Trx h reduction cannot be excluded.

3.2.5 Activity of APX

The increasing activity of APX during radicle elongation (Figure 3.15) was in excellent agreement with the spot pattern of the embryo 2D gels, where APX1 (spot 79; accession # AJ006358) was visible from 24 h PI and increased in intensity during radicle elongation (Figure 3.16). A second APX spot that represented a different gene product (APX2; accession # AF411228) was identified in developing endosperm (Finnie et al., 2003) but it was not identified in silver stained gels of germinating embryos. It cannot be excluded, however, that APX2 is present in the germinated embryo extracts in low amounts not clearly detectable by silver staining. APX1 and APX2 are both cytosolic and share 83.6% sequence identity but they have not been studied with respect to specific activity and relative importance in the barley seed. The appearance of APX1 and APX2 during radicle elongation was investigated by gene expression analysis (Section 3.2.5.1), zymograms (Section 3.2.5.2), and 2D western blotting combined with MS (Section 3.2.5.3).

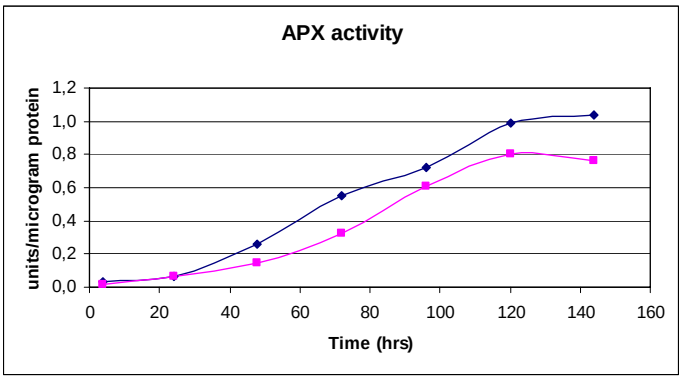

Figure 3.15. APX Activity from 4-144 h PI measured in the embryo extract using a direct spectrophotometric assay that measure depletion of AsA (Section 2.4.1). One unit is defined as the amount of protein (microgram) that catalyzes conversion of 1 millimole substrate per minute. The individual curves represent replicates using freshly prepared extract each time.

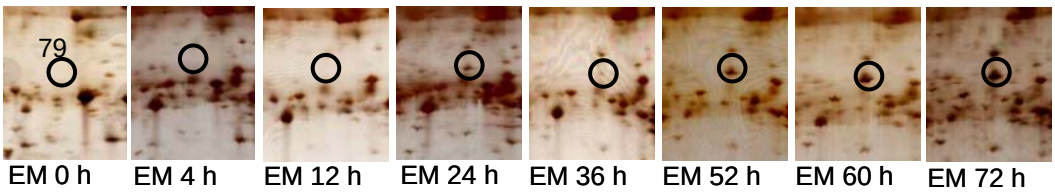

Figure 3.16. 2D gel spot pattern of the APX spot (spot 79, accession # AJ006358) during germination and radicle elongation. The gel sections represent the area of Mw: 25-39 kDa and pH: 6.05-6.42.

3.2.6 Gene expression analysis of APX1 and APX2

In order to confirm the presence of both APX1 and APX2 mRNA in the barley embryos, gene expression analysis was carried out by Ph.D. stud. Azar Shahpiri (EPC, BioCentrum-DTU). This showed that mRNA of both APX1 and APX2 was present in the embryos of mature dry seeds increasing up to 96 h PI and then remained constant until 144 h PI (Figure 3.17). From these experiments it is not possible to quantify the relative amounts of APX1 and APX2 mRNAs because the annealing efficiency of the used primers is probably not the same. To rule out the possibility of annealing of the two primer sets to both APX mRNA's, the PCR products were cloned into a pDrive cloning vector and sequenced. This confirmed that only APX1 and APX2, respectively, were amplified by the two primer sets.

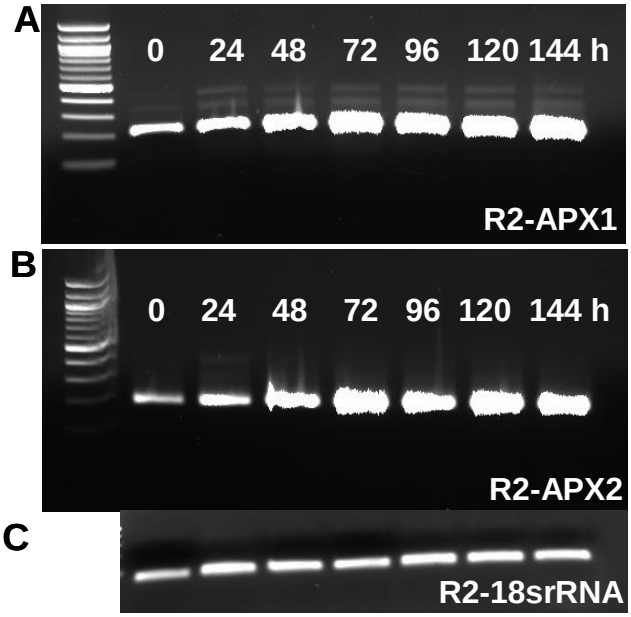

Figure 3.17. Gene expression analysis of A) APX1 and B) APX2 in embryo during 0-144 h PI. C) control experiment using 18srRNA, courtesy of Azar Shahpiri.

3.2.7 APX activity detected in zymogram

The detection of APX activity in zymograms was based on the AsA dependent reduction of NBT (nitroblue tetrazolium) resulting in a purple product. The native Tris-glycine gel soaked in AsA turned purple upon addition of NBT, with cleared zones representing areas that lack AsA due to APX activity.

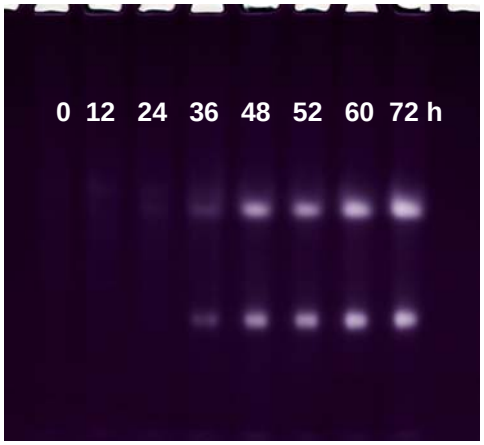

Figure 3.18. Zymogram showing APX activity in embryo extracts 0-72 h PI. Approximately 20 µg embryo protein was applied for each time point. APX activity was detected in a 4-12% Tris-glycine gel at pH 9.0 as described in Section 2.4.6.

The zymogram showed two cleared zones in each lane (from 36 h PI), the upper band being the strongest (Figure 3.18), indicating the presence of two active forms of APX in the embryo extract. In agreement with the 2D gel patterns and the enzyme activity assays, APX activity appeared in the zymogram at 36 h PI and increased thereafter. In an attempt to identify differences between the two forms of APX by MS, the clearing zones were excised from the gel and run on a SDS-PAGE (after reduction and alkylation) which was stained with sbCBB. However, no protein bands with expected size of APX appeared, probably due to low sensitivity of this stain or limitations in amount of protein that enter the SDS-PAGE. More sensitive stain (silver or fluorescence stains) may reveal the APX bands but this was not tested.

The two bands may represent a monomer and a dimer of the same protein. The same pattern and intensity of band was observed when the embryo extract was incubated with DTT prior to the 1D gel (not shown). The possibility of disulfide bond formation through the free Cys32 (Patternson and Paulos, 1995; Sharp et al., 2003; Section 1.1.5.1) was therefore excluded and the dimer would be based on non-covalent interactions.

3.2.8 Immuno-detection of APX forms

Specific antibodies raised against maize APX (Koshiba, 1993) enabled detection of APX in barley embryo extracts. A 1D western blot showed that APX increased in abundance from 24 h (Figure 3.19) in agreement with activity assays and zymogram results described above.

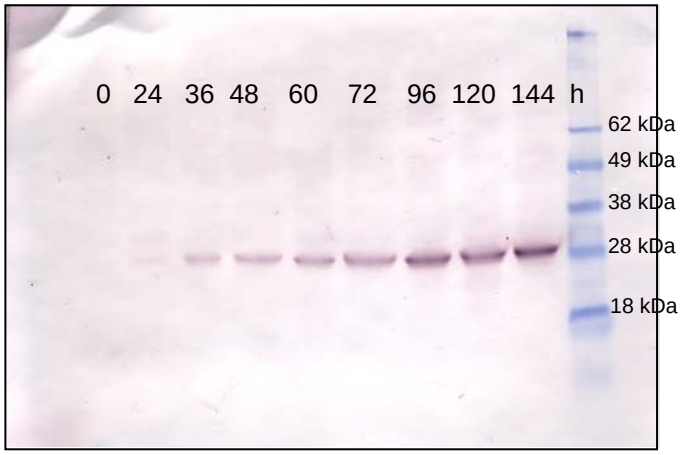

Figure 3.19. 1D western blot of APX in barley seed embryos during germination and radicle elongation. The SeeBlue marker (Invitrogen) indicated the correct molecular size of the APX band. Approximately 5 µg protein was applied to each lane.

A 2D western blot showed a more complex pattern of APX appearance during radicle elongation. Two weak spots were visible at 24 h (encircled on Figure 3.20), one of pI 5.8 at the same position as the APX1 spot (spot 79) observed in the silver stained 2D gels and one at pI 5.0 in approximately the same position as the APX2 isoform in developeing endosperm (Finnie et al, 2003). These two APX spots increased in intensity up to 72 h PI and several new spots, varying in size and pI, appeared.

The reactivity of the antibodies with APX1 and APX2, respectively, is not known and it is possible that they react more specifically with APX1 compared to APX2 as APX1 showed the strongest intensity (Figure 3.20). However, no possible spots of APX2 was visible in the silver stained 2D gel pattern in agreement with the low spot intensity of the proposed APX2 in the 2D western blot. It cannot be excluded that some of the weak spots of the 2D western blot can be ascribed to unspecific immuno-detection of other proteins in the extract that possess the same appearance profile as APX.

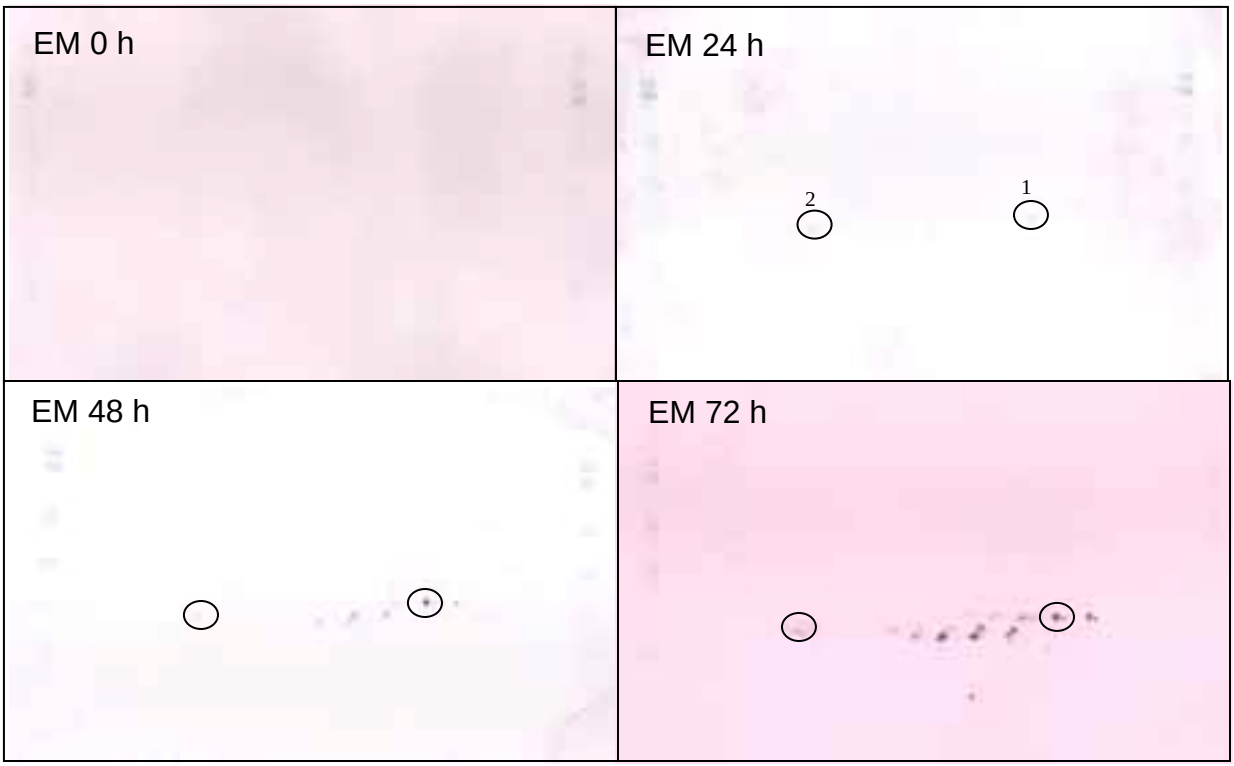

Figure 3.20. 2D Western blot of APX in barley seed protein extracts. 200 µg protein was loaded onto each 2D gel and APX was detected as described in Section 2.5.2 and 2.5.3. Spot 1 corresponds to the position of APX1 in developing barley endosperm and spot 2 corresponds to the position of APX2, i.e. spot 79, in germinated embryo.

3.2.9 Mass spectrometry of APX forms

The multiple APX spots detected in the 2D western blot probably reflected post-translational modifications and/or degradation and this was studied by MS. The spot anticipated to be equivalent to spot 79 in silver stained gels together with spots 4 and 5 had a slightly higher Mw compared to spots 8, 12, 13, 15, 16, 17, and 25 (Figure 3.21A). This indicated that a small part of the N- or C-terminus was truncated resulting in lower pI values. Moreover, the pI differences could represent different oxidation states of the free Cys32 (Section 1.5). This was investigated by MS and described in the following.

When using the endopeptidase trypsin for digestion of APX1 in spot 79 prior to MS, 8 matching peptides were found yielding a sequence coverage of 38% (Figure 3.22). By using AspN and LysC in addition to trypsin, the sequence coverage was increased to 92.4% (Table 3.2). Spots from a corresponding CBB stained gel of an extract from embryos imbibed for 144 h were excised, guided by the corresponding 2D western blot (Figure 3.21) and subjected to proteolytic digestion and MS. In addition to spot 79, 9 APX1 spots were identified (Figure 3.21) with varying sequence coverage (29.2 – 92.4%; Table 3.2) probably due to low amount of protein in some of the spots. For spots 4, 8, and 13 MS/MS was employed to verify the identifications. A number of weak APX spots were not identified by MS or MS/MS probably because it was difficult to locate the spots in the 2D gels and the protein amounts were low (Figure 3.21B). APX1 and APX2 would generate MS spectra with no overlapping peaks according to theoretical trypsin digests using the PeptideMass tool at the ExPASy web site (www.us.expasy.org). No spots containing APX2 were identified.

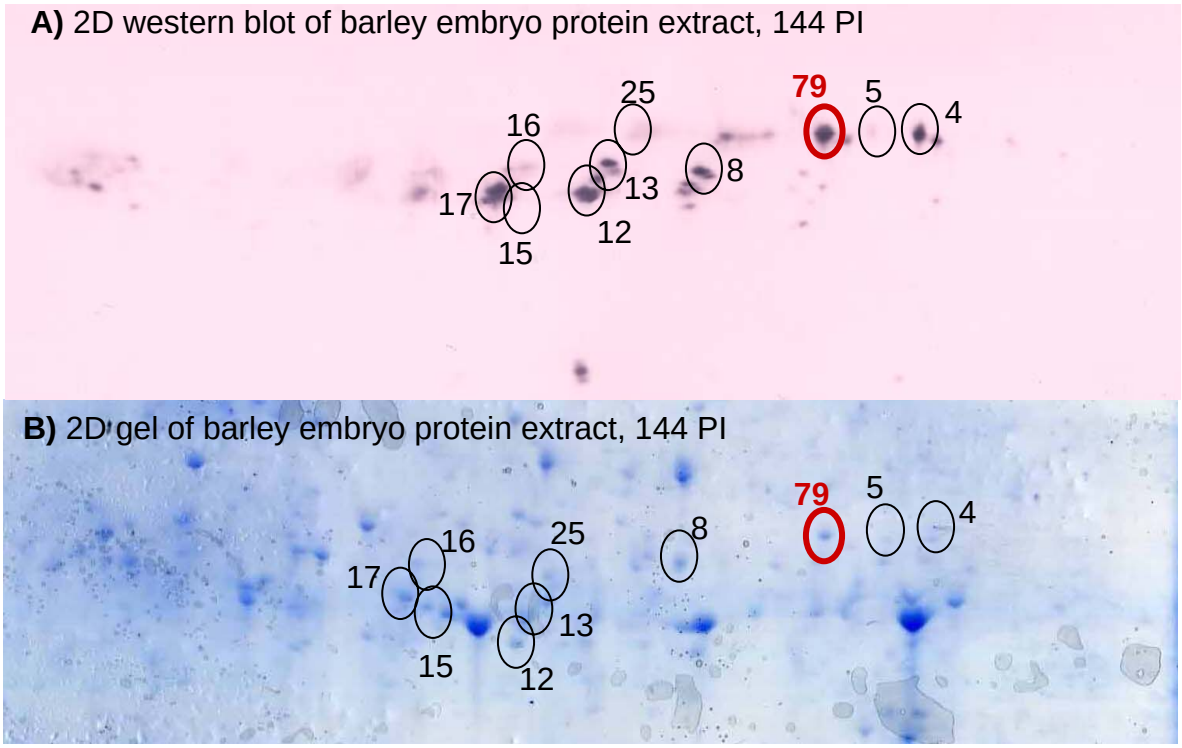

Figure 3.21. Identification of APX forms from a A) 2D western blot and B) CBB stained 2D gel of barley embryo extract 144 h PI. APX1 was identified in all encircled spots which include the spots that strongly react with the antibody.

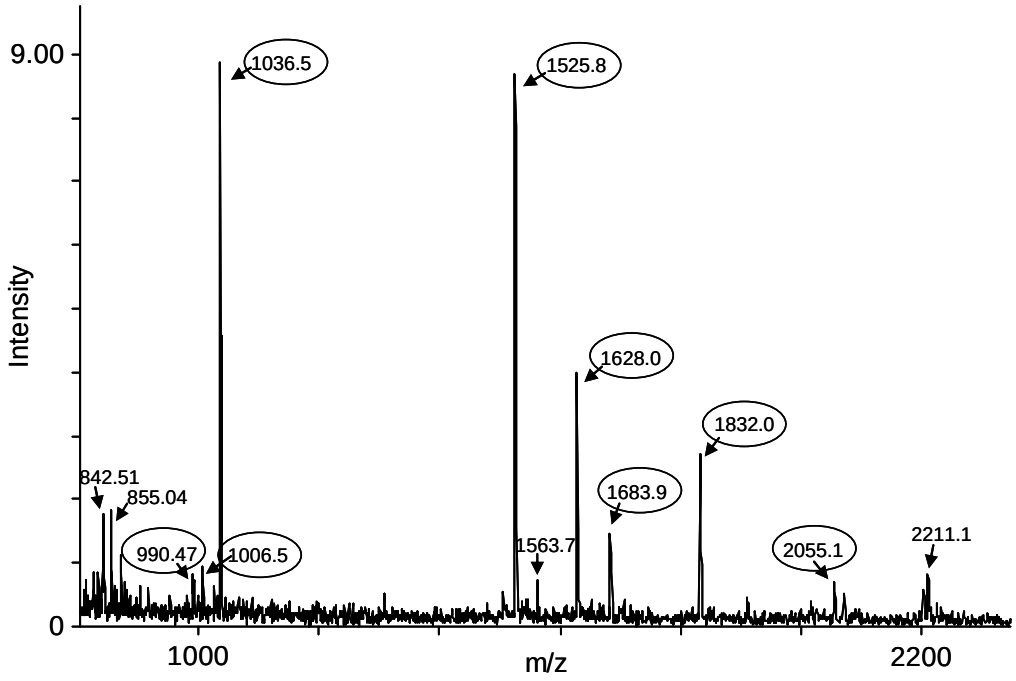

Figure 3.22. Peptides mass fingerprint for APX1 (spot 79) after digestion with trypsin. Recorded by MALDI-TOF MS. Encircled masses are peaks from APX1 peptides.

Table 3.2.Sequence coverage obtained for APX spots using three different endopeptidases, trypsin, AspN and LysC, and total sequence coverage for all three enzymes.

Spot id	Trypsin digest (%)	AspN digest (%)	LysC digest (%)	Total (%)
79	38.0	48.4	52.0	92.4
4	38.0	31.2	34.0	74.0
5	26.4	30.8	20.0	51.2
8	32.0	30.0	46.4	70.0
12	32.0	48.4	48.8	83.2
13	10.0	38.0	20.8	60.8
15	6.0	38.0	nd	38.0
16	32.0	12.4	30.0	29.2
17	÷	48.4	48.8	83.2
25	nd	48.4	39.2	80.0

Nd: not determined and ÷: no peaks form APX fragments present.

If APX1 had undergone over-oxidation of Cys32 during radicle elongation, negatively charged peptides could be generated in the digests (depending on the sequences of the peptides) due to oxidation of cysteines to sulfinic acid (Cys-SO_2H) or sulfonic acid (Cys-SO_3H). Therefore MS was run in negative mode as well as positive mode (Section 1.2.1.3). In negative mode, however, the spectra contained less peaks and no peptides containing the free Cys32 were identified. AspN cleaves proteins N-terminal to over-oxidized cysteine residues in addition to aspartate residues (Wagner et al., 2002). In case of over-oxidation of Cys32 AspN would generate peptides of 1790.13 and 1806.13 (if Met36 is oxidized), which were not seen in any of the spectra. Peptides containing Cys32 generated two peaks after trypsin digestion at 990.48 and 1006.47 m/z units, respectively. These masses corresponded to Asp31-Arg38 with and without oxidation of Met36 (Figure 3.22 and 3.23). These two peaks were of low intensity and only observed in the spectra of spots 4, 5, 8, and 79 (and in the spectra of spots 12 and 13 only peak 1006.47 was observed). These spots had varying pI values and oxidation of Cys32 is therefore not likely to cause the pI differences.

The small decrease in molecular weight according to the western blot (Figure 3.21A) of APX1 spots 8, 12, 13, 15, 16, and 17 compared to 4, 5, 25, and 79 indicated truncation of either that of the N- and/or C-terminus. The N-terminus was only covered in the spectra of spots 4, 13, and 79, and it is possible that the N-terminus had undergone truncation in some of the residual spots resulting in lack of the peak in the mass spectra. The absence of part of the N-terminus could give rise to both the observed pI and Mw shifts by loss of charged residues. The C-terminus was covered in all of the spectra from AspN and/or LysC digestions (Figure 3.23), except for spot 16. Spot 16 generally had low sequence coverage and there is no reason to believe that spot 16 was truncated at the C-terminus (Table 3.2).

Figure 3.23. Sequence coverage of APX1 (spot 79) obtained by mass spectrometry. Black amino acid residues are not covered in any of the mass spectra. Blue arrows indicate peptides identified by using trypsin for digest. Green arrows indicate peptides identified in AspN digest and purple arrows indicate peptides identified in LysC digest. Cys32 is encircled and Met36 is marked with *.

3.2.10 Oxidation of APX in embryo extracts

It was attempted to confirm that oxidation of APX occurred in the embryo extract by exposing the protein extract to oxidation by H_2O_2 and observing changes in pI of the APX forms by western blotting of an IEF gel. Neither activity staining nor western blotting revealed major changes in pI of APX upon oxidation (Figure 3.24). APX activity may increase slightly on treatment with H_2O_2 as judged from activity staining, although it was not possible to quantify the staining. It would be possible to measure the activity change in an activity assay, however, this was not done. To exclude that the APX spots appearing on the 2D gel were artifacts caused by oxidation during the 2DE procedure, the protein extract was alkylated by N-ethylmaleimide prior to the first dimension of 2DE. This did not change the APX spot pattern (not shown).

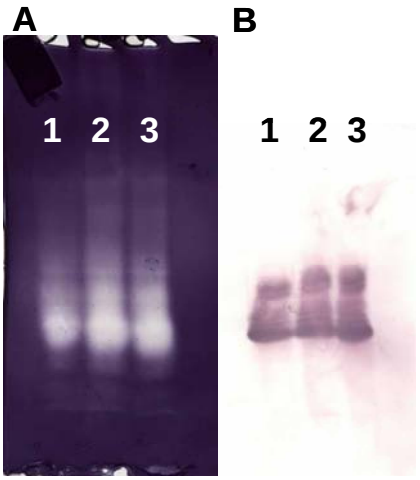

Figure 3.24. Isoelectric focusing of APX in non-oxidized and oxidized embryo protein extract from 96 h germinated seeds. APX was detected by A) APX activity staining and B) specific antibodies. Lane 1: non-oxidized protein extract; lane 2: treatment with 20 mM H_2O_2 for 10 min; lane 3: treatment with 200 mM H_2O_2 for 10 min. Approximately 30 µg protein was loaded in each lane.

3.2.11 Discussion

Generally the 2DE technique can give a broad picture of a proteome, including relative abundance of protein spots, presence of isoforms, post-translational modifications and degradation products. However, the observation of a protein in a 2D gel spot does not necessarily imply that the protein is biologically active. The activity of many proteins is regulated at the post-translational level and this is important for understanding their functionality and a major challenge in protein chemistry. By comparing 2D gel patterns with activity profiles for the individual proteins, it is possible to gain insight about the activity regulation of the proteins. Therefore we aimed at measuring activities of selected proteins of interest in the embryo extracts.

Enzymes of the ascorbate-glutathione cycle (APX, DHAR, MDHAR, and GR) were subjected to enzyme activity assays that were compared to the 2D spot patterns of the individual enzymes during radicle elongaiton. GR and MDHAR showed minor changes in activity during radicle elongation in agreement the 2D gel pattern (GR) and previous analysis of germinating wheat embryos and pine seeds (De Gara et al., 1997; Tomassie et al., 2001). The biological role of these findings is discussed in Section 3.2.11.2. The disagreement between the activity profile and 2DE patterns of DHAR during radicle elongation indicated activity regulation at a post-translational level involving Trx h as suggested previously (Section 1.1.5.3; Wong et al., 2003; Marchand et al., 2004, 2006). This is discussed in Section 3.2.11.1. As expected, APX activity increased 36-144 h PI in excellent agreement with the 2D gel patterns and was further analyzed with respect to different forms and isoforms of APX with focus on oxidation of Cys32 (Section 3.2.11.3).

3.2.11.1 DHAR activity

Two forms of DHAR were identified in the embryo 2D gels. It is not known, however, how many proteins (DHAR or other proteins), that possess DHAR activity in the embryo extracts. Therefore it is difficult to compare profiles of DHA reducing activity with 2D spot patterns.

Using the present DHAR activity assays and the available recombinant barley Trx h2 (Maeda et al., 2003), it was not possible to observe a Trx h-linked change in DHAR activity. This indicated that DHAR is not a target of Trx h. Trx h was shown to reduce DHAR in barley embryo extracts (Section 1.1.5.3; Hägglund et al., in prep) but it is not known if this reduction affects the DHAR activity. It is possible that the used conditions, i.e. the complex proteins mixture, including endogenous Trx h and Trx h interacting proteins, disabled detection of the specific target enzyme reduction.

Purified recombinant DHAR would be a fine tool for further analysis of its putative interaction with Trx h by *in vitro* binding and reduction experiments. However, cloning, expression and purification of DHAR is laborious and a simpler approach could be to enrich the DHAR fraction by pre-fractionation of the embryo extract. This may be done by treatment of the embryo extract with biotinylated, oxidized glutathione (GSSG-biotin), which can bind GSH binding proteins including DHAR. These GSH binding proteins can then be trapped in a streptavidin-agarose containing matrix and eluted by DTT. This strategy was shown to recognize DHAR in Arabidopsis cell cultures (Dixon et al., 2005) along with a number of other GSH binding proteins. Using this approach it may be possible to avoid DHAR-activity-interfering factors. In addition, it may be possible to observe differences in the amount of DHAR fished out of the extract with and without treatment with Trx h.

3.2.11.2 The physiological role of DHAR, MDHAR, and GR in the embryo

The removal of DHA by reduction to AsA in the chloroplasts is essential since a concentration of only 50 μM DHA inhibits the regulatory functions of Trx in chloroplasts metabolism (Morell et al., 1997). However, this may not be a real problem as DHA never accumulates to any significant extent due to high activities of MDHAR and the presence of reduced ferredoxin which can reduce MDHA to AsA. The relatively high DHAR activity during germination may be important for the immediate generation of AsA upon imbibition to control ROS before AsA biosynthesis is adequately restored (Tommasi et al., 2001). During radicle elongation MDHAR may be more important than DHAR for generation of AsA as MDHAR has slightly increasing activity as opposed to DHAR (Arrigoni et al., 1981; Mittova et al., 2000). Also in wheat embryos, decreasing DHAR activity and slightly increasing MDHAR activity were seen during the first 48 h of germination (De Gare et al., 1997). The relative importance of the two enzymes is not known but the specific activity of MDHAR is 10 fold higher than of DHAR in both mitochondria and chloroplasts of tomato (Mittova et al., 2000).

GR and MDHAR, both slightly increase in activity 4-144 h PI and use NADPH as a proton donor in catalysis. This is correlated with an increase in NADPH availability during seed germination, where the pentose phosphate cycle responsible for NADPH generation in non-green tissue is activated by imbibition (Mayer and Poljakoff-Mayber, 1982; Tommasi 2001). The slightly increasing GR activity indicates at least constant utilization of GSH during germination and radicle elongation. The activities of GR and DHAR, which are tightly correlated in the ascorbate-glutathione cycle, change in opposite ways during the analyzed timeframe. This is not surprising since GSH is also involved in other processes, i.e. sulphur metabolism (Noctor et al., 1998; De Kok and Stulen, 1993) and maintaining redox potential.

3.2.11.3 APX appearance in the embryo

The cytosolic APX1 had an interesting 2D spot appearance profile as it is only present in the germinated embryo, in contrast to the other identified redox-active proteins (Section 3.1.7). The present work confirms mRNA of both APX1 and APX2 to be present in the dry mature seed. It is not known if this mRNA survived the desiccation intact and is used as a template for translation. The time frame for synthesis of new mRNA is 30-90 minutes (Potokina et al., 2002) and newly synthesized mRNA may replace the mRNA left from maturation. The level of APX mRNA increases at the end of germination in agreement with the APX1 appearance at 24 h PI in the 2D gels. Although no sequence information of APX2 was obtained, APX2 seemed to be present in small amounts in the germinated embryo extracts as judged by 2D western blotting. The specific activities of APX1 and APX2 has not been reported and it is possible that APX1 has a much higher specific activity than APX2 and represent one of the two APX active bands in the zymogram (Figure 3.18).

In this present work, we focused on the cytosolic APX1 and APX2, however, there may be more APX isoforms present in the embryo extracts. Chloroplastic isoforms of APX are unstable in the absence of AsA and therefore AsA was added to the extraction buffer (Chen and Asada, 1989). We cannot exclude that part of the APX activity in the embryo extracts originates from un-identified APX isoforms.

3.2.11.4. Post-translational modifications of APX

It is evident from numerous large-scale protein identification studies that very often more than one protein form originates from a particular gene. Thus protein profiling of cells and tissues by

2DE showed characteristic trains of spots covering a pI and/or Mw range. Such spot trains can represent multiple forms derived from a single gene product due to post-translational and other processing and/or originate from isoforms of different, but closely related genes and allele variants. For identification of post-translational modifications it is desirable to have high sequence coverage. One way to increase the sequence coverage is to use more than one proteolytic enzyme for protein digestion prior to MS. The first choice is most often trypsin, but enzymes like AspN and LysC are also commonly used. The high sequence coverage of APX1 spot 79 (92.4%) enabled the study of post-translational modifications.

The different pI values of the APX spots, detected by 2D western blotting, could indicate that truncation of either the C- or N-terminus, oxidation of the protein during radicle elongation, or deamination. A target for oxidation could be the free Cys32 located in the vicinity of the active site as seen in the crystal structure (Sharp et al., 2003). Reversible oxidation (sulfenic acid, Cys-SOH) and irreversible oxidation (sulfinic acid, Cys-SO_2H and sulfonic acid, Cys-SO_3H) of an active site cysteine in peroxiredoxin is known both as part of the catalytic mechanism with peroxides in mammalian cells (Wood et al., 2003) and in response to oxidative stress in human cells as shown by MS (Rabilloud et al., 2002). Therefore it was hypothesized that peroxiredoxin could undergo oxidation in barley seeds during development, but this has not been confirmed by MS (Finnie et al., 2006).

Peptides containing Cys32 gave weak signals that were present in five of the ten APX1 mass spectra. If Cys32 exposed different oxidations states, the peptide would shift position in the spectra due to addition of oxygen. This was not the case, as the peptide is present in the spectra of spot 4, 12 and 17 (peak 1006.47) and 4 (peak 990.48), which all differ in pI compared to spot 79. Asn31 in APX1 is a potential N-glycosylation site with the sequence N-X-S (where X is any amino acid except proline) and if a fraction of the peptides are glycosylated this could account for the weak peak intensity. It is possible to de-glycosylate the peptides using N-glycosidase A (specific for glycosylations in plants) prior to MS for further analysis. Since there were no direct indications of oxidation of Cys32 this was not tried. Truncation of APX1 is possible, but could not be confirmed by MS because the C-terminus was not covered by the MS.

APX could be modified at a different site than Cys32. Deamination of aspargines (or glutamines) is another common modification that gives rise to pI shift. In the mass spectrum deamination causes a shift in m/z of +1 Da (for Asn to Asp/isoAsp) or -17 Da (for Asn to succinimide), however, these shifts of m/z values were not observed for any of the asparagines in the APX sequence.

Appearance of a protein in several spots of varying pI has been observed previously in barley seeds, i.e. α-amylase (AMY2 isozyme) appearing in barley malt in six full-length forms in the pI range of 5.66-6.13 (Bak-Jensen et al., 2007), peroxiredoxin appearing in 3 forms separated by a pI difference of 0.3 during development (Finnie et al., 2006), and limit dextrinase appearing in an array of undefined spots of pI 4.4-4.8 (Section 3.3.3). In case of α-amylase and peroxiredxin MS failed to unveil the cause of the observed pI differences. Differences in observed pI values have previously been shown to be caused by oxidation in barley aleurone membrane protein in response to GA (Maya-Ampudia and Bernal-Lugo, 2006). Multiple forms can also represent folding isomery occurring during IEF (Lutter et al., 2001; Veith et al., 2001; Berven et al., 2003).

3.3 Study of the limit dextrinase inhibitor

3.3.1 Cloning of the LDI gene

The protein sequence of LDI was known from MS data and N-terminal sequencing (MacGregor et al., 2000) and the DNA sequence was obtained by a pBLASTn search using an EST database. A number of hits differed slightly at the nucleotide level but showed the same protein sequence. One of these sequences was from barley developing seeds (cv. Morex) and since these seeds were on stock in-house (at -80^{o}C) they were chosen for RNA extraction. The sequence contained no introns and therefore only 2 primers were necessary to clone the gene. PRC using the extracted RNA as template produced a nucleotide sequence of 342 bp corresponding to the LDI sequence (Figure 3.25). This cDNA sequence was verified by sequencing after cloning into the TOPO vector.

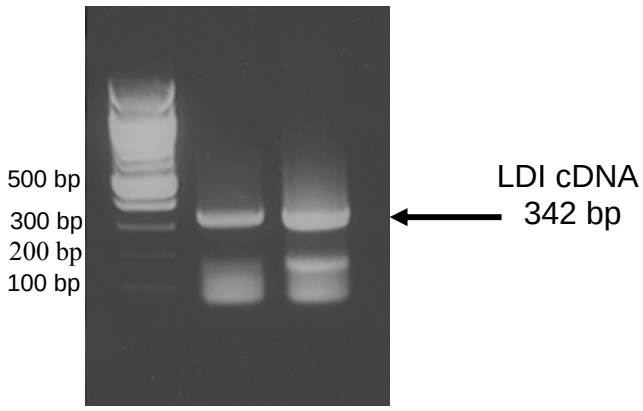

Figure 3.25. Agarose gel showing the LDI cDNA from the PCR on the RNA extraction. The arrow indicates the LDI cDNA. The first lane contains a 100 bp marker (Novagen)

3.3.2 Heterologous expression of LDI

Several constructs were made in an attempt to produce LDI; initially in *E. coli* and later in *P. pastoris* and *L. lactis*. Constructs were made both with and without a C-terminal His_6-tag in all expression vectors (Table 3.3). The His_6-tag could ensure easy purification using a chelating nickel column. Several *E. coli* strains and different growth temperatures were tested, whereas for *P. pastoris* and *L. lactis* only standard conditions were tested according to guidelines from Invitrogen and Gasson et al. (1983). It was not possible to detect LDI in crude protein extracts from *E. coli* using specific antibodies or LD inhibition assays if no N-terminal tag was added. The *E. coli* cells were also analyzed for inclusion bodies, which, however, were not found to be present.

Table 3.3. Overview of LDI expression constructs and choice of organism and strain. ECL: enteropeptidase cleavage site (Section 3.3.2.4).

Expressed sequence	Vector	Organism	Strain
LDI	pET11a	*E. coli*	BL21 (DE3), Oregami pLys, Tunar
LDI-His_6	pET11a	*E. coli*	BL21 (DE3), Oregami pLys, Tunar
LDI (optimized)	pET11a	*E. coli*	Oregami pLys
LDI (optimized)-His_6	pET11a	*E. coli*	Oregami pLys
Trx-ECL-LDI	pET32a	*E. coli*	Rosetta
Trx-ECL-LDI-His_6	pET32a	*E. coli*	Rosetta
LDI	pPICZα	*P. pastoris*	X-33
LDI-His_6	pPICZα	*P. pastoris*	X-33
LDI	pAMJ399	*L. lactis*	MG1363
LDI-His_6	pAMJ399	*L. lactis*	MG1363

3.3.2.1 Optimised codon usage

The LDI gene contains several codons that are less optimal in *E. coli* than in barley and this motivated optimization of codon usage for *E. coli* and *P. pastoris*. A long oligonucleotide encoding 123 nucleotides (constructed using 3 overlapping primers) with optimized codon usage was used as a 5' primer and a low annealing temperature (35°C) enabled construction of the LDI gene that had good codon usage for *E. coli* and *P. pastoris* for the 5' half of the gene (Figure 3.26). However, this did not lead to production of LDI in *E. coli* according to both immuno-detection of LDI and LD inhibition assay in crude protein extracts.

A

```
  T   L   E   S   V   K   D   E   C   Q   P   G
ACC CTG GAG AGC GTC AAG GAC GAG TGC CAA CCA GGG
ACC CTG GAA TCT GTT AAA GAT GAA TGT CAG CCA GGT
  V   D   F   P   H   N   P   L   A   T   C   H
GTG GAC TTC CCG CAC AAC CCG TTA GCC ACC TGC CAC
GTT GAT TTT CCA CAT AAC CCA CTG GCC ACC TGT CAT
  T   Y   V   I   K   R   V   C   G   R   G   P
ACC TAC GTG ATA AAA CGG GTC TGC GGC CGC GGT CCC
ACC TAT GTT ATT AAA AGA GTT TGT GGT AGA GGT CCG
  S   R   P   M   L   V   K   E   R   C   C   R
AGC CGG CCC ATG CTG GTG AAG GAG CGG TGC TGC CGG
TCC AGA CCG ATG CTG
  E   L   A   A   V   P   D   H   C   R   C   E
GAG CTG GCG GCC GTC CCG GAT CAC TGC CGG TGC GAG
  A   L   R   I   L   M   D   G   V   R   T   P
GCG CTG CGC ATC CTC ATG GAC GGG GTG CGC ACG CCG
  E   G   R   V   V   E   G   R   L   G   D   R
GAG GGC CGC GTG GTT GAG GGA CGG CTC GGT GAC AGG
  R   D   C   P   R   E   E   Q   R   A   F   A
CGT GAC TGC CCG AGG GAG GAG CAG AGG GCG TTC GCC
  A   T   L   V   T   A   A   E   C   N   L   S
GCC ACG CTT GTC ACG GCG GCG GAG TGC AAC CTA TCG
  S   V   Q   E   P   G
```

B

	Content (%)		
	Hordeum vulgare	Escherichia coli	Pichia pastoris
GAG	36.7	29.6	18.8
GAA	16.0	40.2	38.9
AGC	15.9	15.0	7.4
TCT	10.9	10.6	23.5
GTC	22.9	14.2	14.5
GTT	14.0	19.9	26.7
AAG	37.8	12.7	34.4
AAA	12.1	35.4	30.2
GAC	33.8	19.2	26.2
GAT	20.7	32.8	37.2
TGC	13.8	6.0	4,5
TGT	6.0	5.2	8,3
CAA	13.7	14.5	14.5
CAG	24.5	28.3	23.9
GGG	17.6	11.4	6.4
GGT	15.6	25.4	26.6
TTC	29.6	16.0	19.1
TTT	13.3	22.2	23.9

Figure 3.26. Construction of the LDI gene with optimized codon usage. A) The LDI DNA and protein sequence. The red nucleotides indicate the sites for nucleotide exchange for optimized codon usage. B) The codon usage in barley (*Hordeum vulgare*), *E. coli* and *P. pastoris* for the codons exchanged in LDI.

3.3.2.2 Pichia pastoris

The LDI sequence was cloned into the *P. pastoris* expression vector pPICZα and the X-33 strain was transformed with the vectors. Fourty clones were tested for production of LDI using immunoblotting directly from agar plates that contained methanol for induction. Only a weak unspecific background reaction appeared, indicating that no LDI was produced from any of the clones.

3.3.2.3 Lactococcus lactis

MG1363/pAMJ399-LDI and MG1363/pAMJ399-LDI-His_6 were grown as described (Section 2.7.4). The plasmid carried the pH-inducible P170 promotor that was induced by the decrease in pH as the fermentation proceeded. Cell pellet and supernatant were analyzed for presence of LDI by SDS-PAGE and LD activity inhibition assay, but no LDI was found.

3.3.2.4 Trx-ECL-LDI-His_6 fusion protein

The difficulties in production of recombinant LDI may be caused by incorrect pairing of the four disulfide bridges. Therefore a cleavable N-terminal thioredoxin tag was added to LDI as this tag is believed to increase the solubility and facilitate disulfide bond formation of the target protein (Figure 3.27; LaVallie et al., 1993). An enteropeptidase cleavage site (ECL; sequence: Asp-Asp-Asp-Asp-Lys) was introduced between the thioredoxin and LDI in order to enable cleavage of the tag without leaving any additional residues of the N-terminus of LDI. Factor Xa could be an alternative choice of a less expensive endopeptidase. However, the LDI sequence contained a site similar to the Factor Xa cleavage site, and this would probably be a target for unspecific cleavage.

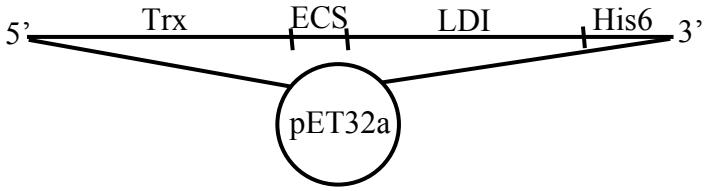

Figure 3.27. Construct of the Trx-ECS-LDI-His_6 fusion protein for production of LDI. The vector was commercially constructed with the Trx sequence and an enteropeptidase cleavage site (ECS), the LDI cDNA and the added His_6-tag sequence and cloned into the pET32a expression vector.

The fusion protein was produced in Rosetta cells at 37°C during 3 h induction with IPTG. The yield was 15 mg/L culture of soluble Trx-ECL-LDI-His_6. The fusion protein bound strongly to a nickel chelating column and was eluted as an almost pure protein of approximately 25 kDa (Figure 3.28, lane 5-7). The protein band of 50 kDa was most likely a dimer as it disappeared upon cleavage with enteropeptidase and it was also recognized by specific antibodies (Figure 3.29).

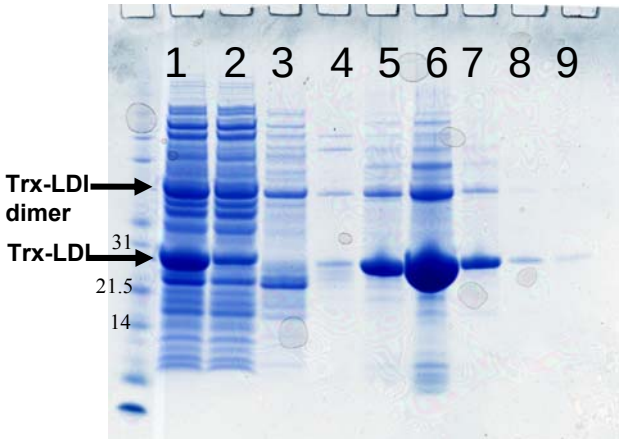

Figure 3.28. SDS-PAGE of the crude *E. coli* protein extract containing overexpressed Trx-LDI (Lane 1) and fractions of the purification of Trx-LDI on a nickel column, lane 2-9. Lane 1: Protein extract, lane 2: flow-through, lane 3: wash, lane 4: wash, 80 mM imidazole, lane 5-9: elution, 400 mM imidazole, fraction 1-5.

The Trx-ECL-LDI-His_6 showed inhibition of LD, however, approximately 16-fold weaker than that of LDI from barley seeds (bLDI; this is a rough estimate, as described in the next section). Upon cleavage the inhibitory activity decreased 3-10 fold and according to SDS-PAGE and western blotting (Figure 3.29) it is likely that enteropeptidase cleaves unspecifically within the LDI sequence. The residual inhibitory activity may be ascribed to correctly folded LDI-His_6 which seems to be strongly recognized by the specific antibodies (Figure 3.29B, lane 5 and 6). Fully active LDI is not a target for enteropeptidase, as tested using bLDI.

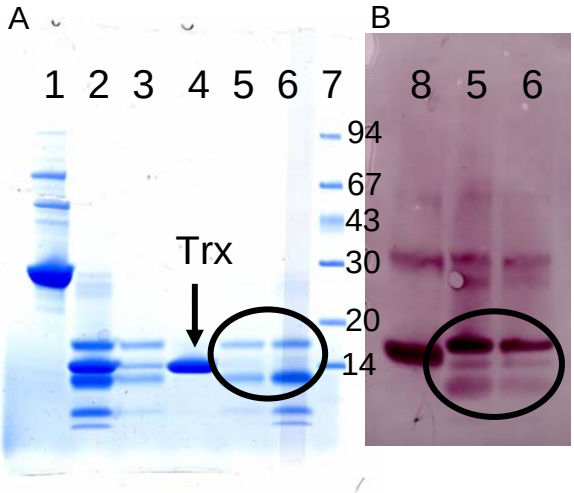

Figure 3.29. A) SDS-PAGE of the cleavage of Trx-ECL-LDI-His_6 with enteropeptidase and purification of LDI-His_6 on a nickel chelating column and B) western blotting of the purified LDI fractions. Lane 1: Trx-ECL-LDI-His_6, 5 µL (3 mg/L), lane 2: Cleaved Trx-LDI, 5 µL, lane 3: Flowthrough 1 from Ni-column, 16 µL, lane 4: Flowthrough 2 from Ni-column, 16 µL, lane 5: Eluate 1, 16 µL, lane 6: Eluate 2, 16 µL, lane 7: Protein marker, numbers are given in kDa, lane 8: bLDI, 1 µg.

Several culture conditions for Trx-ECL-LDI-His_6 producing cells were tested in an attempt to induce chaperones that can aid correct folding. These included growth at low temperature (15°C), induction with different concentrations of IPTG (5 and 100 µM), addition of ethanol (1

and 5%), and cold shock just before induction, but none of these modifications of the standard protocol gave higher yield or increased the inhibitory activity of Trx-ECL-LDI-His_6.

3.3.2.5 LD Inhibition activity

A small amount of bLDI purified from barley was available and mainly used as positive control in SDS-PAGE, western blotting, and LD activity inhibition assays. It is known that LD and LDI form a 1:1 complex and the binding is described as being "strong" (MacGregor, 2004) but no further characterization of the inhibition kinetics has been reported. The small amount of available bLDI did not allow studies of inhibition kinetics. However, a few points on an inhibition curve were generated from control experiments (Figure 3.30) and used as a guideline for estimation of the inhibitory efficiency of recombinant LDI. If the bLDI inhibition curve in Figure 3.30 was extrapolated to zero, linearity up to 70-90% was seen and only approximately 18% LD activity was inhibited at [bLDI]/[LD] = 1. This is less than expected for a strong 1:1 inhibition mechanism. Long term storage of bLDI (at 4°C as freeze-dried protein for years and at -20°C after re-dissolution) may have impaired the inhibitory activity. In this case, the inhibitory activity of Trx-ECL-LDI-His_6 is less than calculated below.

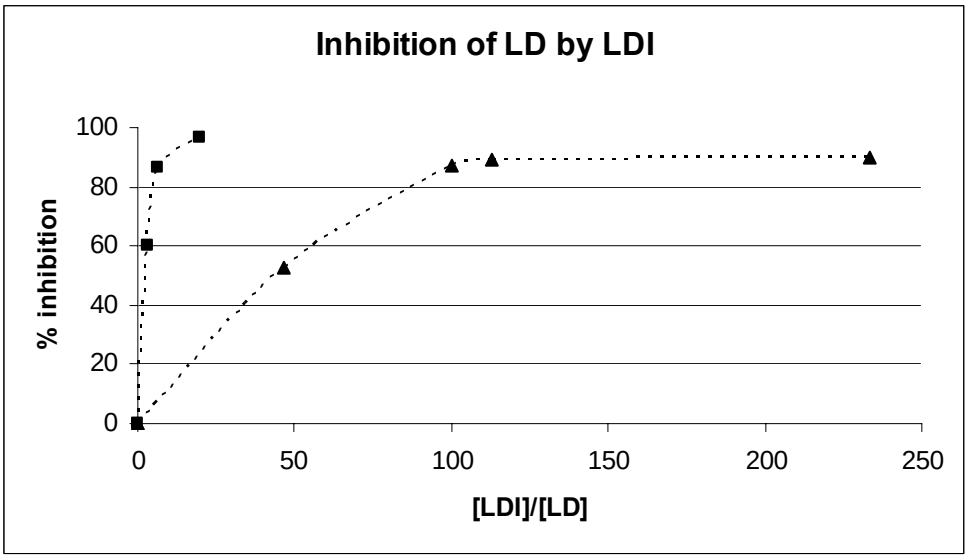

Figure 3.30. Inhibition of LD by bLDI (■) and Trx-ECL-LDI-His_6 (▲). The concentrations of LD an LDI were 0.03 mM and 0.15-3.5 mM, respectively in the assay.

The fusion protein showed 50% inhibition at [LDI]/[LD] = 44 compared to 50% inhibition at [LDI]/[LD] = 2.8 for bLDI. Linearity is assumed for this part of the inhibition curves, and therefore it is valid to conclude that Trx-ECL-LDI-His_6 has 16-fold reduced inhibitory activity compared to bLDI. After cleavage with enteropeptidase the inhibition by LDI-His_6 decreased 3-10 fold. The reduced activity of Trx-ECL-LDI-His_6 could be due to full activity of a small fraction of Trx-ECL-LDI-His_6 or Trx-ECL-LDI-His_6 could make a weak non-specific interaction with LD. Trx had no influence on the inhibition of LD as tested in a separate experiment.

3.3.3.6 Refolding of Trx-ECL-LDI-His_6

A re-folding protocol was set up in order to regain the correct conformation of Trx-ECL-LDI-His_6 before cleavage with enteropeptidase. After denaturation in urea and DTT the fusion protein

was re-folded at a concentration of 50 μg/mL. All combinations of the conditions listed below were tested:

- pH 7.5 or 9.0
- GSH:GSSG 2:1 (2 mM :1 mM) and 10:1 (3 mM : 0.3 mM)
- $(NH_4)_2SO_4$ 0 M, 0.2 M and 0.5 M
- Re-folding time 3½ h and 22 h

Presence of 1 M GdmCl was tested without significant positive effect and different protein concentrations (0.05 – 0.5 μg/μL) during renaturation were tested without any effect. A small increase of 2-5 fold in inhibition activity of Trx-ECL-LDI-His_6 was obtained by renaturation for 22 h compared to 3½ h (0.1 M Tris-HCl, pH 9.0, 1 mM EDTA, 3 mM GSH, 0.3 mM GSSG). Furthermore, the drop in activity upon cleavage with enteropeptidase described above was reduced after refolding. These experiments were repeated by a stud. polyt. Jannick Prentø, but he was not able to achieve increased inhibitory activity upon re-folding at any of the tested conditions (Prentø, 2005). Since full LDI inhibitory activity was not obtained and it was difficult to repeat the experiments, we assumed that the folding of LDI was not significantly improved.

3.3.3 Detection of LDI and LD in barley seed extracts

LD was detected in protein extracts of whole barley seeds to follow the formation and release of LD PI and identify possible post-translational modifications. As the protein is low-abundant we used specific antibodies to detect LD at 0, 72 and 144 h PI. Proteins were extracted with and without the presence of DTT in order to compare the levels of bound and unbound LD during radicle elongation (Section 1.3.1).

1D western blot (Figure 3.31) showed a clear band of the correct molecular size for LD at all three time points as compared to purified barley LD (Figure 3.31, lane 1). As expected, LD increased in abundance with time. DTT added to the extraction buffer had no significant effect on the amount of extracted LD when the LD bands of correct size were compared (Figure 3.31, compare lane 3 and 4, 5 and 6, 7 and 8). This suggested that only a small fraction of LD is in a bound form in the used seeds. Little degradation occurred during the protein extraction even at 144 h PI, where many proteases were active in the endosperm. Protease inhibitors were added during the protein extraction and they seemed to function efficiently.

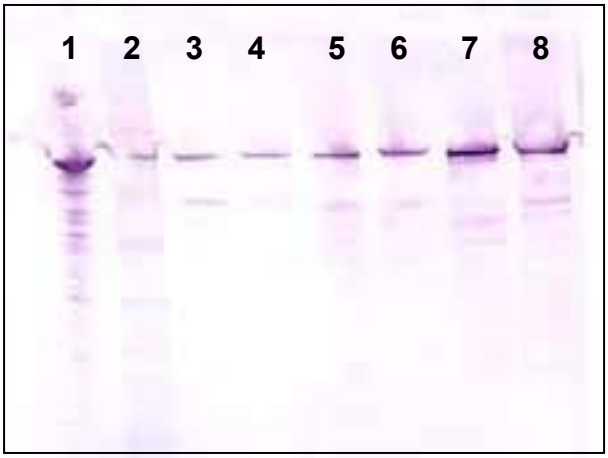

Figure 3.31. Western blot of whole barley seed protein extracts. Proteins were extracted in the presence or absence of DTT. Samples (9 μL) were applied to each lane (9-22 μg protein). Lane 1: barley LD control, lane 2: Marker, lane 3: seeds, 9 μL, lane 4: seeds +DTT, 9 μL, lane 5: 72 h, 9 μL, lane 6: 72 h +DTT, 9 μL, lane 7: 144 h, 9 μL, lane 8: 144 h +DTT, 9 μL.

2D western blots using the Novex system (Invitrogen) for the 2nd dimension showed that LD was present in the dry barley seed as a train of small spots that differed in pI (Figure 3.32). Only one gene encodes LD in barley (Burton et al., 1999) and it is therefore suggested that pI differences represented post-translational modifications. Trains of protein spots were also seen for the related enzyme, α-amylase, but in this case no post-translational modifications were identified by MS despite extensive studies (Bak-Jensen et al., 2007). Folding isomery occurring during IEF can also cause multiple forms of a protein in 2D gels (Lutter et al., 2001; Veith et al., 2001; Berven et al., 2003). After 72 h PI the intensity of the spots increased and a number of lower molecular weight forms were observed at 144 h PI in agreement with low molecular weight bands observed by 1D western blotting. These low molecular weight forms may indicate a specific degradation pattern in the seed but degradation could also occur during protein extraction and running of the 1st dimension as previously reported for β-amylase (Finnie and Svensson, 2002).

Figure 3.32. Detection of LD in 2D western blots of whole seed barley protein extracts using LD antibodies. 20 μL loaded on each gel (~20-50 μg protein)

It was not possible to see the LD spot on a silver stained gel and amount were to low therefore for identification of structural differences causing spot mobility differences by MS. LD exists in

a number of forms of pI 4.7-5.0 and molecular weights of 80-100 kDa (MacGregor, 1987). It was identified in 2D gels from aleurone cells incubated 18 h with GA in one spot (Mw 98 kDa and pI 4.5) out of a train of spots by MS (Christine Finnie, unpublished).

Detection of LDI in barley seed extracts was difficult probably due to the low abundance or in-efficient extraction of the protein. However, LDI was detected in endosperm from mature barley seeds using specific antibodies and 1D western blotting (not shown, as the weak band is not visible in a scanned, printed version of the blot). LDI seemed not be soluble in the normal extraction buffer (5 mM Tris-HCL pH 7.5, 1 mM $CaCl_2$), but when pH was lowered (0.2 M sodium acetate pH 5.0, 20 mM DTT) a weak band appeared of correct molecular size in a 1D western blot of endosperm and single seeds (Finnie and Svensson, 2003) extracts. The total amount of LDI in the seed could be detected in total protein extract, where the extraction buffer contained DTT and SDS, however, this was not done. As judged from the western blot only approximately 100 ng of soluble LDI is present in one mature barley seed and the amount of LDI probably decrease during germination along with related CM-proteins. LDI inhibition of LD may play a role during development and early stages of germination, but during radicle elongation LD is probably present in much higher amount than LDI.

3.3.4 Discussion

3.3.4.1 Heterologous expression of LDI

Several attempts to produce recombinant LDI for characterization of LD/LDI complex formation were carried out. However, pure un-tagged LDI was never obtained.

Only a few proteins from the same class (CM-proteins) as LDI have been produced recombinantly (Garcia-Maroto et al., 1991; Okuda et al., 1997; Klein et al., 1998) indicating the general difficulty with producting these in non-authentic organisms. A synthetic gene of the 0.19 α-amylase inhibitor from wheat was used for heterologous expression in *E. coli*, however, no protein was produced probably due to formation of mRNA hairpin structures interrupting the translation. When these structures were eliminated by degenerate codons, this protein was produced as inclusion bodies (Okuda et al., 1997). After refolding, this inhibitor was fully functional. The CM-proteins contain up to 10 cysteines forming disulfide bonds, which is often a major challenge when using simple organisms for heterologous expression, such as *E. coli*, which do not have the necessary folding machinery. Inter-molecular and incorrect intra-molecular disulfide bonds can form resulting in inclusion bodies. Inclusion bodies can in some cases be purified and refolded *in vitro*. Many soluble disulfide bond containing proteins, however, have been produced in *E. coli* (Bønsager et al., 2003; Braud et al., 2004), and thus the CM-protein family seems to be particular tricky.

LDI was not produced at all without an N-terminal tag – not even as inclusion bodies – neither in *E. coli*, *L. lactis* or *P. pastoris*. In *L. lactis* and *P. pastoris* the produced recombinant protein would be exported to the periplasma and the culture medium, respectively, but this did not aid production of LDI. The problem with LDI production probably occurred at the transcriptional level or initiation of translation. Therefore, the codon usage was optimized for production in *E. coli* and *P. pastoris* for the N-terminal part of the LDI gene, but this did not overcome the problem. As learned from a DNA sequence alignment of closely related genes encoding closely related proteins, the nucleotides in front of the start of the mature proteins are

highly conserved and may be important for transcription and/or translation efficiency (Figure 3.33).

```
Oryzae          MASKN------LLLSAAVLLSVLAIAAAAATASAATTSCQPGMAIPHDPLRGCRRYVLRR 54
Oryzae LDI      MACKSS---CSLLLLAAVLLSVLAAASASG-------SCVPGVAFRTNLLPHCRDYVLQQ 50
Hordeum LDI     MAS----DHRRFVLSGAVLLSVLAVAAATL--ESVKDECQPGVDFPHNPLATCHTYVIKR 54
Triticum        MAS----NHRRFLLSGAVLLSVLAAVAA-L--ESVEDECRPGVAFPHNALATCHTYVIKR 53
Zea             MASSSSSSHRRLILAAAVLLSVLAAASA-----SAGTSCVPGWAIPHNPLPSCRWYVTSR 55
                **.        ::* .******** .:*         .* **  :  : *  *: **  :

Oryzae          ACG-LAAGGRLYDWS-------------LKERCCQELAAVPAYCRCAALAYFMDG--ASE 98
Oryzae LDI      TCGTFTPGSKLPEWMTSASIYSPGKPYLAKLYCCQELAEISQQCRCEALRYFIALPVPSQ 110
Hordeum LDI     VCG----RGPSRPM-------------LVKERCCRELAAVPDHCRCEALRILMDGVRTPE 97
Triticum        VCG----RGPSLPM-------------LVKERCCRELAAVPDYCRCEALRVLMDGVRVEG 96
Zea             TCG----IGPRLPWP------------ELKRRCCRELADIPAYCRCTALSILMDGAIPPG 99
                .**     .                    *  **:*** :.  *** **  ::

Oryzae          ------GRL----LEDLPGCPRETQRGLAAVLTTPGECNLETIH--GGPYCLELTDREMP 146
Oryzae LDI      PVDPRSGNVGESGLIDLPGCPREMQWDFVRLLVAPGQCNLATIH--NVRYCPAV---EQP 165
Hordeum LDI     ------GRVVEGRLGDRRDCPREEQRAFAATLVTAAECNLSSVQEPGVRLVLLADG---- 147
Triticum        ------GHVLEGRLGDRRDCPREAQREFAATLVTAAECNLPTVS--GVGSTLGATGRWMX 148
Zea             P-----DAQLEGRLEDLPGCPREVQRGFAATLVTEAECNLATIS--GVAECPWILGGGTM 152
                      .      * *  .**** *  :.  *.: .:*** ::   .

Oryzae          KY--- 148
Oryzae LDI      LWI-- 168
Hordeum LDI     -----
Triticum        XELPK 153
Zea             PSK-- 155
```

Figure 3.33. Sequence alignment of LDI (Hordeum) related sequences from wheat (Triticum; α-amylase/trypsin inhibitor), maize (Zea; Hageman factor inhibitor), rice LDI (Oryzae LDI), and rice (Oryzae; α-amylase/trypsin inhibitor). The aligned regions preceding the N-terminus of LDI contained highly conserved regions (indicated in red).

3.3.4.2 Trx-ECL-LDI-His$_6$ fusion protein

A Trx tag was added to the N-terminus of LDI-His$_6$ spaced by an enteropeptidase cleavage site (ECL) because Trx is highly soluble and is able to facilitate disulfide bond formation of target proteins in *E. coli* (LaVallie et al., 1993). This vector construct yielded 15 mg/L Trx-ECL-LDI-His$_6$ and the fusion protein was easily purified using the His$_6$-tag. Trx-ECL-LDI-His$_6$ showed 16-fold reduced inhibitory activity towards compared to bLDI (calculated as described in Section 3.3.2.5).

Upon cleavage with enteropeptidase the inhibitory activity of LDI was expected to increase because the N-terminus residues thought to be important in inhibition were freed. However, a decrease in inhibitory activity was observed. This decrease is difficult to explain, but it could be due to unspecific cleavage in the LDI sequence of in-correctly folded LDI that originally had little inhibitory activity. The residual inhibitory activity could be ascribed to full activity of a smaller fraction of LDI of correct molecular size according to a SDS-PAGE (Figure 3.29). This fraction could be responsible for the inhibitory activity seen in the present work both for the fusion protein and for the cleaved protein. It should be possible to identify the low molecular protein contaminants (see Figure 3.29) by MS and remove them by ion exchange or a Superdex Peptide column (GE Healthcare), but this has not yet been done. The major limitation in this expression system is the cost of enteropeptidase.

Addition of an N-terminal highly soluble tag facilitated the production of LDI, however, since LDI is a suggested Trx h target *in vivo*, Trx as fusion partner may carry out a dual function during the folding process. An alternative option could be the intein-tag system in *E. coli* (New England Biolabs), where the tag is self-cleavable as induced by temperature or pH shift and no

external protease is needed. Maybe the most promising expression system for production of recombinant barley LDI would be a tobacco system (Vionnet et al., 2003) since a plant has the most appropriate transcription/translation machinery and mechanism for post-translational modifications for heterologous production of recombinant plant proteins.

3.3.4.3 LD/LDI complex formation – choice of mutants

The purpose of producing recombinant LDI was to obtain sufficient amounts of fully active protein for characterization and for design and production of LDI mutants to perform mutational analysis of the LD/LDI complex formation. LDI may be important during the malting of barley seeds and Trx h is thought to have a role in this context (Cho et al., 1999; Stahl et al., 2004). Based on sequence alignment with related proteins (the cereal type α-amylase/protease inhibitors) and structure of the TMA/RBI complex (Strobl et al., 1998; Section 1.3.3), the suggested LD binding site is located at the N-terminus including Ser4 and Val5 and these residues are targets for mutational analysis. The equivalent residues in RBI (Ser1 and Val2) are directly interacting with the catalytic residues of TMA, which belongs to the same structural family as LD. In addition, the residues preceding Ser4 and Val5 (Thr1, Leu2 and Glu3) are also targets for mutations. Glu3 is able form salt bridges or strong hydrogen bonds with target amino acid residues and such possible effect could be eliminated by mutation. By removing these first three amino acids in LDI it may be possible to change the specificity to inhibition of α-amylase (MacGregor et al., 2000). This is not the primary aim of the study, but the structures of α-amylases are well known as opposed to LD structures and understanding the mechanism of α-amylase inhibition may guide the understanding of the LD inhibition. Arg64 and Arg71 are suggested to be involved in inhibition since arginine specific chemical modification of LDI reduced the inhibitory activity (MacGregor et al., 2000), and these residues are thus are targets for mutational analysis.

The relatively strong inhibitory activity of Trx-ECL-LDI-His_6 toward LD was surprising since N-terminal residues were suggested to be directly involved in binding (MacGregor et al., 2000) and these would only be partially accessible in the fusion protein. We therefore think that other parts of LDI are important for binding to LD and that the mechanism of inhibition is different from that observed in other glycoside hydrolase/CM-protein complexes (Strobl et al., 1998; Payan, 2004; Section 1.3.3). In this case it will be more difficult to find the important residues for inhibition by mutation, but the role of Cys59 ought to be investigated. Barley LD contains 10 cysteines and it is possible that one is free and exposed to interact with LDI. Such an inhibition mechanism involving an intra-molecular disulfide bond would be unique compared to other enzyme-inhibitor interactions. According to the study of MacGregor et al. (2000) this LDI cysteine is modified in the barley seed by either disulfide bound cysteine or glutathione and it is not involved in inhibition of LD. These modifications of a free cysteine would probably not occur in *E. coli*, which is another argument for shifting to a tobacco expression system.

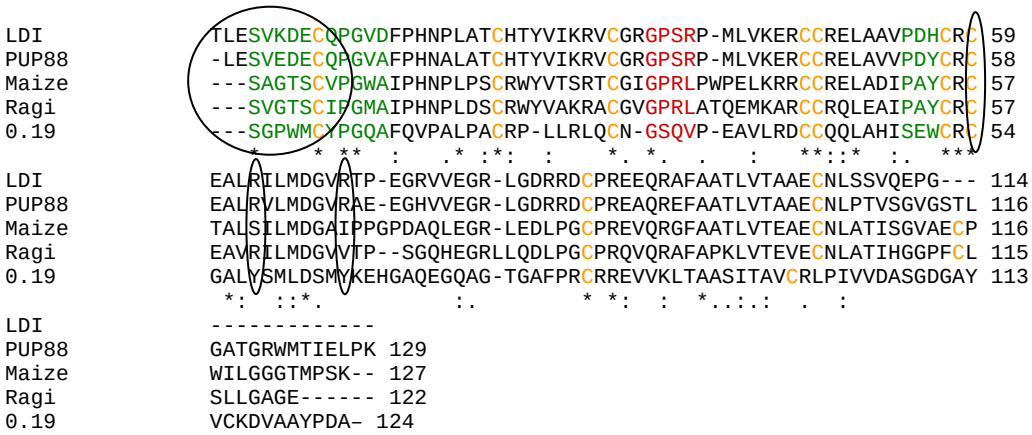

Figure 3.34. Sequence alignment of LDI, PUP88 from wheat, Hagedorn from maize, Ragi bifunctional inhibitor (RBI) and 0.19 from wheat. Residues suggested to involved in binding to α-amylase/limitdextrinase are green and residues suggested to be involved in protease binding are red. Cysteines are showed in orange. Encircled residues are targets for mutational analysis.

The protease binding site for RBI involves Gly-Pro-Arg-Leu (position 32-35) which constitutes a loop that interacts with the protease. In LDI the arginine switched position and probably exposes a different conformation not able to interact with a protease (MacGregor et al., 2000). By engineering the protease binding segment it may be possible to convert LDI to also have protease inhibitory activity, but this was not the objective in the present study.

Chapter 4 – Discussion and conclusions

4.1 Validation of the used methods

In this work, classical proteomic methods were employed in a study of water soluble barley seed proteins during germination and radicle elongation. The starting point was a detailed 2DE analysis of the dissected barley seed tissues which enabled individual proteins to be followed during a complex process and to couple the proteins to the tissue functionalities. The 2DE technique has limitations in the dynamic range, extraction of proteins, and quantitative measurement between two samples, respectively. These limitations were addressed in the present study by optimization of protein extraction conditions (Østergaard, 2003), fractionation of the seed tissues (Finnie and Svensson, 2003), running replicate gels, and comparing 2D gels from close time points. This resulted in reliable quantitative detection and identification of a broad variety of metabolic proteins through germination and radicle elongation. Examples of degradation patterns and protein modification were shown as some proteins were identified in multiple spots. This could provide clues to regulatory mechanisms, and possible post-translational modifications were studied in detail for APX. Homology searches strongly suggested functionalities of the identified proteins, but a major short coming in the 2D gel technology is the lack of information on protein activities and protein-protein interactions. It is not possible to address all aspects of a protein by a single method, but combination of different methods can provide detailed information of selected proteins.

By inspiration from the 2DE analysis it was attempted to understand the regulation of enzymes in redox-regulation involving central processes in the germinated embryo. The enzymes of the ascorbate-glutathione cycle were subjected to activity measurements and compared to the 2D gel patterns. This provided complementing (APX and GR) and in case of DHAR deviating profiles suggesting post-translational regulation of DHAR during radicle elongation. Comparison of 2D gel profiles with enzyme activity profiles has not been reported previously, probably because high through-put methods for detection of protein activities are difficult to set up. One study, however, of diurnal regulation in Arabidopsis compared activity of 23 enzymes and the corresponding transcript profiles (Gibon et al., 2004). There was not observed a direct relation between several of the enzyme activities and change the in transcripts encoding the corresponding enzymes. In some cases, the protein activity level was much delayed compared to the transcript level, while in other cases the protein and transcript profiles showed opposite patterns of appearance. This indicated that the studied enzymes are mainly regulated post-translationally and have a long turn-over.

Working with the protein extracts has the advantage of providing more biological relevant information as opposed to *in vitro* experiments using purified proteins. The drawback of the enzyme activity assayed in the present study is, however, the heterogeneity of the embryo protein extract associated with relatively high standard deviations of the activity measurements. By using a proper choice of control experiments and by conducting several replicates, the shown trends, however, were found to be reliable.

APX was subjected to additional analysis in order to understand the appearance, activity, and regulation of this enzyme. Gene expression analysis thus showed the appearance at the transcription level, 1D western blotting showed the appearance at the translation level, enzyme

assay and zymograms showed the activity at the functional level, and post-translational modifications were shown by 2D western blotting. The various structural changes resulting from the post-translational modifications were not identified by MS, but could provide clues to a possible regulatory mechanism. Thus, the study of APX is a good example of how different methods can provide complementing and overlapping results to understand the entirety of a protein in a biological process.

4.2 Germination of barley seeds

The onset of many cellular processes in the quiescent barley seed upon imbibition gives rise to proteome changes. Apparently all components needed to resume metabolic activity are present in the dry mature seed in a potentially active form (Bewley and Black, 1994), including mRNA, ribosomal proteins, initiation and elongation factors. This was recently supported for Arabidopsis seeds germinating in the presence of the transcriptional inhibitor, α-amanitin (Rajjou et al., 2004), whereas germination was abolished by cycloheximide that inhibits translation (Rajjou et al., 2004). Based on these findings, changes at the protein level are anticipated to precede changes in the transcript profile. Therefore 2DE combined with MS and database searches is a suitable approach to understand germination. In the present 2D gels a large number of proteins changed in abundance in the analyzed period and 79 spots representing 48 gene products were identified by MS. A number of these were related to desiccation stress (e.g. LEA proteins) and these decreased rapidly during germination. Most protein profile changes occurred during the radical elongation, suggesting that many of the proteins involved in the germination-related processes were either already present in the dry mature seed in a potentially active form or they are low abundant proteins for which the temporal appearance was not visible by 2DE.

The protein spots increasing in abundance during 0-72 h PI were either involved in oxidative stress, glycolysis, citric acid cycle, and protein translation or acting as chaperones, emphasizing the onset of metabolic activity. Relatively few proteins involved in cell cycle, translation, transcription and metabolism of nutrients were identified probably due to low abundance of these proteins. Increases, however, in levels of mRNA encoding such proteins were observed at the end of germination (i.e. 18-24 h after imbibition) by cDNA microarray analysis. This relatively late appearance of mRNAs supports that the mRNAs required for germination are present in the dry seed (Potokina et al., 2002; Watson and Henry, 2005). The gene expression analysis of APX supports this conclusion as the APX mRNA is present in the mature dry seed and new mRNA is synthesized during germination and radicle elongation. Both newly synthesized mRNAs and those present in the dry seed are likely to encode proteins essential for the support of normal cellular metabolism, which involves the housekeeping reactions that are not restricted to germination.

Although GA has previously been associated with germination, GA induced genes seems to play a minor role in germination and to be important rather in radicle elongation for mobilization of storage reserves (Gallardo et al., 2002; Bethke et al., 2006). This was supported by the fact that isolated embryos seemed to germinate very similarly to whole seed germinated embryos as judged from 2DE patterns. During radicle elongation, however, the embryo needs amino acids for synthesis of new proteins and if these are not provided by the endosperm, the embryo to certain extent seems to break-down its own proteins (Section 3.1.4).

The present proteome analysis strongly supports that germination is programmed during seed maturation and that the most necessary components, such as mRNAs, are already found in the dry mature seed prior to the onset of germination. Therefore *de novo* protein synthesis can occur concomitantly with mRNA synthesis at germination. As a consequence new proteins appeared in the embryo proteome already at 4 h PI.

4.3 Comparison with cDNA microarray data

Some of the 2DE identified proteome changes during germination and radicle elongation matched cDNA microarray data, e.g. for APX, PDI, and HSP70, whereas others were only found by one of the techniques emphasizing the complementarities of proteome and transcriptome analyses. A strong advantage of 2DE-based proteomics is the description of proteins from several 2DE spots due to post-translational modification, as seen in the present work. Contrasting results from proteome and transcriptome analysis were also reported previously e.g. for maize seeds at cold germination and desiccation (Kollipara et al., 2002). Spatio-temporal variations for proteins in barley seed germination compared with cDNA microarray data show examples of deviating and similar results (Table 4.1). Fragments of jasmonate-induced protein 23 (JIP-23) were found in two forms at 52-72 h PI in embryo (Figure 3.8, spot 370 and 587) in agreement with four JIP-23 transcripts being up-regulated at 48 h PI in embryo (Watson and Henry, 2005). While the present protein spots, however, originated from the same gene, three additional transcripts of the JIP-23 family were induced with almost identical profiles in another study (Watson and Henry, 2005).

Carboxypeptidase 1A (Figure 3.7, spot 593) appeared in embryo and aleurone 2DE at 24 and 52 h PI, respectively, but the corresponding transcript was constant in embryo until 72 h PI and then up-regulated (Potokina et al., 2002; Watson and Henry, 2005). This suggests that translation of the gene started soon after imbibition and that carboxypeptidase 1A increased in abundance also beyond 72 h PI. The gene was preferentially expressed in scutellar epithelium (Potokina et al., 2002), however, scutellar epithelium was included in the embryo fraction both in the present and the cDNA microarray study (Watson and Henry, 2005). An APX transcript found in scutullar epithelium (Potokina et al., 2002) and embryo (Potokina et al., 2002; Watson and Henry, 2005) at 12-24 h PI agreed with the APX protein being found at 24 h PI, although it is not known if the two APX transcripts were the same and corresponded to this protein.

Glutathione *S*-transferase, aconitate anhydrase, and a β-type proteasome subunit showed contrasting protein and transcript profiles and tissue specificity during germination and radicle elongation (Table 4.1). Thus transcription and translation are not necessarily directly coupled which has also been observed previously (Gygi et al., 1999; Tian et al., 2004). Differences may occur due to the use of methods with different detection thresholds preventing simultaneous analysis of all proteins and mRNAs from a tissue. Another factor would be protein stability and turnover. Finally, contrasting results between different sets of cDNA microarray data were also observed, e.g. for glutathione *S*-transferase (Table 4.1).

.

Table 4.1. Appearance of proteins and corresponding mRNA after imbibition identified by the present 2DE analysis and cDNA microarray (Potokina et al., 2002; Watson and Henry, 2005).

			2-DE analysis		cDNA microarray analysis
Protein	**Accesion #[a]**	**Tissue**	**Change in abundance**	**Tissue**	**Change in abundance**
Aconitate anhydrase	BQ458967	emb	↓ 52 h	emb	÷
		aleu	↓ 24 h	scut	÷
		endo	÷	endo+aleu	↑ 12-24 h[b]
Glutathione *S*-transferase	AF109194	emb	→	emb	↑ 12-24 h[b] ↓ 96 h[c]
		aleu	→	scut	÷
		endo	→	endo+aleu	÷
Serine carboxypeptidase	1314177A	emb	↑ 36 h	emb	↑ 12-24 h[b] ↑ 8 h[c]
		aleu	↑ 52 h	scut	↑ 12-24 h[b]
		endo	÷	endo+aleu	÷
Proteasome subunit β-type	O64464	emb	↑ 4 h	emb	↓ 96 h[c]
		aleu	÷	scut	÷
		endo	÷	endo+aleu	÷
Jasmonate induced protein 23	X98124	emb	↑ 52 h	emb	↑ 48 h[c]
		aleu	÷	scut	÷
		endo	÷	endo+aleu	÷
Ascorbate peroxidase (APX)	AJ006358	emb	↑ 24 h	emb	↑ 12-24 h[b]
		aleu	÷	scut	↑ 12-24 h[b]
		endo	÷	endo+aleu	÷

[a] accession numbers are from Table 3.1. [b] Identification made in Potokina et al., 2002. [c] Identification made in Watson and Henry, 2005. The arrows indicate at what time point the proteins spot start to either increase ↑ or decrease ↓ in abundance. → indicates that the protein spot is constant during 0-72 h PI and ÷ indicates that the protein spot or the mRNA does not change in abundance or is not present in the specific tissue. Glutahione *S*-transferase is known from previous work to be constant during germination and radicle elongation (Østergaard et al., 2004).

4.4 Study of LDI and ascorbate-glutathione cycle enzymes

The present work included study of selected proteins comprising LDI and ascorbate-glutathione cycle enzymes that all are related to radicle elongation. They are involved in central processes during radicle elongation, i.e starch degradation and ROS scavenging that are targets for extensive studies.

The small amounts present in the seed or the poor solubility of LDI has not previously allowed detailed characterization of the inhibitor and production of recombinant LDI was therefore necessary. Despite many challenges to overcome, LDI was eventually purified with an N-terminal Trx tag and showed 16-fold reduced inhibitory activity compared to bLDI. It was not possible in the used expression systems to obtain fully functional LDI and it remains to be characterized with respect to interaction with LD and the role of Trx h in this binding, which has relevance for the brewing industry.

By using APX, DHAR, MDHAR, and GR activity assays in the embryo extracts, we were able to obtain information on a functional aspect of these enzymes during radicle elongation and to correlate the data with 2D gel spot patterns. This work inspired to analyze for possible Trx h linked reduction of DHAR and APX by combining different available techniques (enzyme activity assays with and without addition of recombinant Trx h, 2D western blotting,

and MS). Trx h is believed to play a central role in protection against oxidative stress during seed desiccation and germination (reviewed in Gelhaye et al., 2004) and this has been a target for research for many years. The high sequence coverage (up to 92.4%) obtained by MS of 9 APX1 forms was an excellent starting point for determination of post-translational modifications, however, we have not yet been able to identified these modifications.

Chapter 5 - Perspectives

The present application of a proteomics approach to study barley seed germination has provided new insight into the processes of germination and radicle elongation that are not yet understood in molecular detail. The difficulties in working with small amount of biological material and small-scale protein extraction were overcome and good resolution 2D gels enabled us to track proteins during 72 h covering the processes in three different tissues with specific functionalities. We were able to identify proteins changing in abundance as soon as at 4 h PI showing that the present approach indeed is useful for providing novel insight in the germination process. The identified proteins covered a broad spectrum of functionalities and underlined the complexity of the germination process. The identified proteins also correlated nicely with the tissue functionalities. The present proteome analysis of seed germination is to date the most detailed of its kind and makes an excellent starting point for detailed analysis of specific proteins in the process in barley as well as for other cereals and plants in general.

In the present study, the ascorbate-glutathione cycle enzymes were selected for further analysis since they seemed to play a role during radicle elongation as judged from the 2D gel analysis. The comparison of enzyme activities of APX, DHAR, MDHAR, and GR with the corresponding 2D gel patterns during germination and radicle elongation has not been previously reported. This approach provided links between the presence of enzymes and regulation of activities. In case of APX, gene expression and post-translational modifications were also monitored to understand the expression and possible activity regulation patterns. However, the structure of the post-translational modifications of APX remains to be identified. Gene expression analysis could be expanded to include the other ascorbate-glutathione cycle enzymes, preferable in all seed tissues, to gain more information of the ascorbate-glutathione cycle in the seed during germination and radicle elongation. In addition, the analysis (enzyme activity assays and gene expression analysis) can profitably be applied to other enzymes involved in redox control.

Future projects regarding germination and radicle elongation of cereal seeds can with advantage be based on the present proteome analysis. Protein markers for germination are still desirable for understanding this remarkable ensemble of biological processes. A target for further analysis could be the embryo specific protein that is present in intensive spots and has not yet been ascribed a function. It has been suggested to be a Trx h target (Maeda et al., 2004) and is therefore interesting also in the context of understanding Trx h interaction with target proteins.

By heterologous expression of LDI we hoped to be able to study the interaction with LD in detail using mutational analysis of selected amino acid residues anticipated to be important for inhibition. This may be important for the brewing industry and for understanding protein-protein interactions and protein engineering of related inhibitors. LDI belongs to a type of proteins (CM-proteins) that are strongly represented in cereal seed, but the precise functions of these proteins are far from clear. With the present approach we were not yet able to produce fully functional LDI, but did obtain a reasonable amount of partially active inhibitor as a fusion protein. During this work several challenges were faced important for testing new approaches to produce fully functional recombinant LDI.

The present work comprises studies of proteins at different levels: 1) a large scale proteomics approach that gives an overview of many proteins involved in a biological process, 2)

study of selected proteins in protein extracts (enzyme activity assays, specific antibodies, and MS) adding a functional aspect to the proteomics approach, and c) cloning and heterologous expression of a protein that can form the basis for gain of new information regarding structure/function relationships (using e.g. mutational analysis and crystallization).
This work contributed novel identification of early changes in barley seed germination at the protein level and highlighted new aspects of the function of the ascorbate-glutathione cycle enzymes in radicle elongation.

References

Abe, J., Sidenius, U., Svensson, B. (1993) Arginine is essential for the α-amylase inhibitory activity of the α-amylase/subtilisin inhibitor (BASI) from barley seeds. *Biochem. J*. 293, 151-155.

Aebersold, R.H., Leavitt, J., Saavedra, R.A., Hood, L.E., Kent, S.B. (1987) Internal amino acid sequence analysis of proteins separated by one- or two-dimensional gel electrophoresis after *in situ* protease digestion on nitrocellulose. *Proc. Natl. Acad. Sci. USA* 84, 6970-6974.

Agrawal, G.K., Jwa, N.-S., Iwahashi, H., Rakwal, R. (2003) Importance of ascorbate peroxidase OsAPX1 and OsAPX2 in the rice pathogen response pathways and growth and reproduction revealed by their transcriptional profiling. *Gene* 322, 93-103.

Agrawal, G.K., Rakwal, R. (2006) Rice proteomics: a cornerstone for cereal food crop proteomes. *Mass Spectrum. Rev.* 25, 1-53.

Ahn, B.Y., Moss, B. (1992) Glutaredoxin homologue encoded by vaccinia virus is a virion-associated enzyme with thioltransferase and dehydroascorbate reductase activities. *Proc. Natl. Acad. Sci. USA* 89, 7060-7065.

Alam, N., Gourinath, S., Dey, S., Srinivasan, A., Singh, T.P. (2001) Substrate-inhibitor interaction in the kinetics of α-amylase inhibition by Ragi α-amylase/trypsin inhibitor (RATI) and its various N-terminal fragments. *Biochemistry* 40, 978-985.

Alsheikh, M.K., Heyen, B.J., Randall, S.K. (2003) Ion binding properties of the dehydrin ERD14 are dependent upon phosphorylation. *J. Biol. Chem*. 278, 40882-40889.

Amiour, N., Merlino, M., Leroy, P., Branlard, G. (2002) Proteomie analysis of amphiphilic proteins of hexaploid wheat kernels. *Proteomics* 2, 632-641.

Amor, Y., Chevion, M., Levine, A. (2000) Anoxia pretreatment protects soybean cells against H_2O_2-induced cell death: possible involvement of peroxidases and of alternative oxidase. *FEBS Lett*. 477, 175-180.

Andon, N.L., Hollingworth, S., Koller, A., Greenland, A.J., Yates, J.R., Haynes, P.A. (2002) Proteomic characterization of wheat amyloplasts using identification of proteins by tandem mass spectrometry. *Proteomics* 2, 1156-1168.

Arrigoni, O., De Gara, L., Tommasi, F., Liso, R. (1992) Changes in the ascorbate system during seed development of *Vivia faba* L. *Plant Physiol*. 99, 235-238.

Arrigoni, O., Dipierro, S., Borraccino, G. (1981) Ascorbate free radical reductase, a key enzyme of the ascorbic acid system. *FEBS Lett*. 120, 242-244.

Asada, K. (1997) The role of ascorbate peroxidase and monodehydroascorbate reductase in H_2O_2 scavenging in plants. In: Scandalios, J.D. (Ed.) *Oxidative stress and molecular biology of antioxidant defences*. New York: Cold Spring Habour Laboratory Press, 527-568.

Bailly, C. (2004) Active oxygen species and antioxidants in seed biology. *Seed Sci. Res*. 14, 93-107.

Bak-Jensen, K.S., Laugesen, S., Østergaard, O., Finnie, C., Roepstorff, P., Svensson, B. (2007) Mapping multiple forms of barley α-amylase generated at germination by using two-dimensional electrophoresis, immunoblotting, and mass spectrometry. *FEBS J*. 274, 2552-2565.

Bak-Jensen. K.S., Laugesen, S., Roepstorff, P., Svensson, B. (2004) Two-dimensional gel elctrophoresis pattern (pH 6-11) and identification of water-soluble barley seed and malt protein by mass spectrometry. *Proteomics* 4, 728-742.

Barbar, D., Sanchez-Monge, R., Mendez, E., Lazaro, A., Garcia-Olmedo, F., Salcedo, G. (1986) New α-amylase and trypsin inhibitors among the CM-proteins of barley (*Hordeum vulgare*). *Biochim. Biophys. Acta* 869, 115-118.

Bartels, B., Engelhardt, K., Roncarati, R., Schnider, K., Rotter, M., Salamini, F. (1991) An ABA and GA modulated gene expressed in the barley embryo encodes an aldose reductase related protein. *EMBO J.* 10, 1037-1043.

Beavis, R.C., Chaudhary, T., Chait, B.T. (1992) Alpha-cyano-4-hydroxycinnamic acid as a matrix for matrix-assisted laser desorption mass spectrometry. *Org. Mass Spectom*. 27, 156-158.

Berven, F.S., Karlsen, O.A., Murrell, J.C., Jensen, H.B. (2003) Multiple polypeptide forms observed in two-dimensional gels of *Methylococcus capsulatus* (Bath) polypeptides are generated during the separation procedure. *Electrophoresis* 24, 757-761.

Bethke, P., Lonsdale, J.E., Fath, A., Jones, R.L. (1999) Hormonally regulated programmed cell death in barley aleurone cells. *Plant Cell* 11, 1033-1046.

Bethke, P.C., Hwang, Y., Zhu, T., Jones, R.L. (2006) Global patterns of gene expression in the aleurone of wild-type and *dwarf1* mutant rice. *Plant Physiol*. 140, 484-498.

Bewley, J.D. (1997) Seed germination and dormancy. *Plant Cell* 9, 1055-1066.

Bewley, J.D., Black, M. (1994) *Seeds: Physiology and development of germination*. Plenum Publishing Corporation, New York, USA.

Biron, D.G., Brun, C., Lefevre, T., Lebarbenchon, C., Loxdale, H.D., Chevenet, F., Brizard, J., Thomas, F. (2006) The pitfalls of proteomic experiments without the correct use of bioinformatics tools. *Proteomics* 6, 5577-5596.

Bønsager, B.C., Nielsen, P.K., Abou-Hachem, M., Fukuda, K., Prætorius-Ibba, M., Svensson, B. (2005) Mutational analysis of target recognition of the beta-trefoil fold barley alpha-amylase subtilisin inhibitor. *J. Biol. Chem*. 280, 14855-14864.

Bønsager, B.C., Prætorius-Ibba, M., Nielsen, P.K., Svensson, B. (2003) Purification and characterization of the beta-trefoil fold protein barley alpha-amylase/subtilisin inhibitor overexpressed in *Escherichia coli*. *Protein Expr. Purif*. 30, 184-193.

Braud, S., Belin, P., Dassa, J., Pardo, L., Mourier, G., Caruana, A., Priest, B.T., Dulski, P., Garcia, M.L., Ménez, A., Boulain, J.-C., Gasparini, S. (2004) BgK, a disulfide-containing sea anemone toxin blocking K+ chammels, can be produced in *Escherichia coli* cytoplasm as a functional tagged protein. *Protein Expr. Purif*. 38, 69-78.

Briggs, D.E. (1978) *Barley*. Chapman & Hall, London, UK.

Bringhurst, T.A., Broadhead, A.L., Brosnan, J.M., Pearson, S.Y., Walker, J.W. (2001) The identification and behavior of branched dextrins in production of Scotch whisky. *J. Inst. Brew*. 107, 137-148.

Broin, M., Cuiné, S., Eymery, F., Rey, P. (2003) The plastidic 2-cysteine peroxiredoxin is a target for a thioredoxin involved in the protection of the photosynthetic apparatus against oxidative damage. *Plant Cell* 14, 1417-1432.

Burton, R.A., Zhang, X.-Q., Hrmova, M., Fincher, B. (1999) A single limit dextrinase gene is expressed both in the developing endosperm and in germinated grains of barley. *Plant Physiol.* 119, 859-871.

Campos, F.A.P., Richardson, M. (1983) The complete amino acid sequence of the bifunctional α-amylase/trypsin inhibitor from seeds of Ragi (Indian finger millet, Eleusine coracana Gaertneri). *FEBS Lett.* 152, 300-304.

Candiano, G., Bruschi, M., Musante, L., Santucci, L., Ghigger, G.M., Carnemolla, B., Orecchia, P., Luciano, Z., Righetti, P.G. (2004) Blue silver: a very sensitive colloidal Coomassie G-250 staining for proteome analysis. *Electrophoresis* 25, 1327-1333.

Chen, G-X., Asada, K. (1989) Ascorbate peroxidase in tea leaves: occurrence of two isozymes and differences in their enzymatic and molecular properties. *Plant Cell Physiol*. 30, 987-998.

Cho, M.-J., Wong, J.H., Marx, C., Jiang, W., Lemaux, P.G., Buchanan, B.B. (1999) Overexpression of thioredoxin h leads to enhanced activity of starch debranching enzyme (pullulanase) in barley grain. *Proc. Natl. Acad. Sci. USA* 96, 14641-14646.

Choudhary, J.S., Blackstock, W.P., Creasy, D.M., Cottress, J.S. (2001) Matching peptide mass spectra to EST and genomic DNA databases. *Trends Biotechnol*. 19, 17-22.

Cottrell, J.S. (1994) Protein identification by peptide mass finger printing. *Pept. Res*. 7, 115-124.

Creissen, G., Firmin, J., Fryer, M., Kular, B., Leyland, N., Reynolds, H., Pastori, G., Wellburn, F., Baker, N., Wellburn, A., Mullineaux, P. (1999) Elevated glutathione biosynthetic capacity in the chloroplasts of transgenic tobacco plants paradoxically causes increased oxidative stress. *Plant Cell* 11, 1277-1292.

Crosatti, C., Polverino de Laureto, P., Bassi, R., Cattivelli, L. (1999) The interaction between cold and light controls the expression of the cold-regulated barley gene cor14b and the accumulation of the corresponding protein. *Plant Physiol.* 199, 671-680.

Cui, K., Gengsheng, X., Xinmin, L., Gengmei, X., Yafu, W. (1999) Effect of hydrogen peroxide on somatic embryogenesis of *Lycium barbarum* L. *Plant Sci*. 146, 9-16.

Dalton, D.A., Russels, S.A., Hanus, F.J., Pascode, G.A., Evans, H.J. (1986) Enzyme reaction of ascorbate and glutathione that prevent peroxide damage in soybean root nodules. *Proc. Natl. Acad. Sci. USA* 83, 3811-3815.

De Gara, L., de Pinto, M.C., Moliterni, V.M.C., D'Egidio, M.G. (2003) Redox regulation and storage processes during maturation in kernels of *Triticum durum. J. Exp. Bot*. 54, 249-381.

De Gara, L., Pinto, M.C., Arrigoni, O. (1997) Ascorbate synthesis and ascorbate peroxidase activity during the early stage of wheat germination. *Physiol. Plant.* 100, 894-900.

De Kok, L.J., Stulen, I. (1993) Role of glutathione under oxidative stress. In: De Kok, L.J. et al., (Eds.). *Sulphur nutrition and assimilation in higher plants*. The Hague, The Netherlands: SPB Acadmic Publishing, 125-152.

de Pinto, M.C., Tommasi, F., De Gara, L. (2000) Enzymes of the ascorbate biosynthesis and ascorbate-glutathione cycle in cultured cells tobacco Bright Yellow 2. *Plant Physiol. Biochem*. 38, 541-550.

Demus, U. (1999). *Entwicklungs- und jasmonatabhängiges Vorkommen eines 23 kDa Proteins der Gerste (Hordeum vulgare L. cv. Salome)*. Dr. rer. nat. dissertation. Matematisch-Naturwissenschaftlich-Technischen Fakultät der Martin-Luther Universität, Halle-Wittenberg.

DeRocher, A.E., Vierling, E. (1994). Developmental control of small heat shock protein expression during pea seed maturation. *Plant J*. 5, 93-102.

Dixon, D.P., Davis, B.G., Edwards, R. (2002) Functional divergence in the glutathione transferase superfamily in plants. *J. Biol. Chem.* 277, 30859-30869.

Dixon, D.P., Skipsey, M., Grundy, N.M., Eswards, R. (2005) Stress-induced protein *S*-gluthionylation in Arabidopsis. *Plant Physiol*. 138, 2233-2244.

Dommes, J., Van de Walle, C. (1990) Polysome formation and incorporation of new ribosomes into polysomes during germination of the embryonic axis of maize. *Plant Physiol*. 79, 289-296.

Dulhunty, A., Gage, P., Curtis, S., Chelvanayagam, G., Boark, P. (2001) The glutathione transferase structural family includes a nuclear chloride channel and a ryanodine receptor calcium release channel modulator. *J. Biol. Chem*. 276, 3319-3323.

Dunbar, B.D., Bundman, D.S., Dunbar, B.S. (1985) Identification of cultivar specific proteins of winter wheat (*T. aestivum* L.) by high resolution two-dimensional polyacrylamide gel electrophoresis and color-based silver stain. *Electrophoresis* 6, 39-43.

Eastmond, P.J., Germain, V., Lange, P.R., Bryce, J.H., Smith, S.M., Graham, I.A. (2000) Postgerminative growth and lipid catabolism in oilseeds lacking the glyoxylate cycle. *Proc. Natl. Acad. Sci. USA* 97, 5569-5574.

Fath, A., Bethke, P., Lonsdale, J., Meza-Romero, R., Jones, R. (2000) Programmed cell death in cereal aleurone. *Plant Mol Biol*. 44, 255-266.

Fath, A., Bethke, P.C., Jones, R.L. (2001) Enzymes that scavange reactive oxygen species are down-regulated prior to gibberellic acid-induced programmed cell death in barley aleurone. *Plant Physiol.* 126, 156-166.

Feng, C.H., Richardson, M., Chen, M.S., Kramer, K.J., Morgan, T.D., Reeck, G.R. (1996) α-Amylase inhibitors form wheat: amino acid sequence and patterns of inhibition of insect and human α-amylases. *Insect Biochem. Mol. Biol*. 26, 419-426.

Fincher, G.B., Stone, B. (1986) Cell walls and their components in cereal grain technology. *Adv. Cereal Sci. Tech*. 8, 207-295.

Finnie, C., Bak-Jensen, K.S., Laugesen, S., Roepstorff, P., Svensson, B. (2006) Differential appearance of isoforms and cultivar variation in protein temporal profiles revealed in the maturing barley grain proteome. *Plant Sci.* 170, 808-821.

Finnie, C., Melchior, S., Roepstorff, P., Svensson, B. (2002) Proteome analysis of grain filling and seed maturation in barley. *Plant Physiol*. 129, 1308-1319.

Finnie, C., Svensson, B. (2002) Proteolysis during the isoelectric focusing step of two-dimensional gel electrophoresis may be a common problem. *Anal. Biochem*. 311, 182-186.

Finnie, C., Svensson, B. (2003) Feasibility study of a tissue-specific approach to barley proteome analysis: aleurone layer, endosperm, embryo and single seeds. *J. Cereal Sci.* 38, 217-227.

Flengsrud, R. (1993) Separation of acidic barley endosperm proteins by two-dimensional electrophoresis. *Electrophoresis* 14, 1060-1066.

Flengsrud, R., Kobro, G. (1989) A method for two-dimensional electrophoresis of proteins from green plant tissue. *Anal. Biochem.* 177, 33-36.

Foster, J.G., Hess, J.L. (1980) Responses of superoxide dismutase and glutathione reductase activities in cotton leaf tissue exposed to and atmosphere enriched in oxygen. *Plant Physiol*. 66, 482-287.

Foyer, C.H., Noctor, G. (2005) Oxidant and antioxidant signaling in plants: a re-evaluation of the concept of oxidative stress in a physiological context. *Plant Cell Env.* 28, 1056-1071.

Franco, O.L., Ridgen, D.J., Melo, F.R., Bloch, C., Silva, C.P., Grossi de Sa, M.F. (2000) Activity of wheat α-amylase inhibitors toward bruchid α-amylases and structural explanation of observed specificities. *Eur. J. Biochem*. 267, 2166-2173.

Franco, O.L., Ridgen, D.J., Melo, F.R., Grossi-de-Sa, M.F. (2002) Plant α-amylase inhibitors and their interaction with insect α-amylase. Structure, function and potential for crop protection. *Eur. J. Biochem*. 269, 397-412.

Gallardo, K., Job, C., Groot, S.P.C., Puype, M., Demol, H., Vandekerckhove, J., Job, D. (2001) Proteomic analysis of Arabidopsis seed germination and priming. *Plant Physiol.* 126, 835-848.

Gallardo, K., Job, C., Groot, S.P.C., Puype, M., Demol, H., Vandekerckhove, J., Job, D. (2002) Proteomic of Arabidopsis seed germination. A comparative study of wild-type and gibberellin-deficient seeds. *Plant Physiol*. 129, 823-837.

Garcia-Maroto, F., Cabonero, P., Garcia-Olmedo, F. (1991) Site-directed mutagenesis and expression in *Escherichia coli* of WMAI-1, a wheat monomeric inhibitor of insect α-amylases. *Plant Mol. Biol*. 17, 1005-1011.

Gasson, M.J. (1983) Plasmid complements of *Streptococcus lactis* NCDO 712 and other lactic streptococci after protoplast-induced curing. *J. Bacteriol*. 154, 1-9.

Gelhaye, E., Navrot, N., Macdonald, I.K., Rouhier, N., Raven, E.L., Jacquot, J.-P. (2006) Ascorbate peroxidase-thioredoxin interaction. *Photosynth. Res*. 89, 193-200.

Gelhaye, E., Rouhier, N., Jacquot, J.-P. (2004) The thioredoxin *h* system of higher plants. *Plant Physiol. Biochem*. 42, 265-271.

Gengenheimer, P. (1990) Preparation of extracts from plants. *Methods Enzymol*. 182, 174-193.

Ghezzi, P. (2005) Regulation of protein function by glutathionylation. *Free Rad. Res*. 39, 573-580.

Gibon, Y., Blaesing, O.E., Hannemann, J., Carillo, P., Höhne, M., Hendriks, J.H.M., Palacios, N., Cross, J., Selbig, J., Stitt, M. (2004) A robot-based platform to measure multiple enzyme activities in Arabidopsis using a set of cycling assays: comparison of changes of enzyme activities and transcript levels during diurnal cycles and in prolonged darkness. *Plant Cell* 16, 3304-3325.

Giese , H., Hejgaard, J. (1994) Synthesis of salt-soluble proteins in barley. Pulse-labeling study of grain filling in liquid-cultured detached spikes. *Planta* 161, 172-177.

Gobom, J., Nordhoff, E., Mirgorodskaya, E., Ekman, R., Roepstorff, P. (1999) Sample purification and preparation technique based on nano-scale reversed-phase column for the sensitive analysis of complex peptide mixtures by matrix-assisted laser desorption/ionization mass spectrometry. *J. Mass Spectrom.* 24, 105-106.

Goday, A., Jensen, A.B., Culiáñez-Marciá, F.A. (1994) The maize abscisic acid-responsive protein Rab17 is located in the nucleus and interacts with nuclear localization signals. *Plant Cell* 6, 352-360.

Görg, A., Postel, W., Baumer, M., Weiss, W. (1992) Two-dimensional polyacrylamide gelelectrophoresis, with immobilized pH gradients in the first dimension, of barley seed proteins: discrimination of cultivars with different malting grades. *Electrophoresis* 13, 192-203.

Görg, A., Postel, W., Domscheit, A., Gunther, S. (1988) Two-dimensional electrophoresis with immobilized pH gradients of leaf proteins from barley (*Hordeum vulgare*): Method, reproducibility and genetic aspects. *Electrophoresis* 9, 681-692.

Görg, A., Postel, W., Weiss, W. (1992) Detection of polypeptides and amylase isoenzymes modifications related to malting quality during malting process of barley by two-dimensional electrophoresis and isoelectric focusing with immobilized pH gradients. *Electrophoersis* 13, 759-770.

Granier, F. (1988) Extraction of plant proteins for two-dimensional electrophoresis. *Electrophoresis*, 9, 712-718.

Groot, S.P.C., Karssen, C.M. (1987) Gibberellins regulate seed germination in tomato by endosperm weakening: a study with gibberellin-deficient mutants. *Planta* 171, 525-531.

Gygi, S.P., Rochon, Y., Franza, R., Aebersold, R. (1999) Correlation between protein and mRNA abundance in yeast. *Mol. Cell. Biol.* 19, 1720-1730.

Gygi, S.P., Rist, B., Gerber, S.A., Turecek, F., Gelb, M.H., Aebersold, R. (1999) Quantitative analysis of complex protein mixtures using isotope-coded affinity tags. *Nat. Biotechnol*. 17, 994-999.

Harrop, S.J., DeMaere, M.Z., Fairlie, W.D., Reztsova, T., Valenzuela, S.M., Mazzanti, M., Tonini, R., Qiu, M.R., Jankova, L., Warton, D., Bauskin, A.R., Wu, W.M., Pankhurst, S., Campbell, T.J., Breit, S.N., Curmi, P.M.G. (2001) Crystal structure of a soluble form of the intracellular chloride ion channel CLIC1 (NCC27) at 1.4-Å resolution. *J. Biol. Chem*. 276, 44993-45000.

Hejgaard, J. (1978) Free and bound β-amylases during malting of barley. Characterization by two-dimensional immunoelectrophoresis. *J. Inst. Brew.* 84, 43-46.

Hejgaard, J. (1982) Purification and properties of protein Z – a major albumin of barley endosperm. *Physiol. Plant* 54, 174-182.

Heukeshoven, J., Dernick, R. (1988) Improved silver staining procedure for fast staining in PhastSystem Deveopment Unit. I. Staining of sodium dodecyl sulfate gels. *Electrophoresis* 9, 28-32.

Heyen, B.J., Alsheikh, M.K., Smith, E.A., Torvik, C.F., Seals, D.F., Randall, S.K. (2002) The calcium-binding activity of a vacuole-associated, dehydrin-like protein is regulated by phosphorylation. *Plant Physiol*. 130, 675-687.

Hiner, N.P., Rodrïgeuz-López, J.N., Arnao, M.B., Raven, E.L., García-Cánovas, F., Acosta, M. (2000) Kinetic study of the inactivation of ascorbate peroxidase by hydrogen peroxide. *Biochem. J*. 348, 321-328.

Hirano, H. (1997) Screening of rice genes from the cDNA catalogue using the data obtained by protein sequencing. *J. Prot. Chem*. 16, 53-536.

Hoekstra, F.A., Golovina, E. (2003) What do we really know about desiccation tolerance mechanisms? Nicolás, G., Bradford K.J., Côme, D., Pritchard, H.W. (Eds*.). The biology of seeds*. CABI Publishing. pp 259-270.

Hynek, R., Svensson, B., Jensen, O.N., Barkholt, V., Finnie, C. (2006) Enrichment and identification of integral membrane protein from barley aleurone layers by reversed-phase chromatography, SDS-PAGE, and LC-MS/MS. *J. Proteome Res*. 5, 3105-3113.

Ingram, J., Bartels, D. (1996) The molecular basis of dehydration tolerance in plants. *Annu. Rev. Plant Physiol. Mol. Biol.* 47, 377-404.

Irar, S., Oliveira, E., Pagés, M., Goday, A. (2006) Towards the identification of late-embryonic abundant phosphoproteome in Arabidopsis by 2-DE and MS. *Proteomics* 6, S175-S185.

Islam, N., Woo, S.-H., Tsujimoto, H., Kawasaki, H., Hirano, H. (2002) Proteome approaches to characterize seed storage protein related to ditelocentric chromosome in common wheat (*Triticum aestivum* L.). *Proteomics* 2, 1146-1155.

Jabs, T. (1999) Reactive oxygen intermediates as mediators of programmed cell death in plant and animals. *Biochem. Pharmacol*. 57, 231-245.

Jacobsen, J.V., Gubler, F., Chandler, P.M. (1995) Gibberellin action in germinated cereal grains. In: Davies, P.J. (Ed.) *Plant hormones. Physiology, biochemistry and molecular biology*, pp 247-271.

Jacobsen, S.E., Olszewski, N.E. (1993) Mutations in the *SPINDLY* locus of Arabidopsis alter gibberellin signal transduction. *Plant Cell* 5, 887-896.

Jaenicke, R., Rudolph, R. *Protein structure: a practical approach*. Creighton, T.E. (Ed.) IRL Press, Oxford, 1989.

James, P., Quadrom, M., Carafoli, E., Gonnet, G. (1994) Protein identification in DNA database by peptide mass fingerprinting. *Protein Sci.* 3, 1347-1350.

Jamet, E. (2004) Bioinformatics as a critical prerequisite to transcriptome and proteome studies. *J. Exp. Bot*. 55, 1977-1979.

Jeffrey, J., Jörnvall, H. (1983). Enzyme rationships in a sorbitol pathway that bypasses glycolysis and pentose phosphates in glucose metabolism. *Proc. Natl. Acad. Sci. USA*. 80, 901-905.

Jensen, A.B., Goday, A., Figueras, M., Jessop, A.C., Pages, M. (1998) Phosphorylation mediates the nuclear targeting of the maize Rab17 protein. *Plant J.* 13, 691-697.

Jiang, M., Zhang, J. (2002) Role of abscisic acid in water stress-induced antioxidant defence in leaves of maize seedlings. *Free Radic. Res.* 36, 1001-1015.

Johansen, K.S., Svendsen, I., Rasmussen, S.K. (2000) Purification and cloning of the two domain glyoxalase I from wheat bran. *Plant Sci.* 155, 11-20.

Jones, D.P., Go, Y.-M., Anderson, C.L., Ziegler, T.R., Kinkade, J.M., Kirlin, W.G. (2004) Cysteine/cystine couple is a newly recognized node in the circuity for biologic redox signaling and control. *FASEB J.* doi:10.1096/fj.03097fje.

Joo, J.H., Bae, Y.S., Lee, J.S. (2001) Role of auxin-induced reactive oxygen species in root gravitropism. *Plant Physiol*. 126, 1055-60.

Juge, N., Andersen, J.S., Tull, D., Roepstorff, P., Svensson, B. (1996). Overexpression, purification, and characterization of recombinant alpha-amylase 1 and 2 secreted by the methylotrophic yeast *Pichia pastoris*. *Protein Expr. Purif.* 8, 204-214.

Jung, C.-H., Thomas, J.A. (1996) S-glutathionated hepatocyte proteins and insulin disulfides as substrates for reduction by glutaredoxin, thioredoxin, protein disulfide isomerase, and glutathione. *Arch. Biochem. Biophys*. 335, 61-72.

Kamo, M., Kawakami, T., Miyatake, N., Tsugita, A. (1995) Separation and characterization of *Arabidopsis thaliana* proteins by two-dimensional gel electrophoresis. *Electrophoresis* 16, 423-430.

Karas, M., Hillenkamp, F. (1988) Laser desorption ionization of proteins with molecular masses exceeding 10,000 daltons. *Anal. Chem*. 60, 2299-2301.

Karssen, C.M., Zagorski, S., Kepczynski, J., Groot, S.P.C. (1989) Key role for endogenous gibberellins in the control of seed germination. *Ann. Bot. (Lond.)* 63, 71-80.

Kermode, A.R. (1990) Regulatory mechanisms involved in the transition from seed development to germination. *Crit. Rev. Plant Sci.* 9, 155-195.

Kermode, A.R. (1995) Regulatory mechanisms in the transition from seed development to germination: interactions between the embryo and the seed environment. In G. Galili, J. Kigel, (Eds.) *Seed development and germination*. Marcel Dekker, New York, pp 273-332.

Kersten, B., Bürkle, L., Kuhn, E.J., Giavalisco, P., Konthur, Z., Lueking, A., Walter, G., Eickhoff, H., Schneider, U. (2002) Large-scale plant proteomics. *Plant Mol. Biol*. 48, 133-141.

Klein, C., Lamotte-Guéry, F., Gautier, F., Moulin, G. (1998) High-level secretion of a wheat lipid transfer protein in *Pichia Pastoris*. *Protein Expr.Purif.* 13, 73-82.

Kobrehel, K., Wong, J.H., Balogh, A., Kiss, F., Yee, B.C., Buchanan, B.B. (1992) Specific reduction of wheat storage proteins by thioredoxin h. *Plant Physiol*. 99, 919-924.

Koller, A., Washburn, M.P., Lange, B.M., Andon, N.L., Deciu, C., Haynes, P.A., Hays, L., Schieltz, D., Ulaszek, R., Wei, J., Wolthers, D., Yates, J.R. (2002) III: Proteomic survey of metabolic pathways in rice. *Proc. Natl. Acad. Sci. USA* 99, 11969-11974.

Kollipara, K.P.K., Saab, I.N., Wych, R.D., Lauer, M.J., Singletary, G.W. (2002) Expression profiling of reciprocal maize hybrids divergent for cold germination and desiccation tolerance. *Plant Physiol*. 129, 974-992.

Komatsu, S., Yano, H. (2006) Update and challenges on proteomics in rice. *Proteomics* 6, 4057-4068.

Koornneef, M., Karssen, C.M. (1994) Seed dormancy and germination. In: Meyerowitz, E.M., Somerville, C.R. (Eds.) *Arabidopsis*. Cold Spring Harbor, NY: Cold Spring Harbor Laboratory Press, pp 313-334.

Koornneef, M., van der Veen, J.H. (1980) Induction and analysis of gibberellin sensitive mutants in *Arabidopsis thaliana* (L.) *Heynh. Theor. Appl. Genet*. 58, 257-263.

Koshiba, T. (1993) Cytosolic ascorbate peroxidase in seedlings and leaves of maize (*Zea mays*). *Plant Cell Physiol*. 35, 713-721.

Kristensen, M., Lok, F., Planchot, V., Svendsen, I., Leah, R., Svensson, B. (1999) Isolation and characterization of the gene encoding the starch debranching enzyme limit dextrinase from germinating barley. *Biochim. Biophys. Acta* 1431, 538-546.

Kristensen, M., Planchot, V., Abe, J.-I., Svensson, B. (1998) Large scale purification and characterization of barley limit dextrinase, a member of the α-amylase structural family. *Cereal Chem*. 75, 473-479.

Kristoffersen, H.E., Flengsrud, R. (2000) Separation and characterization of basic barley seed proteins. *Electrophoresis* 21, 3693-3700.

Lad, L., Mewies, M., Raven, E.L. (2002) Substrate binding and catalytic mechanism in ascorbate peroxidase: evidence for two ascorbate binding sites. *Biochemistry* 41, 13774-13781.

Laugesen, S., Bak-Jensen, K.S., Hägglund, P., Henriksen, A., Finnie, C., Svensson, B., Roepstorff, P. (2007) Barley peroxidase isozymes: Expression and post-translational modification in mature seed as identified by two-dimensional gel electrophoresis and mass spectrometry. Submitted to *Int. J. Mass Spectrom.*, subject to minor revision.

LaVallie, E.R., DiBlasio, E.A., Kovacic, S., Grant, K.L., Schendel, P.F., MaCoy, J.M. (1993) A thioredoxin gene fusion expression system that circumvents inclusion body formation in *E. coli* cytoplasm. *Biotechnol*. 11, 187-193.

Lazano, R.M., Wong, J.H., Yee, B.C., Peters, A., Kobrehel, K., Buchanan, B.B. (1996) New evidence for a role for thioredoxin h in germinated seedling development. *Planta* 200, 100-106.

Lazaro, A., Rodriguez-Palenzuela, Marana, C., Carbonero, P., Garcia-Olmedo, F. (1988) Signal peptide homology between the sweet protein thaumatin II and unrelated cereal α-amylase/trypsin inhibitors. *FEBS Lett*. 239, 147-150.

Levine, A., Tenhaken, R., Dixon, R., Lamb, C. (1994) H_2O_2 from the oxidative burst orchestrates the plant hypersensitive disease resistance response. *Cell* 79, 583-594.

Lin, Y., Cheng, G., Want, X., Clark, T.G. (2002) The use of synthetic genes for the expression of ciliate proteins in heterologous systems. *Gene* 288, 85-94.

Link, A.J., Eng, J., Schieltz, D.M., Carmack, E., Mize, G.J., Morris, D.R., Garvik, B.M., Yates, J.R. (1999) Direct analysis of protein complexes using mass spectrometry. *Nat. Biotechnol.* 17, 676-682.

Longstaff, M.A., Bryce, J.H. (1993) Development of limit dextrinase in germinated barley (*Hordeum vulgare* L.). *Plant Physiol*. 101, 881-889.

Lutter, P., Meyer, H.E., Langer, M., Witthohn, K., Dormeyer, W., Sickmann, A., Bluggel, M. (2001) Investigation of charge variants of rViscumin by two-dimensional gel electrophoresis and mass spectrometry. *Electrophoresis* 22, 2888-2897.

MacGregor, E.A. (2004) The proteinaceous inhibitor of limit dextrinase in barley malt. *Biochim. Biophys. Acta* 1696, 165-170.

MacGregor, A.W., Donald, L.J. MacGregor, E.A., Duckworth, H.W. (2003) Stoichiometry of the complex formed by barley limit dextrinase with its endogenous inhibitor. Determination by electrospray time-of flight mass spectrometry. *J. Cereal Sci*. 37, 357-362.

MacGregor, A.W., Macri, L.J., Schroeder, S.W., Bazin, S.L. (1994) Purification and characterization of limit dextrinase inhibitors form barley. *J. Cereal Sci.* 20, 33-41.

MacGregor, E.A., Bazin, S.L., Ens, E.W., Lahnstein, J., Macri, L.J., Shirley, N.J., MacGregor, A.W. (2000) Structural models of limit dextrinase inhibitors from barley. *J. Cereal Sci*. 31, 79-90.

Macri, L.J., MacGregor, A.W., Schroeder, S.W., Bazin S.L. (1993) Detection of a limit dextrinase inhibitor in barley. *J. Cereal. Sci.* 18, 103-106.

Maeda, K., Finnie, C., Østergaard, O., Svensson, B. (2003) Identification, cloning and characterization of two thioredoxin h isoforms, HvTrxh 1 and HvTrxh 2, from the barley seed proteome. *Eur. J. Biochem*. 270, 2633-2644.

Maeda, K., Finnie, C., Svensson, B. (2005) Identification of thioredoxin h-reducible disulphides in proteomes by differential labeling of cysteines: insight into recognition and regulation of proteins in barley seeds by thioredoxin h. *Proteomics* 5, 1634-1644.

Maeda, K., Finnie, C., Svensson, B. (2004) Cy5 maleimide labelling for sensitive detection of free thiol in native protein extracts: identification of seed proteins targeted by barley thioredoxin h isoforms. *Biochem. J*. 378, 497-507.

Maeda, K., Hägglund, P., Finnie, C., Svensson, B., Henriksen, A. (2006) Structural basis for target protein recognition by the protein disulfide reductase thioredoxin. *Structure* 14, 1701-1710.

Manners, D.J., Marshall, J.J., Yellowlees, D. (1970) The specificity of cereal limit dextrinases. *Biochem. J*. 116, 539-541.

Marx, C., Wong, J.H., Buchanan, B.B. (2003) Thioredoxin and germinating barley: target and protein redox changes. *Planta* 216, 454-460.

Maskos, K., Huber-Wunderlich, R., Glockshuber, R. (1996) RBI, a one-domain α-amylase/trypsin inhibitor with completely independent binding sites. *FEBS Lett*. 397, 11-16.

Matsudaira, P. (1987) Sequence from picomole quantities of protein electroblotted onto polyvinylidene difluoride membranes. *J. Biol. Chem*. 262, 10035-10038.

May, J.M., Mendiratta, S., Hill, K.E., Burk, R.F. (1997) Reduction of dehydroascorbate to ascorbate by the selenoenzyme thioredoxin reductase. *J. Biol. Chem*. 272, 22607-22610.

Maya-Ampudia, V., Bernal-Lugo, I. (2006) Redox-sensitive target detection in gibberellic acid-induced barley aleurone layer. *Free Rad. Biol. Med*. 40, 1362-1368.

Mayer, A., Poljakoff-Mayber, A. (1982) Metabolism of germinating seeds. In: Wareing, P.F., Galston, A.Y., (Eds.) *The germination of seeds*. New York. Pergamon Press, 85-139.

Merchand, C., Maréchal., P.L., Meyer, Y., Decottignies, P. (2006) Comparative proteomics approaches for the isolation of proteins interaction with thioredoxin. *Proteomics* 6, 6528-6537.

Merchand, C., Maréchal, P.L., Meyer, Y., Miginiac-Maslow, M., Issakidis-Bourguet, E., Decottignies, P. (2004) New targets of Arabiopsis thioredoxins revealed by proteomic analysis. *Proteomics* 4, 2696-2706.

Mittler, R, Vanderauwera, S., Gollery, M., van Breusegem, F. (2004) Reactive oxygen gene network of plants. *Trends Plant Sci*. 9, 490-498.

Mittler, R. (2002) Oxidative stress, antioxidants and stress tolerance. *Trends Plant Sci*. 7, 405-410.

Mittler, R., Zalinskas, B.A. (1993) Detection of ascorbate peroxidase activity in native gels by inhibition of the ascorbate-dependent reduction of nitroblue tetrazolium. *Anal. Biochem*. 212, 540-546.

Mittova, V., Vanderauwera, S., Gollery, M., van Breusegem, F. (2000) Activities of SOD and the ascorbate-glutatione cycle enzymes in subcellular compartments in leaves and roots of the cultivated tomato and its wild salt-tolerant relative *Lycopersicon pennilli*. *Plant Physiol*. 110, 42-51.

Morell, S., Follmann, H., De Tullio, M., Häberlein, I. (1997) Dehydroascorbate and dehydroascorbate reductase are phantom indicators of oxidative stress in plants. *FEBS Lett*. 414, 567-570.

Müller-Uri, F., Cameron-Mills, V., Mundy, J. (2002) The barley *Jip23b* gene. *Biochim. Biophys. Acta* 1576, 231-235.

Mundy, J., Svendsen, I., Hejgaard, J. (1983) Barley α-amylase/subtilisin inhibitor. Isolation and characterization. *Carlsberg Res. Commun*. 48, 81-91.

Naested, H., Kramhoft, B., Lok, F., Bojsen, K., Svensson, B. (2006) Production of enzymatically active recombinant full-length barley high pI alpha-glucosidase of glycoside family 31 by high cell-density fermentation of *Pichia pastoris* and affinity purification. *Protein Exp. Purif*. 46, 53-63.

Nakano, Y., Asada, K. (1981) Hydrogen peroxide is scavenged by ascorbate-specific peroxidase in spinach chloroplasts. *Plant Cell Physiol*. 22, 867-880.

Nambara, E., Akazawa, T., McCourt, P. (1991) Effects of the gibberellin biosynthesis inhibitor uniconazol on mutants of Arabidopsis. *Plant Physiol*. 97, 736-738.

Noctor, G., Foyer, C.H. (1998) ASCORBATE AND GLUTATHIONE: Keeping Active Oxygen Under Control. *Annu. Rev. Plant Physiol. Plant Mol. Biol.* 49, 249-279.

Noctor, G., Arisi, A.C., Aouanin, L., Kunert, K.J., Rennenberg, H., Foyer, C.H. (1998) Glutathione: biosynthesis, metabolism and relationship to stress tolerance explored in transformed plants. *J. Exp. Bot*. 49, 623-647.

O'Farrell, P.H. (1975) High resolution two-dimensional electrophoresis of proteins. *J. Biol. Chem*. 250, 4007-4021.

O'Kane, D., Gill, V., Boyd, P., Burdon, R. (1996) Chilling, oxidative stress and antioxidant responses in *Arabidopsis thaliana* callus. *Planta* 198, 371-377.

Oda, Y., Matsunaga, K., Fukuyiama, K., Miyasaki, T., Morimoto, J.T. (1997) Tertiary and quarternary structures of 0.19 α-amylase inhibitor from what determined by x-ray analysis at 2.06 Å resolution. *Biochemistry* 36, 13503-13511.

Okuda, M., Satoh, T., Sakurai, N., Shibuya, K., Kaji, H., Samenjima, T. (1997) Overexpression in *Escherichia coli* of chemically synthesized gene for active 0.19 α-amylase inhibitor from wheat kernel. *J. Biochem*. 122, 918-926.

Orozco-Cardenas, M.L., Narváez-Vásquez, J., Ryan, C.A. (2001) Hydrogen peroxide acts as a second messenger for the induction of defense genes in tomato plants in response to wounding, systemin, and methyl jasmonate. *Plant Cell* 13, 179-191.

Osborne, T.B. (1907) *The proteins from the wheat kernel*. Carnegie Inst. Washington Publ. 84, Judd and Detweiler, Washington, USA.

Østergaard, H., Rasmussen, S.K., Roberets, T.H., Hejgaard, J. (2000) Inhibitory serpins from wheat grain with reactive centers resembling glutamine-rich repeats of prolamin storage proteins. Cloning and characterization of five major molecular forms. *J. Biol. Chem*. 275, 33272-33279.

Østergaard, O. (2003) Proteome analysis of barley seed and malt. Ph.D. thesis, Department of Chemistry, Carlsberg Laboratory, Valby, Denmark, and Department of Biochemistry and Molecular Biology, University of Southern Denmark, Odense, Denmark.

Østergaard, O., Finnie, C., Laugesen, S., Roeostorff, P., Svensson, B. (2004) Proteome analysis of barley seeds: Identification of major proteins from two-dimensional gels (pI 4-7). *Proteomics* 4, 2437-2447.

Østergaard, O., Melchior, S., Roepstorff, P., Svensson, B. (2002) Initial proteome analysis of mature barley seed and malt. *Proteomics* 2, 733-739.

Ozturk, Z.N., Talamé, V., Deyholos, M., Michalowski, C.B., Galbraith, D.W., Gozukirmizi, N., Tuberosa, R., Bohnert, H.J. (2002) Monitoring large-scale changes in transcript abundance in drought- and salt-stressed barley. *Plant Mol. Biol*. 48, 551-573.

Park, J.B., Levine, M. (1996) Purification, cloning and expression of dehydroascorbic acid-reducing activity from human neutrophils: identification as glutaredoxin, *Biochem. J.* 315, 931-938.

Patternson, W.R., Poulos,T.L. (1995) Crystal structure of recombinant pea cytosolic peroxidase. *Biochemistry* 34, 4331-4341.

Payan, F. (2004) Structural basis for the inhibition of mammalian and insect α-amylases by plant protein inhibitors. *Biochem. Biophys. Acta* 1696, 171-180.

Peck, S.C. (2005) Update on proteomics in Arabidopsis. Where do we go from here? *Plant Physiol*. 138, 591-599.

Pei, Z.-M., Murata, Y., Benning, G., Thomine S., Klüsener, B., Allen, G.J., Grill, E., Schroeder, J.I. (2000) Calcium channels activated by hydrogen peroxide mediate abscisic acid signaling in guard cells. *Nature* 406, 731-734.

Perkins, D.N., Pappin, D.J., Creasy, D.M., Cottress, J.S. (1999) Probability-based protein identification by searching sequence databases using mass spectrometry data. *Electrophoresis* 20, 3551-3567.

Popov, N., Schmitt, M., Schulzeck, S., Matthies, H. (1975) Eine Störungsfreie Mikromethode zur Bestimmung des Proteingehaltes in Gewebehomogenaten. *Acta Biol. Med. Ger*. 34, 1441-1446.

Potokina, E., Sreenivasulu, N., Altschmie, L., Michalek, W., Graner, A. (2002) Differential gene expression during seed germination in barley (*Hordeum vulgare* L.). *Funct. Integr. Genomic*s 2, 28-39.

Potokina, E., Prasa. M., Malysheva, L., Roder, M.S., Graner, A. (2006) Expression genetics and haplotype analysis reveal cis regulation of serine carboxypeptidase I (Cxp1), a candidate gene for malting quality in barley (*Hordeum vulgare* L.). *Funct. Integr. Genomics* 6, 25-35.

Prasad, T.K., Anderson, M.D., Martin, B.A., Stewart, C.R. (1994) Evidence for chilling-induced oxidative stress in maize seedlings and a regulatory role for hydrogen peroxide. *Plant Cell* 6, 65-74.

Prentø, J. (2005) Purification of recombinant limit dextrinase inhibitor. PMP project, Enzyme and Protein Chemistry, BioCentrum-DTU.

Rabilloud. T., Chermont, S. In: Rabilloud, T. (Ed.) *Proteome Research: Two-Dimensional Gel Electrophoresis and Identification Methods*, Springer Verlag, Berlin, Heidelberg 2000, pp. 107-126.

Rabilloud, T. (2002) Two-dimensional gel-electrophoresis in proteomics: Old, old fashioned but still climbs up the mountain. *Proteomics* 2, 3-10.

Rabilloud, T., Heller, M., Gasnier, F., Luche, S., Rey, C., Aebersold, R., Benahmed, M., Louisot, P., Lunard, J. (2002) Proteomics analysis of cellular response to oxidative stress. Evidence for *in vivo* overoxidation of peroxiredoxins at their active site. *J. Biol. Chem*. 277, 19396-19401.

Rajjou, L., Gallardo, K., Debeaujon, I., Vandekerckhove, J., Job, C., Job, D. (2004) The effect of α-amanitin on the Arabidopsis seed proteome highlights the distinct roles of stored and neosynthesized mRNAs during germination. *Plant Physiol.* 134, 1598-1613.

Rakwal, R., Agrawal, G.K. (2003) Rice proteomics: current status and future perspectives. *Electrophoresis* 24, 3378-3389.

Riis, P., Bang-Olsen, K. (1991) Germination profile – a new term in malting barely analyses. *Proceedings of the European Convention Congress*, 23, 101-108.

Riis, P., Meiling, E., Peetz, J. (1995) Determination of germination index- collaborative trial and ruggedness testing. *J. Inst. Brew.* 101, 171-173.

Roncarati, R., Salimini. F., Bartels, D. (1995) An aldose reductase homologous gene from barley: regulation and function. *Plant J.* 7, 809-822.

Rosenfeld, J., Capdevielle, J., Guillemot, J.C., Ferrara, P. (1992) In-gel digestion of proteins for internal sequence analysis after one- or two-dimensional gel electrophorsis. *Anal Biochem*. 203, 173-179.

Rouhier, N., Gelhaye, E., Sautiere, P-E., Brun, A., Laurent, P., Tagu, D., Gerard, J., de Fay, E., Meyer, Y., Jacqout, J.-P. (2001) Isolation and characterization of a new peroxiredoxin from poplar sieve tubes that uses either glutaredoxin or thioredoxin as a proton donor. *Plant Physiol.* 127, 1299-1309.

Rouhier, N., Villarejo, A., Srivastava, M., Gelhaye, E., Keech, O., Droux, M., Finkemeier, I., Samuelsson, G, Dietz, K.J., Jacqout, J.P., Wingsle, G. (2005) Identification of plant glutaredoxin targets. *Antiox. Red. Signal*. 7, 919-919.

Sadimantara, G.R., Abe, T., Suzuki, J.-I., Sasahara, T. (1999) Identification and microsequence analysis of high molecular weight proteins in endosperm of the rice seed. *J. Plant Physiol*. 154, 571-575.

Sambrook, J., Russels, D.W. (Eds.) *Molecular clonning. A laboratory manual*. CSHL Press, 2001.

Sanchez-Monge, R., Gomez, L., Barber, D., Lopez-Otin, C., Armentia, A., Salcedo, G. (1992) Wheat and barley allergens associated with baker's asthma. Glycosylated subunits of the *a*-amylase inhibitor family have enhanced IgE-binding capacity. *Biochem. J*. 281. 401-405.

Sarvas, M., Harwood, C.R., Biron, S., van Dijl, J.M. (2004) Post-translational folding of secretory protein in Gram-positive bacteria. *Biochim. Biophys. Acta* 1694, 311-327.

Seki, M., Narusaka, M., Abe, H., Kasuga, M., Yamaguchi-Shinozaki, K., Carninci, P., Hayashizaki, Y., Shinozaki, K. (2001) Monitoring the expression pattern of 1300 Arabidopsis genes under drought and cold stresses by using full-length cDNA microarray. *Plant Cell* 13, 61-72.

Serrato, A.J., Cejudo, F.J. (2003) Type-h thioredoxins accumulate in the nucleus of developing wheat seed tissues suffering oxidative stress. *Planta* 217, 392-399.

Sharp, K.H., Mewies, M., Moody, P.C.E., Raven, E.L. (2003) Crystal structure of the ascorbate peroxidase-ascorbate complex. *Nat. Struct. Biol*. 10, 303-307.

Shevchenko, A., Wilm, M., Vorm, O., Mann, M. (1996). Mass spectrometric sequencing of proteins from silver-stained polyacrylamide gels. *Anal. Chem*. 68, 850-858.

Shewry, P.R., Finch, R.A., Parmar, S., Franklin, J., Miflin, B.J. (1983) Chromosomal location of *Hor 3*, a new locus govering storage proteins in barley. *Heredity* 50, 179-189.

Singla-Pareek, S.L., Reddy, M.K., Sopory, S.K. (2003) Genetic engineering of the glyoxalase pathway in the tobacco leads to enhanced salinity tolerance. *Proc. Natl. Acad. Sci. USA* 100, 14672-14677.

Sissons, M.J., Lance, R.C.M., Sparrow, D.H.B. (1993) Studies on limit dextrinase in barley. Limit dextrinase in developing kernels. *J. Cereal Sci*. 17, 19-24.

Sjødal, J., Kempka, M., Hermansson, K., Thorsén, A., Roerraade, J. (2005) Chip with twin anchors for reduced ion suppression and improved mass accuracy in MALDI-TOF mass spectrometry. *Anal. Chem*. 77, 827-832.

Skylas, D.J., Copeland, L., Rathmell, W.G., Wrigley, C.W. (2001). The wheat-grain proteome as a basis for more efficient cultivar identification. *Proteomics* 1, 1542-1546.

Skylas, D.J., Cordwell, S.J., Hains, P.G., Larsen, M.R., Basseal, D.J., Walsh, B.J., Blumenthal, C., Rathmell, Copeland, L., Wrigley, C.W. (2002). Heat shock of wheat during grain filling: Proteins associated with heat-tolerance. *J. Cereal Sci.* 35, 175-188.

Skylas, D.J., Mackintosh, J.A., Cordwell, S.J., Basseal, D.J., Walsh, B.J., Harry, J., Blumenthal, C., Copeland, L., Wrigley, C.W., Rathmell, W. (2000) Proteome approach to the characterization of protein composition in the developing and mature wheat-grain endosperm. *J. Cereal Sci.* 32, 169-188.

Stahl, Y., Coates, S., Bryce, J.H., Morris, P.C. (2004) Antisense downregulation of the barley limit dextrinase inhibitor modulates starch granules size distribution, starch composition and amylopectin structure. *Plant J*. 39, 599-611.

Strobl, S., Maskos, K., Weegand, G., Huber, R., Gomis-Rüth, F.X., Glockshuber, R. (1998) A novel strategy for inhibition of α-amylases: yellow meal worm α-amylase in complex with the *Ragi* bifunctional inhibitor at 2.5 Å resolution. *Structure* 6, 911-921.

Strobl, S., Mühlhahn, P., Berbstein, R., Wiltscheck, R., Maskos, K., Wunderlich, M., Huber, R., Glockshuber, R., Holak, T.A. (1995) Determination of the three-dimensional structure of the bifunctional α-amylase/trypsin inhibitor form *Ragi* seeds by NMR spectroscopy. *Biochemistry* 34, 8281-8293.

Svensson, B., Fukuda, K., Nielsen, P.K., Bønsager, B.C. (2004) Proteinaceous α-amylase inhibitors. *Biochim. Biophys. Acta* 1696, 145-156.

Takase, K. (1994) Site-directed mutagenesis reveals critical importance of the catalytic site in binding of α-amylase by wheat proteinaceous inhibitor. *Biochemistry* 33, 7925-7930.

Thiellement, H., Bahrman, N., Damerval, C., Plomion, C., Rossignol, M., Santoni, V., de Vienne, D., Zivy, M. (1999) Proteomics for genetic and physiological studies in plants. *Electrophoresis* 20, 2013-2026.

Tian, Q., Stepaniants, S.B., Mao, M., Weng, L., Feetham, M.C., Doyle, M.J., Yi, E.C., Dai, H.,Thorsson, V., Eng, J., Goodlett, D., Berger, J.P., Gunter, B., Linseley, P.S., Stoughton, R.B., Aebersold, R., Collins, S.J., Hanlon, W.A., Hood, L.E. (2004) Integrated genomics and proteomics analysis of gene expression in mammalian cells. *Mol. Cell. Proteomics* 3, 960-968.

Tommasi, F., Paciolla, C., de Pinto, M.C., De Gara, L. (2001) A comparative study of glutathione and ascorbate metabolism during germination of *Pinus pinea* L. seeds. *J. Exp. Bot*. 52, 1647-1654.

Trümper, S., Follmann, H., Häberlein, I. (1994) A novel dehydroascorbate reductase from spinach chloroplasts homologous to plant trypsin inhibitor. *FEBS Lett*. 352, 159-162.

Tsugita, A., Kamo, M., Kawakami, T., Ohki, Y. (1996) Two-dimensional electrophoresis of plant protein and standardization of gel patterns. *Electrophoresis* 17, 855-865.

Tsugita, A., Kawakami, T., Uchiyama, Y., Kamo, M., Miyatake, N., Nozu, Y. (1994) Separation and characterization of rice proteins. *Electrophoresis* 15, 708-720.

Ünlü, M., Morgan, M.E., Minden, J.S. (1997) Difference gel electrophoresis: A single gel method for detecting changes in protein extracts. *Electrophoresis* 18, 2071-2077.

Veith, P.D., Talbo, G.H., Slakeski, N., Reynolds, E.C. (2001) Identification of a novel heterodimeric outer membrane protein of *Porphyomonas gingivalis* by two-dimensional gel electrophoresis and peptide mass fingerprinting. *Eur. J. Biochem*. 268, 4748- 4757.

Vensel, W.H., Tanaka, C.K., Cai, N., Wong, J.H., Buchanan, B.B., Hurkman, W.J. (2005) Developmental changes in the metabolic protein profiles of wheat endosperm. *Proteomics* 5, 1594-1611.

Verdoucq, L., Vignols, F., Jacqout, J.-P., Cartier, Y., Meyer, Y. (1999) *In vivo* characterization of a thioredoxin h target protein defines a new peroxiredoxin family. *J. Biol. Chem*. 274, 19714-19722.

Vester-Christensen, M.B., Naested, H., Abou Hachem, M., Svensson, B. in prep.

Vionnet, O., Rivas, S., Mestre, P., Baulcombe, D. (2003) An enhanced transient expression system in plants based on suppression of gene silencing by the p19 protein of tomato bushy stunt virus. *Plant J*. 33, 949-956.

Wagner, E., Luche, S., Penna, L., Chevallet, M., Van Dorsselaer, A., Leize-Wagner, E., Rabilloud, T. (2002) A method for detection of overoxidation of cysteines: peroxiredoxins are oxidised *in vitro* at the active site cysteine. *Biochem. J*. 366, 777-785.

Walker, J.V., Bringhurst, T.A., Broadhead, A.L., Brosnan, J.M., Pearson, S.Y. (2000) Survival of limit dextrinase during fermentation in production of Scotch whisky. *J. Inst. Brew*. 107, 99-106.

Wasinger, V.C., Pollack, J.D., Humphery-Smith, I. (2000) The proteome of *Mycoplasma genitalium*. Chaps-soluble component. *Eur. J. Biochem*. 267, 1571-1582.

Watson, L., Henry, R. J. (2005) Microarray analysis of gene expression in germinating barley embryos (*Hordeum vulgare* L.). *Funct. Integr. Genomics* 5, 155-162.

Wehyer, N., Hernandez, L.D., Finkelstein, R.R., Vierling, E. (1996) Synthesis of small heat-shock proteins is part of the developmental program of late seed maturation. *Plant Physiol*. 112, 747-57.

Weiss, W., Postel, W., Görg, A. (1992) Application of sequential extraction procedures and glycoprotein blotting for the characterization of the 2-D polypeptide patterns of barley seed proteins. *Electrophoresis* 13, 770-773.

Wells, W.W., Xu, D.P., Yang, Y., Rocque, P.A. (1990) Mammalian thiotransferase (glutaredoxin) and protein disulfide isomerase have dehydroascorbate reductase activity. *J. Biol. Chem*. 265, 15361-15364.

Whitelegge, J.P. (2004) Mass spectrometry for high throughput quantitative proteomics in plant research: lessons from thylakoid membranes. *Plant Physiol. Biochem*. 42, 919-927.

Wilhelmson, A., Laitila, A., Vilpola, A., Olkku, J., Kotaviita, E., Fagerstedt, K., Home, S. (2006) Oxygen deficiency in barley (*Hordeum vulgare*) grain during malting. *J. Agric. Food Chem*. 54, 409-416.

Wong, J. H., Kobrehel, K., Buchanan, B.B. (1995) Thioredoxin and seed proteins. *Methods Enzymol*. 252, 228-240.

Wong, W.H., Balmer, Y., Cai, N., Tanaka, C.K., Vensel, W.H. Hurkman, W.J., Buchanan, B.B. (2003) Unraveling thioredoxin-linked metabolic processes of cereal starchy endsperm using proteomics. *FEBS Lett*. 547, 151-156.

Wood, Z.A., Schroeder, E., Harris, J.R., Poole, L.B. (2003) Structure, mechanism and regulation of peroxiredoxins. *Trends Biochem. Sci*. 28, 32-40.

Yamazaki, D., Motohashi, K., Kasama, T., Hara, Y., Hisabori, T. (2004) Target proteins of the cytosolic thioredoxins in *Arabidopsis thaliana*. *Plant Cell Physiol*. 45, 18-27.

Yano, H., Kuroda, M. (2005) Disulfide proteome yield a detailed understanding of redox regulations: A model to study thioredoxin linked reactions in seed germination. *Proteomics* 5, 1-7.

Yano, H., Wong, J.H., Lee, Y.M., Cho. M-J., Buchanan, B.B. (2001) A strategy for the identification of proteins targeted by thioredoxin. *Proc. Natl. Acad. Sci. USA* 98, 4794-4799.

Yates, J.R., Speicher, S., Griffin, P.R., Hunkapiller, T. (1993) Peptide mass maps: a highly informative approach to protein identification. *Anal. Biochem*. 214, 397-408.

Zentella, R., Yamauchi, D., Ho, T.D. (2002) Molecular dissection of the gibberellin/abscisic acid signaling pathways by transiently expressed RNA interference in barley aleurone cells. *Plant Cell* 14, 2289-2301.

Zhang, H., Sreenivasulu, N., Wesche, W., Stein, N., Rudd, S., Radchuk, V., Potokina, E., Scholz, U., Schweizer, P., Zierold, U., Langridge, P., Varshney, R.K., Wobus, U., Graner, A. (2004) Large-scale analysis of the barley transcriptome based on expressed sequence tags. *Plant J.* 40, 278-290.

Zhang, X., Zhang, L., Dong, F., Gao, J., Galbraith, D.W., Song, C.-P. (2001) Hydrogen peroxide is involved in abscisic acid-induced stomatal closure in *Vicia faba. Plant Physiol*. 126, 1438-1448.

Zhu, H., Bilgin, M., Bangham, R., Hall, D., Casamayor, A., Bertone, P., Lan, N., Jansen, R., Bidlingmaier, S., Houfek, T., Mitchell, T., Miller, P., Dean, R.A., Gerstein, M., Snyder, M. (2001) Global analysis of protein activities using proteome chips. *Science* 293, 2101-2105.

Appendix 1a

2D gels (pH range 4-7) of embryo extracts during germination and radicle elongation. All time points (0, 4, 12, 24, 36, 52, 60, and 72 h PI) are shown.

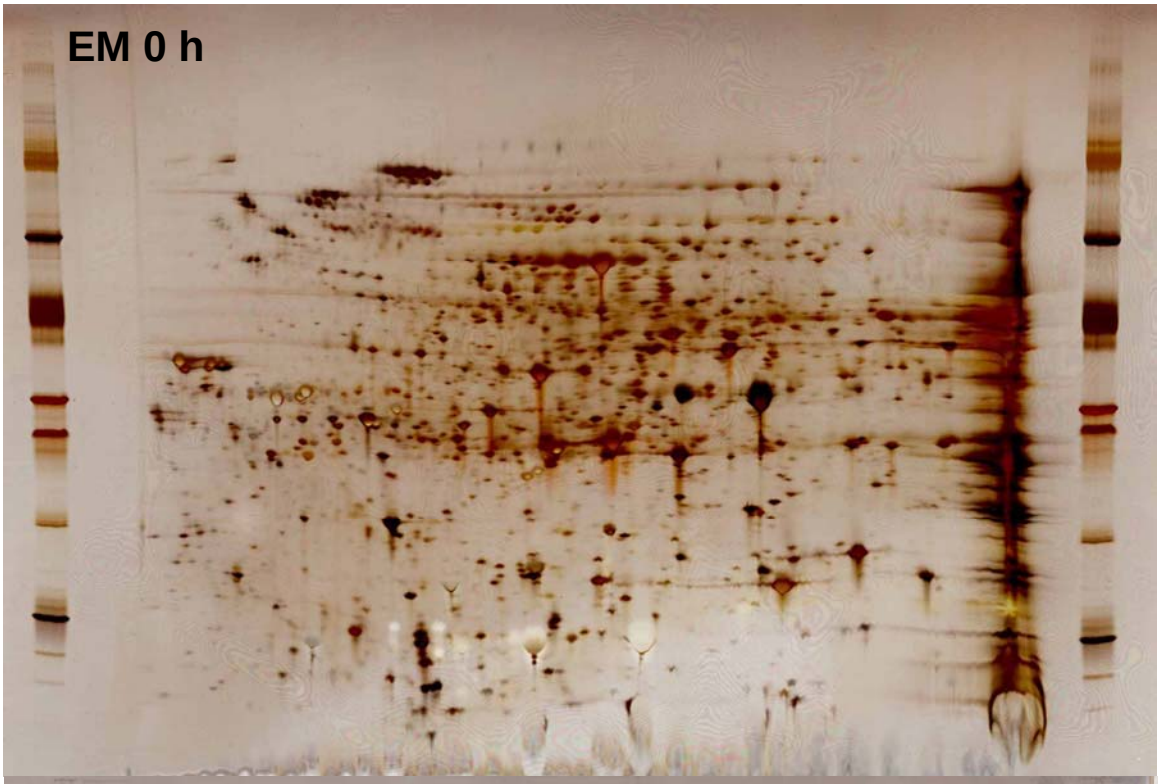

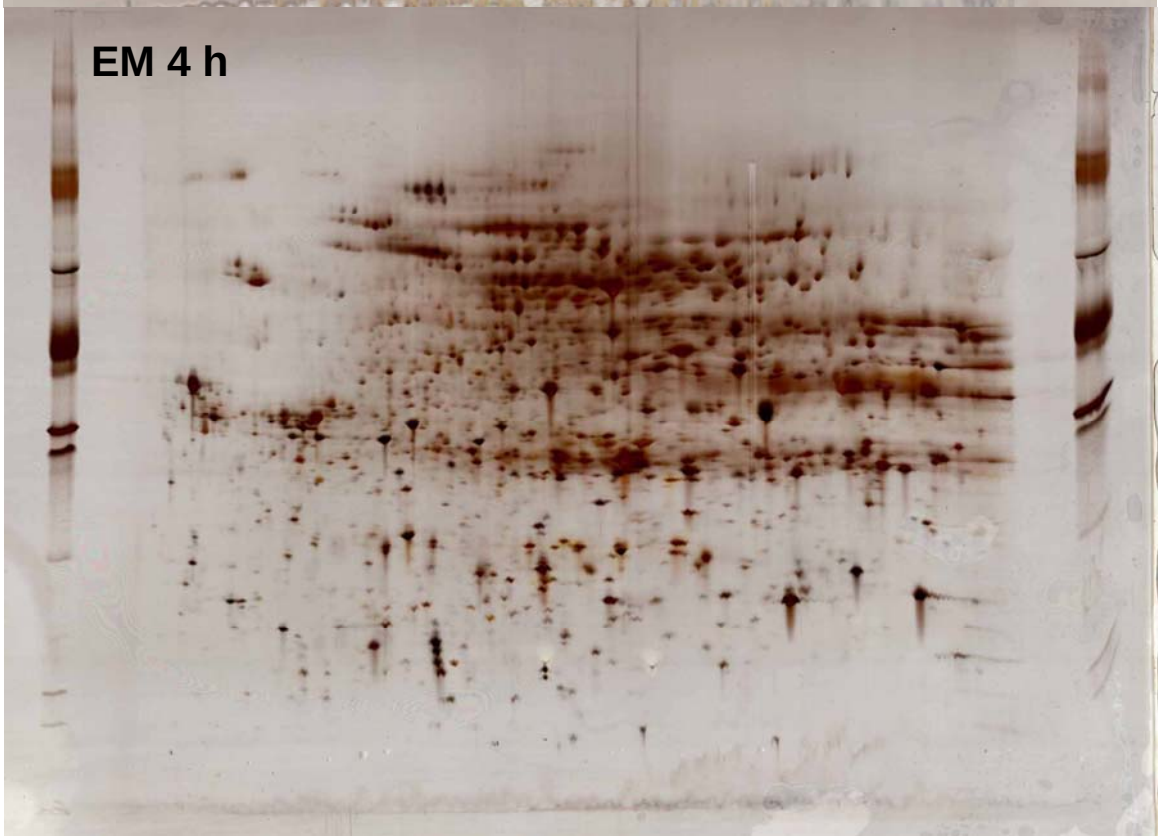


EM 12 h

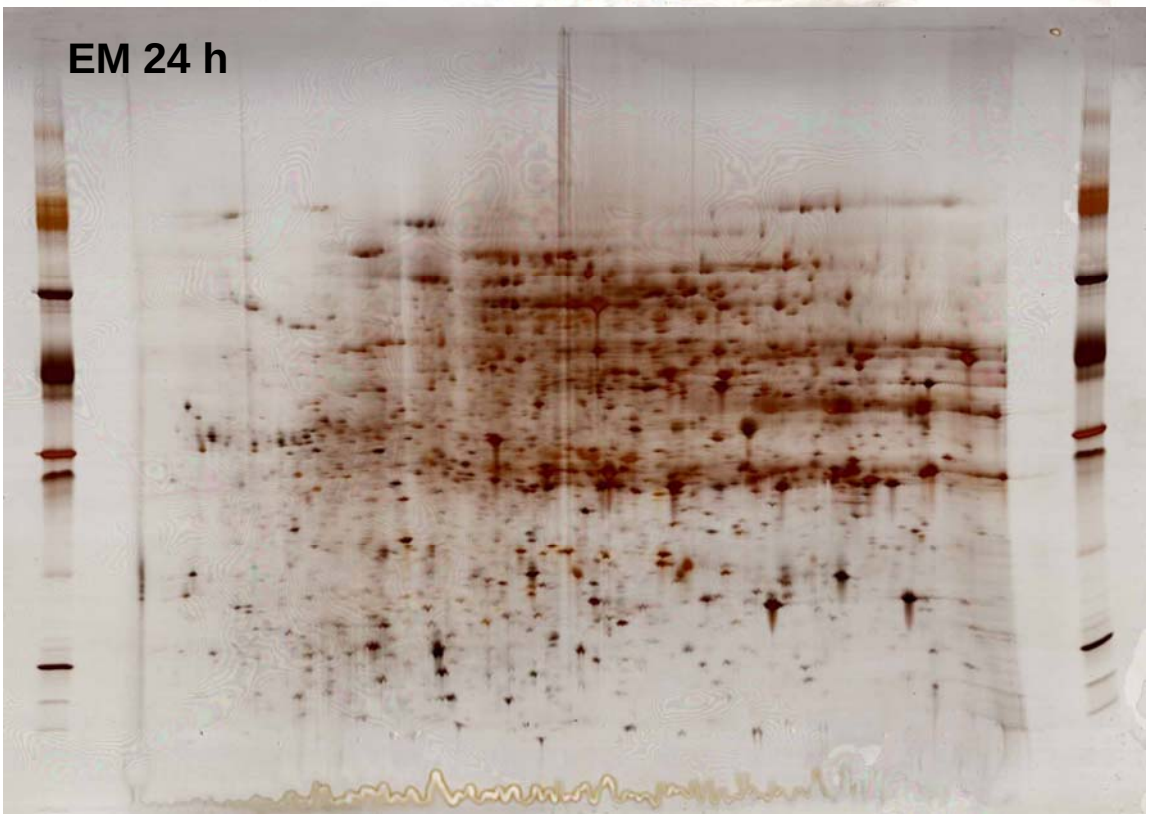
EM 24 h

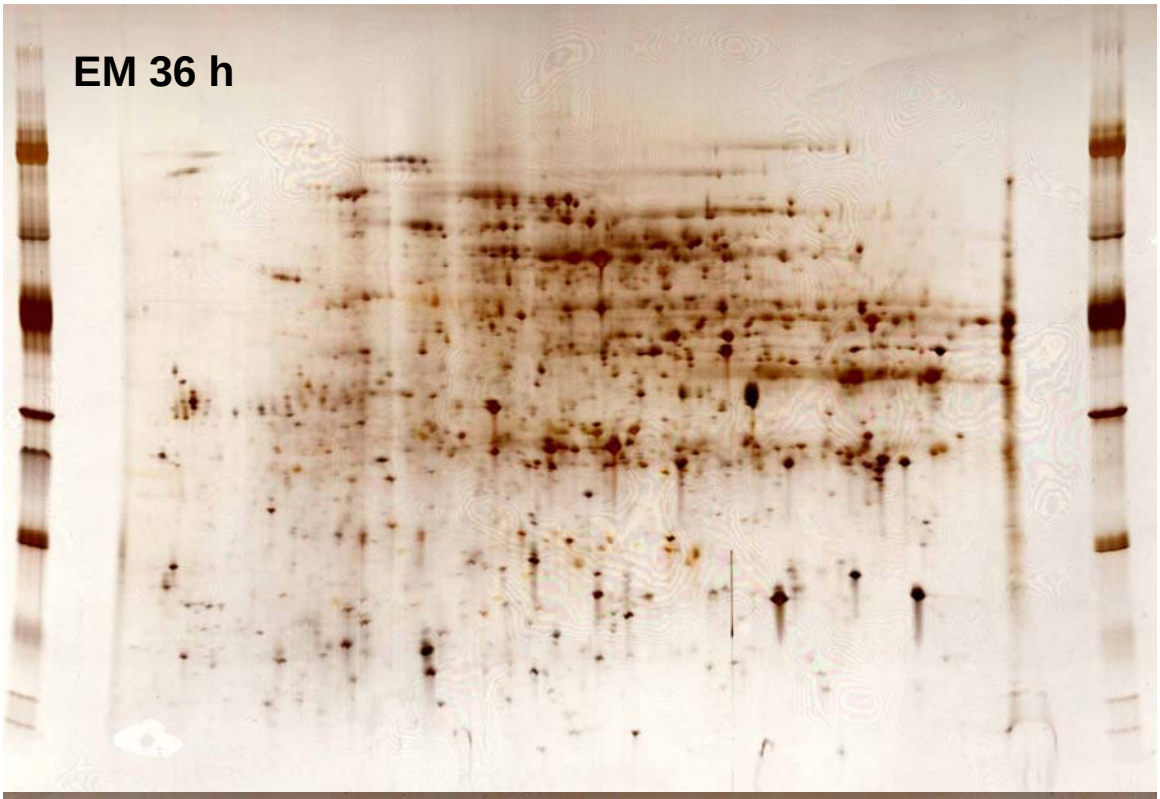
EM 36 h

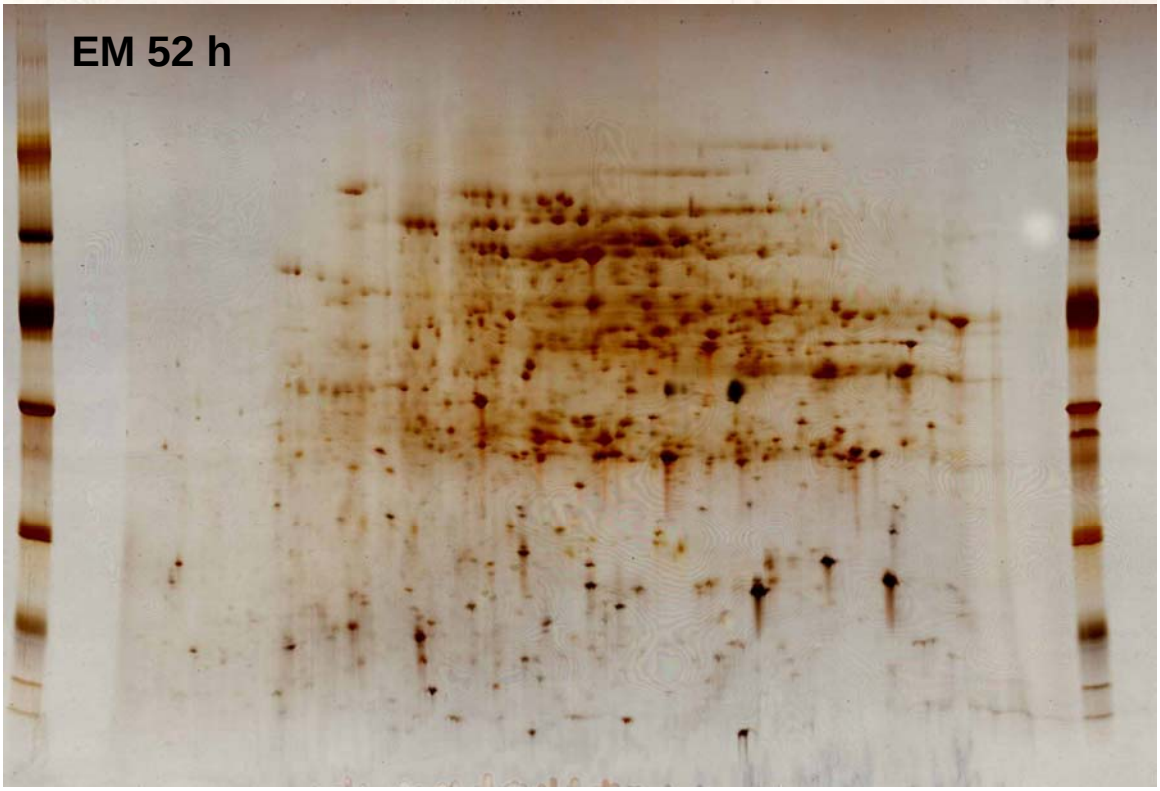
EM 52 h

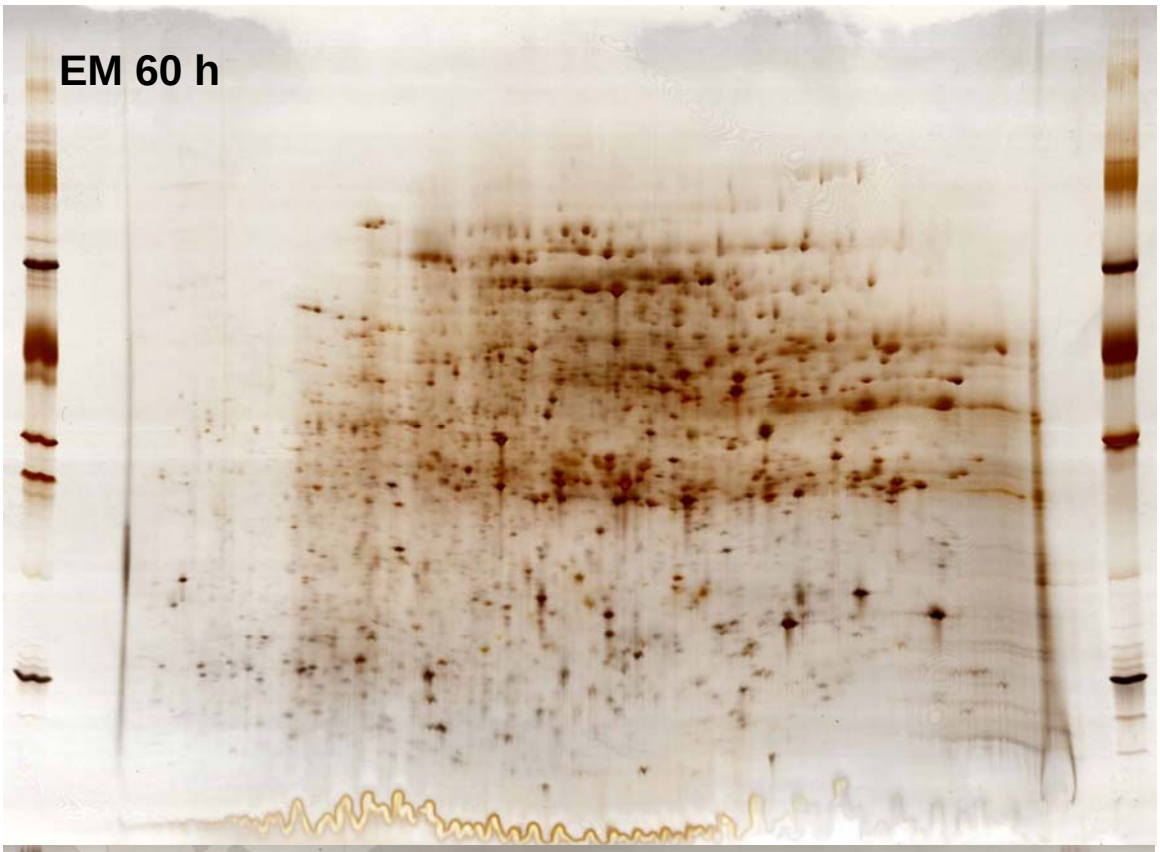
EM 60 h

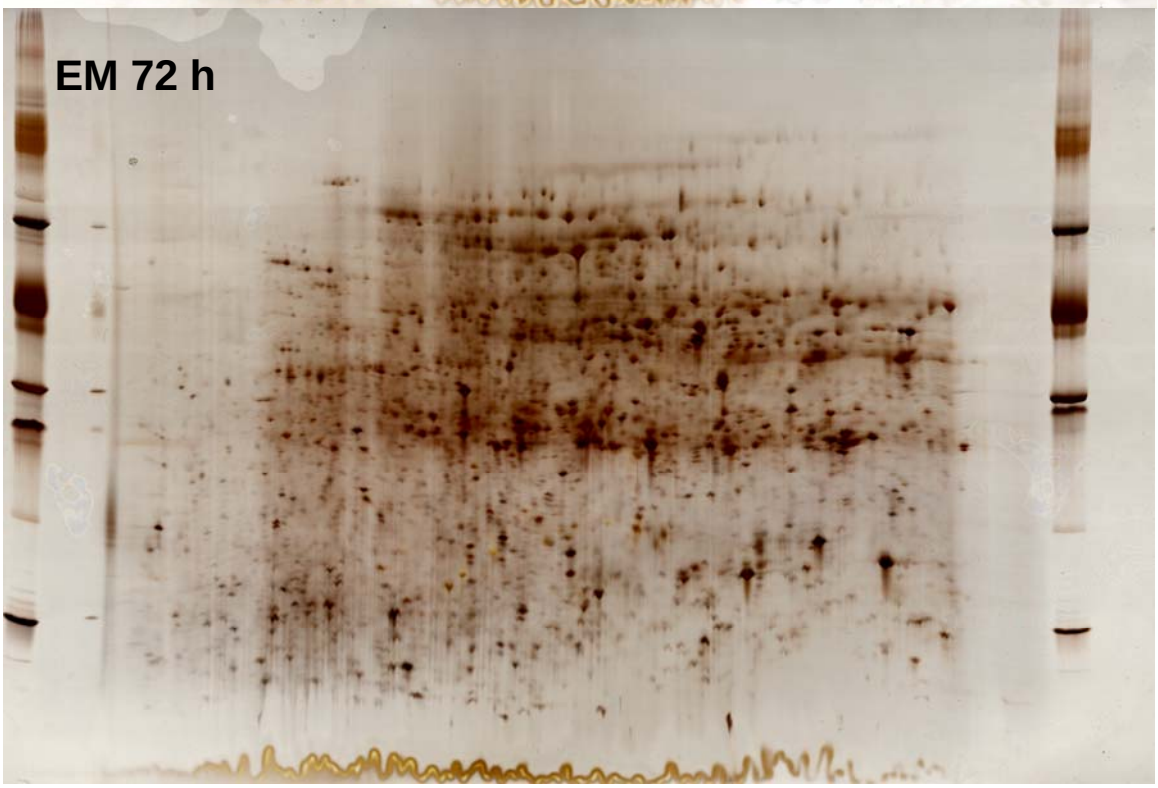
EM 72 h

Appendix 1b

2D gels (pH range 4-7) of aleurone layer extracts during germination and radicle elongation. All time points (0, 4, 12, 24, 36, 52, 60, 72 h PI) are shown.

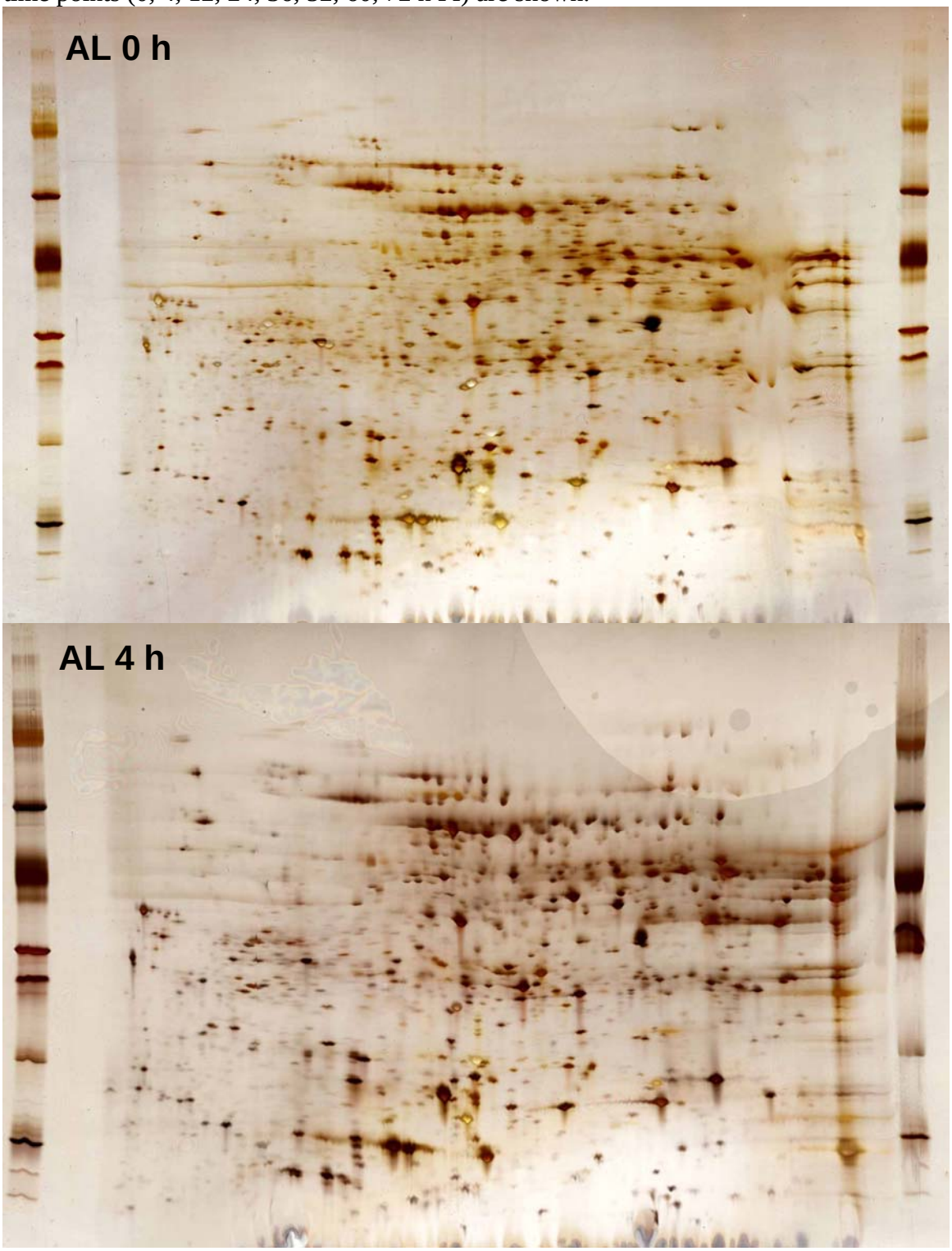

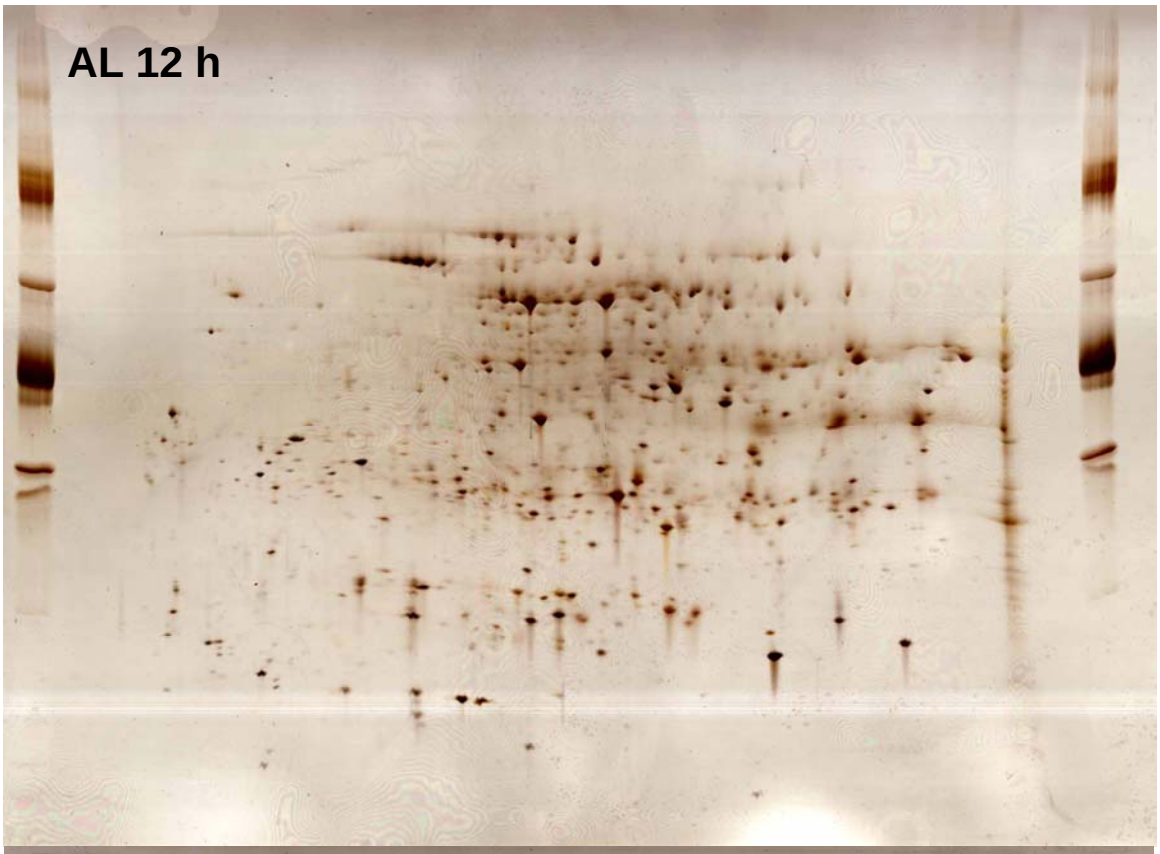
AL 12 h

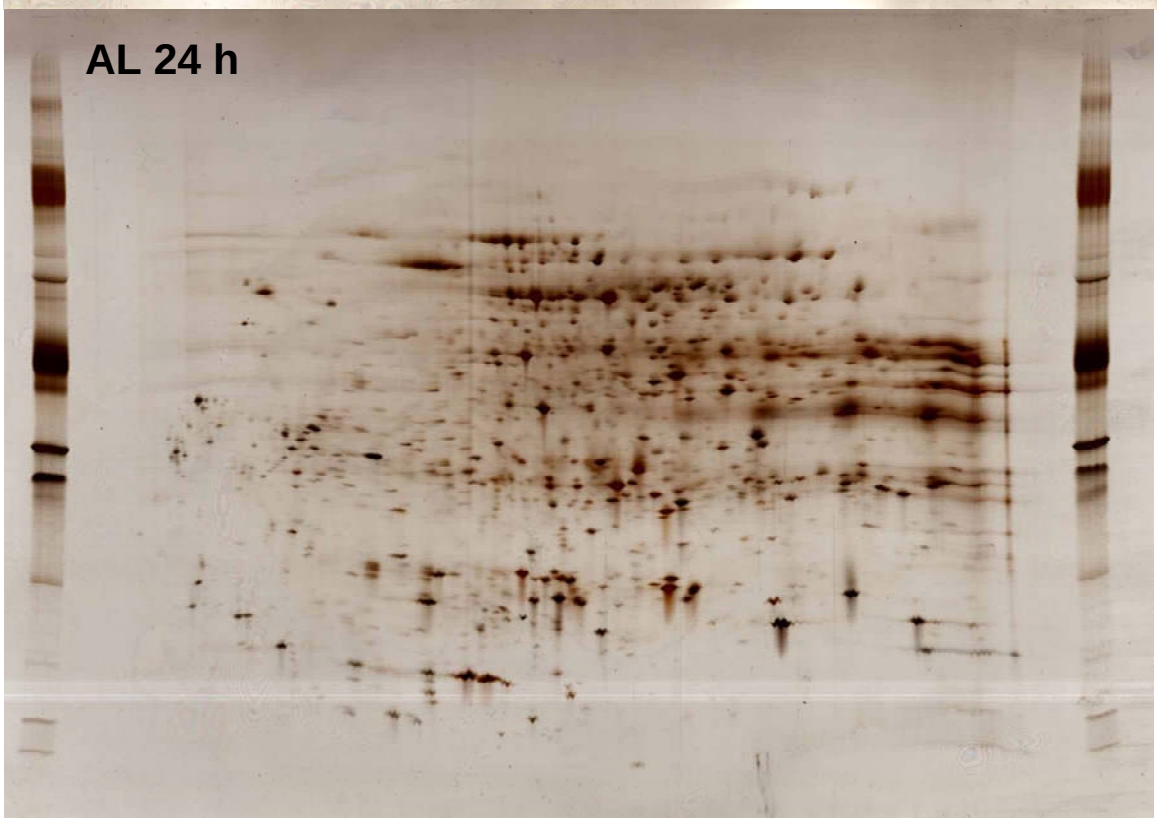
AL 24 h

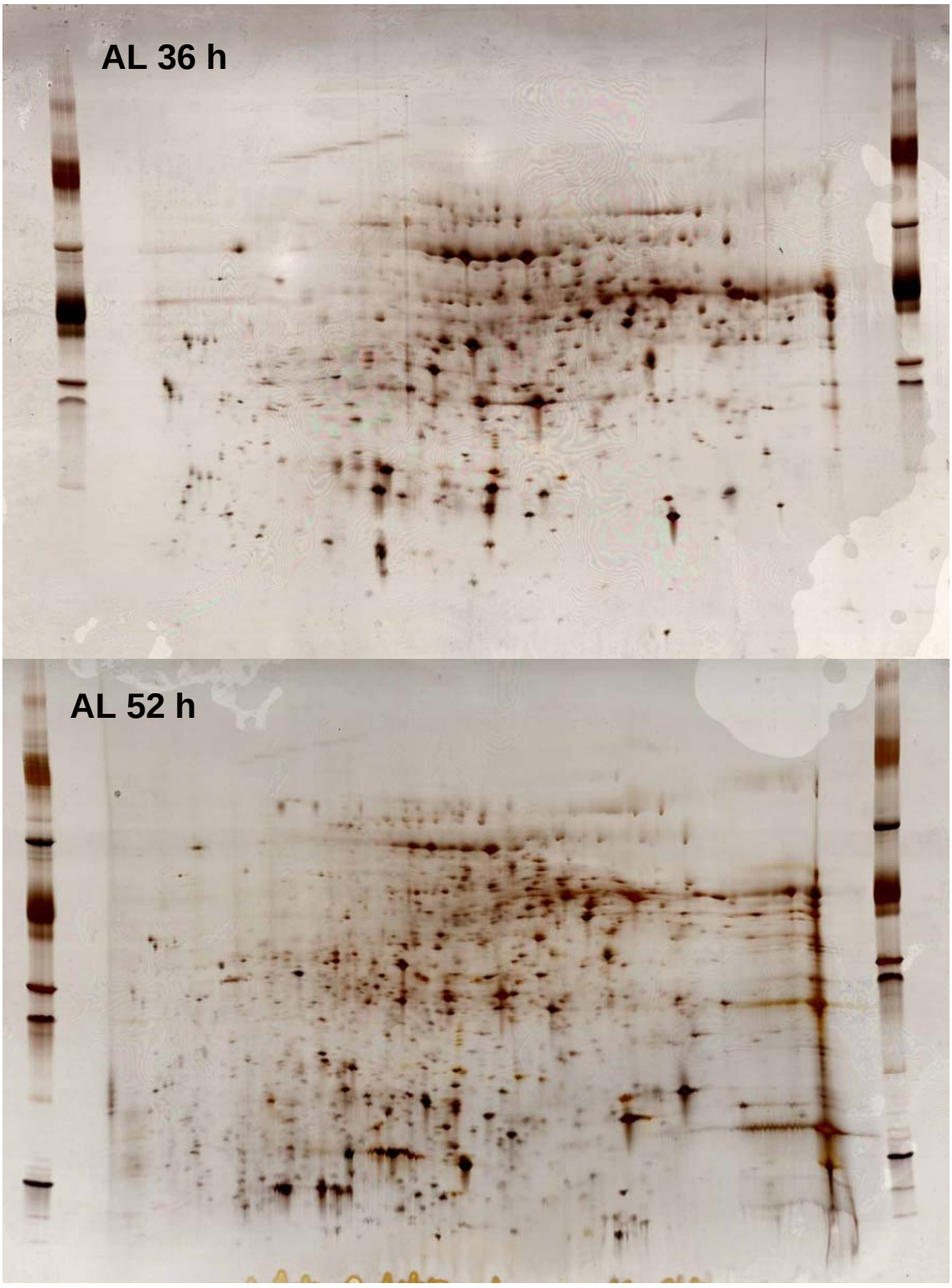
AL 36 h
AL 52 h

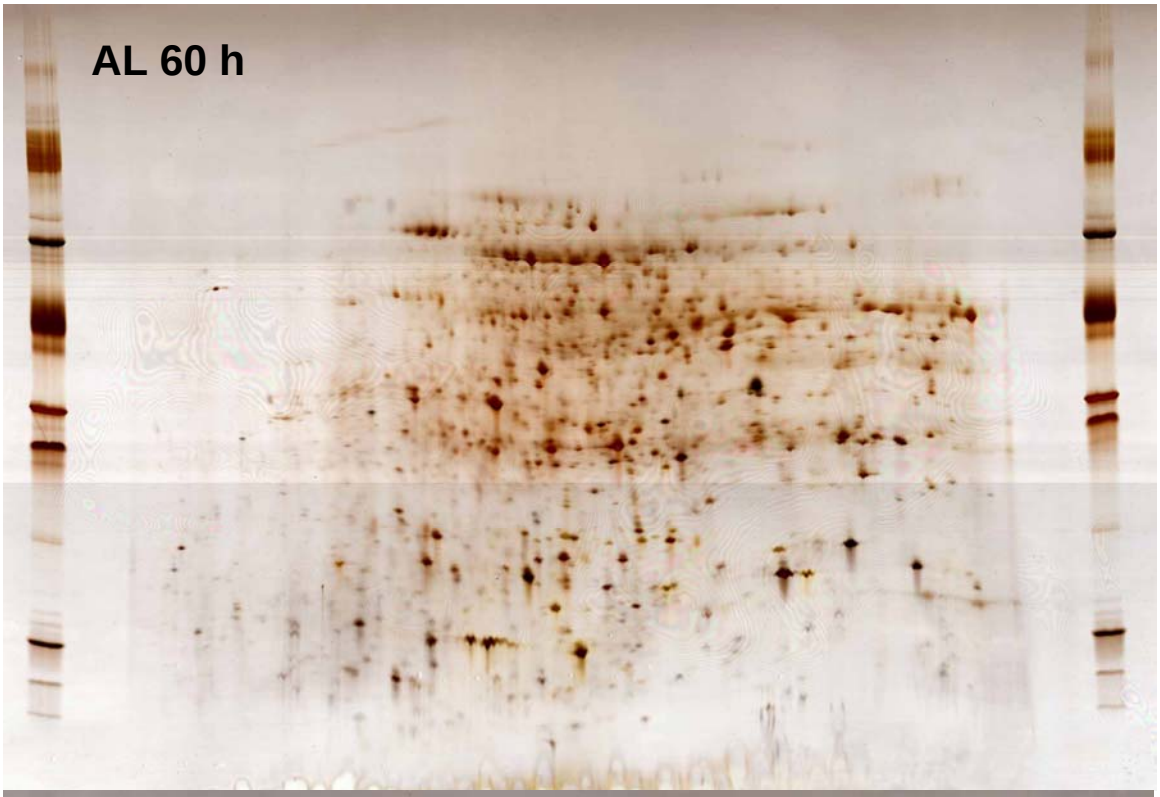
AL 60 h

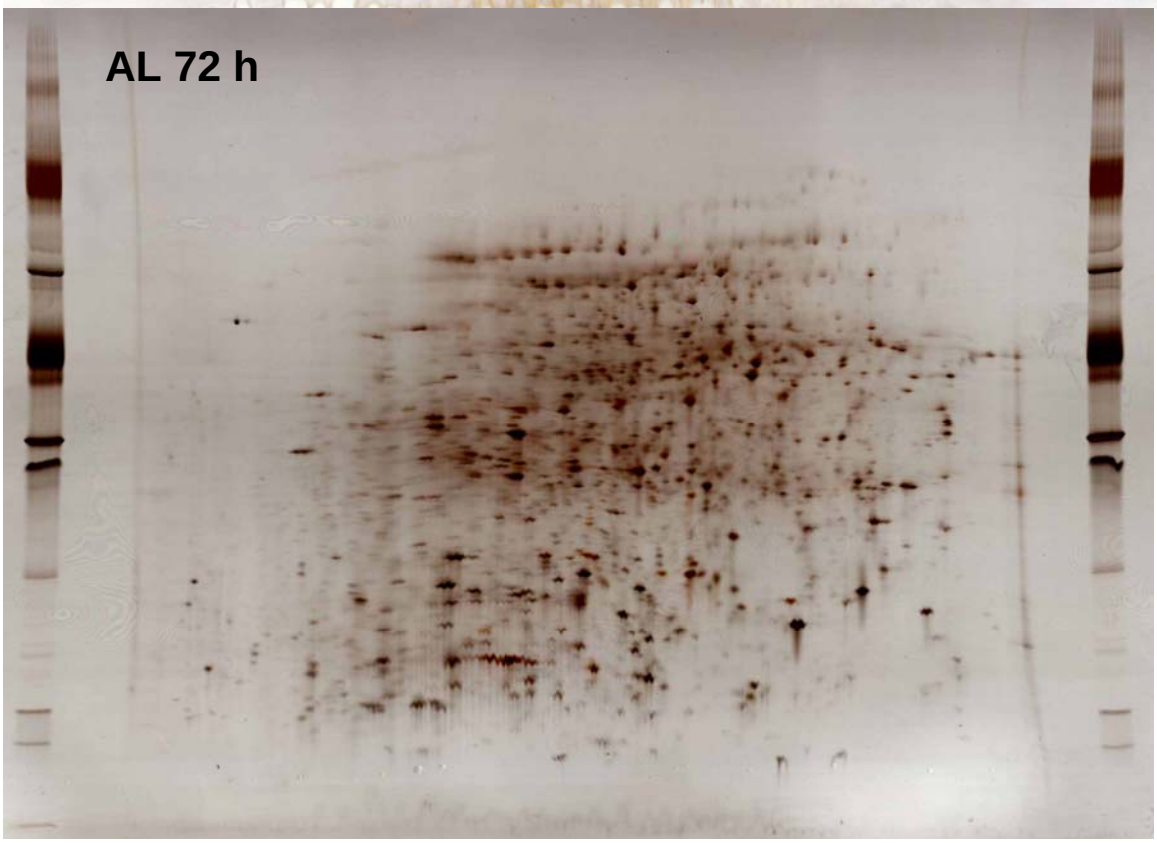
AL 72 h

Appendix 1c

2D gels (pH range 4-7) of endosperm extracts during germination and radicle elongation. All time points (0, 4, 12, 24, 36, 52, 60, 72 h PI) are shown.

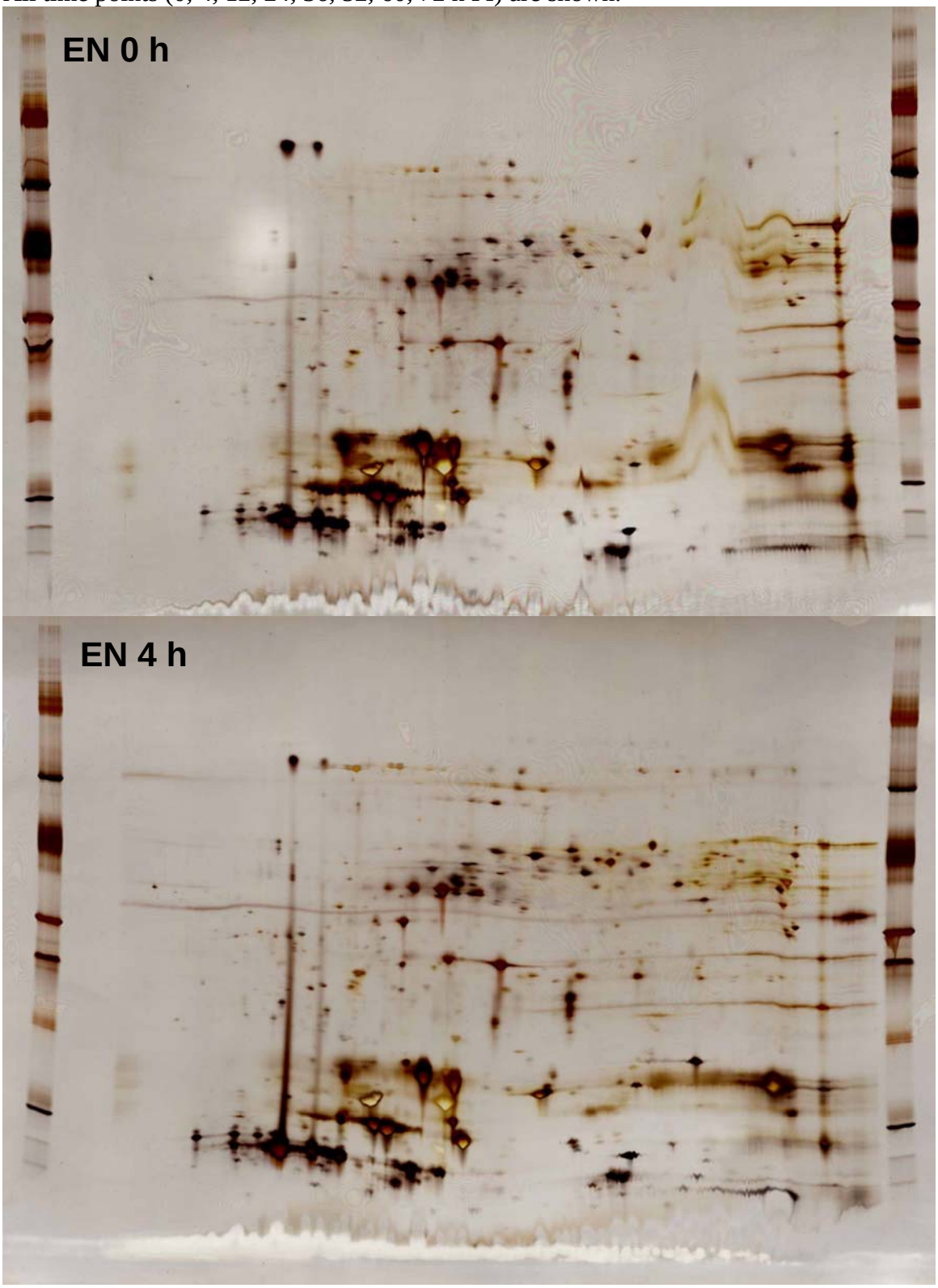

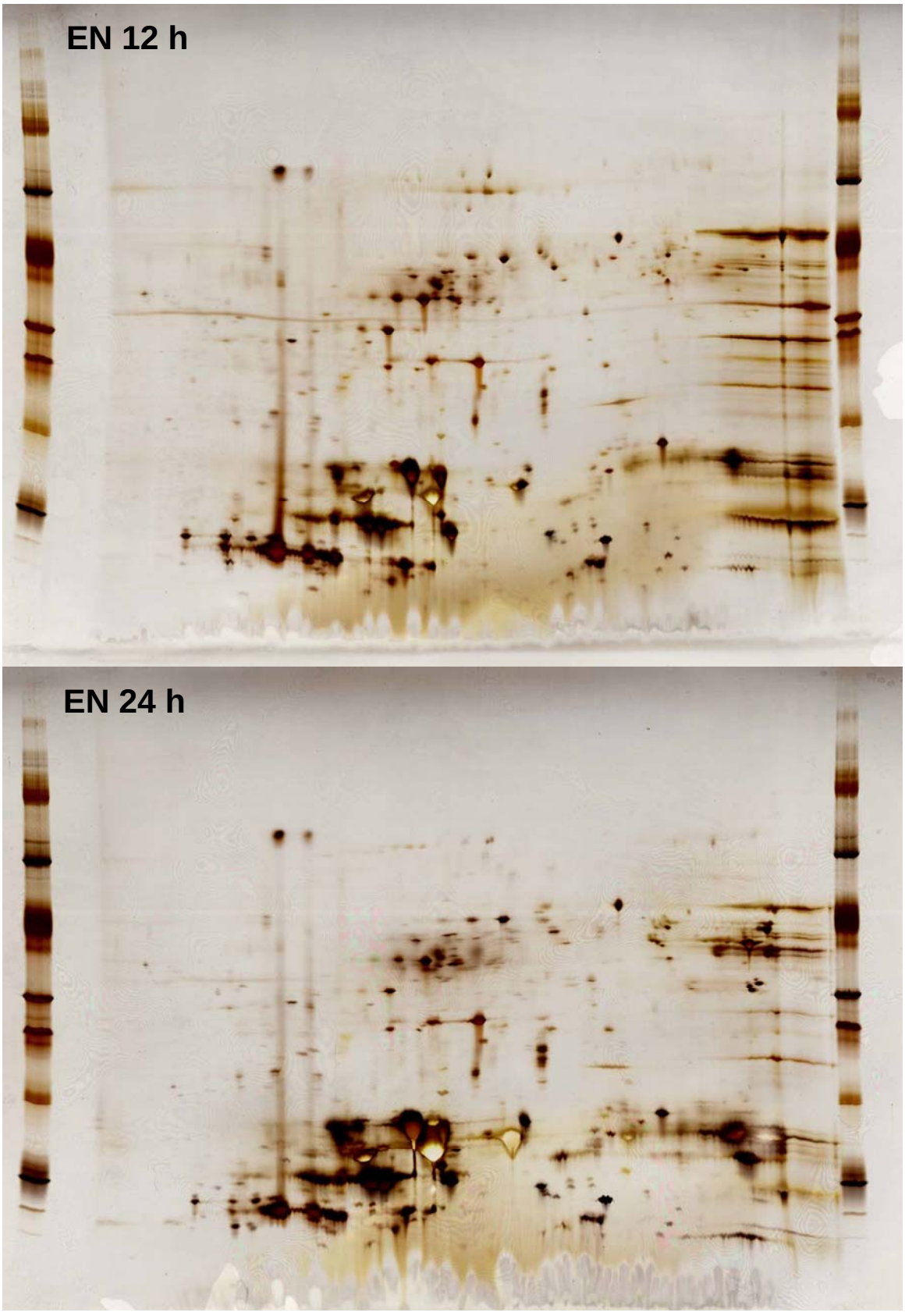
EN 12 h
EN 24 h


EN 36 h


EN 52 h

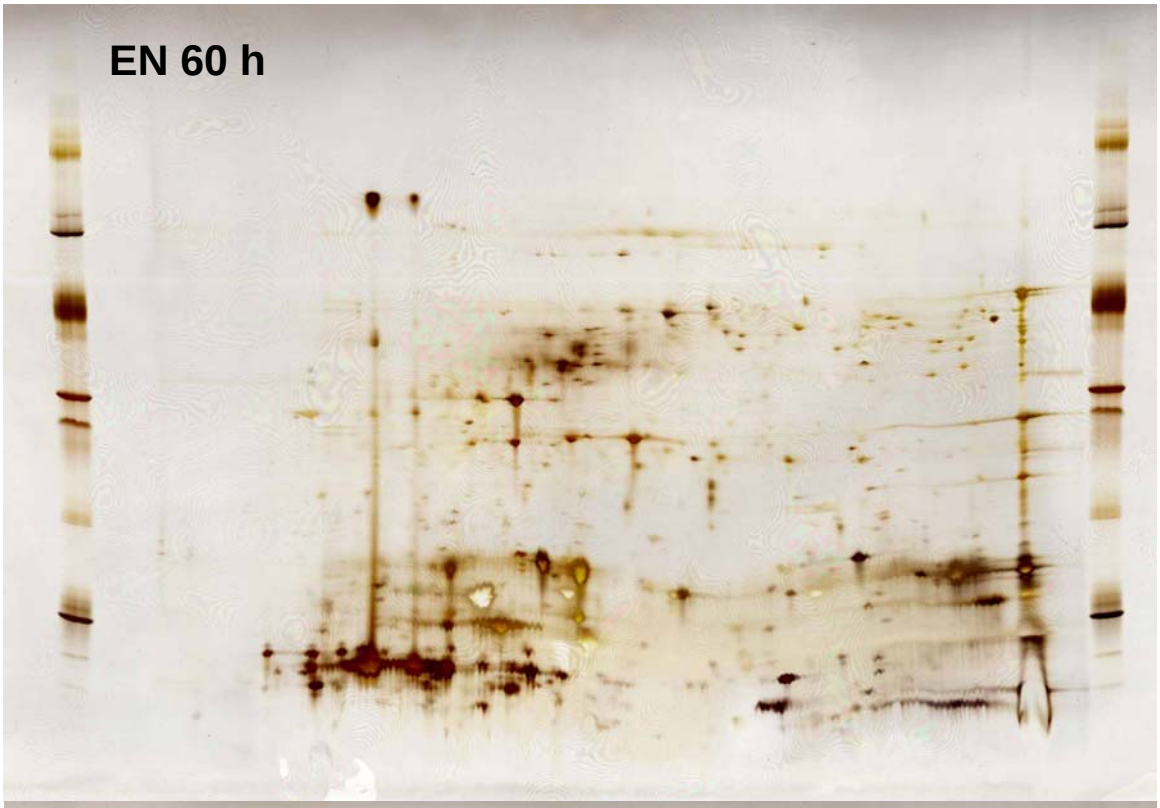
EN 60 h


EN 72 h

Appendix 2

2D gels (pH range 4-7) of extracts from embryos that were germinated for 24 h after isolation from the rest of the seed (b) compared to whole seed germinated embryo extract (a). ABA was added to the embryos germinating in the absence of the surrounding tissues (c).

a) EM 24 h whole seed germination

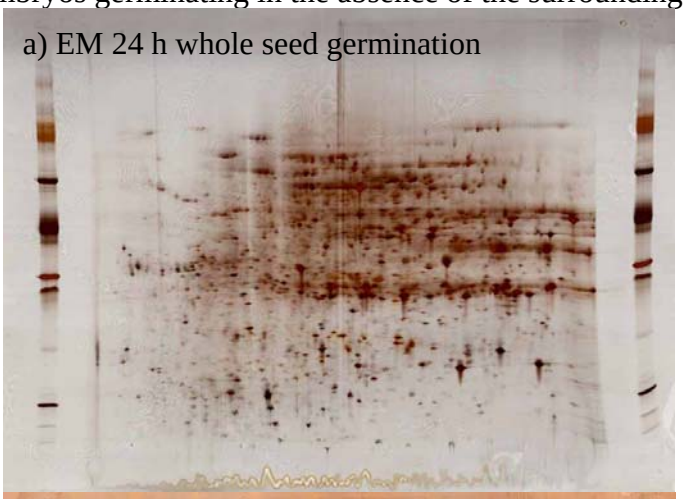

b) EM 24 h isolated and germinated on water

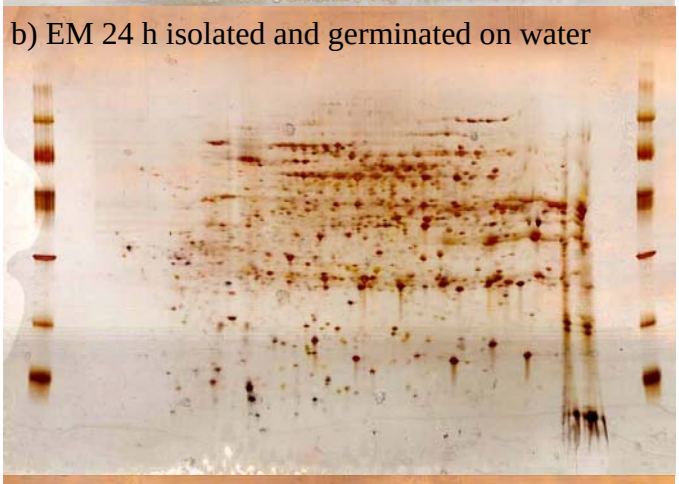

c) EM 24 h isolated and germinated on water/ABA

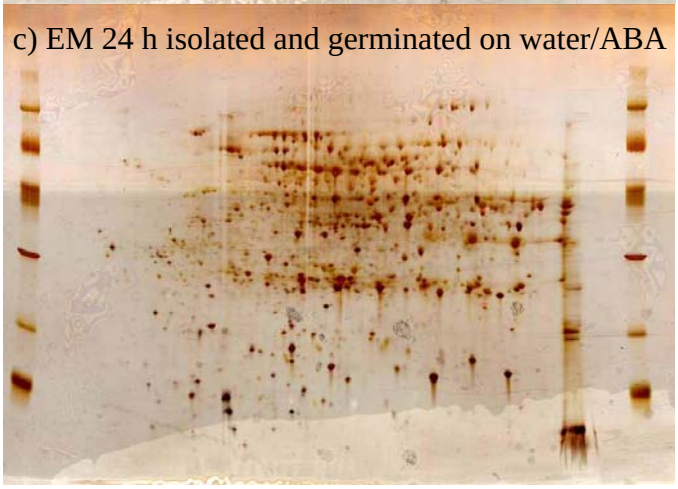

2D gels (pH range 4-7) of extracts from embryos that were germinated for 72 h after isolation from the rest of the seed (b) compared to whole seed germinated embryo extract (a). ABA was added to the embryos germinating in the absence of the surrounding tissues (c).

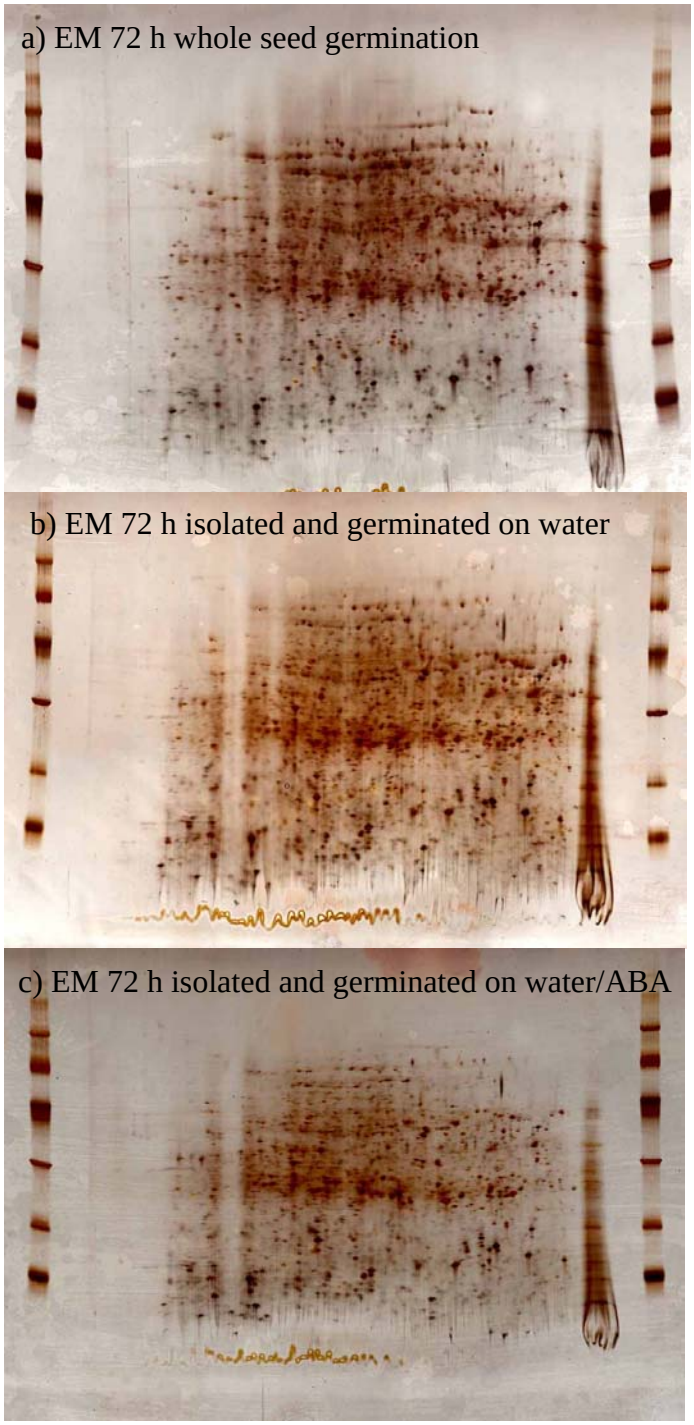

Appendix 3

An example of raw date from an APX assay at all seven time points is given in Figure 3. Based on the slopes of the linear parts of the curves, units were calculated (Table 3). Units are defined as the amount of enzyme (microgram) that catalyzes the conversion of 1 micromole substrate per minute.

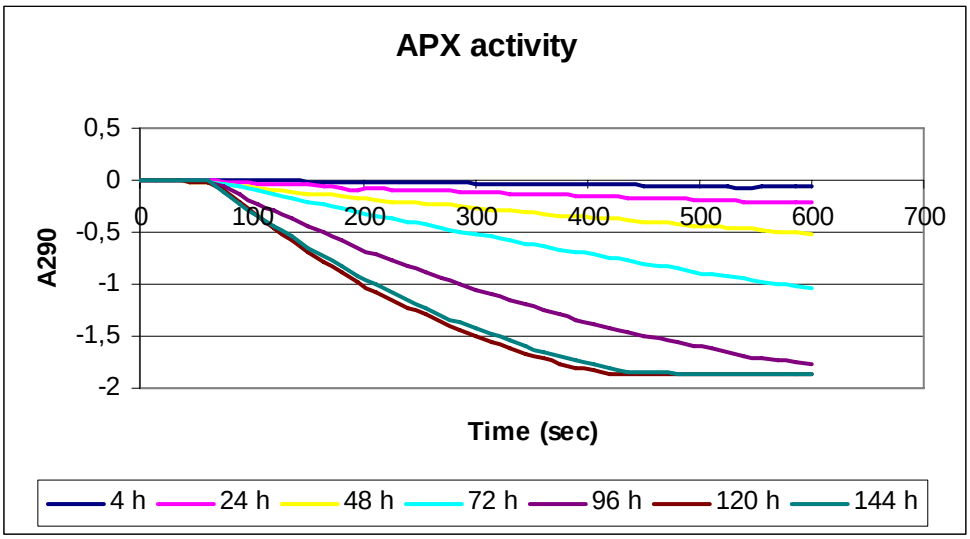

Figure 3. The raw data from a single APX activity assay in the embryo extract. The units/microgram protein was calculated based on the slopes of each time point (Table below).

Table 3. Enzyme activities of APX, DHAR, GR and MDHAR.

	Units/microgram protein			
	APX	**DHAR**	**GR**	**MDHAR**
4 h	0.023 (+/-0.006)	3.232 (+/-0.315)	0.189 (+/-0.031)	0.036 (+/-0.004)
24 h	0.064 (+/-0.002)	2.710 (+/-0.139)	0.202 (+/-0.027)	0.037 (+/-0.003)
48 h	0.203 (+/-0.055)	1.514 (+/-0.117)	0.240 (+/-0.053)	0.053 (+/-0.006)
72 h	0.439 (+/-0.117)	0.355 (+/-0.135)	0.197 (+/-0.051)	0.057 (+/-0.010)
96 h	0.666 (+/-0.056)	0.388 (+/-0.131)	0.282 (+/-0.068)	0.074 (+/-0.014)
120 h	0.898 (+/-0.092)	0.224 (+/-0.195)	0.317 (+/-0.045)	0.074 (+/-0.018)
144 h	0.900 (+/-0.135)	1.640 (+/-0.677)	0.337 (+/-0.067)	0.082 (+/-0.015)

The numbers are mean values of three replicates.

Appendix 2

2D gels (pH range 4-7) of extracts from embryos that were germinated for 24 h after isolation from the rest of the seed (b) compared to whole seed germinated embryo extract (a). ABA was added to the embryos germinating in the absence of the surrounding tissues (c).

a) EM 24 h whole seed germination

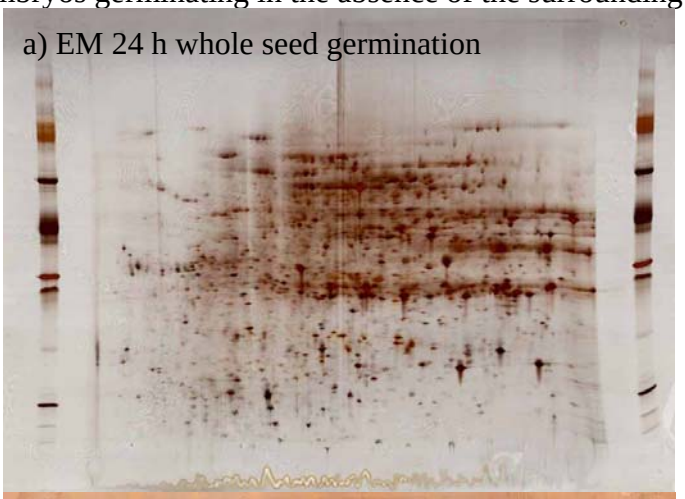

b) EM 24 h isolated and germinated on water

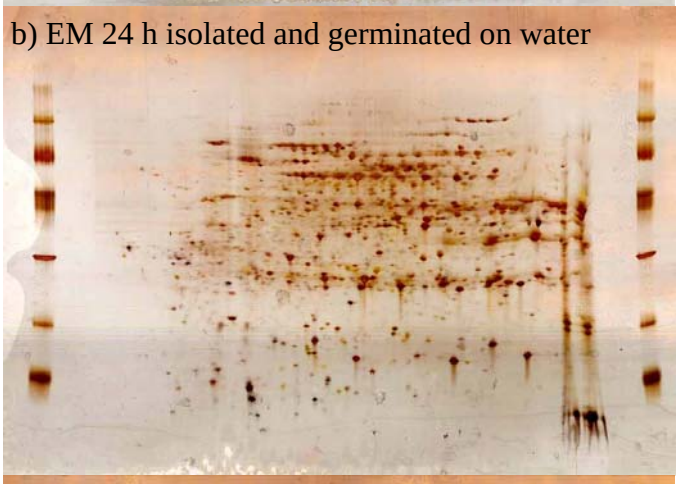

c) EM 24 h isolated and germinated on water/ABA

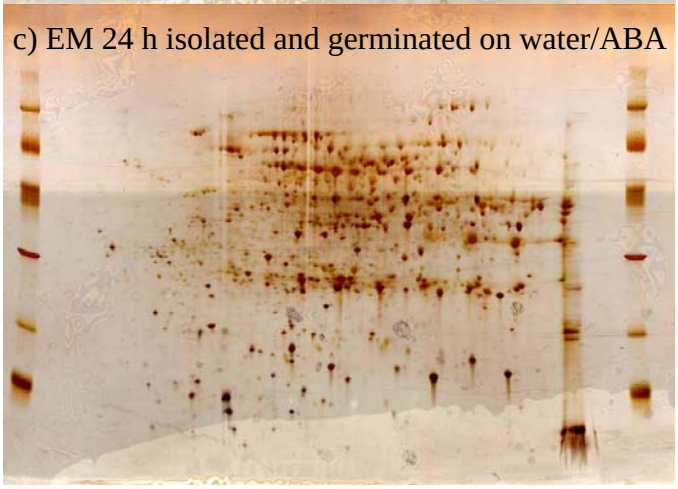

2D gels (pH range 4-7) of extracts from embryos that were germinated for 72 h after isolation from the rest of the seed (b) compared to whole seed germinated embryo extract (a). ABA was added to the embryos germinating in the absence of the surrounding tissues (c).

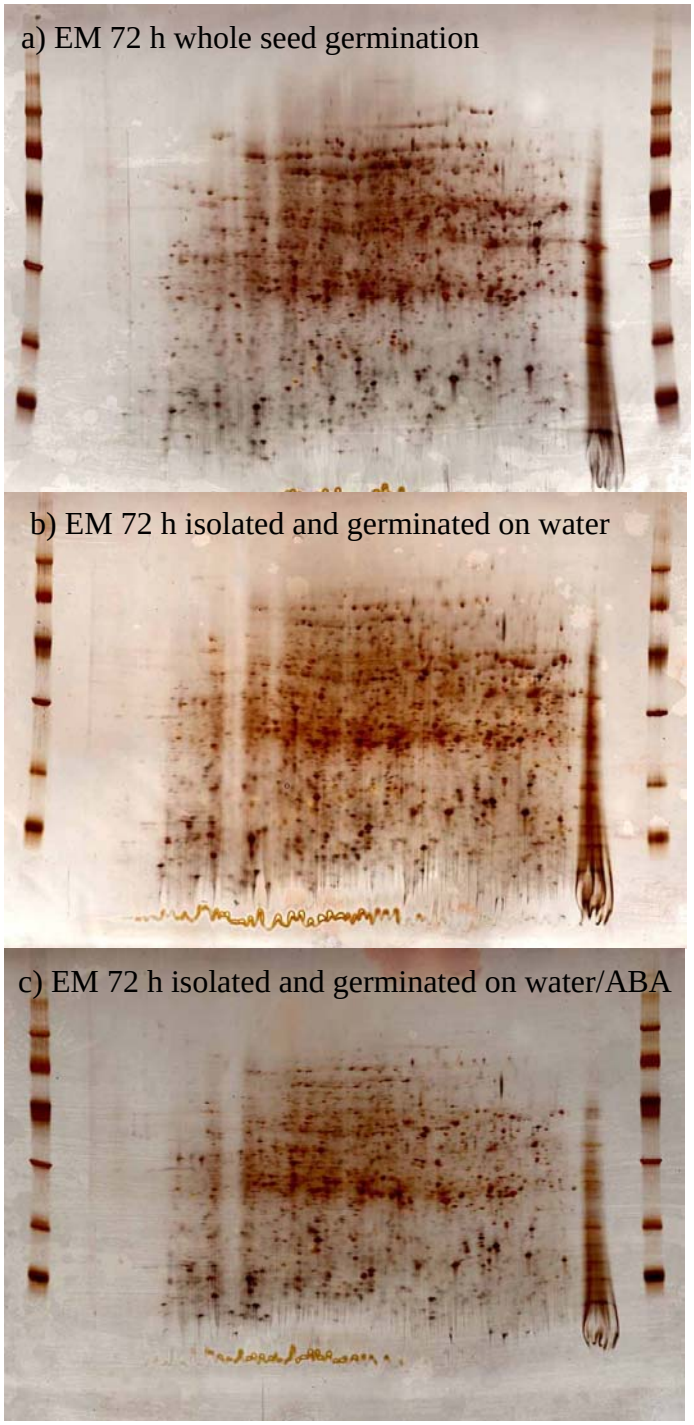

Appendix 3

An example of raw date from an APX assay at all seven time points is given in Figure 3. Based on the slopes of the linear parts of the curves, units were calculated (Table 3). Units are defined as the amount of enzyme (microgram) that catalyzes the conversion of 1 micromole substrate per minute.

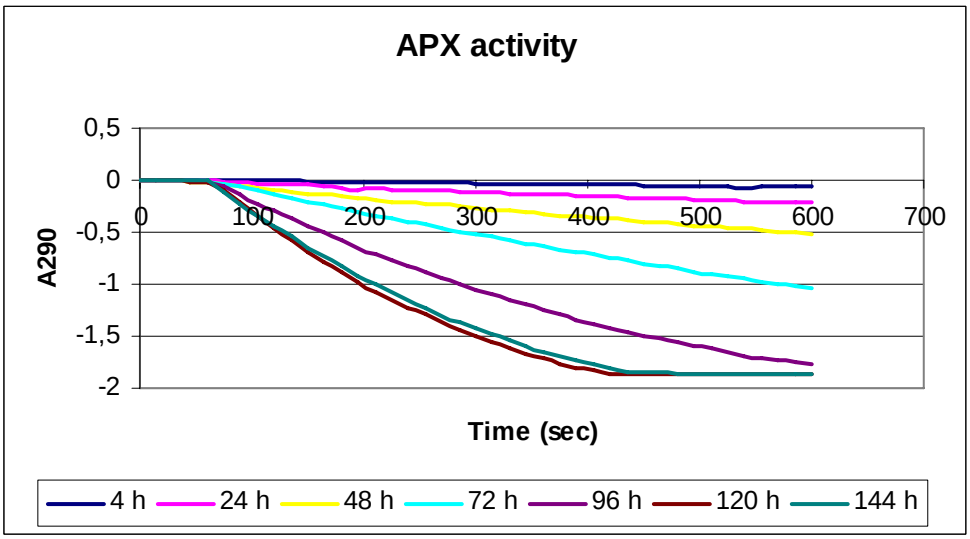

Figure 3. The raw data from a single APX activity assay in the embryo extract. The units/microgram protein was calculated based on the slopes of each time point (Table below).

Table 3. Enzyme activities of APX, DHAR, GR and MDHAR.

	Units/microgram protein			
	APX	**DHAR**	**GR**	**MDHAR**
4 h	0.023 (+/-0.006)	3.232 (+/-0.315)	0.189 (+/-0.031)	0.036 (+/-0.004)
24 h	0.064 (+/-0.002)	2.710 (+/-0.139)	0.202 (+/-0.027)	0.037 (+/-0.003)
48 h	0.203 (+/-0.055)	1.514 (+/-0.117)	0.240 (+/-0.053)	0.053 (+/-0.006)
72 h	0.439 (+/-0.117)	0.355 (+/-0.135)	0.197 (+/-0.051)	0.057 (+/-0.010)
96 h	0.666 (+/-0.056)	0.388 (+/-0.131)	0.282 (+/-0.068)	0.074 (+/-0.014)
120 h	0.898 (+/-0.092)	0.224 (+/-0.195)	0.317 (+/-0.045)	0.074 (+/-0.018)
144 h	0.900 (+/-0.135)	1.640 (+/-0.677)	0.337 (+/-0.067)	0.082 (+/-0.015)

The numbers are mean values of three replicates.

Appendix 4 – Paper 1

B. Svensson, K. Fukuda, P.K. Nielsen, **B.C. Bønsager.** (2004) Proteinaceous α-amylase inhibitors. Biochim. Biophys. Acta, 1696, 145-156.

Available online at www.sciencedirect.com
SCIENCE DIRECT®
Biochimica et Biophysica Acta 1696 (2004) 145–156
BIOCHIMICA ET BIOPHYSICA ACTA
BBA
www.bba-direct.com

Review

Proteinaceous α-amylase inhibitors

Birte Svensson*, Kenji Fukuda, Peter K. Nielsen, Birgit C. Bønsager

Carlsberg Laboratory, Department of Chemistry, Gamle Carlsberg Vej 10, DK-2500 Copenhagen, Denmark

Received 17 March 2003; accepted 15 July 2003

Abstract

Proteins that inhibit α-amylases have been isolated from plants and microorganisms. These inhibitors can have natural roles in the control of endogenous α-amylase activity or in defence against pathogens and pests; certain inhibitors are reported to be antinutritional factors. The α-amylase inhibitors belong to seven different protein structural families, most of which also contain evolutionary related proteins without inhibitory activity. Two families include bifunctional inhibitors acting both on α-amylases and proteases. High-resolution structures are available of target α-amylases in complex with inhibitors from five families. These structures indicate major diversity but also some similarity in the structural basis of α-amylase inhibition. Mutational analysis of the mechanism of inhibition was performed in a few cases and various protein engineering and biotechnological approaches have been outlined for exploitation of the inhibitory function.

Keywords: Protein–protein interaction; Substrate mimicry; Site-directed mutagenesis; Evolution; Transgene; Allergen

1. Introduction

Plant seeds are rich sources of a large number of different proteinaceous inhibitors acting on α-amylases or other polysaccharide processing enzymes—as reviewed in this issue—and proteases [1–3]. The area of α-amylase inhibitors has received increasing interest during the past 40 years and started even by a few reports dating back to 1933 (see in Refs. [1,4]). A recent review describes plant inhibitors active towards insect α-amylases and includes aspects of transgenic protection of plants against insect predators [2]. Earlier reviews cover occurrence, chemical properties, and reaction mechanisms of microbial and plant α-amylase inhibitors [1,3,4] as well as their relation to nutrition [3,4]. The present mini-review addresses the diverse group of α-amylase inhibitors with focus on recent insights in structure and function.

Some α-amylase inhibitors show strict target enzyme specificity and recognise only one out of several closely related isozymes or enzymes from different species [5,6]. Other inhibitors have high affinity for both mammalian and insect α-amylases (see Ref. [2]) that share around 35% sequence identity. Several examples moreover are found of inhibitors acting on insect, but not on mammalian enzymes and vice versa (for reviews see Refs. [2,4]). Inhibitors from bean can influence human and animal nutrition and were once also applied as "starch blockers" in obesity and diabetes therapy [3,7]. The vast majority of endogenous plant enzymes are insensitive to the inhibitors, thus only one inhibitor type acts on certain plant α-amylase isozymes [5,8].

2. Inhibitor classes, forms, and evolutionary aspects

Seven types of proteinaceous α-amylase inhibitors are found in nature as defined by similarities in sequence and three-dimensional structures [2–4,9]. Six types are from higher plants [2,10–20] whereas the remaining type occurs in *Streptomyces* species [21] (Table 1). In addition, artificial α-amylase inhibitors were recently obtained by applying an in vitro evolution strategy using phage

Abbreviations: AAI, amaranth α-amylase inhibitor; αAI, lectin-like α-amylase inhibitor; ASI, α-amylase/subtilisin inhibitor; BASI, barley α-amylase/subtilisin inhibitor; BMAI, barley monomeric α-amylase inhibitor; CBD, cellulose binding domain; Fmoc, 9-fluorenylmethyloxycarbonyl; HPA, human pancreatic α-amylase; PPA, porcine pancreatic α-amylase; RASI, rice α-amylase/subtilisin inhibitor; RATI, ragi α-amylase/trypsin inhibitor (this protein is sometimes referred to as RBI for ragi bifunctional inhibitor); SIα, sorghum α-amylase inhibitor; TMA, *Tenebrio molitor* α-amylase; VHH, camelid heavy chain antibody; WASI, wheat α-amylase/subtilisin inhibitor; WMAI, wheat monomeric α-amylase inhibitor

* Corresponding author. Tel.: +45-3327-5345; fax: +45-3327-4708.
E-mail address: bis@crc.dk (B. Svensson).

1570-9639/$ - see front matter © 2003 Elsevier B.V. All rights reserved.
doi:10.1016/j.bbapap.2003.07.004

Table 1
Properties of proteinaceous α-amylase inhibitors

Inhibitor type [review]	Source	α-Amylase targets	Size (aa residues)	K_i or K_d (M)	Engineered/synthetic analogues	Abbreviation/names
Microbial [4]	*Streptomyces*	Mammalian, bacteria	Approximately 74–76 [31,33]	9×10^{-12} [31]	Depsipeptides [90], β-hairpin [88,89]	Haim, Paim, Tendamistat (HOE 467)
Knottin-like (cluster 5) [24]	Amaranth [10]	Insect	32 [10]	"Strong" [10]	Analogues and HWTX-chimera [9]	AAI
γ-Thionin-like	Sorghum [11]	Insect, (mammalian)	47–48 [36]	"Strong" [11]		SIα1, SIα2, SIα3
CM-proteins [2,4,6]	Barley [12], wheat [15], ragi [14], rye [40]	Mammalian, insect, bacterial	124–160	0.1×10^{-9} [56,93]	Insertion site-directed mutants [12]	RATI (RBI), 0.19, 0.28 (WMAI-1), 0.53, WRP25, WRP26, BMAI-1
Kunitz-type [4,60]	Barley [5,8], wheat [15], rice [16]	Cereal, insect	176–181	0.22×10^{-9} [61]	Site-directed mutants in BASI [60,62,96]	BASI, WASI, RASI
Thaumatin-like [2]	Maize [63]	Insect	173–235	n.d. [63]		
Legume lectin-like [2,4]	Common bean [18,19]	Mammalian, insect, (fungi)	240–250	30×10^{-12} [65]		αAI1, αAI2
Cellulose binding domain mutant [22]	*Trichoderma reesei*, phage display	Mammalian	36	μM range [22]	11 positions allowed to vary [22]	$CBD_{PPA\ 1:4}$, $CBD_{PPA\ 1:5}$
Anti-PPA variant [23]	Dromedary VHH	Mammalian		$3.5–235 \times 10^{-9}$ [23]		AMB7, AMD9, AMD10

display and as scaffold either the cellulose binding domain (CBD) from *Trichoderma reesei* cellobiohydrolase Cel7A [22] or dromedary VHH antibodies raised against porcine pancreatic α-amylase (PPA) [23].

For the six plant α-amylase inhibitor families, non-inhibitory proteins with more or less closely related sequences are available [24–29]. The inhibitors are typically present in several organisms and certain exist in different forms. Dendrograms have been calculated for some families of inhibitors and related proteins to illustrate their structural and evolutionary relationships [24,25,27,30]. Some of the inhibitors are small proteins and may belong to protein hyperfamilies, sharing only fold and no evolutionary relationship, which enables strategies in skeleton protein engineering and peptide synthesis for creation of active designer inhibitors.

2.1. Streptomyces inhibitors

Tendamistat [31], Haim [21], Paim [32], and related proteins constitute a family of small proteins of approximately 75 amino acid residues which have been purified from different *Streptomyces* species. These inhibitors possess about 30% sequence identity and show conserved disulfide topology [33]. They act on α-amylases from animals, *Streptomyces* species, and a *Bacillus* sp. no. 195 [see references in Ref. [34]).

2.2. Knottins

AAI from the Mexican crop plant amaranth (*Amaranthus hypochondriacus*) is the smallest known natural proteinaceous α-amylase inhibitor [10]. Protein knots are extremely rich in disulfides and occur both as individual miniproteins of around 32 amino acid residues and as domains in larger molecules. In a recent dendrogram, knottins group in eight clusters according to the disulfide bond topology [24]. AAI belongs to cluster 5, which presents various distinct characteristics shared by the members of different origin such as a high content of proline and a conserved *cis*-proline. In addition to the α-amylase inhibitor, cluster 5 includes spider and snail venom toxins, of which conotoxins have pharmacological applications. Gurmarin, a plant knottin, suppresses sweet taste in rats and is used in traditional medicin to treat diabetes mellitus. This knottin fold apparently evolved independently in the different kingdoms; AAI structurally is most similar to gurmarin and funnel-web spider toxin [35].

2.3. γ-Thionins

SIα1, SIα2, and SIα3 from sorghum (*Sorghum bicolor*) are small proteins of 47–48 amino acid residues that strongly inhibit insect α-amylases [11]. The three isoforms contain four disulfide bridges and have 42–87% sequence identity [36]. They belong to the γ-thionin superfamily of distantly related proteins, of which several members through a wide variety of mechanisms are involved in plant defence [2].

2.4. CM-proteins

A large protein family from cereal seeds containing 120–160 amino acid residues and five disulfide bonds [12–14] includes inhibitors known for their action on α-amylases from mammals and insects. The name CM-protein refers to the appearance in chloroform/methanol extracts of flour. These inhibitors are also referred to as "cereal-type" [2].

The primary target α-amylases have ≥35% sequence identity and similar three-dimensional structures with some differences in certain surface loops. Many different CM-proteins are found to be abundant in aqueous extracts of developing and mature barley seeds [37] and several are double-headed α-amylase/trypsin inhibitors [12–14,38,39] whereas others inhibit only α-amylase [40] or trypsin [3,41]. Recently limit dextrinase inhibitors belonging to the CM-proteins were purified from barley seeds [42,43], which are directed against the endogenous limit dextrinase that is synthesized during germination to debranch amylopectin for endosperm starch mobilisation. The limit dextrinase inhibitors have been addressed in this issue [44]. The CM-protein family furthermore includes lipid transfer proteins [45–47] and close relatives related to cold tolerance [48], as well as allergens, some of which cause baker's astma or dermatitis [25,49–53].

The double-headed 0.19 α-amylase inhibitor from wheat is acting as a homodimer [6,54], whereas wheat inhibitor 0.28 and the corresponding barley inhibitor BMAI-I are monomers [55]. Other inhibitors are active as heterooligomers [3]. Although wheat inhibitor 0.19 has broad specificity [2,6,56], the 0.53 inhibitor, which is also a homodimer [6], has 94% sequence identity with 0.19, but is specific for insect α-amylases [2,4,6]. The double-headed ragi α-amylase/trypsin inhibitor (RATI) of this family [14] was structure-determined in complex with yellow meal worm α-amylase (see below). Certain inhibitors are glycosylated, a property that has been associated with allergenicity [55,57] whereas a role of the carbohydrate moieties in enzyme inhibition remains to be demonstrated. A most recent dendrogram shows the sequence relationship of the CM-proteins among the small sulfur-rich seed proteins of the prolamin superfamily [25].

2.5. Kunitz-type

The capacity to inhibit subtilisin was earlier discovered for a barley protein [58] of sequence similarity to Kunitz soybean trypsin inhibitor [59]. This barley protein was later identified in complex with an endogenous α-amylase and hence named α-amylase/subtilisin inhibitor (BASI) [5,8]. Homologous proteins with 92% and 58% sequence identity are present in wheat (WASI) [15] and rice (RASI) [16], respectively. The ASIs have around 25% sequence identity with Kunitz trypsin inhibitors [59] and furthermore share structural similarity, without having sequence identity, with members of a hyperfamily of proteins sharing only the β-trefoil fold [26]. The β-trefoil fold proteins are characteristic for being involved in protein–protein interactions. A review in this issue [60] addresses BASI that specifically inhibits barley α-amylase 2 (AMY2) with $K_i = 0.22$ nM [61]. BASI also shows isozyme specific binding to AMY2 as demonstrated by using surface plasmon resonance [62]. A dendrogram has been calculated and is presented (Fig. 1) for the Kunitz inhibitor part of the β-trefoil fold family as this has not been previously available for BASI and related proteins. Clearly the vast majority of the related sequences are serine protease inhibitors, but the different clusters or isolated branches in the dendrogram include storage proteins, tumor-related protein, water-soluble chlorophyll proteins, drought-induced protein, a fucosidase, a biotic cell-death related protein, and a cysteine protease inhibitor (Fig. 1).

2.6. Thaumatin-like inhibitors

Zeamatin from maize inhibits insect, but not mammalian α-amylases. It is a homologue of the sweet protein thaumatin [2,29,63], however, thaumatin and other related proteins do not inhibit α-amylases. Proteins of this family are grouped in pathogen-related group 5 (PR-5) and alter the properties of fungal cell walls. Zeamatin thus binds to β-1,3-glucan and permeabilizes fungal cells resulting in cell death, and has been applied in antifungal drugs [2,64].

2.7. Lectin-like inhibitors

αAI1 and αAI2 are α-amylase inhibitors from common white, red and black kidney beans [4,27,65]. Three inhibitors are encoded by two different alleles, and only αAI1 inhibits both mammalian and insect α-amylases whereas αAI2 inhibits different insect α-amylases [2]. They belong to a lectin-arcelin-αAI1 supergene family exhibiting high degree of sequence similarity; proteolytic processing of homodimers to acquire the subunit composition $\alpha_2\beta_2$ is a prerequisite for inhibitory activity [27,66]. The evolution of the proteins in this family has been illustrated by dendrograms [27,66] and a chimera with a γ subunit has been found as an intermediate between arcelin and the inhibitor [67]. Posttranslational processing also includes both proteolytic trimming of polypeptide chain ends and glycosylation [27,68].

2.8. Designer inhibitors

In two cases, de novo design and engineering were combined to create novel proteinaceous α-amylase inhibitors. First, phage display and selection by biopanning using PPA as target enzyme involved randomization at 11 positions in a 36-amino-acid-residue CBD of the knottin family. The CBD variants contained substitutions in three areas with concomitant loss of cellulose binding ability. Two of the variants binding to PPA have affinity in the micromolar range as judged from surface plasmon resonance analysis [22].

The second approach consisted in immunisation of dromedary with PPA and subsequent phage display after cloning of the antigen binding repertoire of the heavy chain antibodies, VHH, characteristic of camelids. After three rounds of biopanning, several PPA binders were identified. Three were selected for structure determination and produced in recombinant His-tagged forms [23]. One

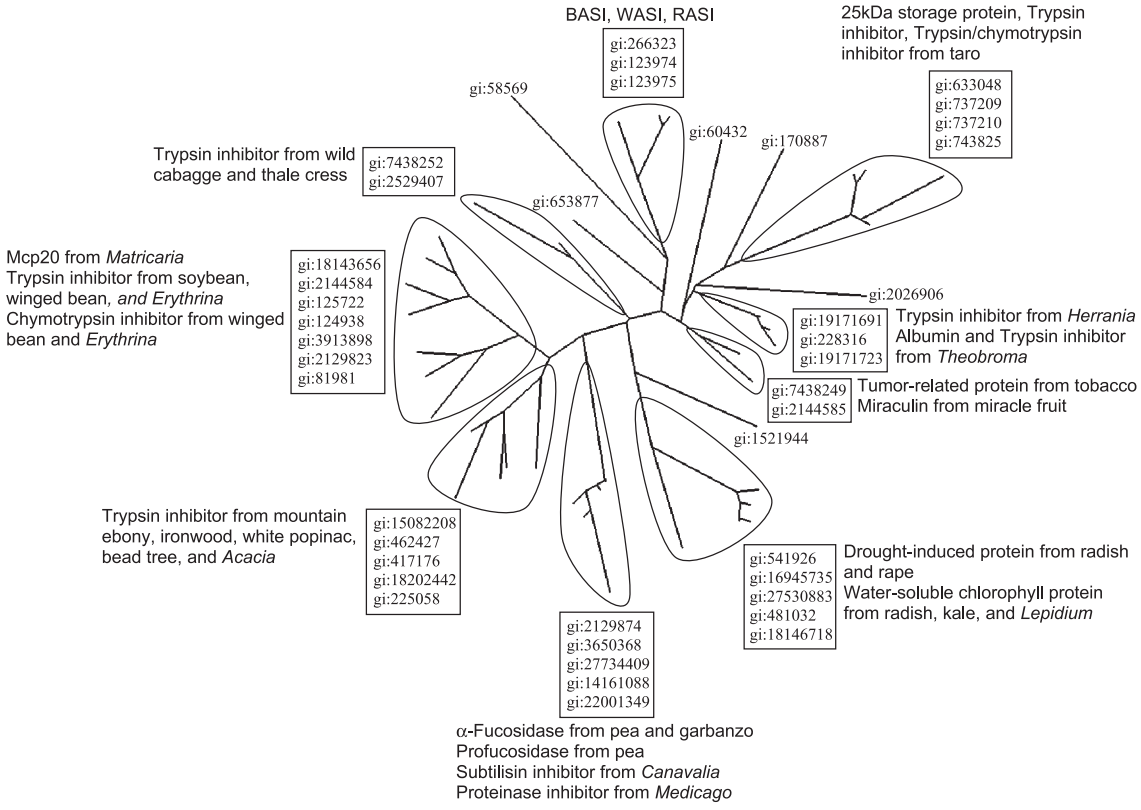

Fig. 1. Dendrogram of Kunitz soybean trypsin inhibitors and related proteins. Based on the maximum likelihood method, a dendrogram of Kunitz soybean trypsin inhibitors and related proteins was generated by the ProML software (http://evolution.genetics.washington.edu/phylip.html). Changes between amino acids were estimated by the Jones–Taylor–Thornton probability model. Each entry is represented by the National Center for Biotechnology Information (http://www.ncbi.nlm.nih.gov/) gi identifier as follows (biological source organisms are in parentheses): gi:266323, α-amylase/subtilisin inhibitor RASI (*Oryza sativa*); gi:123974, α-amylase/subtilisin inhibitor BASI (*Hordeum vulgare*); gi:123975, endogenous α-amylase/subtilisin inhibitor WASI (*Triticum aestivum*); gi:604320, sporamin (*Ipomoea batatas*); gi:1708872, latex serine proteinase inhibitor (*Carica papaya*); gi:633048, 25-kDa storage protein (*Colocasia esculenta*); gi:737209, trypsin inhibitor:ISOTYPE=b (*C. esculenta*); gi:737210, trypsin inhibitor:ISOTYPE=a (*Cyrtosperma chamissonis*); gi:7438250, trypsin/chymotrypsin inhibitor (*Alocasia macrorrhizos*); gi:20269067, protease inhibitor (*Sesbania rostrata*); gi:19171691, trypsin inhibitor (*Herrania albiflora*); gi:228316, albumin (*Theobroma cacao*); gi:19171723, trypsin inhibitor (*Theobroma microcarpum*); gi:7438249, tumor-related protein clone NF34 (*Nicotiana tabacum*); gi:2144585, miraculin (*Richadella dulcifica*); gi:15219441, protease inhibitor Dr4 (*Arabidopsis thaliana*); gi:541926, drought-induced 22K protein (*Raphanus sativus*); gi:16945735, water-soluble chlorophyll protein (*R. sativus* var. *niger*); gi:27530883, water-soluble chlorophyll protein (*Brassica oleracea var. Acephala*); gi:481032, drought-induced protein BnD22 (*Brassica napus*); gi:18146718, water-soluble chlorophyll protein (*Lepidium virginicum*); gi:2129874, α-fucosidase (*Pisum sativum*); gi:3650368, profucosidase (*P. sativum*); gi:27734409, subtilisin inhibitor CLSI-II/CLSI-III (*Canavalia lineata*); gi:14161088, α-fucosidase (*Cicer arietinum*); gi:22001349, proteinase inhibitor 20 (*Medicago truncatula*); gi:15082208, trypsin inhibitor (*Bauhinia variegata*); gi:462427, trypsin inhibitor (*Acacia confusa*); gi:417176, kunitz-type trypsin inhibitor (*Prosopis juliflora*); gi:18202442, kunitz-type trypsin inhibitor LlTI (*Leucaena leucocephala*); gi:225058, trypsin isoinhibitor DE5 (*Adenanthera pavonina*); gi:18143656, Mcp20 (*Matricaria chamomilla*); gi:2144584, trypsin inhibitor A (*Glycine max*); gi:125722, kunitz-type trypsin inhibitor KTI1 (*G. max*); gi:124938, trypsin inhibitor 1A (*Psophocarpus tetragonolobus*); gi:3913898, trypsin inhibitor DE-3 (*Erythrina variegata*); gi:2129823, chymotrypsin inhibitor ECI (*E. variegata*); gi:81981, chymotrypsin inhibitor WCI-x (*P. tetragonolobus*); gi:7438252, trypsin inhibitor (*B. oleracea*); gi:25294075, trypsin inhibitor T18K17.7 (*A. thaliana*); gi:6538778, biotic cell death-associated protein (*Nicotiana glutinosa*); gi:585699, cysteine protease inhibitor 9 (*Solanum tuberosum*).

bound at the PPA active site cleft and two outside of the substrate binding region. The former had IC_{50} of 10 nM, and biosensor measurements gave K_d of 3.5 nM for this VHH, and 7- and 70-fold poorer affinity for the other two (Table 1).

3. High-resolution structures of inhibitors and inhibitor/enzyme complexes

The three-dimensional structures of plant proteinaceous α-amylase inhibitors are addressed elsewhere in this issue [69]. Briefly, structures of enzyme/inhibitor complexes are available for five different types of inhibitors (Fig. 2). Remarkably, the way the inhibitors interact with the three catalytic acid groups of the enzymes shows enormous variation. First of all, binding between the inhibitor and the catalytic site of the enzyme can be either through direct hydrogen bonds or through hydrogen bonds via a water network or a water molecule. One case involves a fully hydrated Ca^{2+} at the protein interface. Finally, two of the five inhibitor types exert substrate mimicry. Various characteristic structural features of the enzyme–inhibitor complexes are summarized in Table 2.

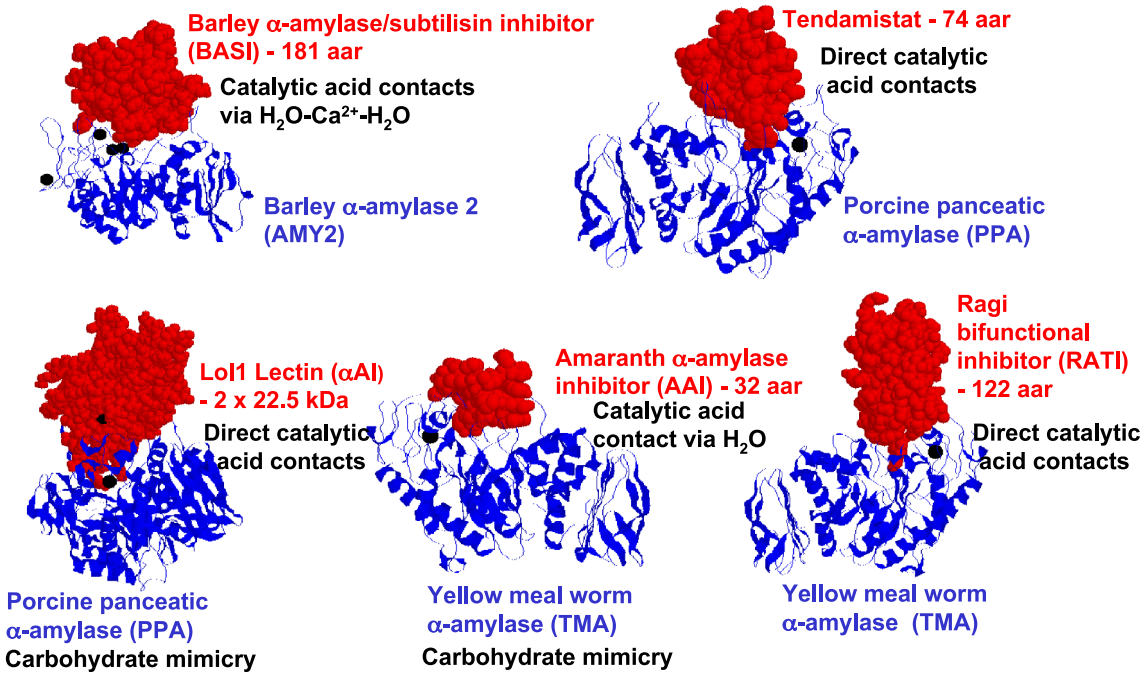

Fig. 2. Diversity in α-amylase/α-amylase inhibitor complexes as shown by examples on all structure-determined types. Calcium is shown as black spheres. The figure was constructed by RasMol Version 2.6 (http://www.umass.edu/microbio/rasmol/) using the protein database entries 1AVA (barley α-amylase 2/BASI), 1BVN (PPA/tendamistat), 1DHK (PPA/bean lectin-like inhibitor), 1CLV (TMA/amaranth inhibitor), and 1TMQ (TMA/RATI).

3.1. Tendamistat

The structure of free tendamistat was determined by both NMR spectroscopy and crystallography [70,71]. A disulfide-stabilized β-turn, earlier identified as the enzyme binding site of tendamistat and Arg19 from a conserved tripeptide Trp18–Arg19–Tyr20 at the tip of this β-turn, was suggested to be involved in the mechanism of inhibition [31]. Thus, in the complex with PPA a strong electrostatic contact is formed between Glu233 OE2 and Glu233 OE1 of the catalytic proton donor and tendamistat Arg19 NH1 and Arg19 NH2, respectively [34]. No direct contact was seen to the other two catalytic carboxyl groups in PPA [34]. Arginine salt-bridge(s) to one or more catalytic acid(s) recur(s) in other α-amylase/inhibitor complexes [24,72].

Table 2
Inhibitors and α-amylase/inhibitor complex structures

Inhibitor	Free inhibitor	α-Amylase complex	Catalytic residue contacts and comments	Interface (Å^2)	Substrate mimicry
Tendamistat	NMR [70], X-ray [71]	PPA/tendamistat [34]	Inhibitor Arg19 forms salt-bridge to Glu233, the catalytic proton donor. No inhibitor bonds to the other two catalytic acids	1330[a]	No
AAI	NMR synthetic [9] NMR natural [73]	TMA/AAI [35]	AA1 Arg7 and Tyr28 are in water-mediated contact with the proton donor and the catalytic nucleophile in TMA, the third catalytic acid makes a salt-bridge to AAI Arg7	2085	Yes
SIα1	NMR [83]	n.d.			
RATI from *Ragi* 0.19 from wheat	X-ray [76] X-ray [54]	TMA/RATI [74]	RATI Ser1 N, O, Oγ hydrogen bonds with the catalytic proton donor, nucleophile, and the third catalytic acid	2404	No
BASI	n.d.	Barley AMY2/BASI [77]	Inhibitor side chains E168 and Tyr170 are in contact with the three catalytic acids via a fully hydrated Ca^{2+} network	2345	No
WASI	X-ray [78]				
Zeamatin	X-ray [84]	n.d.			
αAI1 from bean	n.d	PPA/αAI1 [72], TMA/αAI [80], HPA/αAI [82]	αAI1 Tyr186, Tyr37, Tyr190 are hydrogen bonding with the catalytic proton donor, nucleophile, and the third catalytic acid, respectively	3050	Yes
Dromedary anti-PPA		PPA/AMD9 [23]	No hydrogen bond with catalytic acids, but stacking with aromatic active site groups	2259	No

[a] Sum for contact residues [34].

3.2. AAI

The structure was determined of the knottin miniprotein AAI from amaranth by NMR spectroscopy on a synthetic [9] and a natural protein [73]. This revealed that a *cis*-proline present only in the natural inhibitor [73] may be important by restricting the conformation of the inhibitor also in the enzyme complex [24]. Hydrogen exchange studies showed that only three residues in AAI were not exposed to solvent, which reflects the high conformational flexibility of the free inhibitor [24]. In the crystal structure of the complex with the target enzyme, α-amylase from yellow meal worm (*Tenebrio molitor*, TMA), the inhibitor blocks the central four subsites of the substrate binding groove in TMA. At the protein interface, the enzyme segment Thr291–Ser294 undergoes a dramatic conformational change and two of the inhibitor side chains are reoriented. One of the catalytic acids, Asp287, forms a strong salt-bridge with Arg7 of the inhibitor, whereas the two other catalytic acids are connected to the Arg7 side chain via an intricate water-mediated hydrogen-bond network [35]. The AAI *cis*-proline is found in the structure of the TMA complex and the inhibitor exerts substrate mimicry [35].

3.3. CM-proteins

The structure of RATI, an α-amylase/trypsin inhibitor from ragi, has been solved in complex with TMA [74]. This reveals that the N-terminal segment Ser1–Ala11 points into the enzyme active site groove. Ser1 makes several hydrogen bonds with Asp185 and Glu222, two of the three catalytic acids, while Val2 and Ser5 from the inhibitor interact with the third catalytic acid, Asp287. To gain insight into the target enzyme specificity of different inhibitory CM-proteins from wheat, modelling was performed using the RATI/TMA complex. The modelled complexes provide support for the finding that wheat inhibitors of even 98% sequence identity can have different specificity and biochemical properties [6]. Related proteins have been reported from barley [4,13,37,49,55]. The NMR structure of RATI [75] varies at the N-terminal region from the crystal structure [76] as found also by superpositioning of the crystal structure of the complex, indicating lack of conformational change for free and bound RATI [74]. Trypsin binding involves Arg34, which is situated on the opposite site of the RATI molecule [76]. The crystal structure was determined of the free 0.19 α-amylase inhibitor from wheat [54] and several related non-inhibitory proteins in this family were also structure-determined [25].

3.4. ASIs

Structures have been solved of a number of β-trefoil fold proteins, albeit for BASI only in complex with the target enzyme barley α-amylase 2 [77]. The structures of the free inhibitor from wheat, WASI [78], and its complex with proteinase K [79] are also solved. The AMY2/BASI complex contains a unique fully hydrated Ca^{2+} ion at the protein interface and two side chains from BASI hydrogen bond to one water molecule, whereas four other water molecules in the sphere, co-ordinated by the Ca^{2+}, are hydrogen bonded with the three catalytic acids [77]. The interaction of BASI with AMY2 covers a large surface area [77] involving distinct isozyme specific sites. BASI is reviewed elsewhere in this issue [60]. The protease site occurs in a specific surface loop on the other side of the BASI molecule as deduced from the structure of WASI in complex with proteinase K [79].

3.5. Lectin-like inhibitors

The structures of the $\alpha_2\beta_2$ heterotetrameric αAI1 in complex with PPA and TMA show two sites [72,80] that bind enzyme tightly [81]. αAI1 exerts substrate mimicry and interacts directly with the catalytic residues via hydrogen bonds. A more recent study of the complex with human pancreatic α-amylase (HPA) indicated that a flexible loop typical of mammalian α-amylases existed in two different conformations, suggesting a pH-dependent loop closure [82]. Moreover, Arg74 in αAI1 that interacts with a long loop in the enzyme adopts two different conformations in the HPA and the TMA complexes, respectively.

3.6. γ-Thionin SIα1 and zeamatin

For the two plant α-amylase inhibitors related to purothionin and thaumatin, structures were only solved of the free inhibitors, not of enzyme–inhibitor complexes [83,84].

3.7. Dromedary VHH

Three inhibitory engineered VHH antibodies bind to PPA, of these two bind outside of the active site, whereas the third and stronger binding VHH AMD9 interacts directly with the active site region. Arg59 from the inhibitor established strong contact with the indole ring of Trp59 PPA situated in the substrate binding site [23]. A similar stacking has been reported for the tendamistat complex with PPA [34].

4. Mechanism of inhibition, mutational analysis, protein engineering, designer inhibitors and mimetics

The inhibition kinetics has been described in highly varying detail for the different types of inhibitors. Three types of inhibitors, however, have been studied quite thoroughly; red kidney bean inhibitor (αAI) inhibiting PPA [65], BASI inhibiting AMY2 from barley [85] (covered elsewhere in this issue [60]), and wheat inhibitor 0.19 acting on a *Bacillus subtilis* α-amylase [56]. While K_i values are

reported for analogues of tendamistat [31], no K_i, $IC_{50,}$ or K_d values are available for AAI, SIα1, SIα2 and SIα3, and zeamatin.

4.1. Tendamistat

PPA and tendamistat form a very tight 1:1 complex as demonstrated kinetically [31,32] and by electrospray ionization mass spectrometry [86]. The K_i was 9 pM over a certain pH range [31]. Competition experiments with the pseudotetrasaccharide inhibitor acarbose demonstrated that tendamistat inhibits PPA with about 10^6-fold lower K_i than acarbose [31]. This is in agreement with independent measurements of the K_i for acarbose to be 1.7 μM [87]. A large number of peptides have been synthesized based on the structure and amino acid sequence of tendamistat. Some of these have been examined for protein structure and folding [88,89]. Others were made in attempts to generate enzyme inhibitors, e.g. depsipeptide mimetics of tendamistat having K_i values in the 30–390 μM range [90].

4.2. AAI

The type of inhibition and K_i values remain to be reported for the knottin type of inhibitor from amaranth, as only a functional concentration level of AAI has been indicated [9,91]. A series of synthetic analogues at different segments of the AAI structure were screened and scored for inhibition below a certain threshold as well as for folding [9]. This resulted in the N-terminal segment being identified as essential for inhibition. Further support for this conclusion was provided by formation of a chimera between a short N-terminal segment of AAI and Huwentoxin-I, a spider neurotoxin. Compared to AAI, the resulting chimeric knottin molecule showed significant, albeit weak, inhibition of insect α-amylase [9].

4.3. CM-proteins

The first assessment of the inhibition kinetics described the 0.19 and 0.53 wheat inhibitors acting on an α-amylase from *B. subtilis* [56]. A $K_d = 0.11$ nM was reported for the 0.53 inhibitor and 0.19 was described to be more efficient than the 0.53 inhibitor [56]. Whereas mutation of each of the three catalytic acids of the *Bacillus* α-amylase to the corresponding amides had only marginal effect on the binding of the inhibitors, substitution of a histidine conserved in the α-amylase family and interacting with substrate at subsite +1 [92], reduced the affinity for the 0.19 and 0.53 inhibitors by 13- and 25-fold, respectively [56]. A similar study, however, has not been conducted using insect target enzymes of the two wheat inhibitors [2,4].

RATI from ragi exhibited purely competitive inhibition with $K_i = 15$ nM for PPA catalyzed hydrolysis of the poor substrate 4-nitrophenylmaltoside [93]. By using the superior substrates 4-nitrophenylmaltoheptaoside and starch, the mode of inhibition became complex and depended on the substrate concentration. This was moreover complicated by the inhibitor being bound to the starch substrate. However, by assessing the amount of RATI that binds to substrate and correction of the activity data, the inhibition was shown to be competitive with $K_i = 0.1$ nM [93]. Synthetic peptides of the RATI N-terminal segment gave K_i in the range 140 – 1610 μM for all three substrates. A peptide composed of RATI residues 1–9 was a slightly superior inhibitor than peptides corresponding to either seven or eleven N-terminal residues. Substitution of the N-terminal serine in RATI by alanine reduced K_i of the synthetic heptapeptide from around 300 to 1600 μM, and blocking the N-terminal α-amino group in this peptide by an Fmoc group caused complete loss of inhibitory activity [93]. These results are in agreement with Ser1 playing a very important role in the interaction with the target enzyme as evident from the crystal structure of RATI/TMA [74]. Earlier site-directed insertion mutagenesis of the 0.28 monomeric wheat inhibitor (WMAI-1), another CM-protein family member, surprisingly showed structural changes at position 1 or 4 to reduce, but not completely destroy the ability to inhibit [12]. However, insertion of different segments at positions 4 or 58 in WMAI-1 led to complete inactivation of the inhibitor [12].

4.4. Kunitz-type

The K_i was 0.22 nM for BASI acting on barley AMY2 [61], while WASI was less potent [15], and RASI even less so for plant α-amylase [94]. A fast and tight simple two-step mechanism was determined for the binding of BASI to AMY2 [85]. The structural basis of the inhibition and the contribution of individual residues in both the target enzyme [95] and the inhibitor [62,96] have been addressed by structure-guided site-directed mutagenesis and monitored by inhibition kinetics and surface plasmon resonance measurements. Furthermore, preliminary changes of target enzyme specificity have been obtained by rational protein engineering of both the barley α-amylase [95] and BASI [96]. More details on BASI are given elsewhere in this issue [60].

4.5. Lectin-like inhibitor

A detailed analysis of the kinetics of inhibition of the red kidney bean inhibitor αAI acting on PPA indicated a two-step non-competitive slow, tight binding mechanism with a $K_d = 31$ μM for the first binding step and an overall $K_i = 30$ pM [65]. In this PPA/αAI complex the active site of the enzyme was available for catalysis. A recent study of the same system demonstrated that two inhibitor binding sites were present both on free PPA and in a PPA–substrate complex [97]. The mechanism of inhibition was found to be mixed non-competitive and the formation of both the EI and ESI complexes was slow and required preincubation for

efficient inhibition [97]. The kinetics of αAI inhibition of PPA is described in detail elsewhere in this issue [98]. Remarkably, the crystal structure of PPA/αAI has two PPA molecules bound to the homodimeric αAI [72] and this 2:1 stoichiometry was also found in solution [81]. A major difference from the inhibition kinetics study was an inhibitor to enzyme ratio of 1–2 used in crystallisation as opposed to a ≥100 excess of inhibitor used for the enzyme inhibition measurements. This may explain why the kinetics analysis gave two inhibitor binding sites per molecule of PPA [97]. A chimera of αAI1 that contains an α, a β, and a γ-subunit, of which the latter corresponds to a subunit in an α-amylase inhibitor-like protein, which is an evolutionary intermediate between arcelin and αAI1, was without inhibitory activity [67].

Arg74, Trp188, and Tyr190 of αAI were suggested based on mutagenesis to be involved in the inhibitory site and creating a triad of Trp, Arg, and Tyr, reminiscent of the sequential triade present at the active site of tendamistat [99]. Subsequent three-dimensional structure analysis showed, however, that Tyr190 interacted with one of the catalytic groups, whereas Arg74 and Trp188 had no contact with the enzyme [72].

4.6. Designer inhibitors and mimetics

The binding mechanism of the CBD-derived PPA inhibitors was not described; however, increasing concentration (5 nM–500 μM) of the pseudotetrasaccharide acarbose, a PPA inhibitor [87], was capable of suppressing the formation of the complex between CBD variants and PPA [22]. The crystal structure and functional analysis of the three dromedary VHHs that inhibit PPA indicated interaction with three different epitopes on the enzyme, and it was proposed that different enzyme inhibition modes may apply to the formation of the three different complexes [23].

4.7. γ-Thionin and thaumatin

No kinetics analysis or protein engineering has been conducted on α-amylase inhibitors from the γ-thionin and thaumatin families, for which also enzyme complexes remain to be structure-determined.

4.8. Bifunctional proteins

The ASIs of the Kunitz soybean trypsin inhibitor family and many inhibitors of the CM-protein family are double-headed. While the CM-proteins are targeted to exogenous proteins typically from insects, but also from microorganisms, and mammals and different types of joint specificities occur, two of the ASIs, BASI and WASI, act on a specific endogenous α-amylase iozyme and proteases of the subtilisin family in both cases with subnanomolar affinity. RASI, however, acts on insect α-amylase and subtilisin [16]. The ternary complex containing BASI, subtilisin, and barley α-amylase 2 has been reported in solution [8]. Although no crystal structures are available of ternary complexes, since BASI in complex with barley α-amylase 2 [77] and WASI in complex with proteinase K [79] are both determined, it is possible to build a model of the ASI-ternary complex. For the CM-protein inhibitors RATI in complex with TMA is available, however, a complex with a target protease was not reported although the structural determinants for both enzymes have been assessed by model building starting with the bifunctional corn Hageman factor inhibitor [100].

A different dual function has been proposed in a preliminary study of a protein prepared from Job's tears (*Coix lachrymal-jobi*) that specifically acts on insect α-amylase and has a weak endochitinase activity. The partial protein sequence shows similarity to wheat germ agglutinin, but the inhibitory potency remains to be assessed for highly purified protein [101].

5. Application of inhibitors as insecticides and impact of inhibitors in nutrition, health, and disease

A range of biotechnological applications of α-amylase inhibitors has been addressed elsewhere in this issue [102] as are the potential physiological roles of the inhibitors in plants [103]. Experiments conducted, in which certain α-amylase inhibitors were demonstrated to act as insecticides, are of particular agronomical relevance. Concerns on the application of transgenic plants producing inhibitors include potential unwanted effects on non-target organisms such as man and animals, the stability of the transgenic inhibitor to the host plant environment, and the ability of transgene seeds to germinate without the transgenic inhibitor influencing endogenous α-amylases. (for a recent review see Ref. [2]).

Certain plant α-amylase inhibitors have been demonstated to have adverse effect in nutrition (antinutrients) due to their inhibition of digestive enzymes in man and animals [1,4,7,104–106]. The inhibitors have also been proposed for application in obesity and diabetes therapy [3,7]. Gurmarin, a knottin related to the amaranth α-amylase inhibitor, although not reported to be an α-amylase inhibitor, has been used in folkloric treatement of diabetes [107]. Other inhibitors, e.g. corn Hageman factor inhibitor, is developed for utilization of its protease inhibitor specificity on Factor VIIa [100]. Moreover, several inhibitors of the CM-protein family have been associated with allergies [25,51–53] perhaps elicited by carbohydrate moeities [55,57]. These studies took advantage of available recombinant CM-proteins (Ref. [53] and references therein). Food allergens, despite the harsh conditions in the alimentary tract, retain sufficient structural integrity to be taken up by the gut and sensitize the mucosal immune system [108], a behaviour also associated with certain CM-proteins. Finally, some proteins which are evolutionarily related to the inhibitors of the different families and from the same biological sources as the inhibitors have

been reported to be toxic. This may complicate both the application of the inhibitors in therapy as well as the identification of the agent exerting the negative effects.

6. Conclusion and future prospects

The present review has addressed all of those inhibitor classes for which function is proven for a purified thoroughly characterized molecular form. The vast knowledge on proteinaceous α-amylase inhibitors spans from high-resolution crystal structures of their complexes with target enzymes to effects as antinutrients on animals and humans. The understanding across the entire range of properties between these two extremes focuses on (i) the covalent structure of variants and posttranslationally processed forms and the relation between structure and function, including target enzyme specificity; (ii) the reaction mechanism and the kinetics of inhibition; (iii) evolutionary relationships; (iv) rational engineering and generation of designer inhibitors; (v) applications in plant defence, obesity and diabetes therapy.

Most probably, new classes of inhibitors are still to be discovered. It would be very useful if a database for plant α-amylase inhibitors and their genes was established. A database, PLANT-PIs, is thus available for protease inhibitors [41]. This database currently comprises 10 families, of which two are relevant to the field of α-amylase inhibitors: (i) cereal trypsin/α-amylase inhibitors and (ii) soybean trypsin inhibitors (Kunitz) http://bighost.area.ba.cnr.it/PLANT-PIs).

Acknowledgements

This work was supported by the EU project GEMINI (QLK-2000-0081).

References

[1] J.R. Whitaker, α-Amylase inhibitors of higher plants and microorganisms, in: J.E. Kinsella, W.G. Soucie (Eds.), Proc. Protein Co-prod. Symp., Am. Oil Chem. Soc., Champaign, IL, 1988, pp. 354–380.
[2] O.L. Franco, D.J. Rigden, F.R. Melo, M.F. Grossi-de-Sà, Plant α-amylase inhibitors and their interaction with insect α-amylases. Structure, function and potential for crop protection, Eur. J. Biochem. 269 (2002) 397–412.
[3] F. Garcia-Olmedo, G. Salcedo, R. Sanchez-Monge, L. Gomez, J. Royo, P. Carbonero, Plant proteinaceous inhibitors of proteinases and α-amylases, Oxford Surv. Plant Mol. Cell Biol. 4 (1987) 275–334.
[4] M.F. Ho, F.F. Yin, F. Lajolo, J.R. Whitaker, Naturally occurring α-amylase inhibitors: structure/function relationships, in: R.Y. Yada, R.L. Jackman, J.L. Smith (Eds.), Protein Structure–Function Relationships in Foods, Blackie Academic & Professional, London, 1994, pp. 89–119.
[5] R.J. Weselake, A.W. MacGregor, R.D. Hill, An endogenous α-amylase inhibitor in barley kernel, Plant Physiol. 72 (1983) 809–812.
[6] O.L. Franco, D.J. Ridgen, F.R. Melo, C. Bloch Jr., C.P. Silva, M.F. Grossi de Sa, Activity of wheat α-amylase inhibitors toward bruchid α-amylases and structural explanation of observed specificities, Eur. J. Biochem. 267 (2000) 2166–2173.
[7] P. Layer, G.L. Carlson, E.P. DiMagno, Partially purified white bean amylase inhibitor reduces starch digestion in vitro and inactivates intraduodenal amylase in humans, Gastroenterology 88 (1985) 1895–1902.
[8] J. Mundy, I. Svendsen, J. Hejgaard, Barley α-amylase/subtilisin inhibitor. Isolation and characterization, Carlsberg Res. Commun. 48 (1983) 81–90.
[9] S. Lu, P. Deng, X. Liu, J. Luo, R. Han, X. Gu, S. Liang, X. Wang, F. Li, V. Lozanov, A. Patthy, S. Pongor, Solution structure of the major α-amylase inhibitor of the crop plant amaranth, J. Biol. Chem. 274 (1999) 20473–20478.
[10] A.L. Chagolla-Lopez, A. Blanco-Labra, A. Patthy, R. Sanchez, S. Pongor, A novel α-amylase inhibitor from Amaranth (*Amaranthus hypochondriacus*) seeds, J. Biol. Chem. 269 (1994) 23675–23680.
[11] C. Bloch Jr., M. Richardson, A new family of small (5 kD) protein inhibitors of insect α-amylase from seeds of sorghum (*Sorghum bicolor* (L.) Moench) have sequence homologies with wheat γ-purothionins, FEBS Lett. 279 (1991) 101–104.
[12] F. Garcia-Maroto, P. Cabonero, F. Garcia-Olmedo, Site-directed mutagenesis and expression in Escherichia coli of WMAI-1, a wheat monomeric inhibitor of insect α-amylase, Plant Mol. Biol. 17 (1991) 1005–1011.
[13] D. Barber, R. Sanchez-Monge, E. Mendez, A. Lazaro, F. Garcia-Olmedo, G. Salcedo, New α-amylase and trypsin inhibitors among the CM-proteins of barley (*Hordeum vulgare*), Biochim. Biophys. Acta 869 (1986) 115–118.
[14] F.A.P. Campos, M. Richardson, The complete amino acid sequence of the bifunctional α-amylase/trypsin inhibitor from seeds of ragi (Indian finger millet, *Eleusine coracana* Gaertneri), FEBS Lett. 152 (1983) 300–304.
[15] J. Mundy, J. Hejgaard, I. Svendsen, Characterization of a bifunctional wheat inhibitor of endogenous α-amylase and subtilisin, FEBS Lett. 167 (1984) 210–214.
[16] K.-I. Ohtsubo, M. Richardson, The amino acid sequence of a 20 kDa bifunctional subtilisin/α-amylase inhibitor from bran of rice (*Oryza sativa* L.) seeds, FEBS Lett. 309 (1992) 68–72.
[17] A. Blanco-Labra, F.A. Iturbe-Chinas, Purification and characterization of an α-amylase inhibitor from maize (*Zea mays*), J. Food Biochem. 193 (1980) 1–12.
[18] J.J. Marshall, C.M. Lauda, Purification and properties of phaseolamine, an inhibitor of α-amylase, from the kidney bean, *Phaseolus vulgaris*, J. Biol. Chem. 250 (1975) 8030–8037.
[19] M.F. Ho, J.R. Whitaker, Purification and some physical properties of red kidney bean (*Phaseolus vulgaris*) α-amylase inhibitors from two experimental cultivars, J. Food Biochem. 17 (1993) 15–33.
[20] A.M. Fakhoury, C.P. Wolosuk, Inhibition of growth of *Aspergillus flavus* and fungal alpha-amylases by a lectin-like protein from *Lablab pupureus*, Mol. Plant-Microb. Interact. 14 (2001) 955–961.
[21] S. Murao, A. Goto, Y. Matsui, K. Ohyama, New proteinous inhibitor (Haim) of animal α-amylase from *Streptomyces griseosporeus* YM-25, Agric. Biol. Chem. 44 (1980) 1679–1681.
[22] J. Lehtiö, T.T. Teeri, P.-Å. Nygren, Alpha-amylase inhibitors selected from a combinatorial library of a cellulose binding domain scaffold, Proteins 41 (2000) 316–322.
[23] A. Desmyter, S. Spinelli, F. Payan, M. Lauwereys, L. Wyns, S. Muyldermans, C. Cambillau, Three camelid VHH domains in complex with porcine pancreatic α-amylase, J. Biol. Chem. 277 (2002) 23645–23650.
[24] O. Carugo, S. Lu, J. Luo, X. Gu, S. Liang, S. Strobl, S. Pongor, Structural analysis of free and enzyme-bound amaranth α-amylase inhibitor: classification within the knottin fold superfamily and analysis of its functional flexibility, Protein Eng. 14 (2001) 639–646.

[25] P.R. Shewry, F. Beaudoin, J. Jenkins, S. Griffith-Jones, E.N.C. Mills, Plant protein families and their relationships to food allergy, Biochem. Soc. Trans. 30 (2002) 906–909.
[26] S.R. Brych, S.I. Blaber, T.M. Logan, M. Blaber, Structure and stability effects of mutations designed to increase the primary sequence symmetry within the core region of a β-trefoil, Protein Sci. 10 (2001) 2587–2599.
[27] S.-C. Lee, P.L. Gepts, J.R. Whitaker, Protein structures of common bean (*Phaseolus vulgaris*) α-amylase inhibitors, J. Agric. Food Chem. 50 (2002) 6618–6627.
[28] A. Vigers, W. Roberts, C.P. Selitrennikoff, A new family of plant antifungal proteins, Mol. Plant-Microb. Interact. 4 (1991) 315–323.
[29] M. Bruix, M.A. Jimeniz, J. Santoro, C. Gonzáles, F.J. Colilla, E. Méndez, M. Rico, Solution structure of γ1-H and γ1-P thionins from barley and wheat endosperm determined by ^{1}H-NMR: a structural motif common to toxic arthropod proteins, Biochemistry 32 (1993) 715–724.
[30] F. Sparvoli, C. Lanave, A. Santucci, R. Bollini, L. Lioi, Lectin and lectin-related proteins in Lima bean (*Phaseolus lunatus* L.) seeds: biochemicals and evolutionary studies, Plant Mol. Biol. 45 (2001) 587–597.
[31] L. Vértesy, V. Oeding, R. Bender, K. Zepf, G. Nesemann, Tendamistat (HOE 467), a tight-binding α-amylase inhibitor from *Streptomyces tendae* 4158, Eur. J. Biochem. 141 (1984) 505–512.
[32] S. Murao, N. Oouchi, A. Goto, M. Arai, New proteinous α-amylase inhibitor (Paim) from *Streptomyces corchorushii*, Agric. Biol. Chem. 47 (1983) 453–454.
[33] O. Hoffman, L. Vértesy, G. Braunitzer, The primary structure of α-amylase inhibitor Z-2685 from *Streptomyces parvullus* FH-1641, Biol. Chem. 366 (1985) 1161–1168.
[34] G. Wiegand, O. Epp, R. Huber, The crystal structure of porcine pancreatic α-amylase in complex with the microbial inhibitor Tendamistat, J. Mol. Biol. 247 (1995) 99–110.
[35] P.J. Barbosa Pereira, V. Lozanov, A. Patthy, R. Huber, W. Bode, S. Pongor, S. Strobl, Specific inhibition of insect α-amylases: yellow meal worm α-amylase in complex with *Amaranth* α-amylase inhibitor at 2.0 Å resolution, Structure 7 (1999) 1079–1088.
[36] G. Nitti, S. Orrù, C. Bloch Jr., L. Morhy, G. Marino, P. Pucci, Amino acid sequence and disulfide-bridge pattern of three α-thionins from *Sorghum bicolor*, Eur. J. Biochem. 228 (1995) 250–256.
[37] C. Finnie, S. Melchior, P. Roepstorff, B. Svensson, Proteome analysis of grain filling and seed maturation in barley, Plant Physiol. 129 (2002) 1308–1319.
[38] A. Lyons, M. Richardson, A.S. Tatham, P.R. Shewry, Characterization of homologous inhibitors of trypsin and the α-amylase, Biochim. Biophys. Acta 915 (1987) 305–313.
[39] S. Alagiri, T.P. Singh, Stability and kinetics of a bifunctional amylase/trypsin inhibitor, Biochim. Biophys. Acta 1203 (1993) 77–84.
[40] J. Iulek, O.L. Franco, M. Silva, C.T. Slivinski , C. Bloch Jr., D.J. Rigden, M.F. Grossi de Sa, Purification, biochemical characterization and partial primary structure of a new α-amylase inhibitor from *Secale cereale* (rye), Int. J. Biochem. Cell Biol. 32 (2000) 1195–1204.
[41] F. De Leo, M. Volpicella, F. Licciulli, S. Liuni, R. Gallerani, L.R. Ceci, PLANT-PIs: a database for plant protease inhibitors and their genes, Nucleic Acids Res. 30 (2002) 347–348.
[42] L.J. Macri, A.W. MacGregor, S.W. Schroeder, S.L. Bazin, Detection of limit dextrinase inhibitor in barley, J. Cereal Sci. 19 (1993) 103–106.
[43] E.A. MacGregor, S.L. Bazin, E.W. Ens, J. Lahnstein, L.J. Macri, N.J. Shirley, A.W. MacGregor, Structural models of limit dextrinase inhibitors from barley, J. Cereal Sci. 31 (2000) 79–90.
[44] E.A. MacGregor, The proteinaceous inhibitor of limit dextrinase in barley and malt, this issue.
[45] B. Svensson, K. Asano, I. Jonassen, F.M. Poulsen, J. Mundy, I. Svendsen, A 10 kD barley seed protein homologous with an α-amylase inhibitor from Indian finger millet, Carlsberg Res. Commun. 51 (1986) 493–500.
[46] J.-C. Kader, Lipid-transfer proteins in plants, Annu. Rev. Plant Physiol. Plant Mol. Biol. 47 (1996) 627–654.
[47] M.H. Lerche, F.M. Poulsen, Solution structure of barley lipid transfer protein complexed with palmitate. Two different binding modes of palmitate in the homologous maize and barley nonspecific lipid transfer proteins, Protein Sci. 7 (1998) 2490–2498.
[48] D.K. Hincha, Cryoprotectin: a plant lipid-transfer protein homologue that stabilizes membranes during freezing, Philos. Trans. R. Soc. Lond., B 357 (2002) 909–916.
[49] G. Garcia-Casado, A. Armentia, R. Sanchez-Monge, L.M. Sanchez, C. Lopez-Otin, G. Salcedo, A major baker's asthma allergen from rye flour is considerably more active than its barley counterpart, FEBS Lett. 364 (1995) 36–40.
[50] J.W. Park, D.B. Kang, C.W. Kim, S.H. Soh, H.Y. Yum, K.E. Kim, C.S. Hong, K.Y. Lee, Identification and characterization of the major allergens of buckwheat, Allergy 55 (2000) 1035–1041.
[51] M. Kusaba-Nakayama, M. Ki, M. Iwamoto, R. Shibata, M. Sato, K. Imaizumi, CM3, one of the wheat alpha-amylase inhibitor subunits, and binding of IgE in sera from Japanese with atopic dermatitis related to wheat, Food Chem. Toxicol. 38 (2000) 179–185.
[52] R. Nakamura, T. Matsuda, Rice allergenic protein and molecular-genetic approach for hyperallergenic rice, Biosci. Biotechnol. Biochem. 60 (1996) 1215–1221.
[53] M. Kusaba-Nakayama, M. Ki, E. Kawada, M. Sato, I. Ikeda, T. Mochizuki, K. Imaizumi, Intestinal absorbality of wheat allergens, subunits of a wheat alpha-amylase inhibitor, expressed in bacteria, Biosci. Biotechnol. Biochem. 65 (2001) 2448–2455.
[54] Y. Oda, T. Matsunaga, K. Fukuyiama, T. Miyasaki, J.T. Morimoto, Tertiary and quarternary structures of 0.19 α-amylase inhibitor from wheat determined by X-ray analysis at 2.06 Å resolution, Biochemistry 36 (1997) 13503–13511.
[55] R. Sanchez-Monge, L. Gomez, D. Barber, C. Lopez-Otin, A. Armentia, G. Salcedo, Wheat and barley allergens associated with baker's asthma. Glycosylated subunits of the α-amylase inhibitor family have enhanced IgE-binding capacity, Biochem. J. 281 (1992) 401–405.
[56] K. Takase, Site-directed mutagenesis reveals critical importance of the catalytic site in binding of α-amylase by wheat proteinaceous inhibitor, Biochemistry 33 (1994) 7925–7930.
[57] G. Garcia-Casado, R. Sanchez-Monge, M.J. Chrispeels, A. Salcedo, G. Salcedo, L. Gómez, Role of complex asparagine-linked glycans in allergenicity of plant glycoproteins, Glycobiology 6 (1996) 471–477.
[58] M.T. Yoshikawa, T. Iwasaki, M. Fujii, M. Oogaki, Isolation and some properties of a subtilisin inhibitor from barley, J. Biochem. (Tokyo) 79 (1976) 765–773.
[59] S. Onesti, P. Brick, D.M. Blow, Crystal structure of a Kunitz-type trypsin inhibitor of *Erythrina caffra* seeds, J. Mol. Biol. 217 (1991) 153–176.
[60] P.K. Nielsen, B.C. Bønsager, K. Fukuda, B. Svensson, Barley α-amylase/subtilisin inhibitor: structure, biophysics and protein engineering, Biochim. Biophys. Acta, this issue.
[61] J. Abe, U. Sidenius, B. Svensson, Arginine is essential for the α-amylase inhibitory activity of the α-amylase/subtilisin inhibitor (BASI) from barley seeds, Biochem. J. 293 (1993) 151–155.
[62] P.K. Nielsen, B.C. Bønsager, C.R. Berland, B.W. Sigurskjold, B. Svensson, Kinetics and energetics of the binding between barley α-amylase/subtilisin inhibitor and barley α-amylase 2 analyzed by surface plasmon resonance and isothermal titration calorimetry, Biochemistry 42 (2003) 1478–1487.
[63] R. Schmioler-O'Rourke, M. Richardson, C.P. Selitrennikoff, Zeamatin inhibits trypsin and α-amylase activities, Appl. Environ. Microbiol. 67 (2001) 2365–2366.
[64] W.K. Roberts, C.P. Selitrennikoff, Zeamatin, an antifungal protein

from maize with membrane-permeabilizing activity, J. Gen. Microbiol. 136 (1990) 1771–1778.
[65] E.R. Wilcox, J.R. Whitaker, Some aspects of the mechanism of complexation of red kidney bean α-amylase inhibitor and α-amylase, Biochemistry 23 (1984) 1783–1791.
[66] T.E. Mirkov, J.M. Wahlstrom, K. Hagiwara, F. Finardi-Filho, S. Kjemtrup, M.J. Chrispeels, Evolutionary relationships among proteins in the phytohemagglutinin-arcelin-α-amylase inhibitor family of the common bean and its relatives, Plant Mol. Biol. 26 (1994) 1103–1113.
[67] S.-I. Wato, K. Kamei, T. Arakawa, J.S. Philo, J. Wen, S. Haram, H. Yamaguchi, A chimera-like α-amylase inhibitor suggesting the evolution of *Phaseolus vulgaris* α-amylase inhibitor, J. Biochem. 128 (2000) 139–144.
[68] N.M. Young, P. Thibault, D.C. Watson, M.J. Chrispeels, Post-translational processing of two alpha-amylase inhibitors and arcelin from the common bean, *Phaseolus vulgaris*, FEBS Lett. 446 (1999) 203–206.
[69] F. Payan, Structural basis for the inhibition of mammalian and insect α-amylases by plant protein inhibitors, this issue.
[70] A.D. Kline, W. Braun, K. Wüthrich, Studies by ^{1}H nuclear magnetic resonance and distance geometry of solution conformation of the α-amylase inhibitor tendamistat, J. Mol. Biol. 189 (1986) 377–382.
[71] J.W. Pflugrath, G. Wiegand, R. Huber, L. Vértesy, Crystal structure determination, refinement and the molecular model of the α-amylase inhibitor Hoe-467A, J. Mol. Biol. 189 (1986) 383–386.
[72] C. Bompard-Gilles, P. Rousseau, P. Rougé, F. Payan, Substrate mimicry in the active centre of a mammalian α-amylase: structural analysis of an enzyme inhibitor complex, Structure 4 (1996) 1441–1452.
[73] J.C. Martins, M. Enassar, R. Willem, J.-M. Wieruzeski, G. Lippens, S.J. Wodak, Solution structure of the main α-amylase inhibitor from amaranth seeds, Eur. J. Biochem. 268 (2001) 2379–2389.
[74] S. Strobl, K. Maskos, G. Wiegand, R. Huber, F.X. Gomis-Rüth, R. Glockshuber, A novel strategy for inhibition of α-amylases: yellow meal worm (α-amylase in complex with the *Ragi* bifunctional inhibitor at 2.5 Å resolution, Structure 6 (1998) 911–921.
[75] S. Strobl, P. Mühlhahn, R. Berbstein, R. Wiltscheck, K. Maskos, M. Wunderlich, R. Huber, R. Glockshuber, T.A. Holak, Determination of the three dimensional structure of the bifunctional α-amylase/trypsin inhbitor from Ragi seeds by NMR spectroscopy, Biochemistry 34 (1995) 8281–8293.
[76] S. Gourinath, N. Alam, A. Srinivasan, Ch. Betzel, T.P. Singh, Structure of the bifunctional inhibitor of trypsin and α-amylase from ragi seeds at 2.2 Å resolution, Acta Crystallogr. D56 (2000) 287–293.
[77] F. Vallée, A. Kadziola, Y. Bourne, M. Juy, K.W. Rodenburg, B. Svensson, R. Haser, Barley α-amylase inhibitor bound to its endogenous protein inhibitor BASI: crystal structure of the complex at 1.9 Å resolution, Structure 6 (1998) 649–659.
[78] K.J. Zemke, A. Müller-Farhnow, K.-D. Jany, G.P. Pal, W. Saenger, The three dimensional structure of the bifunctional proteinase K/α-amylase inhibitor from wheat (PKI3) at 2.5 Å resolution, FEBS Lett. 279 (1991) 240–242.
[79] G.P. Pal, C.A. Kavounis, K.-D. Jani, D. Tsernoglou, The three-dimensional structure of the complex of proteinase K with its naturally occurring inhibitor PKI3, FEBS Lett. 341 (1994) 167–170.
[80] V. Nahoum, F. Farisei, V. Le-Berre-Anton, M.P. Egloff, P. Rougé, E. Poerio, F. Payan, A plant-seed inhibitor of two classes of alpha-amylases: X-ray analysis of *Tenebrio molitor* larvae alpha-amylase in complex with the bean *Phaseolus vulgaris* inhibitor, Acta Crystallogr. D55 (1999) 360–362.
[81] K. Kasahara, K. Hayashi, T. Arakawa, J.S. Philo, J. Wen, S. Hara, H. Yamaguchi, Complete sequence, subunit structure and complexes with pancreatic α-amylase of an α-amylase inhibitor from *Phaseolus vulgaris* white kidney beans, J. Biochem. 120 (1996) 177–183.
[82] V. Nahoum, G. Roux, V. Anton, P. Rougé, A. Puigserver, H. Bischoff, B. Henrissat, F. Payan, Crystal structure of human pancreatic α-amylase in complex with carbohydrate and proteinaceous inhibitors, Biochem. J. 348 (2000) 201–208.
[83] C. Bloch Jr., S.U. Patel, F. Baud, M.J. Zvelebil, M.D. Carr, P.J. Sadler, J.M. Thornton, H-NMR structure of an antifungal γ-thionin protein SIα1: similarity to scorpion toxin, Proteins 32 (1998) 715–724.
[84] M.A. Batalia, A.F. Mozingo, S. Ernst, W. Roberts, J.D. Robertus, The crystal structure of the antifungal protein zeamatin, a member of the thaumatin-like, PR-5 protein-family, Nat. Struct. Biol. 3 (1996) 19–23.
[85] U. Sidenius, K. Olsen, B. Svensson, U. Christensen, Stopped-flow kinetics of the reaction of barley α-amylase/subtilisin inhibitor and the high pI barley α-amylase, FEBS Lett. 361 (1995) 250–254.
[86] D.J. Douglas, B.A. Collings, S. Numao, V.J. Nesatyy, Detection of noncovalent complex between α-amylase and its microbial inhibitor tendamistat by electrospray ionization mass spectrometry, Rapid Commun. Mass Spectrom. 15 (2001) 89–96.
[87] M. Alkazaz, V. Desseaux, G. Marchis-Mouren, F. Payan, E. Forest, M. Santimone, The mechanism of porcine pancreatic α-amylase. Kinetic evidence for two additional carbohydrate-binding sites, Eur. J. Biochem. 241 (1996) 787–796.
[88] F.J. Blanco, M.A. Jiménez, M. Rico, J. Santoro, J. Herranz, J.L. Nieto, Tendamistat (12–26) fragment. NMR characterization of isolated β-turn folding intermediates, Eur. J. Biochem. 200 (1991) 345–351.
[89] A.M. Bonvin, W.F. van Gunsteren, Beta-hairpin stability and folding: molecular dynamics studies of the first beta-hairpin of tendamistat, J. Mol. Biol. 296 (2000) 255–268.
[90] A.M. Sefler, M.C. Kozlowski, T. Guo, P.A. Bartlett, Design, synthesis, and evaluation of a depsipeptide mimic of tendamistat, J. Org. Chem. 62 (1997) 93–102.
[91] V. Lozanov, C. Guarnaccia, A. Patthy, S. Foti, S. Pongor, Synthesis and cystine/cysteine-catalyzed oxidative folding of the amaranth α-amylase inhibitor, J. Pept. Res. 50 (1997) 65–72.
[92] E.A. MacGregor, S. Janecek, B. Svensson, Relationship of sequence and structure to specificity in the α-amylase family of enzymes, Biochim. Biophys. Acta 1546 (2001) 1–20.
[93] N. Alam, S. Gourinath, S. Dey, A. Srinivasan, T.P. Singh, Substrate-inhibitor interaction in the kinetics of α-amylase inhibition by Ragi α-amylase/trypsin inhibitor (RATI) and its various N-terminal fragments, Biochemistry 40 (2001) 4229–4233.
[94] H. Yamagata, K. Kunimatsu, H. Kamasaka, T. Kuramoto, T. Iwasaki, Rice bifunctional α-amylase/subtilisin inhibitor: characterization, localization, and changes in developing and germinating seeds, Biosci. Biotechnol. Biochem. 62 (1998) 978–985.
[95] K.W. Rodenburg, F. Vallée, N. Juge, N. Aghajari, X.-J. Guo, R. Haser, B. Svensson, Specific inhibition of barley α-amylase 2 by barley α-amylase/subtilisin inhibitor depends on charge interactions and can be conferred to isozyme 1 by mutation, Eur. J. Biochem. 267 (2000) 1019–1029.
[96] B.C. Bønsager, P.K. Nielsen, M. Prætorius-Ibba, B. Svensson, Mutational analysis of the complex formation between barley α-amylase/subtilisin inhibitor and the target enzymes barley α-amylase 2 and savinase, submitted for publication.
[97] R. Koukiekolo, V. Le Berre-Anton, V. Desseaux, Y. Moreau, P. Rougé, G. Marchis-Mouren, M. Santimone, Mechanism of porcine pancreatic α-amylase. Inhibition of amylose and maltopentaose hydrolysis by kidney bean (*Phaseolus vulgaris*) inhibitor and comparison with that by acarbose, Eur. J. Biochem. 265 (1999) 20–26.
[98] M. Santimone, R. Koukiekolo, Y. Moreau, V. Le Berre, P. Rougé, G. Marchis-Mouren, V. Desseaux, Porcine pancreatic α-amylase inhibition by the kidney bean (*Phaseolus vulgaris*) inhibitor (α-II) and structural changes in the α-amylase inhibitor complex, Biochim. Biophys. Acta, this issue.
[99] T.E. Mirkov, S.V. Evans, J. Wahlstrom, L. Gomez, N.M. Young,

M.J. Chrispeels, Location of the active site of the bean α-amylase inhibitor and involvement of a Trp, Arg, Tyr triad, Glycobiology 5 (1995) 45–50.

[100] C.A. Behnke, V.C. Yee, I. Le Trong, L.C. Petersen, R.E. Stenkamp, S.-S. Kim, G.R. Reeck, D.C. Teller, Structural determinants of the bifunctional corn Hageman factor inhibitor: X-ray crystal structure at 1.95 Å resolution, Biochemistry 37 (1998) 15277–15288.

[101] M.B. Ary, M. Richardson, P. Shewry, Purification and characterization of an insect α-amylase inhibitor/endochitinase from seeds of Job's tears (*Coix lachryma-jobi*), Biochim. Biophys. Acta 999 (1989) 260–266.

[102] J.F. Sørensen, K.M. Kragh, O. Sibbesen, J. Delcour, H. Goesaert, B. Svensson, T.A. Tahir, Joachim Brufau, A.M. Perez-Vendrell, D. Bellincampi, R. D'Ovidio, L. Camardella, A. Giovane, E. Bonnin, N. Juge, Potential role of glycosidase inhibitors in industrial biotechnological applications, Biochim. Biophys. Acta, this issue.

[103] D. Bellincampi, L. Camardella, J.A. Delcour, V. Desseaux, R. D'Ovidio, A. Durand, G. Elliot, K. Gebruers, A. Giovane, N. Juge, J.F. Sørensen, B. Svensson, D. Vairo, Potential physiological role of plant glycosidase inhibitors, Biochim. Biophys. Acta, this issue.

[104] A. Pusztai, G.G. Bardocs, R. Alonso, M.J. Chrispeels, H.E. Tabe, L.M. Tabe, T.J. Higgins, Expression of the insecticidal bean alpha-amylase inhibitor transgene has minimal detrimental effect on the nutritional value of peas fed to rats at 30% of the diet, J. Nutr. 139 (1999) 1597–1603.

[105] K. Kataoka, E.P. DiMagno, Effect of prolonged intraluminal alpha-amylase inhibition on eating, weight, and the small intestine of rats, Nutrition 15 (1999) 123–129.

[106] H. Yoshikawa, M. Kotaru, C. Tanaka, T. Ikeuchi, M. Kawabata, Characterization of kintoki bean (*Phaseolus vulgaris*) alpha-amylase inhibitor: inhibitory activities against human salivary and porcine pancreatic alpha-amylases and activity changes by proteolytic digestion, J. Nutr. Sci. Vitaminol. 45 (1999) 797–802.

[107] T. Imoto, A. Miyasaka, R. Ishima, K. Akasaka, A novel peptide isolated from the leaves of *Gymnema sylvestre*: I. Characterization and its suppressive effect on the neural responses to sweet taste stimuli in the rat, Comp. Biochem. Physiol. 100 (1991) 309–314.

[108] G.R. Burnett, M. Wickham, A. Fillery-Travis, J.A. Robertson, P.S. Gilbert, S.M. Gilbert, A.S. Tatham, P.R. Shewry, E.N.C. Mills, Interaction between protein allergens and model gastric emulsions, Biochem. Soc. Trans. 30 (2002) 916–918.

Appendix 5 – Paper 2

B.C. Bønsager, C. Finnie, P. Roepstorff, B. Svensson. Spatio-temporal changes in germination and radical elongation of barley seeds tracked by proteome analysis of dissected embryo, aleurone layer and endosperm tissues. Submitted to Proteomics.

Spatio-temporal changes in germination and radical elongation of barley seeds tracked by proteome analysis of dissected embryo, aleurone layer and endosperm tissues

Birgit C. Bønsager[1,2], Christine Finnie[1,2], Peter Roepstorff[3] and Birte Svensson[1,2]*

[1]*Carlsberg Laboratory, Gamle Carlsberg Vej 10, DK-2500 Valby Copenhagen, Denmark*

[2]*Enzyme and Protein Chemistry, BioCentrum-DTU, Technical University of Denmark, Søltofts Plads, Bldg 224, DK-2800 Kgs. Lyngby, Denmark*

[3]*Department of Biochemistry and Molecular Biology, University of Southern Denmark, Campusvej 55, DK-5230 Odense, Denmark*

*Corresponding Author: Birte Svensson, Enzyme and Protein Chemistry, BioCentrum-DTU, Søltofts Plads, Building 224, Technical University of Denmark, DK-2800 Kgs. Lyngby, Denmark. bis@biocentrum.dtu.dk, Fax: +45 4588 6307

Abbreviations: ABA: abscisic acid; APX: ascorbate peroxidase; cCBB: colloidal Commassie Brilliant Blue; EST: expressed sequence tag; GA: gibberellic acid; GSH: glutathione; HSP: heat shock protein; JIP: jasmonate-induced protein; LEA protein: late embryogenesis abundant protein; PDI: protein disulfide isomerase; PI: post imbibition; PMF: peptide mass fingerprint; ROS: reactive oxygen species; sHSP: small heat shock protein; TC: tentative consensus

Keywords: spatio-temporal proteomics; 2-dimensional gel electrophoresis; seed tissue dissection; protein categories; barley (*Hordeum vulgare*)

Abstract

Germination of barley is accompanied by changes in water soluble seed proteins. 2-DE was used to describe spatio-temporal proteome differences in dissected seed tissues associated with germination and the subsequent radicle elongation. Protein identification by mass spectrometry enabled assignment of proteins and functions to the seed embryo, aleurone, and endosperm. Abundance in 2-DE patterns was monitored for 48 different proteins appearing in 79 gel spots at 8 time-points up to 72 h post imbibition (PI). In embryo a β-type proteasome subunit and a heat shock protein 70 fragment were among the earliest proteins to appear (at 4 h PI). Other early changes were observed that affected spots containing desiccation stress-associated late embryogenesis abundant and abscisic acid induced proteins. From 12 h PI proteins characteristic for desiccation stress disappeared rapidly, as did a putative embryonic protein and an abscisic acid induced protein, suggesting that these proteins are also involved in desiccation stress. Several redox-related proteins differed in spatio-temporal patterns at the end of germination and onset of radicle elongation. Notably, ascorbate peroxidase that was observed only in the embryo, increased in abundance at 36 h PI. The surprisingly early changes seen in the protein profiles already 4 h after imbibition indicate that germination is programmed during seed maturation.

1 Introduction

Seed germination starts with water uptake by the quiescent dry seed, terminates with extension of the embryonic axis 24-36 h after imbibition (PI) [1], and is followed by radicle elongation. Upon imbibition, metabolic activity in the seed rapidly increases. Enzymes and cellular structures required for resumption of metabolism are assumed to be synthesized during grain filling and be present in the mature seed, having survived the desiccation process [2]. Early events after the start of imbibition correspond to the steeping process of industrial malting.

The embryo, starchy endosperm (referred to as endosperm in this work), and aleurone layer of the barley seed each host processes required for germination and radicle elongation. Metabolic activity needed for cell growth is immediately resumed by embryo and aleurone cells upon imbibition. The embryo synthesizes the phytohormone gibberellic acid (GA) inducing *de novo* synthesis of hydrolytic enzymes in the aleurone layer, of which α-amylase is the most abundant [3]. These enzymes mobilize storage reserves in the endosperm for growth of the embryonic axis [4, 5]. The endosperm is dead tissue, while aleurone cells are non-dividing and eventually undergo programmed cell death [6-8].

Germination in Arabidopsis was recently described using 2-DE, including identification of 39 proteins that changed in abundance during 24 h PI, which were involved in cell cycle activities and mobilization of protein and lipid reserves [9]. Extensive microarray analysis of transcriptome changes during germination in barley [10, 11] and wheat [12, 13] revealed significant transcription to take place at 18-24 h PI. Surprisingly, less than 60 genes respond specifically to GA in the barley aleurone layer

during germination [14]. In Arabidopsis the role of GA during germination seems to be softening of the seed coat prior to penetration of the radicle [15].

Descriptions of the barley seed protein 2-DE profiles were presented in the early nineties [16, 17]. More recently, 2-DE in conjunction with MS identified about 260 soluble proteins in 450 spots from developing, mature and germinating barley seeds [18-22]. Efficient and reproducible extraction of proteins from small amounts of dissected seed tissues was also established [23]. In the present work, proteome changes associated with the early stages of germination and radicle elongation are described for dissected embryo, endosperm, and aleurone tissues, using 2-DE and MS. In addition, embryos isolated from dry seeds were germinated on water/agar plates to evaluate the impact on the germination process of the surrounding tissues. The results are discussed with regard to the biological roles of the tissues and compared with proteome and cDNA microarray analyses of developing and germinating barley seeds [10, 11, 18-22]. This approach provides novel information on spatio-temporal changes in 79 identified spots representing 48 different gene products, occurring during seed germination and radicle extension.

2 Materials and Methods

2.1 Preparation of plant material and extracts

Seeds from the malting barley cultivar Barke (2002 harvest) were provided by Sejet Plantbreeding. Only five seeds were used for the small scale extractions and since germination of a batch cereal seeds is not strictly synchronous, special care was taken to characterize the seed material used. Germination efficiency and homogeneity were determined by a preliminary test where 100 seeds in 9 cm Petri dishes were incubated

with 4 mL tap water at 20°C in the dark (standard germination conditions according to European Brewing Convention). After 24 h and 48 h, 88.3% and 99.3% of the seeds germinated, respectively, corresponding to a germination index of 8.87 [24, 25]. A germination index above 7 is required for malting barley [24, 25], thus the seeds were considered to be of sufficient quality for the analysis. Portions of hundred seeds (germinated at 15°C as in related studies [20-22]) were frozen in liquid nitrogen at 4, 12, 24, 36, 52, 60, and 72 h PI and stored at -80°C until use. Five seeds from each time-point were selected based on visual homogeneity of germination and dissected prior to extraction of proteins in 5 mM Tris-HCl, pH 7.5, 1 mM $CaCl_2$ as described [23]. Protein extracts were stored at -80°C. Protein concentrations were determined by the Popov assay [26] using bovine serum albumin as a standard.

2.2 2-D gel electrophoresis

For each time-point 40 µg (embryo and aleurone layer) or 80 µg protein (endosperm) was precipitated from extracts by addition of 4 volumes of acetone at -20°C for > 24 h. Precipitated proteins were redissolved in reswelling buffer (8 M urea, 2% (w/v) CHAPS, 0.5% (v/v) IPG buffer 4-7 (GE Healthcare), 20 mM DTT and a trace of bromophenol blue) and the first dimension IEF was run on 18 cm IPG strips with a linear gradient of pH 4-7 using an IPGphor (GE Healthcare) [18]. The IPG strips were soaked (20 min) in equilibration buffer (50 mM TrisHCl pH 8.8, 6 M urea, 30% (v/v) glycerol, 2% (w/v) SDS and a trace bromophenol blue) containing 10 mg/mL DTT followed by incubation (20 min) in equilibration buffer containing 25 mg/mL iodoacetamide. The second dimension SDS-PAGE (12-14%, 18 × 24 cm, GE Healthcare) was run on a Multiphor

(GE Healthcare) according to the manufacturer's recommendations and stained with either silver nitrate [27] or cCBB [28].

2.3 Analysis of 2-D gels

2-D gels from the 8 time points (see 2.1) were compared manually for each tissue. The reproducibility was ensured by 2-3 replicates (with freshly prepared extract for each replicate) and through the comparison of 8 close time-points. The large number of time-points ensured confident and consistent appearance profiles for each spot analyzed during the process. Spots that appeared to be constant at all time-points served as markers for relative intensity, i.e. # 220 and # 103, both of which contain superoxide dismutase and # 95 containing triose phosphate isomerase (Fig. 1). Spots judged by this procedure to be increasing or decreasing in abundance during 0-72 h PI were excised from cCBB stained gels, digested in-gel with sequence-grade trypsin (Promega) [18, 29] and identified by MS.

2.4 Mass spectrometric protein identification

Tryptic digests were analyzed by MALDI-TOF-MS (Voyager DE-STR mass spectrometer; Applied Biosystems Inc. or Bruker Ultraflex I). The MS data were processed using the software programs m/z (ProteoMetrics) for MS data and Data Explorer (Applied Biosystems, version 4.4) for MS/MS data. Proteins were identified by peptide mass mapping and searching the National Center for Biotechnology Information non-redundant database (NCBInr) and if necessary an EST database, using the internet version of the search engine MASCOT [30]. Most searches were carried out from November 2003 to October 2004 and the following parameters were set: taxonomy: viridiplantae; fixed modifications: carbamidomethyl cysteine; variable modifications:

oxidized methionine; peptide tolerance: 0.1 Da; up to one missed cleavage. For a positive identification, at least 5 matching peptides were required, together with a significant MASCOT score and a sequence coverage of at least 20% (see supporting information). Tentative consensus (TC) sequences of matched ESTs were found by searching the Institute for Genome Research (TIGR) barley (or in a few cases wheat) index (www.tigr.ord/tdb/hvgi). Proteins not identified by this approach were analyzed by MS/MS (Bruker Ultraflex I or II) to obtain peptide fragmentation data. In a few cases the MASCOT search results became significant when the ion score was included (see supporting information). A few identifications were carried out using Mascot server 2.1 and NCBInr downloaded in september 2006. Despite good quality MS data, protein identification was not always successful due to the limited number of barley protein sequences available in databases. Hence 37% of the protein identifications were achieved using EST information. Thirty-three unidentified MS spectra were subjected to a new search in July 2007 resulting in no additional identifications probably due to the limited increase in barley ESTs between 2004 (340.000) and 2007 (370.000).

3 Results

3.1 Barley seed material

The germination of the excellent malting barley cultivar Barke finished at 24-36 h PI where the radicle penetrated the seed coat and began to elongate. Visually homogeneous seeds were carefully selected at the 8 time points and dissected prior to protein extraction. Extraction conditions were chosen to enable comparison with previously published barley

seed proteome maps [20, 21] and to exclude storage proteins (i.e. hordeins) allowing enrichment for metabolically active proteins [20].

3.2 Comparison of 2-D gels and protein identification

Reproducibility of the 2-D gels was ensured by 2-3 replicates for each of the 8 time-points. The spot pattern for each tissue was recognized in previously published proteome maps of whole barley seeds [18-23], and these maps supported the spot recognitions and identifications. Due to the complex protein patterns, individual gel spots were followed at 8 time-points and compared between the tissues by manual overlay of gels. This enabled us to monitor changes in spot patterns of the individual spots during a series of gels over many time-points to ensure that the observations reflected real trends. A total of 48 proteins were identified in 79 selected spots of varying abundance (Table 1). In the first place 54 of these spot identifications were from previous work; however, in the present it was possible to obtain extra information about tissue distribution and appearance patterns during germination and radicle elongation. An additional 75 spots of decreasing or increasing abundance were selected and of these 25 were identified (see supplemental data). The relatively low success rate for identification was caused by the fact that the most abundant and readily identifiable proteins were already identified. Only identified protein spots were numbered and discussed below. The numbering is in accordance with previously published data on barley seed proteome maps [18-21; 23], however, in the present work the listing is according to functional categories (Table 1).

Tissue-specific functions in germination and radicle elongation could be inferred from spot changes occurring in only one or two of the three tissues. In total, changes were recorded for 44 spots from the embryo, 42 in aleurone, and 19 in the endosperm. Of

these changing spots 32 were shared by embryo and aleurone, 6 by embryo, aleurone and endosperm, and 10 changing spots were common to aleurone and endosperm. The temporal patterns however for these common changing spots mostly differed, the exceptions for embryo and endosperm being two of the five LEA protein entries, ABA-induced protein, 1-Cys peroxiredoxin, one of the sHSP entries, and the embryo specific protein (Table 1). One of the glyoxalase 1 fragment spots decreased with the same time profile in aleurone and endosperm, and finally one of the two thioredoxin 1 spots decreased at the same time in all three tissues. Selected individual spots will be further discussed (3.3 – 3.8).

3.3 Proteome changes in barley seed tissues

The 2-DE patterns revealed variation during germination (0-24 h) and radical elongation (24-72 h) for each of the tissues (Figs. 1 and 2; Table 1) reflecting intensive metabolic activity. Changes in spot patterns can be due to protein degradation and synthesis or post-translational modifications. Furthermore it is possible that some spots vary due to altered extractability of certain protein forms during the 72 h period.

The first new protein spot was observed at 4 h PI in the embryo 2D gel and contained a β-type proteasome subunit (Fig. 5; # 578). Its appearance was accompanied by increased intensity of a spot containing a heat shock protein 70 (HSP70) fragment (Fig. 4; # 603). This was followed by appearance of an α-type proteasome subunit at 24 h PI, coinciding with the end of germination (Figs. 1 and 4; # 602). Several early changes were moreover observed in the acidic area of the embryo 2D gels involving (LEA) proteins (Fig. 3A; # 572) and ABA-induced protein (Fig. 3A; # 576, 577). These spots were also present in aleurone layers prior to germination, but were absent in endosperm (Fig. 3B). Proteins

that decreased in abundance during germination included LEA proteins in six spots (Fig. 1; # 16, 254, 272, 441, 474 579) corresponding to five different gene products (Table 1), a putative embryonic protein (Fig. 4; # 573, 574, 575), glyoxalase 1 (Fig. 4; # 6, 468), GSH-dependent dehydroascorbate reductase (Fig. 1; # 294), aconitate anhydrase (Fig. 1; # 454, 455), transcription factor homolog BTF3-like protein (Fig. 5; # 601), and two fragments of aldose reductase (Fig. 5; # 100, 293). At 60 h PI a spot appears close to the position of spot # 601 (Fig. 5); however, this spot remains to be identified. All of these identified spots are either associated with desiccation, osmotic, salt or oxidative stresses, or belong to the citric acid cycle. Changes in spot pattern were also very significant and complex at the start of radicle elongation (24-36 h PI) and included a decrease in abundance of proteins involved in oxidative stress, glycolysis, citric acid cycle, protein translation or acting as chaperones (Table 1).

The greatest number of new spots appeared at 36-72 h PI. These included ascorbate peroxidase (APX; Fig. 5; # 79), jasmonate-induced protein (Fig. 5; # 370, 587), serine carboxypeptidase A1 (Fig. 4; # 593), α-amylase (Fig. 2B; # 352, 353, 355, 390), the serpin protein Z (Z4) (Fig. 2A; # 598, 599, 600), and fragments of HSP70 (Fig. 2; # 582), barley seed peroxidase 1 (Fig. 1; # 571; ref. 31), and aldose reductase (Fig. 2A; # 583), respectively. The appearance of these fragments indicated degradation of the corresponding full length proteins.

The identified proteins were categorized (Table 1) into five classes according to function; desiccation-, osmotic-, and salt stress (S (D)), oxidative stress (S (O)), protein synthesis, folding and storage (P), housekeeping (H), enzymes for storage compound degradation (E), and proteins with other or unknown function (U). Proteins in the same

functional class were often observed to share temporal profiles during germination and radicle elongation as discussed below (Table 1).

3.4 Desiccation stress related proteins

Initial changes observed at 4 h PI in embryo (Figs. 1 and 3) involved LEA and ABA-induced proteins, which are implicated in desiccation tolerance. The abundant LEA proteins were extensively degraded at 12 h PI resulting in very faint spots remaining after 36 h PI in embryo. These proteins occurred in lower amounts in aleurone (Fig. 3A and B). LEA proteins belong to the dehydrin superfamily and contain several phosphorylation sites [32] that can play a role in subcellular localization [33], binding and retention of specific targets [34], ion binding capacity and calcium-dependent chaperone functions [35, 36]. The shifts in spot position at 4 h PI may therefore reflect phosphorylation changes. However, it was not possible to assign pI changes to specific proteins as the complexity of the spot pattern made it unclear which of the protein spots shifted (Fig. 3A) and the MS provided insufficient sequence coverage to disclose modifications. Other spots share spatio-temporal appearance with LEA proteins, including two charge variants of ABA-induced protein (Fig. 3; # 576, 577) and three forms of embryonic cell protein that vary both in size and pI (Fig. 4; # 573, 574, 575). The function of these proteins is unknown, but their simultaneous disappearance with the LEA proteins indicates that they might play a role during desiccation. Finally, the cold regulated protein (Fig. 1; # 17) involved in desiccation stress [37] and found in both the embryo and aleurone 2D patterns, also decreased slightly after 4 h PI, but was still present 72 h PI.

Two forms of the highly abundant glyoxalase 1, slightly differing in pI, decreased in abundance in all three tissues during germination (Fig. 4; # 6, 468), albeit more slowly

in endosperm in which two additional spots containing glyoxalase I fragments appeared during radical elongation (Fig. 2; # 585, 586). Peptide mass data suggested that these five glyoxalase I forms stemmed from the same gene (Table 1) but the analysis did not allow identification of the cause for the varying molecular weight and pI. Glyoxalase I is involved in protection against cold, salt and desiccation stress [38, 39]. In contrast to the other desiccation stress-related proteins discussed here, glyoxalase 1 is abundant in the endosperm.

Aldose reductase is induced by ABA at the onset of desiccation in the embryo, where it plays a role in protection against osmotic stress [40]. Several aldose reductase fragments were observed in distinct spot patterns in embryo and aleurone layer 2D gels. Spots # 100 and # 293 (Fig. 5), found both in embryo and aleurone layer of non-germinated seeds, disappeared from the embryo spot pattern at 12-24 h PI. However, they increased in intensity in aleurone layer at 24-72 h PI and a third fragment of the same gene product also appeared (Fig. 2A; # 583). This suggested that degradation of aldose reductase occurred at different rates in embryo and in aleurone layer. Three full-length forms and one fragment of aldose reductase, all originating from the same gene, were identified in whole-seed extracts run on 2D gels covering the basic pH range 6-11 [22]. In agreement with the present data, the full-length forms decreased in intensity 72 h after imbibition while a spot containing a fragment increased [22].

3.5 Oxidative stress related proteins

Changes in oxidative stress-related proteins occurred with different spatio-temporal profiles in all three tissues (Table 1). Most of the changes in these protein spots were observed during radicle elongation, however, a low molecular weight form (presumably a

fragment) of GSH-dependent dehydroascorbate reductase showed an early decrease in abundance after 12 h PI in the aleurone layer and endosperm, and after 24 h PI in embryo (Fig. 1; # 294). Notable, the corresponding full length forms remained at a constant level in all tissues (Fig. 1; # 142).

APX, which reduces hydrogen peroxide using ascorbate as an electron donor [41], was found only in the embryo (Fig. 5; # 79). The same spot, however, was previously observed in the endosperm at the start of grain filling together with a second APX isoform [23]. The spots were not observed in mature barley seeds. This pattern for developing and germinating seeds agreed with previous studies showing that APX activity decreased during desiccation of cereal seeds [42, 43], which suggested that the ascorbate system was not involved in desiccation tolerance [44]. The level of an APX mRNA was up-regulated in embryo late in germination [10], in accordance with the present protein profile.

In the endosperm one spot containing superoxide dismutase decreased and another disappeared during germination (Fig. 2; # 301, 302, respectively). This protein form was not visible in 2D gels of embryo and aleurone layer. Two different superoxide dismutase-containing spots, however, remained constant up to 72 h PI in all tissues (Fig. 1 and 5; # 220, 103). Peroxiredoxin (Fig. 5; # 99, 104) decreased after 24 h PI and was only observed in embryo and aleurone layer gels. Three different forms of peroxiredoxin, displaying distinct temporal profiles in grain filling and desiccation, were previously analyzed in detail during barley seed development [19].

A probable fragment of barley seed peroxidase 1 was found in a single spot present in all seed tissues at 60 h PI, with an apparent molecular mass of 28.8 kDa, (Fig.

1; # 571). A full-length form of the same protein (36.1 kDa) was identified in whole seed extracts on 2D gels covering the basic pH range, among a total of 13 peroxidase spots representing three gene products [22, 31]. Glutathione reductase (Fig. 1; # 409) decreased slightly during radicle elongation (from 52 h PI) in embryo and aleurone and was not observed in endosperm.

Two thioredoxin h1 (Trx h1) and one thioredoxin h2 (Trx h2) spots were identified in all tissues [45]. Trx h1 (Fig. 1; # 296) was most abundant in embryo, and whereas it remained essentially constant in the three tissues, the other Trx h1 (Fig. 1; # 297) and the Trx h2 (Fig. 1; # 313) spot decreased in intensity in all tissues at radicle elongation. Trx h is proposed have a central role in germination by reducing disulfide bonds in endosperm storage proteins and small cysteine-rich proteins (e.g. hydrolase inhibitors) increasing their susceptibility to proteolytic breakdown [46].

3.6 Protein folding and storage

Five spots containing protein disulfide isomerase (PDI), four full length forms and two fragments of HSP70 and six spots containing various sHSPs were observed in all tissues and generally decreased in intensity at radicle elongation. The fastest loss occurred in the endosperm where PDI may serve as a storage protein. PDI was present throughout seed development, whereas HSP70 and sHSPs appeared during grain filling and after onset of desiccation, respectively [19]. sHSPs might act as molecular chaperones in seed dehydration and during the first few days of rehydration [47].

Serpin Z4 was identified in the endosperm of the non-germinated seed and in three intense spots appearing after 52 h PI (Fig. 2; # 598, 599, 600). After imbibition

protein Z is released from a bound form by cysteine proteases [48]. The very high abundance in the endosperm suggests that protein Z has a role as a storage protein.

3.7 Housekeeping proteins

Enzymes involved in glycolysis were present throughout germination, reflecting the high energy demand of this process, but decreased during radicle elongation. Strong expression of genes encoding enzymes of the pentose-phosphate pathway in germinating seeds was previously reported [49]. Full length enolase occurred in all three tissues in two or three isoforms, albeit less abundantly in the metabolically inactive endosperm. Enolase fragments appearing in embryo and aleurone (Fig. 1; # 581, 590, 591) suggested turnover of enolase although significant decrease of full length forms was not observed. Three spots (Fig. 1; # 143, 341, 341a) on gels from embryo and aleurone layer contained 2,3 bisphosphoglycerate-independent phosphoglycerate mutase encoded by two different genes. Spot # 341a decreased in abundance after 12 h and 52 h PI in the aleurone layer and embryo, respectively, # 341 decreased only in the aleurone layer at 52 h PI , whereas # 143 remained constant (Fig. 1). These three spots and an additional spot containing the same 2,3 bisphosphoglycerate-independent phosphoglycerate mutase gene product were previously reported to differ in temporal appearance in grain filling [19]. Aconitate hydratase (Fig. 1; # 454, 455) involved in the citric acid cycle and observed in embryo and aleurone layer gels, decreased during radicle elongation.

3.8 Enzymes degrading storage reserves

α-Amylase, the major starch degrading enzyme in barley seeds, was identified in the aleurone layer at 52 h PI in three spots and in the endosperm at 60 h PI in four spots (Fig. 2A and B). A few additional spots containing α-amylase fragments appeared in

endosperm gels after 72 h PI that were previously identified by western blotting and MS [50]. Carboxypeptidase 1A (Fig. 4; # 593) was found both in embryo and aleurone layer gels at 36 h and 52 h PI, respectively. According to cDNA microarray data, carboxypeptidase 1A is expressed in the scutellum and not the embryo [10], but these two tissues were not separated in the present work. Carboxypeptidase 1A catalyses release of amino acids for *de novo* protein synthesis and has been proposed as a marker for malting quality [51].

3.9 Germination of isolated embryos

The influence of aleurone layer and endosperm on germination was tested by germinating isolated embryos on agar plates. Comparison of 2-DE from embryos germinated in isolation and embryos dissected from germinating whole seeds showed degradation of LEA proteins to occur equally fast and APX (Fig. 6A) to appear at the same time and with the same intensity in the two samples. This suggests that the surrounding tissues do not significantly influence germination and that the embryo is self-sufficient until the GA-induced degradation of storage reserves at the radicle elongation [1]. The 2-DE patterns were also very similar at 72 h PI, although several spots in the high molecular weight area of gels from isolated embryos were slightly reduced in abundance in comparison with embryos dissected from the seeds after germination (Fig. 6B). Identification of the proteins in these spots was not successful. The presence of ABA during germination and radicle elongation seemed not to influence germination of isolated embryos, as the 2-DE patterns closely resembled those of embryos from germinated whole seeds (not shown). This suggests that ABA plays a minor role in the non-dormant seeds.

4 Discussion

The onset of many cellular processes in the quiescent barley seed upon imbibition gives rise to dramatic changes in the proteome. All components needed to resume metabolic activity are apparently present in a potentially active form in the dry mature seed [1], including mRNA, ribosomal proteins, initiation and elongation factors. Supporting evidence for this was recently obtained for Arabidopsis seeds that were able to germinate in the presence of the transcriptional inhibitor α-amanitin but not in the presence of the translational inhibitor cycloheximide [15]. Based on these findings, changes at the protein level may be expected to precede changes in the transcript profile. Barley embryos germinated in isolation from the rest of the seed gave similar 2-DE patterns to embryos dissected from germinated whole seeds 0-24 h PI, suggesting that changes in the embryo at the protein level are independent from the breakdown of storage products in the endosperm. The phytohormone GA induces expression of genes required for seedling growth rather than germination, supported by germination of GA-deficient Arabidopsis seeds [52] and their failure to complete seedling development. Recently, it was shown that relatively few genes are specifically up-regulated by GA in rice aleurone layers [14] suggesting that water uptake by the embryo is sufficient to induce genes required for germination.

During germination, many of the proteins observed to increase or decrease in abundance were related to changes in the desiccation state of the seeds, including loss of desiccation-related LEA proteins from embryo and aleurone layer. These proteins were suggested to be induced by the dormancy-promoting hormone ABA [53] and were

proposed to protect living tissues of the mature dry seeds by mimicking water molecules thus stabilizing proteins and the cell wall [54]. Notably, LEA proteins decreased under cold and drought stress in barley, maize, and Arabidopsis [55-57] and were shown to be involved in heat tolerance in wheat [58], Arabidopsis [59] and pea seeds [60].

During radicle elongation the seed seemed to respond to variations in oxidative, salt and osmotic stress as well as to changes in glycolysis, citric acid cycle, and hydrolysis of storage compounds. Rehydration of the seeds thus alters both water balance and ROS production and the living tissues – embryo and aleurone layer – respond to this by regulating stress protective enzymes. The present data show clearly that the regulation differs in the two tissues and may take place at the transcriptional, translational or post-translational level, giving rise to differences in the 2-DE patterns.

In the endosperm most changes occurred during radicle elongation where the tissue fulfills its function as a storage reserve mobilized by an array of hydrolases. PDI spots decreased rapidly and were among the soluble endosperm proteins to be degraded first, providing amino acids for seedling growth along with non-water-soluble storage proteins that were not monitored in the present study.

A number of proteins expected to vary during germination are involved in the cell cycle, translation, transcription, and metabolism of nutrients, and are of very low abundance preventing detection in 2-DE. Increases in levels of mRNA encoding such proteins were however reported to occur at the end of germination (18-24 h PI) based on cDNA microarray analysis, supporting the hypothesis that mRNAs required for germination are already present in the dry mature seed [10, 11]. These and newly synthesized mRNAs are likely to encode proteins essential for normal cellular

metabolism and not restricted to germination. The overlap between the transcriptome and proteome data was limited, preventing a comprehensive comparison. This in fact highlights the value of the proteomics study in providing complementary data.

In the case of APX, PDI, and HSP70 the proteome changes during germination and radicle elongation observed by 2-DE confirmed cDNA microarray data. Others were observed only by one of the techniques emphasizing the complementarity of proteome and transcriptome analyses. A strong advantage of 2-DE-based proteomics is the ability to distinguish between proteins in multiple 2-DE spots due to post-translational modification, closely related isoforms, or degradation. Proteome and transcriptome analyses have sometimes produced contrasting results e.g. for maize seeds undergoing cold germination and desiccation [56]. Protein spatio-temporal variation and cDNA microarray data for barley seed germination show examples both of contrasting and similar patterns of gene expression and protein appearance (Table 2). Two fragments of jasmonate-induced protein 23 (JIP-23) appeared at 52-72 h PI in embryo (Fig. 5) in agreement with four JIP-23 transcripts being up-regulated at 48 h PI in embryo [11]. While the protein spots, however, originated from the same gene, three additional transcripts of the JIP-23 gene family were induced with almost identical profiles [11].

Carboxypeptidase 1A (Fig. 4; # 593) appeared in embryo and aleurone 2-DE at 24 and 52 h PI, respectively, but the corresponding transcript was constant in embryo until 72 h PI and then up-regulated [10, 11]. This suggests that translation of the gene started soon after imbibition and that carboxypeptidase 1A protein would be expected to increase further in abundance after 72 h PI. The gene was preferentially expressed in scutellar epithelium [10], however, this tissue was included with the embryo, both in the present

and the cDNA moicroarray study [11]. An APX transcript found in scutullar epithelium [10] and embryo [10, 11] at 12-24 h PI agreed with the appearance of APX in the embryo 2D-gels at 36 h PI, although it is not known if the APX transcripts identified in these studies were the same and corresponded to the protein observed here.

Glutathione *S*-transferase, aconitate anhydrase, and a β-type proteasome subunit showed divergent protein and transcript profiles and tissue specificity during germination and radicle elongation (Table 2). Thus, as previously observed [61, 62], transcription and translation may not be directly coupled. Such differences could also be the consequence of using methods with different detection thresholds, preventing the simultaneous analysis of all protein and mRNA species from a tissue. Stability and turnover rate also affect protein abundance and clear evidence of protein turnover was provided here by identification of protein fragments. Contrasting results were also observed when comparing different sets of cDNA microarray data, e.g. for glutathione *S*-transferase (Table 2).

Concluding remarks: The present proteome analysis is a biologically important extension of previously published proteome maps of whole barley seeds. Small-scale protein extractions of dissected seed tissues at close time-points through germination and radicle elongation enabled the study of spatio-temporal changes in the protein appearance. Differences in appearance profiles of the proteins in the individual tissues suggested differential timing of the protein functions. Thus, ascorbate peroxidase seems to be an important enzyme only in the embryo during radicle elongation, whereas other redox-related enzymes seem to function also in the aleurone layer and to a lesser extent in the endosperm. The surprisingly early changes observed in the 2-D gels provide supporting

evidence for programming of germination during seed maturation so that the most necessary components, such as mRNA, are found in the dry mature seed prior to the onset of germination. Therefore *de novo* protein synthesis could occur concomitantly with mRNA synthesis at germination leading to the appearance of new proteins in the embryo proteome as soon as 4 h PI. Detection of these early events highlights the value of proteome analysis as a tool for investigation of the germination process.

Acknowledgements

Sejet Plantbreeding (Sejet, Denmark) is thanked for providing barley seeds. Jørgen Larsen and Ella Meiling (Carlsberg Research Laboratory) are thanked for advice regarding germination conditions, Andrea Lorentzen (University of Southern Denmark) for technical assistance with Voyager DE-STR and Bruker Ultraflex II. Birgit Andersen (BioCentrum-DTU) is thanked for technical assistance with the Bruker Ultraflex III. Torben Steenholdt is thanked for helpful discussion regarding protein identification. Carlsberg Laboratory and the Technical University of Denmark are acknowledged for two separate portions of the Ph.D. grant (BCB). The Danish Research Agency SUE programme and the Danish Agricultural and Veterinary Research Council are thanked for financial support.

5 References

1. Bewley, J. D., Black, M. *Seeds: Physiology and development of germination*. Plenum Publishing Corporation, New York, USA 1994, pp 147-197.

2. Bewley, J. D. Seed germination and dormancy. *Plant Cell* 1997, 9, 1055-1066.

3. Zentella, R., Yamauchi, D., Ho, T. D. Molecular dissection of the gibberellin/abscisic acid signaling pathways by transiently expressed RNA interference in barley aleurone cells. *Plant Cell* 2002, 14, 2289-2301.

4. Fincher, G. B. Molecular and cellular biology associated with endosperm mobilization in geminating cereal grain. *Annu. Rev. Plant Physiol. Plant Mol. Biol.* 1989, 40, 305-346.

5. Jones, R. L., Jacobsen, J. V. Regulation of synthesis and transport of secreted proteins in cereal aleurone. *Int. Rev. Cytol.* 1991, 126, 49-88.

6. Wang, M., Oppedijk, B., Lu, X., van Duijn, B., Schilperoort., R. A. Apoptosis in barley aleurone during germination and its inhibition by abscisic acid. *Plant Mol. Biol.* 1996, 32, 1125-1134.

7. Bethke, P., Lonsdale, J. E., Fath, A., Jones, R. L. Hormonally regulated programmed cell death in barley aleurone cells. *Plant Cell* 1999, 11, 1033-1046.

8. Fath, A., Bethke, P., Lonsdale, J., Meza-Romero, R., Jones, R. Programmed cell death in cereal aleurone. *Plant Mol. Biol*. 2000, 44, 255-266.

9. Gallardo, K. et al. Proteomic analysis of Arabidopsis seed germination and priming. *Plant Physiol.* 2001, 126, 835-848.

10. Potokina, E., Sreenivasulu, N., Altschmie, L., Michalek, W., Graner A. Differential gene expression during seed germination in barley (*Hordeum vulgare* L.). *Funct. Integr. Genomics* 2002, 2, 28-39.

11. Watson, L., Henry, R. J. Microarray analysis of gene expression in germinating barley embryos (*Hordeum vulgare* L.). *Funct. Integr. Genomics* 2005, 5, 155-162.

12. Wilson, I. D. et al. Alteration of the embryo transcriptome of hexaploid winter wheat (*Triticum aestivum* cv. Marcia) during maturation and germination. *Funct. Integr. Genomics* 2005, 5, 144-154.

13. Li-Pook-than, J., Carrillo, C., Bonen, L. Variation in mitochondrial transcript profiles of protein-coding genes during early germination and seedling development in wheat. *Curr. Genet*. 2004, 46, 374-380.

14. Bethke, P. C., Hwang Y., Zhu, T., Jones, R. L. Global patterns of gene expression in the aleurone of wild-type and *dwarf1* mutant rice. *Plant Physiol*. 2005, 140, 484-498.

15. Rajjou, L. et al. The effect of α-amanitin on the Arabidopsis seed proteome highlights the distinct roles of stored and neosynthesized mRNAs during germination. *Plant Physiol*. 2004, 143, 1598-1613.

16. Weiss, W., Postel, W., Görg, A. Barley cultivar discrimination: II. Sodium dodecyl sulfate-polyacrylamide gel electrophoresis and isoelectric focusing with immobilized pH gradients. *Electrophoresis* 1991, 12, 330-337.

17. Görg, A., Postel, W., Baumer, M., Weiss, W. Two-dimensional polyacrylamide gelelectrophoresis, with immobilized pH gradients in the first dimension, of barley seed proteins: discrimination of cultivars with different malting grades. *Electrophoresis* 1992, 13, 192-203.

18. Finnie, C., Melchior, S., Roepstorff, P., Svensson, B. Proteome analysis of grain filling and seed maturation in barley. *Plant Physiol*. 2002, 129, 1308-1319.

19. Finnie, C., Bak-Jensen, K. S., Laugesen, S., Roepstorff, P., Svensson, B. Differential appearance of isoforms and cultivar variation in protein temporal profiles revealed in the maturing barley grain proteome. *Plant Sci*. 2006, 170, 808-821.

20. Østergaard, O., Melchior, S., Roepstorff, P., Svensson, B. Initial proteome analysis of mature barley seed and malt. *Proteomics* 2002, 2, 733-739.

21. Østergaard, O., Finnie, C., Laugesen, S., Roepstorff, P., Svensson, B. Proteome analysis of barley seeds: Identification of major proteins from two-dimensional gels (pI 4-7). *Proteomics* 2004, 4, 2437-2447.

22. Bak-Jensen, K. S., Laugesen, S., Roepstorff, P., Svensson, B. Two-dimensional gel electrophoresis pattern (pH 6-11) and identification of water-soluble barley seed and malt proteins by mass spectrometry. *Proteomics* 2004, 4, 728-742.

23. Finnie, C., Svensson, B. Feasibility study of a tissue-specific approach to barley proteome analysis: aleurone layer, endosperm, embryo and single seeds. *J. Cereal Sci.* 2003, 38, 217-227.

24. Riis, P., Bang-Olsen, K. Germination profile – a new term in malting barley analyses. *Proceedings of the European Convention Congress* 1991, 23, 101-108.

25. Riis, P. Meiling, E., Peetz, J. Determination of germination index- collaborative trial and ruggedness testing. *J. Inst. Brew*. 1995, 101, 171-173.

26. Popov, N., Schmitt, M., Schulzeck, S., Matthies, H. Eine störungsfreie Mikromethode zur Bestimmung des Proteingehaltes in Gewebehomogenaten. *Acta Biol. Med. Ger.* 1975, 34, 1441-1446.

27. Heukeshoven, J., Dernick, R. Improved silver staining procedure for fast staining in PhastSystem Deveopment Unit. I. Staining of sodium dodecyl sulfate gels. *Electrophoresis* 1988, 9, 28-32.

28. Rabilloud, T., Chermont, S. In: Rabilloud, T. (Ed.) *Proteome Research: Two-Dimensional Gel Electrophoresis and Identification Methods*, Springer Verlag, Berlin, Heidelberg 2000, pp. 107-126.

29. Shevchenko, A., Wilm, M., Vorm, O., Mann, M. Mass spectrometric sequencing of proteins silver-stained polyacrylamide gels. *Anal. Chem*. 1996, 68, 850-858.

30. Perkins, D. N., Pappin, D. J., Creasy, D. M., Cottress, J. S. Probability-based protein identification by searching sequence databases using mass spectrometry data. *Electrophoresis* 1999, 20, 3551-3567.

31. Laugesen, S. et al. Barley peroxidase isozymes: Expression and post-translational modification in mature seed as identified by two-dimensional gel electrophoresis and mass spectrometry. Submitted to *Int. J. Mass Spectrom*., subject to minor revision.

32. Irar, S., Oliveira, E., Pagés, M., Godau, A. Towards the identification of late-embryonic abundant phosphoproteome in Arabidopsis by 2-DE and MS. *Proteomics* 2006, 6, S175-S185.

33. Jensen, A. B., Goday, A, Figueras, M., Jessop, A. C., Pages, M. Phosphorylation mediates the nuclear targeting of the maize Rab17 protein. *Plant J.* 1998, 13, 691-697.

34. Goday, A., Jensen, A. B., Culiáñez-Marciá, F. A. The maize abscisic acid-responsive protein Rab17 is located in the nucleus and interacts with nuclear localization signals. *Plant Cell* 1994, 6, 352-360.

35. Alsheikh, M. K., Heyen, B. J., Randall, S. K. Ion binding properties of the dehydrin ERD14 are dependent upon phosphorylation. *J. Biol. Chem*. 2003, 278, 40882-40889.

36. Heyen, B. J. et al. The calcium-binding activity of a vacuole-associated, dehydrin-like protein is regulated by phosphorylation. *Plant Physiol.* 2002, 130, 675-687.

37. Crosatti, C., Polverino de Laureto, P., Bassi, R., Cattivelli, L. The interaction between cold and light controls the expression of the cold-regulated barley gene

cor14b and the accumulation of the corresponding protein. *Plant Physiol*. 1999, 199, 671-680.

38. Johansen, K. S., Svendsen, I., Rasmussen, S. K. Purification and cloning of the two domain glyoxalase I from wheat bran. *Plant Sci.* 2000, 155, 11-20.

39. Singla-Pareek, S. L., Reddy, M. K., Sopory, S. K. Genetic engineering of the glyoxalase pathway in the tobacco leads to enhanced salinity tolerance. *Proc. Natl. Acad. Sci. USA* 2003, 100, 14672-14677.

40. Roncarti, R., Salimini, F., Bartels, D. An aldose reductase homologous gene from barley: regulation and function. *Plant J.* 1995, 7, 809-822.

41. Agrawal, G. K., Jwa, N.-S., Iwahashi, H., Rakwal, R. Importance of ascorbate peroxidase OsAPX1 and OsAPX2 in the rice pathogen response pathways and growth and reproduction revealed by their transcriptional profiling. *Gene* 2003, 322, 93-103.

42. Arrigoni, O., De Gara, L., Tommasi, F., Liso, R. Changes in the ascorbate system during seed development of *Vivia faba* L. *Plant Physiol*. 1992, 99, 235-238.

43. De Gara, L., de Pinto, M. C., Moliterni, V. M. C., D'Egidio, M. G. Redox regulation and storage processes during maturation in kernels of *Triticum durum. J. Exp. Bot*. 2003, 54, 249-381.

44. Bailly, C. Active oxygen species and antioxidants in seed biology. *Seed Sci. Res*. 2004, 14, 93-107.

45. Maeda, K., Finnie, C., Østergaard, O., Svensson, B. Identification, cloning and characterization of two thioredoxin h isoforms, HvTrxh 1 and HvTrxh 2, from the barley seed proteome. *Eur. J. Biochem*. 2003, 270, 2633-2644.

46. Lozano, R. M. et al. New evidence for a role for thioredoxin h in germinated seedling development. *Planta* 1996, 200, 100-106.

47. Hoekstra, F. A., Golovina, E. *The Biology of seeds* (Eds. Nicolás, G., Bradford, K. J., Côme, D., Pritchard, H. W.) CABI Publishing. 2003, pp 259-270.

48. Hejgaard, J. Purification and properties of protein Z – a major albumin of barley endosperm. *Physiol. Plant.* 1982, 54, 174-182.

49. Zhang, H. et al. Large-scale analysis of the barley transcriptome based on expressed sequence tags. *Plant J*. 2004, 40, 278-290.

50. Bak-Jensen, K. S., Laugesen, S., Østergaard, O., Roepstorff, P., Svensson, B. Multiple forms of barley α-amylase generated during germination identified by two-dimensional electrophoresis, immunoblotting, and mass spectrometry. *FEBS J.* 2007, 274, 2552-2565

51. Potokina, E. et al. Expression genetics and haplotype analysis reveal cis regulation of serine carboxypeptidase I (Cxp1), a candidate gene for malting quality in barley (*Hordeum vulgare* L.). *Genomics* 2006*,* 6, 25-35.

52. Gallardo, K. et al. Proteomic of Arabidopsis seed germination. A comparative study of wild-type and gibberellin-deficient seeds. *Plant Physiol*. 2002, 129, 823-837.

53. Jiang, M., Zhang, J. Role of abscisic acid in water stress-induced antioxidant defence in leaves of maize seedlings. *Free Radical Res*. 2002, 36, 1001-1015.

54. Ingram, J., Bartels, D. The molecular basis of dehydration tolerance in plants. *Annu. Rev. Plant Physiol. Mol. Biol.* 1996, 47, 377-404.

55. Ozturk, Z. N. et al. Monoring large-scale changes in transcript abundance in drought- and salt-stressed barley. *Plant Mol. Biol*. 2002, 48, 551-573.

56. Kollipara, K. P., Saab, I. N., Wych, R. D., Lauer, M. J., Singletary, G. W. Expression profiling of reciprocal maize hybrids divergent for cold germination and desiccation tolerance. *Plant Physiol*. 2002,129, 974-992

57. Seki, M. et al. Monitoring the expression pattern of 1300 arabidopsis genes under drought and cold stresses by using full-length cDNA microarray. *Plant Cell* 2001, 13, 61-72.

58. Skylas, D. J. et al. Heat shock of wheat during grain filling: Proteins associated with heat-tolerance. *J. Cereal Sci*. 2002, 35, 175-188.

59. Wehyer, N., Hernandez, L. D., Finkelstein, R. R., Vierling, E. Synthesis of small heat-shock proteins is part of the developmental program of late seed maturation. *Plant Physiol*. 1996, 112, 747-57.

60. DeRocher, A. E., Vierling, E. Developmental control of small heat shock protein expression during pea seed maturation. *Plant J.* 1994, 5, 93-102.

61. Gygi, S. P., Rochon, Y., Franza, R., Aebersold, R. Correlation between protein and mRNA abundance in yeast. *Mol. Cell. Biol.* 1999, 19, 1720-1730.

62. Tian, Q. et al. Integrated genomics and proteomics analysis of gene expression in mammalian cells. *Mol. Cell. Proteomics* 2004, 3, 960-968.

Figure legends:

Figure 1: 2-DE of embryo (EM) from A) non-germinated seeds and B) 72 h PI, pH range 4-7. Encircled and squared spots are identified proteins that decrease and increase in abundance, respectively, during germination and radicle elongation (Table 1). Underlined numbers mark spots that remain constant up to 72 h PI. Spot # 220 [21], containing superoxide dismutase remains constant in all tissues and is not listed in Table 1. Boxes 1-3 indicate regions for which close-up views are shown in Figs. 3, 4, and 5, respectively.

Figure 2: 2-DE of A) aleurone layer (AL) and endosperm (EN) from non-germinated seeds and 72 h PI (Mw 14-94 kDa and pI 4.5-7). Spots (Table 1) that appear only in aleurone layer or endosperm, respectively, are indicated. The boxes 1-4 indicate regions for which close-up views are shown in B. B) the area of the 2-DE where α-amylase appears in aleurone layer and endosperm during radicle elongation. Mw 40-60 kDa, pI 4.87-5.24. Un-numbered squared spots contain α-amylase based on previous identifications by western blotting and MS [48].

Figure 3: A) Temporal changes in subpattern 1 (see Fig. 1, box 1, Mw 29-43 kDa and pI 4.1-4.9) of the embryo (EM) up to 72 h PI and comparison to B) aleurone layer (AL) and endosperm (EN) 2-DE from dry mature seeds. Encircled spots are defined as in Fig. 1.

Figure 4: Temporal changes in subpattern 2 (see Fig. 1, box 2, Mw 26-41 kDa and pI 5.05-5.7) of the embryo (EM) during 0-72 h PI. Encircled and squared spots and underlined numbers are defined as in Fig. 1.

Figure 5: Temporal changes in subpattern 3 (see Fig. 1, box 3, Mw 25-35 kDa and pI 6.1-6.8) of the embryo (EM) during 0-72 h PI. Encircled and squared spots and underlined numbers are defined as in Fig. 1.

Figure 6: Differences in 2-DE of embryos isolated from germinated whole seeds (a) in comparison with dissected embryos germinated in isolation from the rest of the seed (b). A) Close-up of a gel section spanning 25-39 kDa and pH 6.05-6.42 showing the presence of APX at 72 h PI in the two spot patterns. B) Close-up of a gel section spanning 56-86 kDa and pH 4.7-6.0 showing a decrease in high molecular protein spots between 24 h and 72 h PI in isolated embryos.

Table 1. Identification and spatio-temporal appearance of proteins 0-72 h PI

Functional class[a]	Spot ID	Protein	Change in abundance			
			Embryo	Aleurone layer	Endosperm	Accesion #
S (D)	254[c]	Late embryogenesis abundant proteinB19.1A*	↓ 24 h	÷	÷	Q05190
S (D)	579[b]	Late embryogenesis abundant protein B19.1B*	↓ 24 h	÷	÷	P46532
S (D)	474[d]	Late embryogenesis abundant protein B19.3	↓ 24 h	÷	÷	Q02400
S (D)	572[b]	Late embryogenesis abundant protein [wheat EST]	↓ 24 h	↓ 24 h	÷	TC191711
S (D)	16[d], 441[d]	Late embryogenesis abundant protein [EST]	↓ 24 h	↓ 24 h	÷	BG366433
S (D)	576[b]	Homolog to rice putative abscisic acid-induced protein [EST]	↓ 24 h	↓ 24 h	÷	TC191428
S (D)	577[b]	Homolog to rice putative abscisic acid-induced protein [EST]	↓ 24 h	↓ 24 h	÷	TC191428
S (D)	573[b], 574[b]	Homolog of rice putative embryonic protein [EST]	↓ 12 h	↓ 24 h	÷	TC142245
S (D)	575[b]	Homolog of rice putative embryonic protein [EST]	↓ 24 h	↓ 12 h	÷	TC142245
S (D)	17[d]	Cold-regulated protein Cor14b (barley)	↓ 36 h	↓ 60 h	÷	AJ29125
S (D)	100[c]	Aldose reductase (fragment)	↓ 12 h	↑ 72 h	÷	P23901
S (D)	293[c]	Aldose reductase (fragment)	↓ 24 h	↑ 24 h	÷	P23901
S (D)	583[b]	Aldose reductase (fragment)	÷	↑ 52 h	÷	P23901
S (D)	6[d], 468[c]	Homologous to glyoxalase I from rice [EST]	↓ 24 h	↓ 52 h	↓ 52 h	Q9ZWJ2
S (D)	149[c]	Homologous to glyoxalase I from rice (fragment) [EST]	→	↑ 36 h	↑ 24 h	Q9ZWJ2
S (D)	585[b]	Homologous to glyoxalase I from rice (fragment) [EST]	÷	÷	↑ 24 h	Q9ZWJ2
S (D)	586[b]	Homologous to glyoxalase I from rice (fragment) [EST]	÷	÷	↑ 36 h	Q9ZWJ2
S (O)	409[d]	Glutathione reductase	→	↓ 52 h	÷	AV916384
S (O)	103[d]	Superoxide dismutase Mn	→	→	÷	T06258
S (O)	301[d]	Superoxide dismutase Cu-Zn, (chloroplast) [EST]	÷	÷	↓ 36 h	T06800
S (O)	302[d]	Superoxide dismutase Cu-Zn 2 (chloroplast) [EST]	÷	÷	↓ 60 h	T06800
S (O)	99[c]	Peroxiredoxin (1-Cys peroxiredoxin)	↓ 36 h	↓ 36 h	÷	P52571
S (O)	104[d]	Peroxiredoxin (1-Cys peroxiredoxin)	↓ 36 h	↓ 36 h	÷	P52571
S (O)	571[b]	Barley seed peroxidase 1 (fragment) [EST]	↑ 4 h ↓ 52 h	↑ 12 h ↓ 52 h	↑ 60 h	Z34917
S (O)	75[d]	Thioredoxin peroxidase (2-Cys peroxiredoxin)	→	→	÷	BM376549
S (O)	296[d]	Thioredoxin h1	→	↓ 60 h	→	BM374793
S (O)	297[d]	Thioredoxin h1	↓ 36 h	↓ 36 h	↓ 36 h	BM445252
S (O)	313[d]	Thioredoxin h2	↓ 52 h	↓ 60 h	↓ 36 h	BM445252
S (O)	79[c]	Ascorbate peroxidase	↑ 36 h	÷	÷	AJ006358
S (O)	142[c]	GSH-dependent dehydroascorbate reductase 1 [EST]	→	→	↓ 12 h	BE601917

S (O)	294[c]	GSH-dependent dehydroascorbate reductase 1 [EST]	↓ 24 h	↓ 12 h	↓ 12 h	BE601917
P	185[d], 186[d], 187[d], 188[d], 189[d]	Protein disulphide isomerase	↓ 60 h	↓ 36 h	↓ 4 h	P80284
P	133[d], 180[d], 181[d], 183[d]	Heat shock protein 70	↓ 60 h	↓ 36 h	÷	P11143
P	603[b]	Heat shock cognate protein 70 (fragment) [EST]	↑ 4 h	→	÷	TC138918
P	304[d]	sHSP- Class I small heat shock protein	÷	↓ 12 h	÷	CAA69172
P	305[d]	sHSP- Class I small heat shock protein	↓ 36 h	↓ 12 h	÷	TC135297
P	306[d]	sHSP- Low molecular mass heat shock protein	↓ 52 h	↓ 36 h	÷	TC56126
P	288[d]	sHSP- Class II small heat shock protein [EST]	↓ 36 h	→	÷	TC45769
P	310[d]	sHSP- Class II small heat shock protein [EST]	↓ 36 h	↓ 12 h	÷	TC45769
P	308[d]	sHSP- Class II small heat shock protein [EST]	↓ 36 h	↓ 36 h	÷	TC45773
P	504[d]	sHSP 16.9B	↓ 36 h	→	÷	S21600
P	289[d]	sHSP 17.3 kDa	↓ 36 h	→	÷	S16525
P	598[b], 599[b], 600[b]	Protein Z (Z4) serpin	÷	÷	↑ 52 h	CAA66232
P	582[b]	Heat shock protein 70 (fragment) [EST]	÷	↑ 60 h	÷	TC169366
E	352[d]	α-Amylase	÷	↑ 60 h	↑ 72 h	P04063
E	353[c]	α-Amylase	÷	↑ 52 h	↑ 60 h	P04063
E	355[c]	α-Amylase	÷	↑ 52 h	↑ 72 h	P04063
E	390[d]	α-Amylase	÷	÷	↑ 72 h	P04063
E	593[b]	CPase I A carboxypeptidase	↑ 36 h	↑ 52 h	÷	1314177A
H	95[d]	Triose phosphate isomerase	→	→	↑ 36 h	P34937
H	588[b]	Triose phosphate isomerase	÷	÷	↑ 60 h	P34937
H	454[d]	Aconitate hydratase (cytoplasmic)	↓ 52 h	↓ 24 h	÷	BQ458967
H	455[d]	Aconitate hydratase (cytoplasmic)	↓ 52 h	↓ 24 h	÷	BQ466008
H	341a[d]	2,3-Bisphosphoglycerate-independent phosphoglycerate mutase [EST]	↓ 52 h	↓ 12 h	÷	BM371359
H	341[d]	2,3-Bisphosphoglycerate-independent phosphoglycerate mutase [EST]	→	↓ 52 h	÷	BM371359
H	143[d]	2,3-Bisphosphoglycerate-independent phosphoglycerate mutase [EST]	→	→	÷	TC63693
H	590[b]	Enolase (fragment) [EST]	↑ 24 h	↑ 36 h	÷	AW039978
H	581[b]	Enolase (fragment) [EST]	↑ 24 h	↑ 36 h	÷	CA017808
H	591[b]	Enolase (fragment) [EST]	÷	↑ 36 h	÷	CAA63121
H	287[c]	Initiation Factor 5A (eIF-5a)	↓ 24 h	↓ 12 h	÷	BF259508
H	578[b]	Proteasome subunit β-type [EST]	↑ 4 h	↓ 52 h	÷	O64464
H	602[b]	Proteasome α-subunit [EST]	↑ 24 h	÷	÷	TC147115
H	78[d]	Alanine aminotransferase	↓ 72 h	↓ 36 h	÷	P52894

H	601[b]	Transcription factor homolog BTF3-like protein [EST]	↓ 24 h	÷	÷	TC131691
U	587[b]	Probable jasmonate induced protein	↑ 52 h	÷	÷	X98124
U	370[c]	Probable jasmonate induced protein	↑ 52 h	÷	÷	X98124
U	8[c]	Embryo specific protein	↓ 52 h	↓ 52 h	÷	Q9ZNS9

The arrows indicate at what time point the protein spot starts to either increase ↑ or decrease ↓ in abundance. Some proteins disappear, others only decrease in abundance (most spots can be followed in Figures 1-5). → indicates that the protein spot is constant during 0-72 h PI and ÷ indicates that the protein spot is not present in the specific tissue.

*appears only in cCCB stained gels because it is negatively stained by silver staining.

[a] Functional categories: S (D): desiccation-, osmotic-, and salt stress; S (O): oxidative stress; P: protein synthesis, folding and storage; H: housekeeping; E: enzymes for storage compound degradation; U: proteins with unknown function.

[b] Identified in the present work. Identification data is given in supporting information.

[c] Published in [20, 21] and re-identified in the present work.

[d] Published in [20, 21].

Table 2. Appearance of proteins and corresponding mRNA PI identified by the present 2-DE analysis and cDNA microarray analysis [10,11].

		2-DE analysis		cDNA microarray analysis	
Protein	accession #[a]	tissue	Change in abundance	tissue	Change in abundance
Aconitate anhydrase	BQ458967	emb	↓ 52 h	emb	÷
		aleu	↓ 24 h	scut	÷
		endo	÷	endo+aleu	↑ 12-24 h[b]
Glutathione S-transferase	AF109194	emb	→	emb	↑ 12-24 h[b] ↓ 96 h[c]
		aleu	→	scut	÷
		endo	→	endo+aleu	÷
Serine carboxypeptidase 1A	1314177A	emb	↑ 36 h	emb	↑ 12-24 h[b] ↑ 8 h[c]
		aleu	↑ 52 h	scut	↑ 12-24 h[b]
		endo	÷	endo+aleu	÷
Proteasome subunit b-type	O64464	emb	↑ 4 h	emb	↓ 96 h[c]
		aleu	÷	scut	÷
		endo	÷	endo+aleu	÷
Jasmonate induced protein 23	X98124	emb	↑ 52 h	emb	↑ 48 h[c]
		aleu	÷	scut	÷
		endo	÷	endo+aleu	÷
Ascorbate peroxidase	AJ006358	emb	↑ 36 h	emb	↑ 12-24 h[b]
		aleu	÷	scut	↑ 12-24 h[b]
		endo	÷	endo+aleu	÷

[a] accession numbers are from Table 1. [b] Identification made by Potokina et al. [10].[c] Identification made by Watson and Henry [11]. The arrows indicate at which time point the protein spot or the mRNA starts to either increase ↑ or decrease ↓ in abundance. → indicates that the protein spot or the mRNA is constant during 0-72 h PI and ÷ indicates that the protein spot or the mRNA is not present in the specific tissue.

Supporting information regarding protein spots identified in the present work

Spot ID	Protein	Id. method	Mascot score	Sequence coverage	Peptides matching	Theoretical		Observed		Accession
						Mw (kDa)	pI	Mw (kDa)	pI	
579	Late embryogenesis abundant protein B19.1B*	MS	59	43	4*	9.97	5.49	13.80	5.75	P46532
572	Late embryogenesis abundant protein [wheat EST]	MS/MS	108		2					TC191711
576	Homolog to rice putative abscisic acid-induced protein [EST]	MS/MS	146	23	6					TC191428
577	Homolog to rice putative abscisic acid-induced protein [EST]	MS/MS	148	23	6					TC191428
573	Homolog of rice putative embryonic protein [EST]	MS	98	63	6					TC142245
574	Homolog of rice putative embryonic protein [EST]	MS	106	63	6					TC142245
575	Homolog of rice putative embryonic protein [EST]	MS	70	63	6					TC142245
583	Aldose reductase (fragment)	MS	66	22	11	36.1	6.51	25.50	5.87	P23901
585	Homologous to glyoxalase I from rice (fragment) [EST]	MS	94	42	8					Q9ZWJ2
586	Homologous to glyoxalase I from rice (fragment) [EST]	MS	94	42	8					Q9ZWJ2
571	Barley seed peroxidase 1 (fragment) [EST]	MS	138	52	11					Z34917
603	Heat shock cognate protein 70 (fragment) [EST]	MS/MS	104(78, 116)		2					TC138918
598	Protein Z (Z4) serpin	MS	120	28	9	43.3	5.61	36.00	5.20	CAA66232
599	Protein Z (Z4) serpin	MS	98	18	7	43.3	5.61	38.00	5.43	CAA66232
600	Protein Z (Z4) serpin	MS	123	26	8	43.3	5.61	36.00	5.38	CAA66232
582	Heat shock protein 70 (fragment) [EST]	MS	106	28	12	34.96	4.86	35.20	6.19	TC169366
593	CPase I A carboxyepeptidase	MS	77	29	6	29.10	4.96	37.90	5.20	1314177A
588	Triose phosphate isomerase	MS	115	31	7	26.95	5.39	27.7	4.98	P34937
590	Enolase (fragment) [EST]	MS/MS	144	20	3					AW039978
581	Enolase (fragment) [EST]	MS	74	36	5					CA017808
591	Enolase (fragment) [EST]	MS/MS	131	20	3					CAA63121
578	Proteasome subunit β-type [EST]	MS	84	30	4*					O64464
602	Proteasome α-subunit [EST]	MS/MS	88(81, 125)	44	8					TC147115
601	Transcription factor homolog BTF3-like protein (EST)	MS/MS	80(177, 170, 125)	44	8					TC131691
587	Probable jasmonate induced protein	MS	92	69	15	16.17	6.39	29.00	6.47	X98124

For proteins identified by MS/MS the Mascot score including the ion score is given or in case of # 602 and 603 the ion scores for each fragmented peptide are given in parenthesis. Theoretical and observed Mw and pI is only given for protein identified from the NCBI database and not for identification based on EST's.

*: The identification was considered confident with only 4 matching peptides because the spectrum only contained few peaks and the sequence coverage was relatively high.

Figure 1,
Bønsager et al.

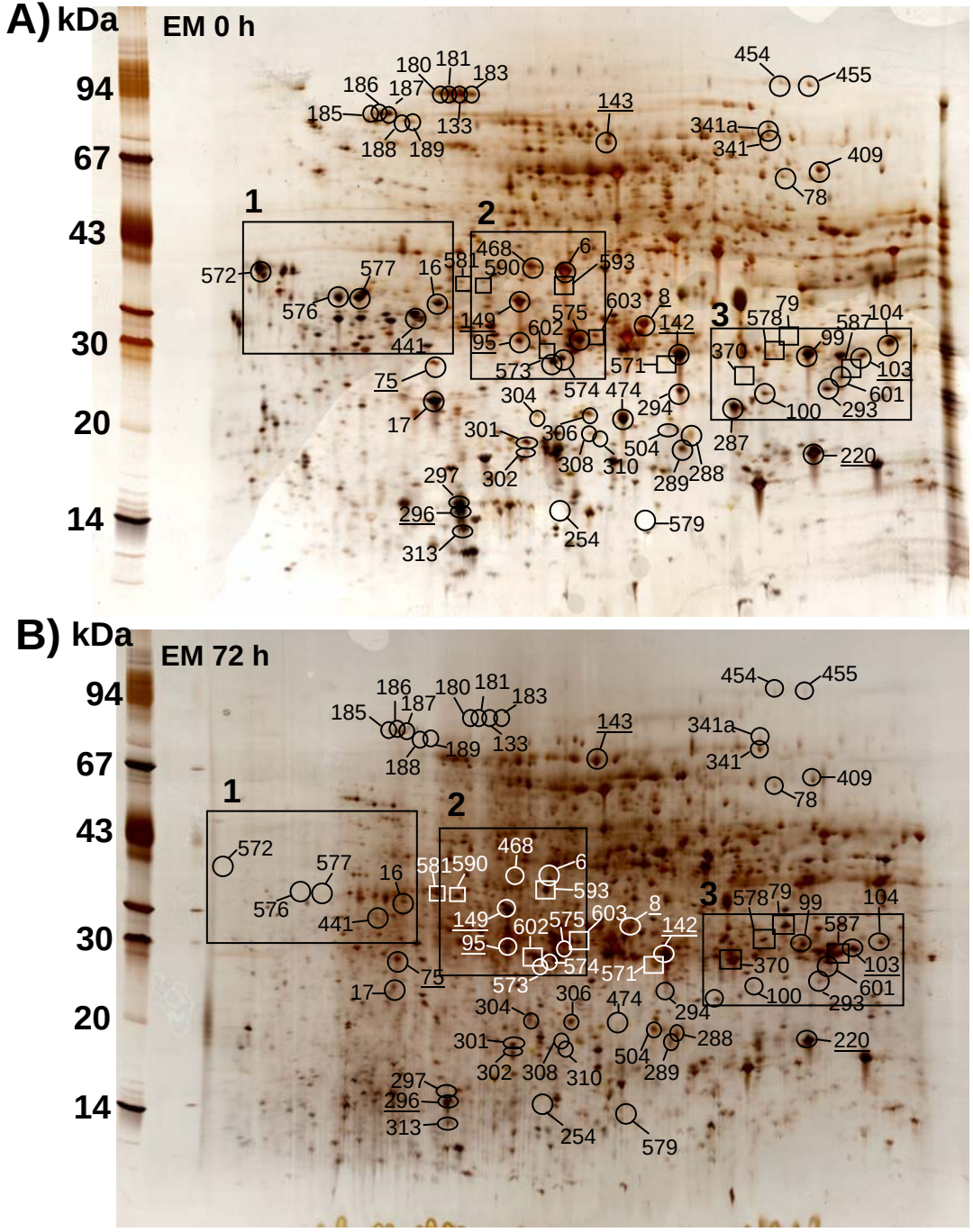

Figure 2, Bønsager et al.

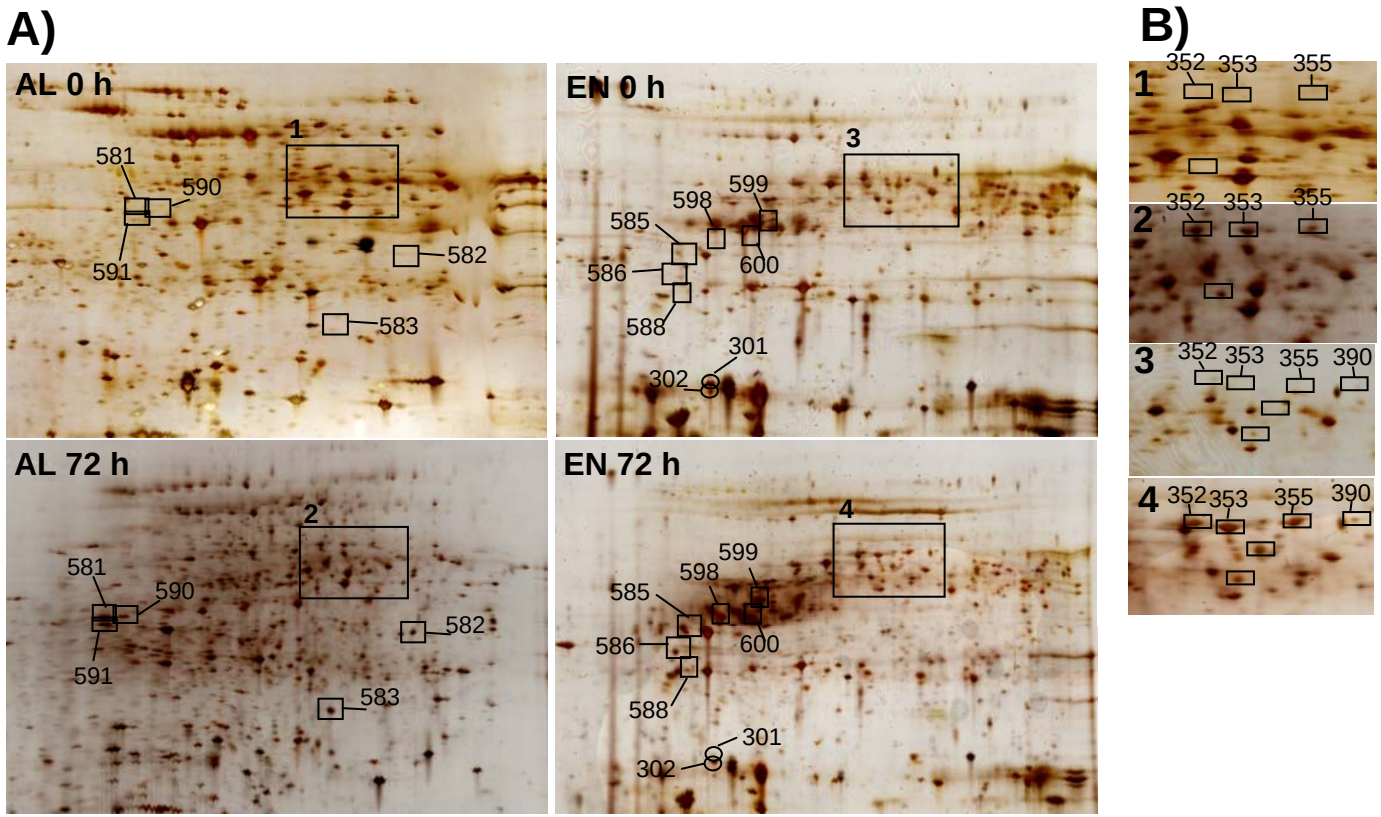

Figure 3, Bønsager et al.

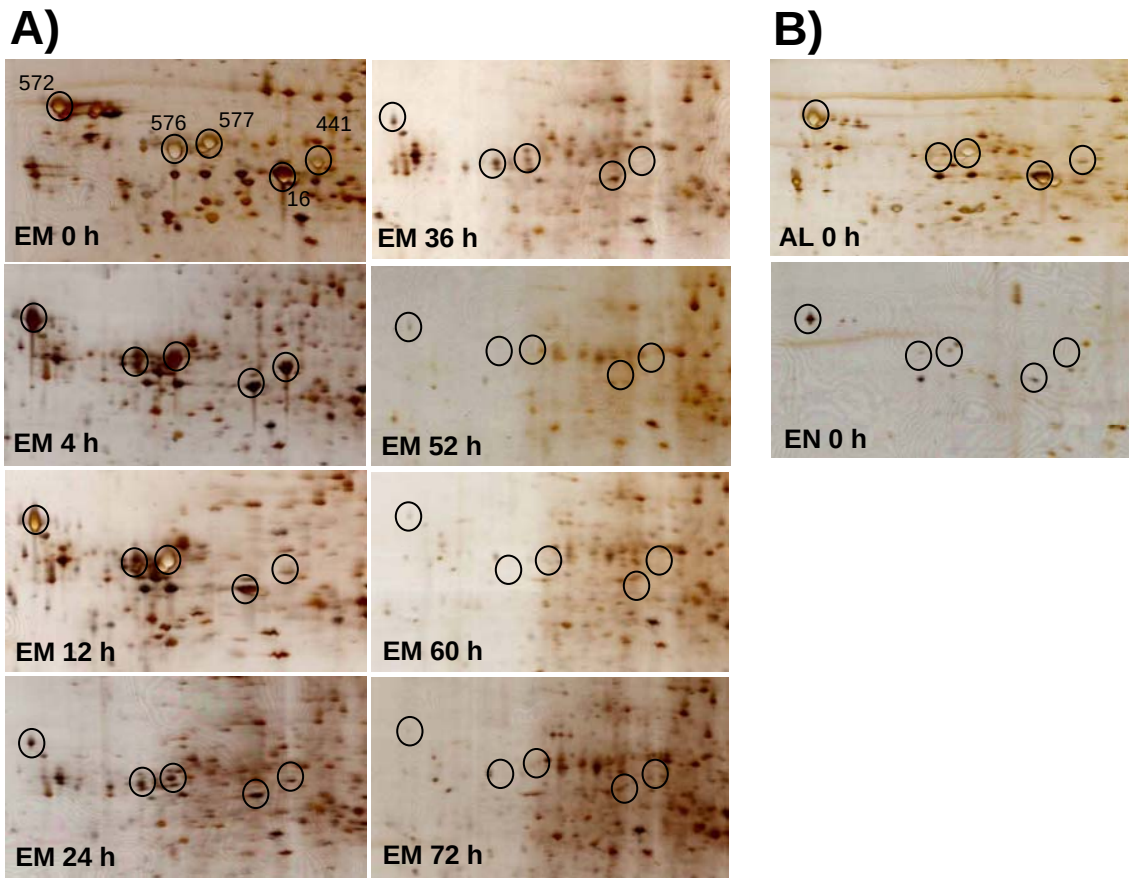

Figure 4, Bønsager et al.

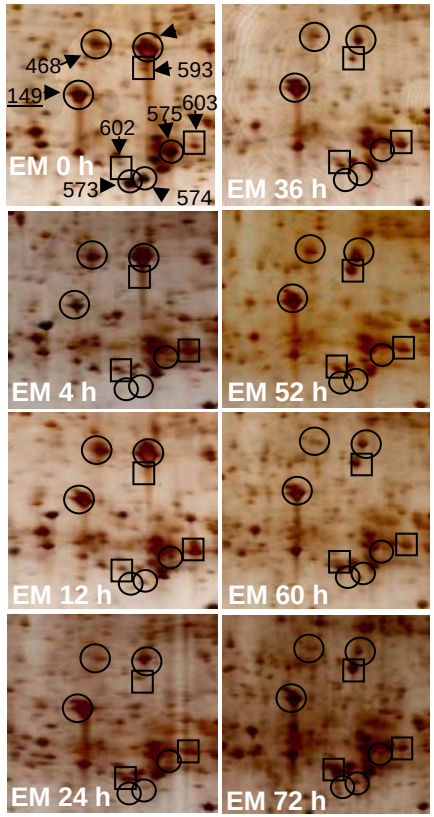

Figure 5, Bønsager et al.

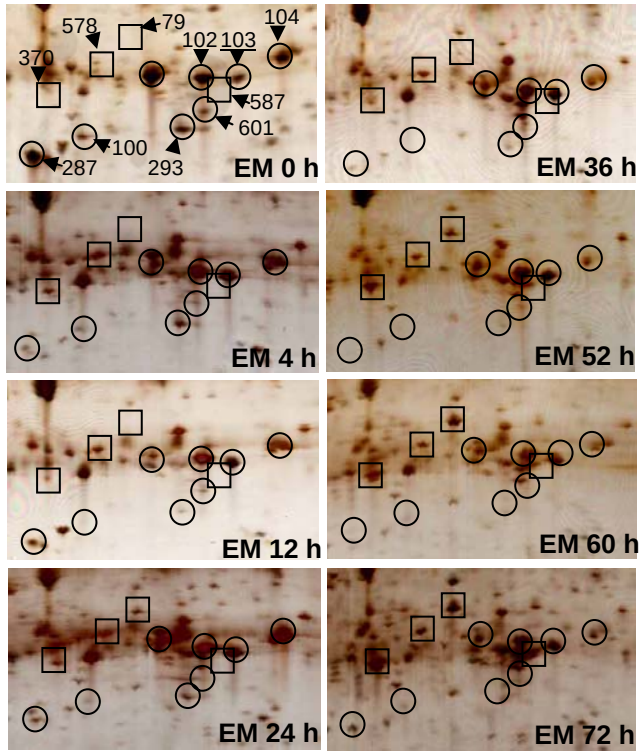

Figure 6, Bønsager et al.

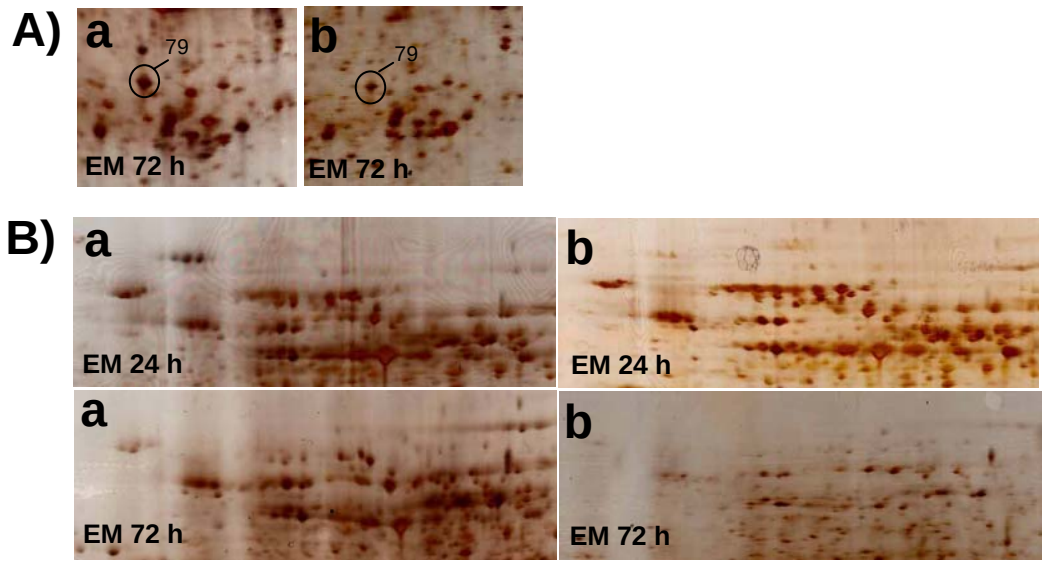

Appendix 6 - Presentations

Conferences

Oral presentations

Plant Biotech Denmark annual meeting 2007, KVL, January 2007.
Oral Presentation: "Germination and radical elongation in barley embryo, aleurone layer and endosperm tracked using proteome analysis of the dissected tissues" by **B.C. Bønsager** (selected from abstract)

The Federation of European Societies in Plant Biology XV. Lyon, France, July 17-21, 2006.
Oral presentation: "Proteome analysis of dissected barley seed tissues during early germination" by **B.C. Bønsager** (selected from abstract)

Birgit Bønsager, Christine Finnie, Kenji Maeda, Per Hägglund, Anette Henriksen and Birte Svensson. Stress and the barley proteome during grain filling, seed maturation, and germination. Plant stress network workshop. Odense, Feb. 2006. (Invited oral presentation, B. Svensson).

Poster presentations

Plant Biotech Denmark annual meeting 2006. KVL, Febuary 2006.
Poster presentation: "Analysis of the barley proteome during early germination" by **B.C. Bønsager**, C. Finnie, and B. Svensson.

Birgit C. Bønsager, Christine Finnie, and Birte Svensson. Proteome analysis of dissected barley seed tissues during early germination. Danish Biotechnology Conference XI. Vejle, June 2005 (Poster, B. Svensson).

Christine Finnie, **Birgit C. Bønsager**, Birte Svensson. Proteome analysis of the barley aleurone layer: a model system for plant signalling. Biochemical Society Focused Meeting. Glasgow, UK. Nov. 2004.

Danish Biotechnology Conference X: Applied Proteomics. From protein function to biotechnology and biomedicine. Munkebjerg, Vejle, Denmark, May 2004.
Poster presentation: "Analysis of the barley proteome during early germination" by **B.C. Bønsager**, C. Finnie, and B. Svensson.

Talks

“Germination and radical elongation in barley embryo, aleurone layer and endosperm tracked using proteome analysis of the dissected tissues” Protein Science annual meeting (The Protein Science Ph. D. School, University of Copenhagen), Tisvildeleje, May, 11, 2007.

“Proteome analysis of barleys seeds during early germination: stress related proteins”. The Protein Science Ph. D. School (University of Copenhagen) Annual Meeting, Tisvildeleje, April 18, 2006.

“Germination of barley: Initial changes in the barley proteome and identification of the high molecular weight protein limit dextrinase”. The Protein Science Ph. D. School (University of Copenhagen) Annual Meeting, Tisvildeleje, January 20, 2004.

“Analysis of the barley proteome during early germination”. The Protein Science Ph. D. School (University of Copenhagen) Annual Meeting, Tisvildeleje, April 20, 2005.

“Analysis of the barley proteome during early germination”. Biochemistry and Nutrition Group, BioCentrum-DTU. Juni 16, 2004.

“Analysis of the barley proteome during early germination”. The Protein Science Ph. D. School (University of Copenhagen) The Island of Spetzes, Greece, May, 2004.